School of Electrical and Computer Engineering

High Renewable Energy Penetration Hybrid Power System for Rural and Desert Areas

Shaji Varukunnel Mathews

This thesis is presented for the Degree of

Doctor of Philosophy

Of

Curtin University

January 2015

Declaration

To the best of my knowledge and belief this thesis contains no material previously published by any other person except where due acknowledgment has been made. This thesis contains no material which has been accepted for the award of any other degree or diploma in any university.

Signature : _____
(SHAJI VARUKUNNEL MATHEWS)

Date : _____

I dedicate this thesis to my parents, wife, children and brothers.

Abstract

This thesis focuses on the development of high renewable energy penetration off-grid remote area power systems combining an innovative variable speed diesel generator, battery storage , solar photovoltaic panels and power electronic interface and control systems. Each chapter in this thesis refers to various aspects of renewable energy sources, integration and its effects to improve the current environmental problems created due to high carbon emissions. A synopsis is provided for each chapter to highlight the crucial elements.

Harvesting the energy of the sun and converting DC energy into the same voltage and frequency which can be used as a utility, is a revolution and a solution to the current world energy deficiency problem. A detailed theoretical analysis, modelling and simulation of the variable speed diesel generator using various generation technologies has also been explained where simulation results using Matlab/Simulink validate the use of VSDG to realize variable speed operation for diesel engine. The analysis demonstrated that variable speed system produced high quality power and also produced high quality DC voltages independent of diesel engine speed.

In many remote areas, decentralized distributed generation systems (DDGS) are commonly used for increasing the capacity and reducing diesel fuel consumption. A renewable energy power generator such as a PV array can be integrated with the conventional diesel generator to supply local load. Unfortunately, the introduction of the renewable energy sources may result resulted in longer time periods of low load diesel operation. By applying VSDG in decentralized distributed generation systems, the problem caused by the conventional diesel generator could be avoided. Three innovative configurations of decentralized distributed generation systems were proposed. One configuration for small scale remote area power supply systems (RAPS), one configuration for medium scale mini grid remote area power supply system and the third for high solar PV penetration into a township utility network.

Firstly, an innovative solar hybrid energy system incorporating a variable speed diesel generator with minimum battery storage is described. Simulation and experimental results confirm that combination of the generator, battery and photovoltaic is ideally suited for

remote community applications. This system has been installed at the Veterans Recreation Centre in Marble Bar and it is operating at its optimal for more than 20 months.

Secondly, a study was conducted on a five year old, large hybrid power system to integrate more renewable energy without upgrading the existing system, to reduce the diesel consumption thereby saving running cost, extending the life of existing diesel generators and incorporation of storage battery. This method limits the power from constant speed diesel generator sources using variable speed generator and hybrid control system which was simulated and implemented. The simulation showed the system operating very well given the increased loads in recent years and the additional PV to be added to the system to allow a maximum penetration of renewable energy given the new loads.

Thirdly, design and modelling methodology was used to define the hosting capacity of Horizon Power's isolated networks to accommodate one hundred percent integration of distributed PV installations. These include stability and reliability, network capacity, power quality and minimum loading of generating unit criteria. A mathematical model has been developed and implemented to visualise interaction among various system parameters. The model can be utilised as an analysis tool to define the hosting capacity and to assess system impacts due to integration of PV generation. The model utilisation has been demonstrated using case study and performance monitoring of a selected network. This paper presents the complete system modelling, designing and controlling of an islanded mini-grid power supply to the town of Carnarvon, Western Australia.

In a hybrid power system with a minimum energy storage element, it is important not to oversize the renewable energy generator unless the power converter has the ability to control the energy production. To achieve optimal system performance accounting for economic feasibility, the renewable energy generator should be sized to supply the day time load directly and sufficiently without producing too much excess energy.

In summary, this control system is the heart of the hybrid power system, which has the capability to decentralise an existing centralised utility network and monitor the load and energy source. This leads the control system to regulate the energy source by providing priority for renewable energy. Therefore, it is concluded that the off-grid & utility integrated PV-VSDG hybrid power system with advanced power management capability has great potential in the market of power generation.

Acknowledgements

First and foremost I want to thank my Almighty Father who gave me the strength, opportunity and courage to come this far in my journey. The past few years has given me a greater insight into the renewable energy sector, I have not only learnt a lot but the journey has been most exciting and rewarding. Though I had a great interest in the field of renewable energy, the concept of renewable energy and various sources were further groomed only after coming to Western Australia. It really blossomed after I started my research studies under the guidance of Professor Chem Nayar. With his constant support and supervision I was lucky enough to be part of the engineering team to implement the largest hybrid renewable energy system project in Broome; and many other pilot projects both overseas and nationally since 2008 till date. I would like to express my sincere gratitude and thanks to Professor Nayar who has been like a backbone to all of my research till date and who was a continuous source of motivation, who took the additional efforts to share his immense knowledge.

I would like to thank Dr. Sumedha Rajakaruna, who started as my co-supervisor but has since moved on to become my supervisor. He has been a very encouraging and supportive mentor, who never let me leave a stone unturned. Irrespective of the time or day, he has been a constant source of inspiration and we spent many an hour pondering over the nuances of my work.

A special note of thanks to Prof Kevin Fynn, Chairperson for arranging industrial scholarship with Regen Power to commence this project, without which this was not possible. I sincerely thank Prof Fynn for his support. I would also like to thank staff at Curtin University with special mention of Curtin Technical staff, Dept of Power Engineering, especially Mark Fowler. Thanks to the Learning Centre and Library at Curtin University for providing assistance to students like me to improve various skills beneficial for our research work. I thank all my colleagues for sharing their research experiences during my study and for giving friendly advice.

I would like to thank my team at AICA Engineering for their love and understanding that they showed during my research period. The team at Regen Power have also played an important role in helping me make my project a success, I thank every one of them. A special thanks to Louise Lathbury, Babbin Mathews and Sridhar Raja for their assistance with the proof reading and bringing this manuscript to its finale. Many people especially friends and

colleagues have put in efforts towards the success of my research, all of which can't be mentioned but I gratefully acknowledge.

Last but never the least I acknowledge my family for their love and enduring care through this challenging journey.

List of Publications

1. Shaji V Mathews, S Rajakaruna and C V Nayar, "Design and Implementation of an Offgrid Hybrid Power Supply with Reduced Battery Energy Storage", Australasian Universities Power Engineering Conference, AUPEC 2013, Hobart, TAS, Australia, 29 September – 3 October 2013.

2. Shaji V Mathews, S Rajakaruna and C V Nayar "Design and Implementation of an Offgrid Hybrid Power Supply with Reduced Battery Energy Storage", ELSEVIER (Renewable Energy an International Journal), 2014. (Currently under revision)

3. Shaji V Mathews, S Rajakaruna and C V Nayar, "Design and Modeling of a Hundred Percent Renewable Energy Based Suburban Utility", Australasian Universities Power Engineering Conference, AUPEC 2014, Perth, WA, Australia, 28 September – 1 October 2014.

Table of Contents

Table of Figures

Table of Tables

List of Acronyms and Symbols

ACRONYMS

AM	Asynchronous machines
AGM	Absorbed glass matt
ASA	Australian Safety Approvals
APVA	Australian Photovoltaic Association
AS	Australian Standards
AC	Alternating Current
BD-INV	Bi-Directional Inverter
BP	British Petroleum
CRC	Catalytic recombination cap
CO2	Carbon dioxide
CSP	Concentrating solar thermal power
CCS	Conformity Certification Services
CSRIO	The Commonwealth Science and Industrial Research Organisation
CC	Current Controlled
CT	Current Transformer
CSDG	Constant speed diesel generator
CEEM	Centre for Energy and Environmental Markets
DF	De-rating factor
DNS	North to south shadow length
DEW	East to West shadow length
DC	Direct Current
DG	Diesel Generator
DDGS	Decentralized distribution generation system
DOD	Depth of Discharge
ESV	Energy Safe Victoria
EIA	Environmental impact assessment

FL	Fuzzy Logic
GW	Giga Watt
GDP	Gross Domestic Product
GUI	graphical user interface
GPRS	General Packet Radio Service
HAS	Hybrid automation system
HMI	Human Machine Interface
HRPSoC	high-rate-partial-state-of-charge
HCCU	Hybrid System Control Command Unit
IM	Induction machines
IC	Internal Combustion
ISG	Integrated Starter Generator
IPCC	Intergovernmental Panel on Climate Change
JAS-ANZ	Joint Accreditation System of Australia and New Zealand
KW	Kilowatt
L-L	Line to line
MPPT	Maximum Power Point Tracking
MWh	Megawatt hour
NOCT	Nominal operating cell temperature
NT	Northern Territory
NOx	mono-nitrogen oxides
NSW	New South Wales
OECD	Organisation for Economic Cooperation and Development
OM	Operation modes
PU	Power vs Speed
PV-VSDG	Photovoltaic-Variable Speed Diesel Generator
PV	Photovoltaic cell
PSoC	Partial State of Charge
PMSM	Permanent Magnet Synchronous Machines

RCP	Representative Concentration Pathways
PMHH	Permanent Magnet Hybrid Homopolar
PWM	Pulse Width Modulation
PSIM	Power Electronic Simulation software from Powersim
RPM	Revolution per minute
SRM	Switched- reluctance machines
STC	Standard test conditions
SLI	Starting, Lighting, and Ignition
SMA	Inverter Manufacturer
SWIS	South West Interconnected System
SMPS	Switched-mode power supply
SOC	State-of-charge
U.S	United States
U.S.S.R	United State of Soviet Russia
VRLA	Valve Regulated Lead Acid
VSI	Voltage source inverter
VSDG	Variable Speed Diesel Generator
VC-VSI	Voltage Controlled VSI
WA	Western Australia

Unit and Symbol

bbl/day	Barrel per day
GJ/m2	Giga Joule per square metre
KW/m2	Kilowatt per square metre
PJ	Petajoule
W/m	Watt per metre
BKWh	Billion Kilowatt hour
V	voltage
Voc	Open Circuit voltage

I	Current
Isc	Short Circuit current
P	Power
Imp	Maximum power current
Ah	Ampere Hour
I_d	Diode current
V_d	Diode voltage
T	Cell temperature
Qd	Diode quality
KVA	Kilo Volts Ampere
p.u	Per unit
Hz	Hertz
k	Boltzmann constant
Ah/day	Design Month Load
V oc	Open circuit voltage
P_{pv}	Power output from PV module
β	Altitude angle
Φs	Azimuth angle
L	latitude
η	efficiency
kg	Kilogram
t	time
MW	Megawatt

Chapter 1

1. Introduction

1.1 Research Background

Energy or Power is among the most commonly used terms since its advent many centuries ago! To tap the various resources together are beyond any human till date but with the progress of time, each era has brought with it a revolution in itself. The ups and downs of each invention, creation and discovery have given mankind a plethora of choices and options to resolve the ever growing demand for energy! Mankind has been in the 'spell' of energy sources since the late 18th C when they became heavily dependent upon energy for sustained social and economic development. As a result of commercial, industrial and domestic activities, electrical energy demand has increased remarkably over recent decades.

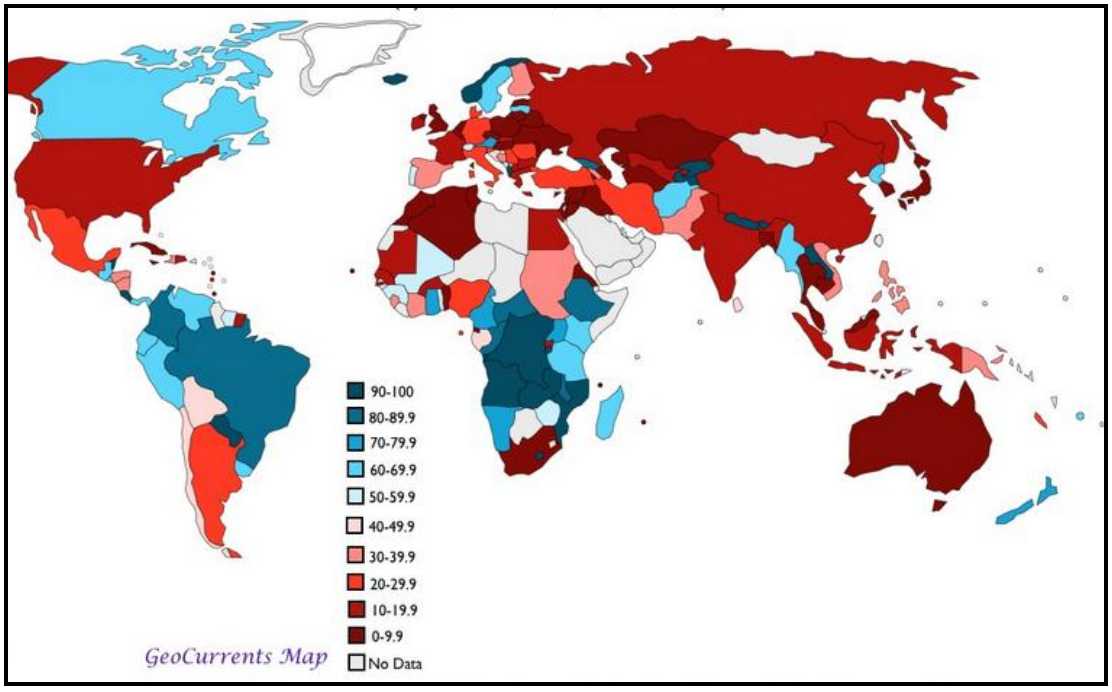

Figure 1. 1: Percentage of electricity generation from renewables [1]

Many countries rely overwhelmingly on fossil fuels for electricity generation, however Figure 1 depicts the lower percentage of countries depending on renewable energy. Large-scale fossil fuel power plants have been built to meet the growing electrical energy demand, particularly in metropolitan areas [2]. In contrast, diesel mini-grids are relied upon in remote areas with low demographic density, where people have no immediate access to

reliable electricity grids. Reasonable costs and general availability of diesel generators have resulted in their widespread applications in rural areas. It is not uncommon to find various sizes of privately owned diesel generators that supply a number of households for their daily energy needs in those areas [3].

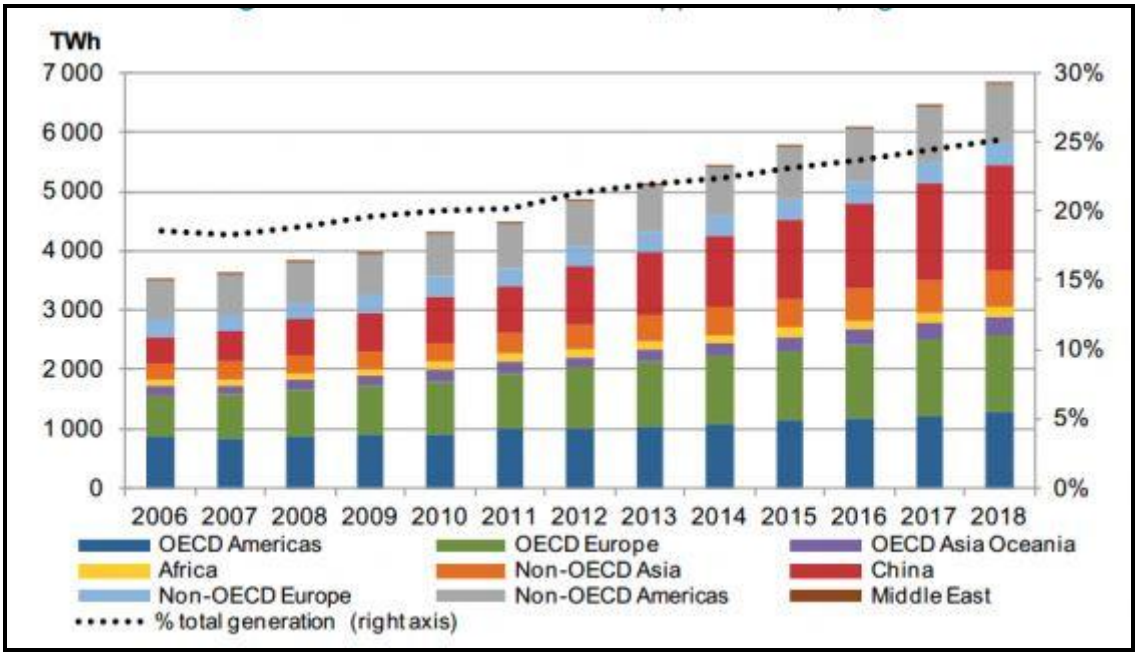

Figure 1. 2: Global renewable electricity production by region [1]

As graphically illustrated in Figure 2, the global renewable energy production will have steady growth. Renewable energy produces almost nil waste products such as carbon dioxide or other chemical pollutants which in turn has minimal impact on the environment. Among all the renewable energy resources, currently the solar and wind energies have the greatest potential as a power generating energy source, because of their many advantages like low or zero emission of pollutant gases, low cost, inexhaustible sources and easy availability. However, these systems are also heavily dependent on natural forces, i.e. weather conditions. One of the major disadvantages with renewable energy is that it is difficult to generate the quantities of electricity that are as large as those produced by traditional fossil fuel generators. We can reduce the dependency of solar or wind power system on weather conditions by using some backup supply like batteries and variable speed gensets. This thesis presents a hybrid PV/Variable speed diesel generator/lead acid super capacitor battery energy system for standalone and utility level grid connected system. Currently the best way to

ensure smooth functioning is by combining different power sources to meet the growing energy demands.

The IEA's Medium-Term Oil Market Report 2014 has predicted that global growth in oil demand may start to slow down as soon as the end of this decade, due to environmental concerns and cheaper alternatives, and despite boosting its 2014 forecast of global demand by 960,000 barrels per day [1]. While supply is forecasted to remain strong, or "tight", an oil revolution currently underway in North America – the IEA says it expects the global market to hit an "inflexion point", by the end of 2019, "after which demand growth may start to decelerate due to high oil prices, environmental concerns and cheaper fuel alternatives." It's worrying news for the over-invested and under-prepared; not least of all oil importing nations, to which, as Samuel Alexander noted in this article last September. "When oil gets expensive, everything dependent on oil gets more expensive: transport, mechanised labour, industrial food production, plastics, etc," he wrote. "This pricing dynamic sucks discretionary expenditure and investment away from the rest of the economy, causing debt defaults, economic stagnation, recessions, or even longer-term depressions. That seems to be what we are seeing around the world today, with the risk of worse things to come."

These factors, says the report, will lead to fuel-switching away from oil, as well as overall fuel savings. In short, it says, "while 'peak demand' for oil – other than in mature economies – may still be years away, and while there are regional differences, peak oil demand growth for the market as a whole is already in sight."

1.1.1 Energy trends in recent times

According to BP energy [4], projected future energy trends and factors affecting the fossil fuel industry have changed markedly in recent times. Global energy demand is expected to grow by 36% between 2011 and 2030, a trend driven by the emerging economies. Without continuous improvements in energy efficiency, supply would have to grow much more rapidly simply to sustain economic growth.

BP's energy outlook also describes the power of competition and market forces in driving efficiency and innovation not only in unlocking new supplies such as unconventional oil and gas reserves, but also in improving energy efficiency and consequently limiting the

growth of carbon emissions. The overall conclusion is that increased demand can be met as long as competition is present to drive innovation, unlock resources and encourage efficiency.

Growth in population size and per capita income are the key drivers behind growing demand for energy [5]. The world population is projected to reach more than eight billion and world income to double by 2030 as compared to the 2011 level in real terms. Low and medium income economies outside the OECD are predicted to account for over 90% of population growth to 2030. Due to their rapid industrialization, urbanization and motorization, these economies are also expected to contribute 70% of the global GDP growth and over 90% of the global energy demand growth.

World primary energy consumption is projected to grow by 1.6% p.a. from 2011 to 2030, adding 36% to global consumption by 2030. Almost all (93%) of the energy consumption growth is expected to occur in non-OECD countries. Non-OECD energy consumption in 2030 is predicted to be 61% above the 2011 level, with growth averaging 2.5% p.a. (or 1.5% p.a. per capita), accounting for 65% of world consumption (compared to 53% in 2011).

During the time period between 2011 and 2030, the power sector will continue to diversify its fuel mix, driven by the high prices for fossil fuels. The fastest growing fuels will be renewables (including biofuels) with growth averaging 7.6% p.a. Nuclear (2.6% p.a.) and hydro (2.0% p.a.) generated power sources are both expected to grow more rapidly than other energy sources during this period.

Among fossil fuels, gas use is predicted to grow the fastest (2.0% p.a.), followed by coal (1.2% p.a.), and oil (0.8% p.a.).

Renewable energy supply will more than treble from 2011 to 2030, accounting for 17% of the increase in global energy supply [6]. Hydro and nuclear together are predicted to account for another 17% of the growth. Renewables are projected to gain market share in power, at a slower but perhaps more sustainable rate than nuclear power did in the 1970/80s. At that time, nuclear power gained share rapidly, but peaked in the 1990s as safety concerns, rising costs, and continued public opposition led to a loss of policy support. Renewables will face a different set of challenges; the most key factor being the affordability of subsidies [7] .

However, carbon emissions from energy use continue to grow, increasing by 26% between 2011 and 2030 (1.2% p.a.) [8]. We assume continued tightening in policies to

address climate change, yet emissions will remain well above the required path to stabilise the concentration of greenhouse gases at the level recommended by scientists (450 ppm). Overall, there will be some progress in greenhouse gas production[9]. The changing fuel mix, in particular the rising share of renewables and substitution of coal with gas, will results in a gradual decoupling of emissions growth from primary energy growth [10].

1.1.2 Carbon dioxide in atmosphere

Scientific instruments showed that the gas had reached an average daily level above 400 parts per million in 2011 [11]. The best available evidence suggests the amount of the gas in the air has not been this high for at least three million years, before humans evolved, and scientists believe the rise portends large changes in the climate and the level of the sea. It symbolizes that so far we have failed miserably in tackling this problem [12].

Climate-change contrarians point out that carbon dioxide represents only a tiny fraction of the air. Climate scientists, however, reject this argument, saying that it is like claiming a tiny bit of arsenic or cobra venom cannot have much effect. Research shows that even at such low levels, carbon dioxide is potent at trapping heat near the surface of the earth.

1.1.3 Climate Science

The Intergovernmental Panel on Climate Change (IPCC) has reported that the world's atmosphere warmed by about 0.85°C between 1880 and 2012 [13]. The oceans are also warming, absorbing 90% of the increased energy stored in the climate system. Ice cover in the Artic, Antarctica and Greenland is declining. Sea levels are rising, the ocean is acidifying and atmospheric concentrations of greenhouse gases are rising.

1.1.3.1 Factors of Climate Change

Climate scientists measure the drivers of climate change using a metric called 'radiative forcing'. This quantifies the change in energy fluxes at the top of the atmosphere due to different climate drivers [14]. Substances with a positive forcing, like carbon dioxide, are those warming the earth whereas substances with negative forcing, like sulphate aerosols, are those cooling the earth [15].

The new IPCC report estimates total human radiative forcing in 2011 relative to 1750 to be 2.29 watts per square meter (W m^{-2}) [16]. The following waterfall chart is an attempt to explain, as simply as possible, the drivers of climate change [17] in terms of radiative forcing.

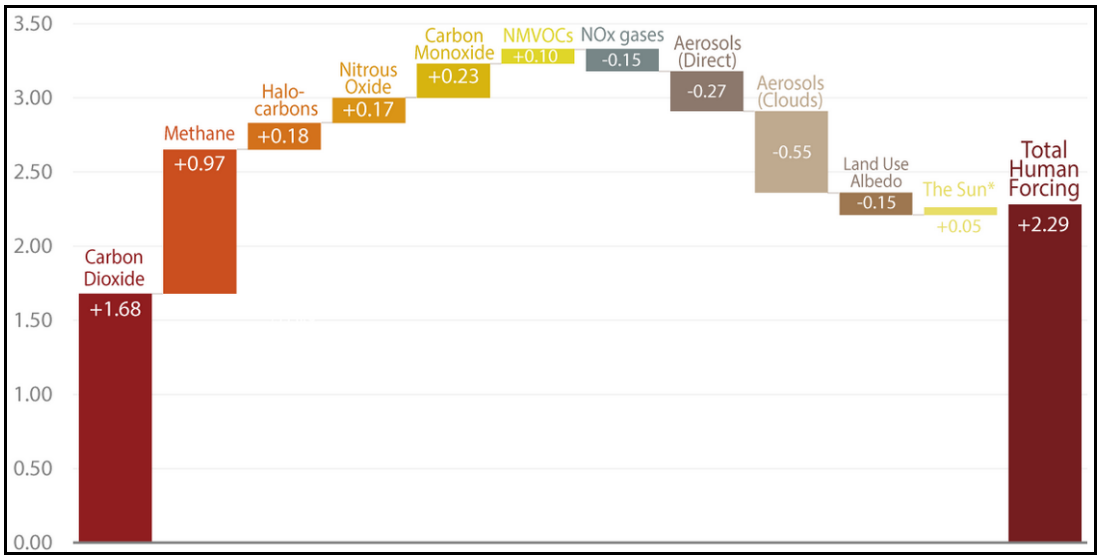

Figure 1. 3 Chart showing relative importance of different compounds in heating and cooling [15]

Emissions of carbon dioxide have been responsible for over half of the warming influences to date. Methane, carbon monoxide, halo-carbons and nitrous oxide have also had a substantial influence on warming [18]. The major cooling influences during this time were NOx gase,

and aerosols (like sulphates and organic carbon). Aerosols also had a cooling effect on clouds, although this could not be accurately quantified [19].

The IPCC, in their fifth assessment report, have brought together a wide ensemble of climate models that involve different forcing and sensitivity estimates, and provided some potential scenarios for global warming this century [20]. The representative concentration pathways, or RCP, are named after their approximate total radiative forcing in the year 2100 relative to 1750. The four RCPs are 2.6 (rapid mitigation), 4.0, 6.5 and 8.5 (runaway emissions) W m^{-2} (Figure 1.3). All of these are higher than the 2011 estimate of 2.29 W m^{-2} [21].

For the rapid mitigation pathway (RCP 2.6) the expected warming this century is 1.0°C (the likely range is shown in the bars). For the fast stabilization pathway (RCP 4.5) 1.8°C of warming is predicted. For the slower stabilization pathway (RCP 4.5) the mean estimate of warming is 2.2°C and for the runaway emissions scenario (RCP 8.5) it is 3.7°C [22].

This warming is over and above the 0.6°C already observed in the 1986-2005 reference period. Therefore in every case but the rapid mitigation scenario (RCP 2.6), the temperature is expected to warm beyond 2°C above the pre-industrial period [23].

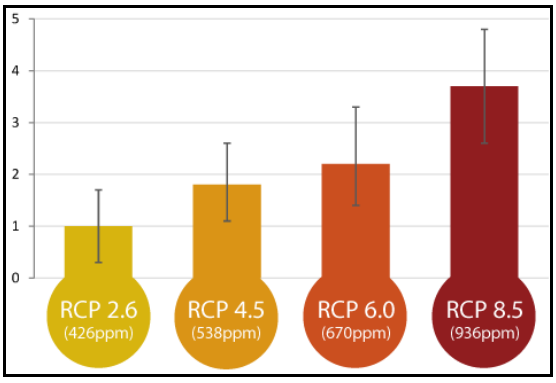

Figure 1. 4: Representative Concentration Pathway [15]

1.1.4 Australia Overview

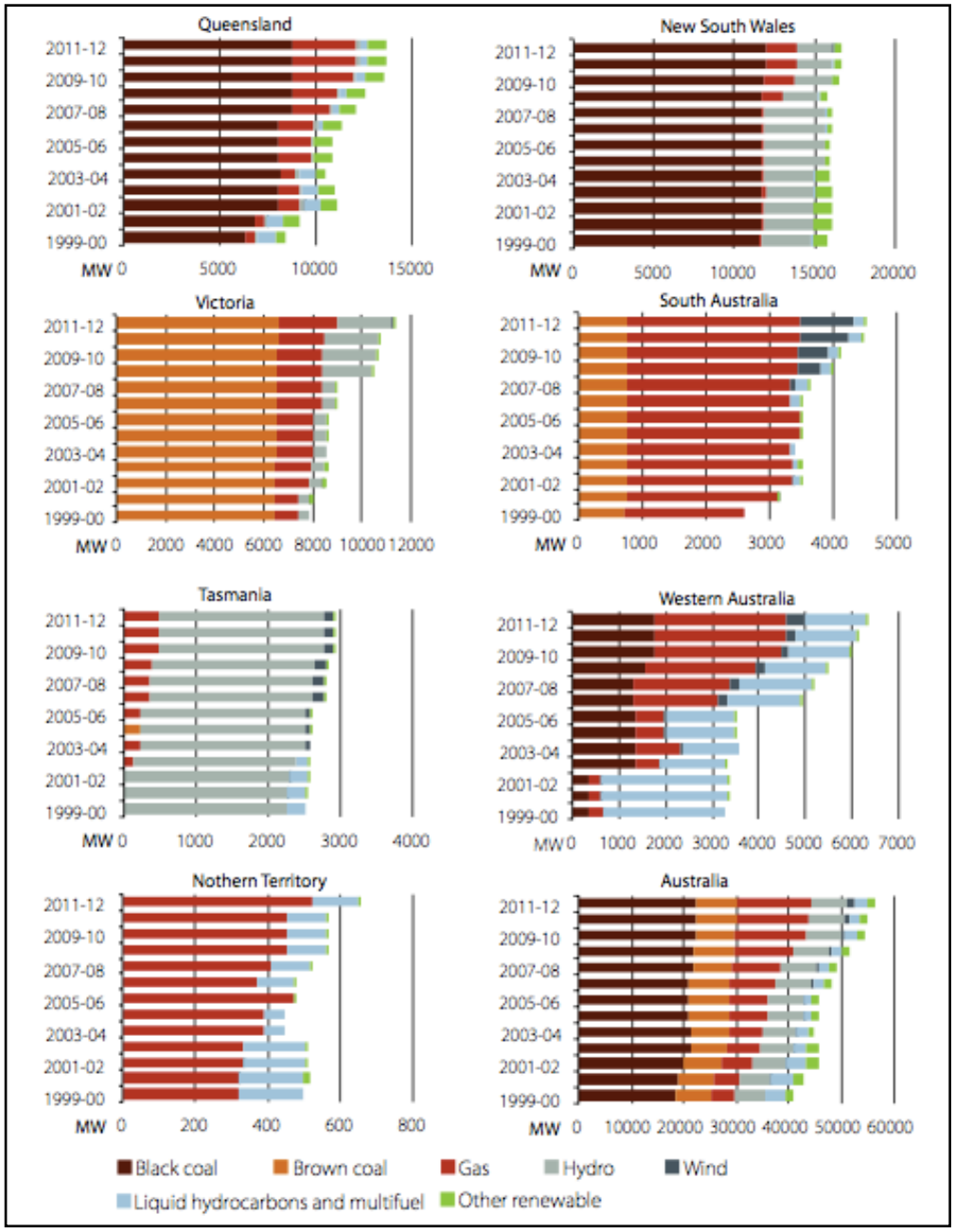

Figure 1. 5: Color-coded chart of Australia Electric Power Generation Profile

Figure 1.5 presents a summary of Australia's electrical power generation profile, and shows that each state has its own unique mode of using natural and non-renewable sources to produce energy. Queensland and New South Wales produce black coal whereas Victoria depends mostly on brown coal, with South Australia largely deriving energy from gas. Natural energy sources like wind and roof top solar power sources were producing almost

one third of the energy for South Australia. Tasmania relies heavily on hydro sources for energy while NT depend on gas and WA derives energy from both coal and gas. The NSW grid supplies the electricity to the ACT, but interestingly this territory plans to source 90 per cent of its electricity needs from renewables by 2020.

The ever increasing electrical energy consumption worldwide has led to rapid depletion of fossil fuel resources and severe environmental impacts. Indeed, each stage in the exploration, extraction, processing, transportation and consumption of fossil fuels has significant impacts and suspected risks for humans and ecosystems. For example, energy generation from fossil fuel involves combustion that releases toxic and carcinogenic gases into the atmosphere. Some of these emissions, also known as greenhouse gases, may be contributing to the earth's climate change.

Realizing the impacts of this energy consumption in exacerbating global warming, international efforts have been initiated by introducing the Kyoto protocol in 1997, which gathered international agreement on reduction of greenhouse gas emissions by 5.2% of the 1990 level. The Kyoto protocol expired in 2012, and the Copenhagen Climate Conference was held in 2009 to discuss efforts in addressing global warming issues. The report drafted by the United States, China, India, Brazil and South Africa on 18 December, The document recognised that climate change is one of the greatest challenges of the present day and that actions should be taken to keep any temperature increases to below 2 °C [24].

Many people believe that oil dependence for electricity generation must be reduced and carbon dioxide emissions from fossil fuel burning must be curbed to address climate change and fossil fuel depletion concerns. However, very few of them realize that fossil fuel electrical energy generation technologies can be modified or improved at relatively low incremental costs to help address these concerns. With the conventional technologies of electrical energy generation being so widely applied over past decades, it will require a long period of time to totally switch from the existing old style power plants to modern ways of generating electrical energy. During this transition period, new technologies such as high efficiency fossil fuel generators have important roles in decelerating the fossil fuel consumption of electrical energy generation. As for the reduction of greenhouse gas emissions, a carbon capture and storage procedure is one of the vital solutions that can tackle this emission problem.

In some well-developed nations, local authorities are driven to opt for alternative energy deployment that is environmentally benign to meet their fast growing energy demand. Enthusiasm for nuclear power is intense due to its low-carbon output in the energy generation process. However, historical records of nuclear reactor accidents at Three Mile Island in the U.S (1979), Chernobyl in the U.S.S.R (1986) and the latest Fukushima nuclear disaster in Japan (2011) have raised global public awareness regarding the safety of nuclear plants for commercial use.

Despite being environmentally benign, these renewable energies have stochastic characteristics due to the varying climate conditions. This explains why renewable-based power generation requires complex design, planning and control optimization methods. On the other hand, fossil fuel energy generation technologies that have long been applied for steady power supply will remain cheaper than the non-conventional renewable energy generation technologies for the coming decades. During the course of developing renewable energy technologies and making nuclear power safer and more appealing, fossil fuels remain important in electricity generation. Comparisons between the diesel generator-only power systems and renewable energy generator-only power systems are summarized in Table 1.1.

Table 1.1: Comparison between diesel-only and renewable energy-only systems

	Diesel generator-only	Renewable energy generator-only
Pros	• Low capital costs • Reliable • Easy to obtain, market available • Easy to operate • Energy storage not required	• Use FREE renewable resources • Environmentally friendly • Low maintenance
Cons	• Fluctuating fuel price • Spew pollution • Regular maintenance • Minimal loading operation restriction • Machine sized to supply peak load	• High capital costs • Fluctuation of renewable resources. • Low system efficiency • Battery replacement & recycling problems • Complex supervisory control

With all of the pros and cons of both electrical energy generation practices taken into account, renewable energy generators are usually installed to augment the grid power supply, thus forming a grid-connected hybrid power system. The renewable energy generators can also be operated along with batteries and diesel generators in stand-alone mode to form off-grid hybrid power systems, with their operation monitored and controlled by a supervisory controller.

1.2 Thesis Overview

The research presented in this thesis has investigated, studied and tested prototype off-grid hybrid power systems, and modelled isolated utility scale integration of one hundred percentage renewable energy with reduced battery bank storage. This power generation combination depends entirely on control systems which have been investigated in this thesis and explained in detail in chapter six and seven. This control system is the heart of the hybrid power system, which has the capability to decentralise an existing centralised utility network and monitor the load and energy source. This leads the control system to regulate the energy source by providing priority for renewable energy. To get optimum output an entirely new class of variable speed generators, High MPPT tracking systems and advanced VRLA batteries have been integrated with the solar energy.

This technology allows the continuous management of variability and shifting of energy, crucial for both the stand alone system and the large scale integration of renewables. Indeed, the Variable speed generator integrated system has already been successfully implemented in two projects, demonstrating the endurance and longevity of this system to manage the ramp rate of renewable energy and to shift renewables output. The superior performance of these systems has the potential to reduce the cost of each MWh of storage used to control renewable energy variability.

The main areas of power electronics, solar energy concepts and diesel generator theory with a basic premises of these areas and the key equations is used. The various energy generation sources around the world and the hybridising of these sources through the technology of power electronics are further investigated. Although fossil fuels are currently the main source of energy there is a global trend towards the use of renewable resources. Various methods used to extract maximum power from solar sources with new advanced battery technology are also analysed.

The simulation of variable speed diesel generator is done in Matlab/Simulink. A Matlab programme was also developed to size components and perform simulations of a system with a variable speed generator. A PSpice/ HOMER model was used to allow comparison of the new hybrid system with the traditional interconnection topologies. Experimental results from an ongoing project are presented and analysed. Focus is given to a novel energy management system and frequency shift control which are used to limit the distributed renewable sources and allow the addition of a variable speed generator and solar panels to a project commissioned five years ago.

Methods to integrate solar and advanced battery technology and a variable speed generator into new or existing conventional power plants are also studied/analysed. Generator loading characteristics are included to allow a comprehensive approach to the controller methodology for any such power station. The common and split bus topologies are presented as methods to integrate central inverter systems with battery storage into conventional generation plants.

1.3 Research Objectives

The main objective of this research is to obtain a solution for power management of various off-grid hybrid power systems and utility scale integration of one hundred percentage renewable energy with reduced battery bank storage.

An innovative predictive method is incorporated into the power management strategy for such system configuration. The aims of the power management strategy are to:

- Balance power production and consumption;
- Directly utilise renewable power;
- Decentralise the utility network;
- Decrease fuel consumption and greenhouse gas emission;
- Decrease diesel generator start-up cycles;
- Equalise the diesel generator accumulated operation time.

The research presented in this thesis strives to provide a framework for future off-grid and edge-of-grid electricity generation systems. Four main objectives were defined:

- To develop power electronics and control topologies for stable on-grid and off-grid renewable energy generation systems.
- To maximize the use of renewable energy sources in electric power systems.
- To increase overall hybrid system efficiencies.
- To decrease the dependence on fossil fuel based energy sources, and as a direct consequence, reduce carbon dioxide emissions.

1.4 Identification of Original Contributions

The original contributions of this thesis are:

- Development of the hybrid power system component sizing and operation control programs using Matlab functions (Chapter 6 to 7)
- Economic analyses of various hybrid power systems (Chapter 5 to 7)
- Estimation of load demand scenario (Chapter 5)
- Development of logistical models for hybrid power system components using *Simulink* (Chapter 6 and 7)
- Development of the predictive and adaptive dispatch strategies (Chapter 7)
- Simulation and performance studies of the utility scale renewable energy integrated power system with various dispatch methods (Chapter 7)

1.5 Thesis Structure

This thesis is divided into eight chapters -

Chapter one, the introductory chapter, gives the justifications for the research and the framework in which the work will be presented. The background theory and literature review of the areas of power electronics, solar energy concepts and diesel generator theory is contained in this chapter. The basic premises of these areas and the key equations used throughout the rest of the work are also defined in chapter one.

Chapter two, discusses the key energy generation sources around the world and the hybridising of these sources through the technology of power electronics. Sources from which energy can be derived include well known sources such as coal, diesel, gas, wind,

solar, hydro and oil, as well as other less known sources such as biodiesel, biofuel, tidal, nuclear, and geothermal. Although fossil fuels are currently the main source of energy there is a global trend towards the use of renewable resources. Chapter two also goes through the energy sources of major countries and their policy on renewable energy.

Chapter three, presents the methods used to extract maximum power from solar sources, introduces new advanced battery technology developed by CSRIO, and the DC variable speed diesel generator. The theory of advanced MPPT is explained, derived and simulated. In order to allow accurate analysis of solar MPPT, an accurate mathematical model was developed based upon the Newton-Raphson algorithm.

Chapter four, explains the mathematical modelling and control of variable speed diesel generator. The steady state and dynamic models of VSDG in both in grid connected and stand-alone operation mode were created. The diesel engine modelling is also built up. The simulation of variable speed diesel generator is done in Matlab/Simulink. A Matlab programme was also developed to size components and perform simulations of a system with a variable speed generator.

Chapter five, introduces the new complementary hybrid system and compares this with other traditional interconnection topologies. A PSpice/ HOMER model is developed to allow comparison of the systems. Matlab and HOMER are used to create a mathematical model that can approximate the energy yield from each of the systems based upon a location. The concept of crossover loss for the complementary system is defined and calculated for differing solar sources. Experimental results from the Veterans project are presented and analysed. Finally, other locations are selected and the most ideal hybrid system topology is defined for each one.

Chapter six, presents the design, simulation and implementation of the Broome Eco Resort expansion project. This project was commissioned in April 2009 and has been operating successfully for five years. The design methodology presented in Chapters three and four is applied, with a special focus on the systems controller. A novel energy management system and frequency shift control are used to limit the distributed renewable sources and to allow the addition of a variable speed generator and solar panels. PSpice, Matlab and HOMER are used to simulate this controller, which is based upon the load, renewable energy available and battery SOC. The four modes of systems inverter operation are also outlined in chapter six.

Chapter seven, presents methods to integrate solar and advanced battery technology and a variable speed generator into new or existing conventional power plants. The Western Australian country town, Carnarvon, was selected for this case study. The centralised and distributed concepts are explained with methods to control and increase the renewable energy penetration levels. Eight design points are encapsulated into a generalised design methodology for any medium to large scale renewable based power system. Generator loading characteristics are included to allow a comprehensive approach to the controller methodology for any such power station. The common and split bus topologies are presented as methods to integrate central inverter systems with battery storage into conventional generation plants.

Chapter eight, sums up the work and findings of the author through this thesis. It gives in brief an outline of the results achieved and studied through the various projects carried out using hybrid gen. The purpose and the objective of the thesis has been summarised in this chapter.

1.6 References

[1] International Energy Agency, "World Energy Investment Outlook," 2014.

[2] D. Berkowitz and A. Squires. (2003, 20/05/2014). *Fossil Fuer Power (1 ed.)*.

[3] A. G. Bakirtzis and E. S. Gavanidou, "Optimum operation of a small autonomous system with unconventional energy sources," *Electric Power Systems Research,* vol. 23, pp. 93-102, 3// 1992.

[4] BP, "Energy Outlook 2035 Shows Global Energy Demand Growth Slowing," ed, 2014.

[5] M. Gaetani, T. Huld, E. Vignati, F. Monforti-Ferrario, A. Dosio, and F. Raes, "The near future availability of photovoltaic energy in Europe and Africa in climate-aerosol modeling experiments," *Renewable and Sustainable Energy Reviews,* vol. 38, pp. 706-716, 10// 2014.

[6] M. T. Islam, S. A. Shahir, T. M. I. Uddin, and A. Z. A. Saifullah, "Current energy scenario and future prospect of renewable energy in Bangladesh," *Renewable and Sustainable Energy Reviews,* vol. 39, pp. 1074-1088, 11// 2014.

[7] A. B. A. Boxall, "Global Climate Change and Environmental Toxicology," in *Encyclopedia of Toxicology (Third Edition)*, P. Wexler, Ed., ed Oxford: Academic Press, 2014, pp. 736-740.

[8] S. Marcott, "A reconstruction of regional and global temperature for the past 11,300 years " *Science* vol. 339 no. 6124 pp.1198-1201, 2013.

[9] World Widelife Fund and Office for Metropolitan Architecture, "The Energy Report 100% Renewable Energy By 2050," 2011.

[10] B. Lin and M. Moubarak, "Renewable energy consumption – Economic growth nexus for China," *Renewable and Sustainable Energy Reviews,* vol. 40, pp. 111-117, 12// 2014.

[11] M. Ozcan, "Assessment of renewable energy incentive system from investors' perspective," *Renewable Energy,* vol. 71, pp. 425-432, 11// 2014.

[12] J. Paska and T. Surma, "Electricity generation from renewable energy sources in Poland," *Renewable Energy,* vol. 71, pp. 286-294, 11// 2014.

[13] Bates, B. C, Z. W. Kundzewicz, S. Wu, and J. P. Palutikof, "Climate Change and Water. Technical Paper of the Intergovernmental Panel on Climate Change," IPCC, Geneva2008.

[14] K. S. Reddy, M. Kumar, T. K. Mallick, H. Sharon, and S. Lokeswaran, "A review of Integration, Control, Communication and Metering (ICCM) of renewable energy based smart grid," *Renewable and Sustainable Energy Reviews,* vol. 38, pp. 180-192, 10// 2014.

[15] L. Wilson. Climate Science for Beginners [Online]. Available: http://shrinkthatfootprint.com/climate-science-beginners

[16] M. E. Bildirici and T. Bakirtas, "The relationship among oil, natural gas and coal consumption and economic growth in BRICTS (Brazil, Russian, India, China, Turkey and South Africa) countries," *Energy,* vol. 65, pp. 134-144, 2/1/ 2014.

[17] A. P. Brunger and F. C. Hooper, "Anisotropic sky radiance model based on narrow field of view measurements of shortwave radiance," *Solar Energy,* vol. 51, pp. 53-64, 7// 1993.

[18] L.-G. Giraudet, C. Guivarch, and P. Quirion, "Exploring the potential for energy conservation in French households through hybrid modeling," *Energy Economics*, vol. 34, pp. 426-445, 3// 2012.
[19] A. T. Mohammad, S. B. Mat, M. Y. Sulaiman, K. Sopian, and A. A. Al-abidi, "Artificial neural network analysis of liquid desiccant regenerator performance in a solar hybrid air-conditioning system," *Sustainable Energy Technologies and Assessments*, vol. 4, pp. 11-19, 12// 2013.
[20] J. Park, I. Hung, Z. Gan, O. J. Rojas, K. H. Lim, and S. Park, "Activated carbon from biochar: Influence of its physicochemical properties on the sorption characteristics of phenanthrene," *Bioresource Technology*, vol. 149, pp. 383-389, 12// 2013.
[21] A. M. Schneider, "Elasticity of demand for gasoline since the 1973 oil embargo," *Energy*, vol. 2, pp. 45-52, 3// 1977.
[22] Y.-H. Shih and C.-H. Tseng, "Cost-benefit analysis of sustainable energy development using life-cycle co-benefits assessment and the system dynamics approach," *Applied Energy*, vol. 119, pp. 57-66, 4/15/ 2014.
[23] H. Song, R. Zhang, Y. Zhang, F. Xia, and Q. Miao, "Energy Consumption Combination Forecast of Hebei Province Based on the IOWA Operator," *Energy Procedia*, vol. 5, pp. 2224-2229, // 2011.
[24] Kyoto Protocol. (2009). *2009 United Nations Climate Change Conference*. Available: http://en.wikipedia.org/wiki/Kyoto_Protocol

Chapter 2

2. Renewable Energy System Components and Various Integration Technologies

2.1 Introduction

Every fifth person in the world lacks access to electric power while more than three billion people depend on wood, coal or animal waste for cooking. According to an IPCC report the direct carbon dioxide emission in 2010 from the energy supply sector is projected to double by 2050 [1]. Renewable resources such as solar power and modern forms of energy are becoming increasingly important with the growing concerns about the future and security of the world's energy supply. Even though various solar energy technologies have been used through millennia of human history, photovoltaic study and the resulting industry and the direct conversion of solar energy into electricity has a very short history of only about 50 years. Photovoltaic systems use wafers, such as crystalline silicon and thin film, which are sensitive to sunlight and produce a small direct current when exposed to sunlight.

Electricity supplied by a PV system displaces electricity from other power-generating technology. If the alternative is very expensive, such as a utility connection to a remote location, then the PV system may save the consumer a substantial amount of money. Furthermore, other advantages and benefits of PV systems add value beyond the potential financial savings. Photovoltaic is an environmentally friendly technology that produces energy with no noise or pollution. In addition, PV systems can be adapted to many different applications, are extremely reliable and require minimal maintenance for a long initial time period. PV users have an energy source that is completely independent, one that utilizes sunlight, a free and readily available resource.

There are some disadvantages which have limited the use of PV systems. The most significant issue is the high initial cost of a PV system compared to the price of competing power generating technologies [2]. PV systems also require a relatively large array area to produce a significant amount of power. Lack of community awareness about the potential of photovoltaic, retailer ignorance about the availability of different systems, limited infrastructure, the limited availability of qualified installers or problematic installation due to technician inexperience or the limited knowledge of PV system requirements of local energy utility staff, are additional factors that continue to affect the use of PV systems.

Although PV technology has been developing for more than 160 years it has only progressed exponentially in the last decade. The first true PV cells were developed by American inventor Charles Fritts in 1883 [3]. He covered a selenium wafer with transparent gold film, which produced a tiny current. The first cells had efficiencies of up to 6%, unimpressive by today's standards. PV cells were ideal power generators for satellites and spacecraft because of the complexity of supplying power by other means and the abundant solar resource available outside Earth's atmosphere [4]. Cells were first developed for the Vanguard I satellite in 1958 and have been used on nearly every spacecraft and satellite since.

2.2 PV Applications

The earliest applications of PV systems were in situations where connections to the utility grid were unavailable or cost prohibitive. Today, PV systems can be used in almost any application where electricity is needed and can support DC loads, AC loads, or both [5]. Space applications are extreme examples of off-grid remoteness, in that there is no possible way to connect satellites and spacecraft to a steady source of terrestrial electricity. Solar radiation outside the Earth's atmosphere is even greater than that on the ground. Satellites were the first practical applications of PV technology and did much to increase the public's knowledge of PV systems. Space bound PV systems are designed for high efficiency and low weight, with cost being less important. Portable PV systems power mobile loads such as vehicles, handheld electronic devices and temporary signs and lighting [6]. Small PV systems with batteries can be added to the signs to power them continuously [7]. Temporary lighting for short-term projects or night time construction work may be PV powered because the short duration of the project may not warrant the time or expense of connecting to utility power. Most portable PV systems are relatively small and can power only modest loads. The systems should be relatively light for ease of transportation. Recreational vehicles and boats can benefit greatly from PV systems [8]. Portable power units can also be brought in to supply critical services during emergency conditions.

The photovoltaic system is an ideal choice for remote areas. Off-grid residences utilize other sources of energy such as wind turbines or engine generators-to supplement or back up the PV system. PV systems can be used for remote lighting applications in communications stations at higher elevations, to power communication signals from emergency call boxes and

electronic information signs. Small PV systems can provide power for remote signage and signal devices. They can also be used as a power source for remote station monitoring and for transmitting meteorological, seismic, structural or other data. PV powered water pumping is also used to provide water for campgrounds, irrigation, and remote village water supplies.

Systems that are connected to the utility grid and use PV energy as a supplemental source of power offer the greatest flexibility in possible system configurations. PV systems can be used to provide supplemental power to any utility connected building or structure including residences, commercial buildings, factories and institutions.

2.3 Solar Energy Technologies

Apart from Photovoltaic there are many other technologies that utilize solar energy. A solar energy collector absorbs solar radiation and converts it to another form, usually heat or electricity. Solar thermal energy systems convert solar radiation into heat energy. Working fluids are heated by the sun in a solar collector and then distributed to a reservoir to store the heat energy. Solar cookers use energy from the sun to heat food or beverages [9].

2.3.1 The sun and its energy

The sun is a gaseous body composed mostly of hydrogen, with some helium and traces of heavier elements. The sun fuses hydrogen into helium at its core and the resulting energy radiates outward. The energy escapes into space in the form of visible light and other radiation. A relatively tiny fraction of the sun's total output, approximately 170 million GW, reaches the earth, but this amount is millions of times greater than the maximum power demand of Earth's entire population. Various factors affect the quantity and composition of the solar energy that reaches the Earth's surface and that can be harnessed by PV devices. Solar irradiance is the power of solar radiation per unit area and it is expressed in units of watts per square meter or kilowatts per square meter [10].

Solar irradiation quantifies the amount of energy received on a surface over time, and is the principal data needed for sizing and estimating the performance of PV systems. The

magnitude of solar irradiance changes throughout the day. Solar irradiance equals the area under the irradiance curve [2].

It can be calculated by applying the formula; H= E x t, where H = solar irradiation,

E= average solar irradiance and t = time.

Almost all of the energy received from the sun is electromagnetic radiation. Solar radiation includes more types of energy than just visible light. Solar radiation is absorbed, scattered, and reflected by components of the atmosphere, including ozone, carbon dioxide and water vapour as well as other gases and particles. The two major types of radiation reaching the ground are direct radiation and diffuse radiation [11]. Direct radiation is solar radiation directly from the sun that reaches Earth's surface without scattering. Diffuse radiation is solar radiation that is scattered by the atmosphere and clouds. Typical flat plate PV arrays utilize both the direct and diffuse components of the total radiation reaching the array surface, while concentrating collectors can utilize only the direct radiation component.

One third of the total solar irradiance is either reflected from clouds back into space or scattered and absorbed by the atmosphere, and the remaining two-thirds reaches the surface of Earth. Since the electrical power output of PV modules is rated at peak sun condition, knowing the number of peak sun hours on a given surface at a given location is used to estimate PV system performance. Peak sun is an estimate of maximum terrestrial solar irradiance around solar noon at sea level and has a generally accepted value of 1000 W/m^2 [12].

To optimize performance and minimize shading from obstructions sun path is important. Sun position and sun path at any given time or location on earth can be calculated and the application of this information for each location allows solar collector orientation to maximize energy collection.

2.3.2 Sun position

Two angles are used to define the sun's position, relative to an observer on Earth. Solar radiation data indicates how much solar energy strikes a surface at a particular location on Earth during a particular period of time. PV systems produce electrical energy in direct proportion to the amount of solar energy received on the surface of the array [13].

2.4 System Components and Configurations

Renewable energy can be integrated into grid connected systems and standalone off grid systems. For maximum benefit, the system must be optimized. In this thesis the integration of solar PV systems into both the existing grid utility and with a stand-alone off grid system has been explored. Other renewable energy resource integration was not part of this study [13].

The major solar components required for renewable energy integrated systems are described below-

2.4.1 Modules and Arrays

A basic explanation of the operation of PV module technology is required before any discussion of PV array shading and harvest optimization. This section reviews the characteristic electrical behaviour of a PV module. To illustrate the key concepts we first start with the PV cell, then combine PV cells to form sub-module sections and finally show the electrical behaviour of a complete PV module. It should be noted that the following discussion applies specifically to market-leading crystalline silicon PV technology. Other PV technologies may vary slightly in their behaviour [13].

$$I = Isc' - I_o \left(e^{\frac{q(V+I\times R_S)}{kT}} - 1 \right) - \left(\frac{V + I \times Rs}{Rsh} \right)$$

Where,

Isc' is the light-generated current (short-circuit value assuming no series/shunt resistance)

I_o is the dark saturation current

q is the charge of an electron (coul)

k is Boltzmen constant (j/K)

T is the cell temperature (K)

I, V, Rs, Rsh are cell current (A), Voltage (V), series and shunt resistance as indiacted in below figure 2.1.

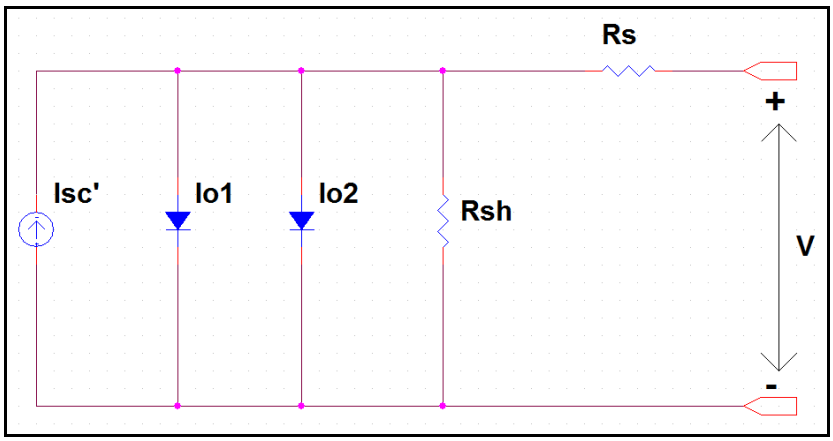

Figure 2. 1: PV cell equivalent circuit model

The PV cell is the central building block of larger PV arrays ranging from a few watts to hundreds of megawatts. The electrical characteristics of a PV cell can be approximated by the simplified electrical model of figure 2.2. The equation presented defines the key relationship between PV cell voltage (V) and current (I). This I-V relationship is the basis of all issues related to harvest efficiency [14]. The relationship between cell voltage (V) and cell power (P) can also be illustrated by plotting the relationship of V and I x V = thus creating the I- P curve. The I-P curve clearly shows a singular maximum power peak of a PV occurring at what we can define as the maximum power operating voltage, Vmp.

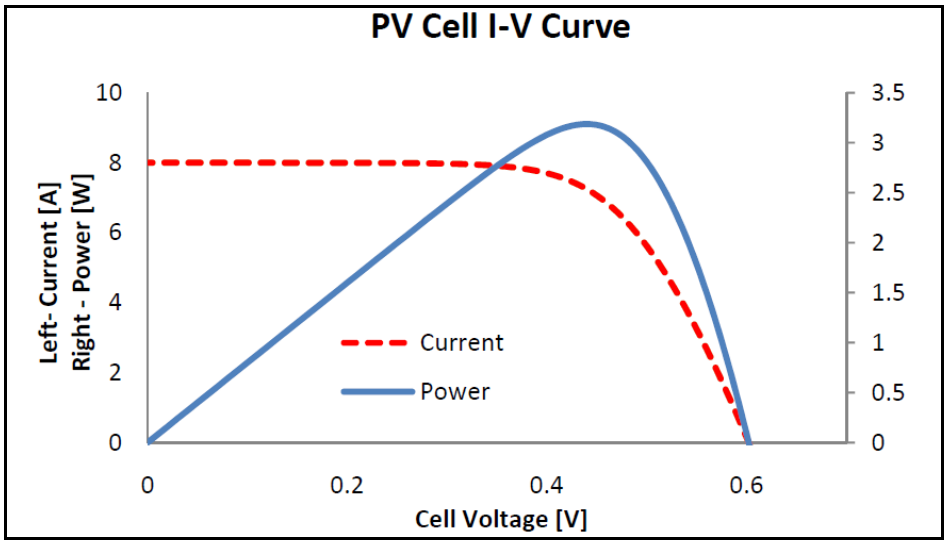

Figure 2. 2: The PV Cell I-V Curve [15]

Achieving 100% PV array harvest efficiency is solved, ideally, by ensuring that each PV cell operates continuously at its maximum power-generating voltage.

2.4.2 Series Cell Module Section with Bypass Diode

Generating electrical power at approximately 0.5V is not very practical. In order to generate useful voltages, cells are connected together in series. However, series cells introduce a new problem of imposing significant voltage across a cell with less ability to generate current. If series cells form a circuit and one cell is shaded (the current source of figure 2 is reduced) then the series voltage of the remaining cells can appear across the shaded cell. Depending on the voltage this may cause destructive heating in the shunt resistance, Rsh, of the cell. To solve this problem, bypass diodes are installed across a limited number of series cells to control the maximum voltage and thermal damage to a shaded cell. We will see later that bypass diodes also play a critical role in allowing shade-tolerant operation of partially shaded PV modules and PV arrays [16].

Figure 3.3 illustrates the relationship between 20 series cells (a common number) and a bypass diode. The voltages of the cells add together and create the same I-V shape as figure 3 only at 20 times the voltage. The other defining characteristic of the module section is the effect of an approximately 0.4V Schottky bypass diode on the I-V curve relationship. The bypass diode prevents any significant reverse voltage from appearing across the module section and also limits the reverse voltage seen by any shaded cell within the section. The bypass diode allows for maximum array currents to be shunted by a shaded module section(s) thus creating the multi-maxima I-P curves characteristic of partial PV module and PV array shading.

A complete PV module is comprised of a number of module sections connected in series. A common wiring configuration is for module sections to be long or “portrait” pairs of cells. This has to do with the electrical interconnections on each cell requiring a linear layout and where right angle corner- turning connections are located at the top and bottom of the module [17].

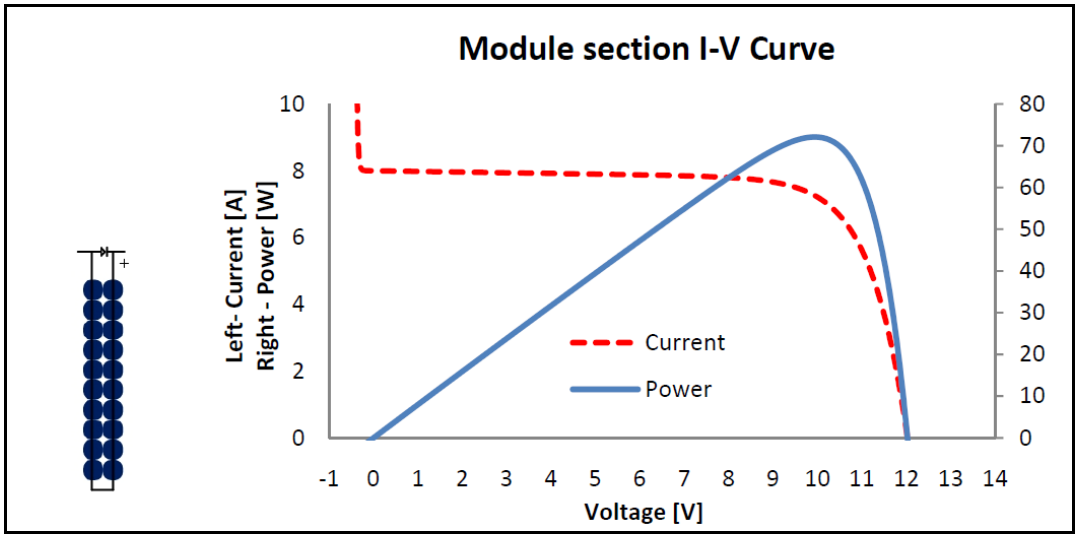

Figure 2. 3: Module Section I-V curve with bypass diode [15].

In this example the I-V curve is now 60 times the voltage of the PV cell and requires 0.4V x 3 volts to forward bias the three series bypass diodes. The I-V curve has the same overall shape and qualities as the individual PV cell plus the added behaviour of the thee bypass diodes.

All PV modules will include the following four data points at the standard test conditions (STC: G = 1000W/m^2, module temp, T = 25C): Short Circuit Current (Isc), Open circuit voltage (Voc), Max Power Voltage (Vmp), and Max Power Current (Imp) [18].

Manufacturers tend not to provide information regarding the placement of bypass diodes within their modules. The characteristic I-V curve of any PV cell is influenced by two main external factors; solar irradiance and cell temperature. The PV cell current source, IL, of the equation within figure 2 is directly proportional to the solar irradiance, G, to which the cell is exposed. The value of IL varies with the position/angle of the sun, clouds passing, dirt, and shade. The effect of varying IL has on the I-V curve, figure 5 showing the PV cell equation of figure 2.3 to represent a consistently solar irradiated Sunpower 250W 90 60 cell solar panel.

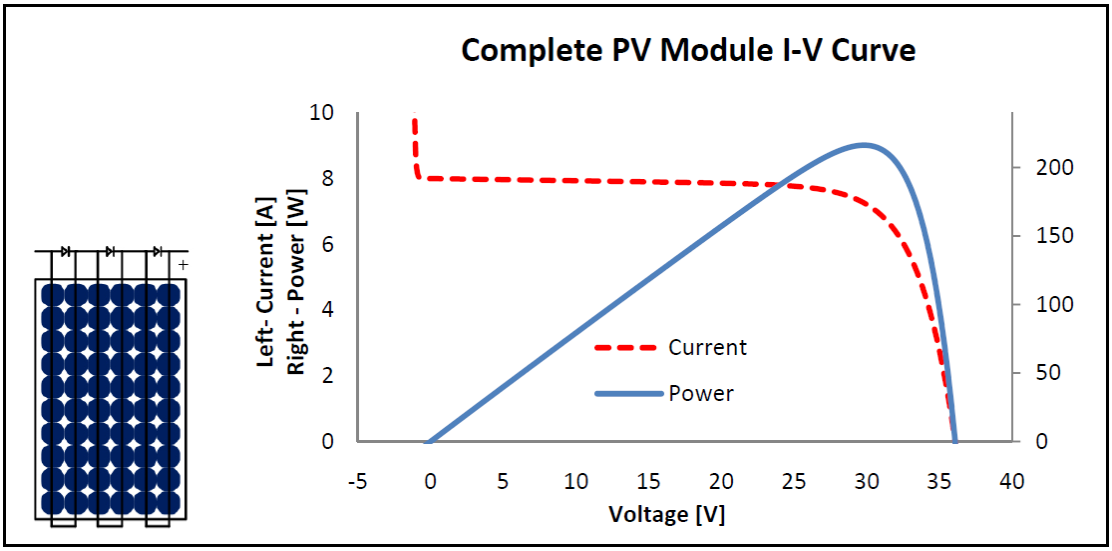

Figure 2. 4: PV Module Curve with Bypass Diodes. IV Curve Behaviour [15]

The top I-V (blue) curve shows the module characteristics at STC and the bottom I-V curve (red) shows module characteristics when solar irradiance has been reduced to 15% of STC. It is clear that the maximum power voltage moves slightly to the left as the irradiance is reduced. In order to harvest maximum power from the PV module during normal changes in irradiance, one has to insure a method of strategically controlling the PV voltage accordingly in real time. Temperature also has a significant influence on the I-V curve of a PV cell. For crystalline silicon Isc varies by about -0.05% per deg C temperature rise and Voc is more sensitive varying by about -0.3% per deg C rise. The effects of varying temperature are shown in figure 2.5.

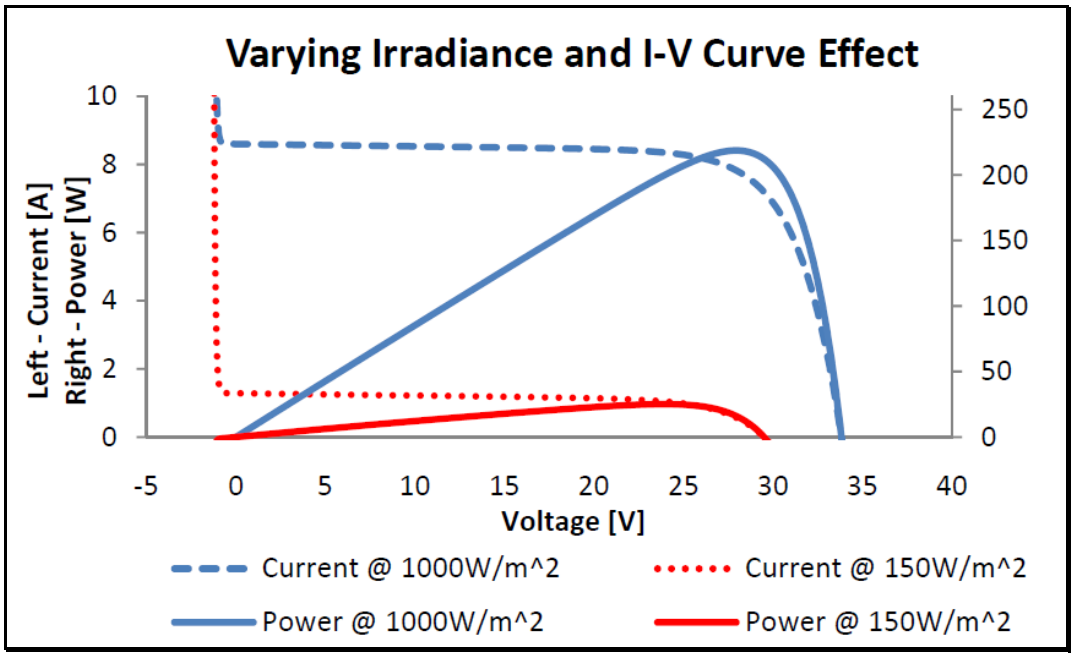

Figure 2. 5: Irradiance and I-V Curve Characteristics [15].

When designing PV arrays one has to ensure that the worst-case cold Voc doesn't exceed the max input voltage rating of the PV inverter, and that the worst- case warm module temperature results in a Vmp that is within the MPPT operating voltage window of the inverter. Cooler cells produce higher voltages, notably Voc, and can produce more power output than warmer cells. The I-V curve effectively compresses to the left for warmer cells and stretches to the right for cooler cells. Figures 2.5 and 2.6 show how Vmp varies with irradiance and temperature [19]. Interestingly, when the sun comes out and the irradiance increases, pushing the I-V curve right, the cell temperature increase seconds afterwards, pushing it back left.

2.4.3 PV Harvest Efficiency by Active Maximum Power Point Tracking

Achieving 100% harvest efficiency requires the PV inverter to continuously harvest energy from the PV cells at their Vmp. For a homogenously irradiated PV module or array of identical cells this requires the inverter to operate continuously at the PV voltage that produces the characteristic singular maximum power "bump".

Since Vmp is dynamic, the inverter must incorporate a maximum power tracking system that has the ability to search for the maximum power point. Historically, these control technologies assumed that the challenge was to find the characteristic max power bump in figures A2-A6 and operate at the peak power. The challenge would be simple if the I-V curve was static, but the I-V curve is dynamic. In order to notice movement in the Vmp, the control system must be constantly checking to see if and where the Vmp is moving [20]. The only way it can do this is to move away from where it is currently operating to see what's happening elsewhere – thus it's theoretically impossible to achieve 100% harvest efficiency.

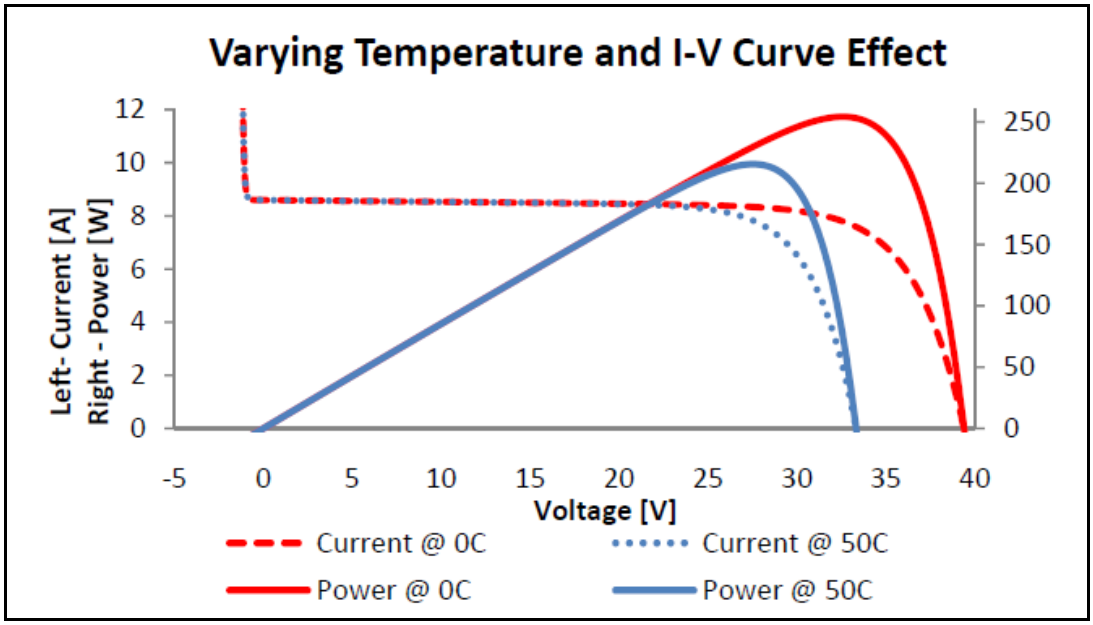

Figure 2. 6: Temperature and I-V Characteristics [15].

2.4.4 Any MPPT control system has two main challenges:

1. The MPPT control strategy needs good static efficiency for slowly varying arrays. This can be achieved by a slow MPPT tracking approach that finds the Vmp and stays there without moving too much away from Vmp [21].

2. The MPPT control strategy needs to have good dynamic efficiency for quickly varying arrays. This can be achieved by a fast MPPT approach that can quickly find the new Vmp. This requires more searching and will compromise static efficiency.

Any real array will therefore need an appropriate balance of dynamic and static efficiency.

The only way to evaluate static and dynamic MPPT efficiency is to operate the MPPT controller on accepted reference I-V curves where the theoretical Vmp is known. A static efficiency test performed with a static I-V curve provided by a PV simulator is straight-forward. However, the dynamic evaluation depends entirely on the selected I-V dynamics modelled, thus requiring a defined reference set of data for comparative tests to be meaningful [22].

Unfortunately, standardized MPPT efficiency tests are not yet established. Some evolving approaches simply vary the irradiance over time, as shown in figure 3.6. Other approaches involve using reference profiles of I-V curve data based on measured data from real PV array measurements thus accounting for cloud, weather and temperature dynamics [23]. An example of this is the ISORIP test profile from the Austrian Institute of Technology. There is currently no definitive standard for evaluating MPPT efficiency. That being said, MPPT efficiency should be in the 99%+ range regardless of the testing method.

There is currently no established method to evaluate the MPPT harvest efficiency for PV inverters operating on partially shaded or non-homogenously irradiated PV arrays [24].

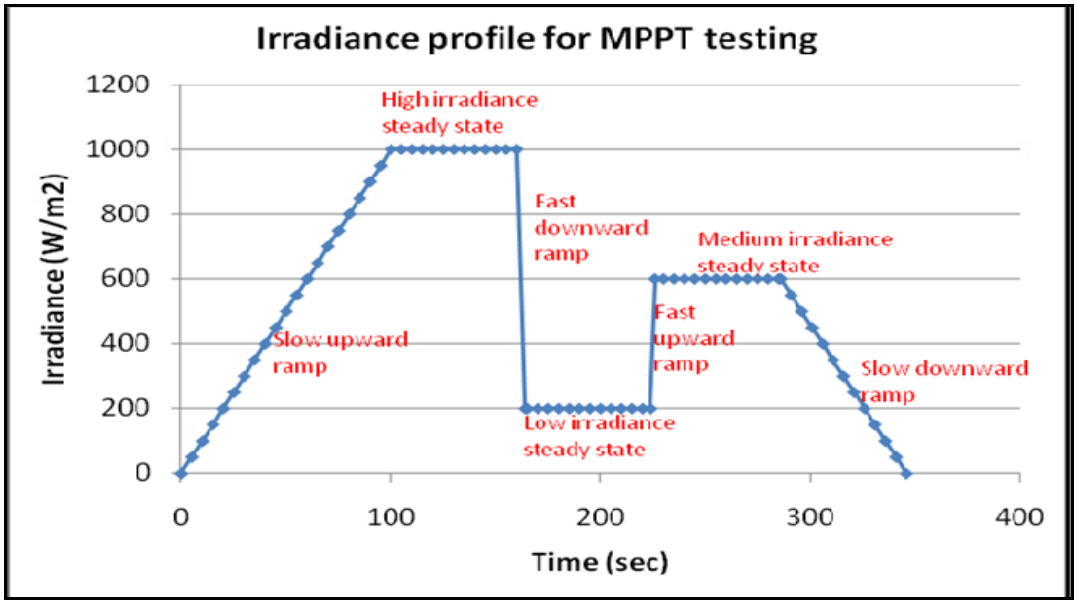

Figure 2. 7: Sample Homogeneously Irradiated PV Array Irradiance Profile [15].

2.5 Batteries

Battery life depends on many design and operational factors, including composition, operating temperatures, cycle frequency, depth of discharges, average state of charge, and charging method. Battery life is expressed in terms of cycles or years and is roughly proportional to its average state of charge. Operating temperature has a significant effect on battery life. Higher operating temperatures also accelerate corrosion of the positive plate grids, resulting in greater gassing and electrolyte loss. Lower operating temperatures generally increase battery life, but capacity is significantly reduced, particularly for lead acid batteries [25]. Lead–acid batteries are most common due to their wide availability in many sizes, low cost, and well-understood performance characteristics. Nickel-cadmium batteries are used in low-temperature applications but high initial cost limits their use in most PV systems.

Table 2. 1: Various types of Batteries

Starting, Lightning, and Ignition Batteries.	Allow the battery to deliver high currents for short periods, designed primarily for shallow-discharge cycle service. Not recommended for PV applications because it is not designed for deep discharges. However, SLI batteries are sometimes used for PV systems in developing counties.
Stationary Batteries.	Designed for occasional deep-discharge, limited-cycle service, not recommended for most PV applications.
Flooded-Electrolyte Batteries	Electrolyte in the form of a liquid, classified as either open-vent or sealed-vent types.
Open-Vent Batteries	Allow charging gases to freely escape. A catalytic recombination cap (CRC) is a vent cap that reduces electrolyte loss from an open-vent flooded battery by recombining vented gases into water.
Sealed-Vent Batteries	Contain non-removable caps on the cells that allow only excess charging gases to escape through pressure-relief vents. Excessive overcharge, however, can increase the internal gas pressure to the point of opening the pressure relief vents and releasing gas.
Captive-Electrolyte Batteries	Sealed, include pressure-relief vents, ideal for remote applications where maintenance is infrequent or unavailable, most common types are the gelled electrolyte and absorbed glass mat electrolyte designs.
Lead-Acid Batteries	Deep-cycle characteristics make them ideal for PV applications, but they do not tolerate extreme temperatures well and may require frequent maintenance The electrolyte is a solution of sulphuric acid and water. The most common types of grid alloys for lead acid batteries are lead-antimony, lead-calcium and hybrids.

Hybrid Batteries	Most common type uses lead-calcium positive plate grids and lead-antimony negative plate grids, design combines the advantages of the lead-calcium and lead-antimony designs, including good deep-cycle performance, low water loss, and long life.
Nickel-Cadmium Batteries	Secondary batteries with features that include a long life, low maintenance, excessive discharge tolerance, excellent low temperature capacity retention, and noncritical voltage regulation requirements. Two primary types of Ni-Cd batteries are sintered plate and pocket plate batteries.
Ultrabattery	Entirely new class of lead-acid technology with performance enhancing features and capacity to perform with high efficiency at the Partial State of Charge (PSoC) band, without the deteriorating effects of conventional lead-acid technology. The Ultrabattery combines an asymmetric electrochemical supercapacitor in parallel with a lead-acid battery, a design that improves cycling and power performance.

2.5.1 Battery Classifications

Secondary batteries are classified based on their design and composition. Categories include tract ion, starting, lighting, and ignition (SLI) or stationary batteries. A traction battery which has fewer plates per cell, and is thick and durable, a design that allows repeated deep discharge cycle service, is very common in PV systems.

2.5.2 Ultrabattery [26]

UltraBattery technology is an entirely new class of lead-acid technology that has performance enhancing features and the capacity to perform in high efficiency at the Partial State of Charge (PSoC) band, while mitigating the deteriorating effects of conventional lead-acid technology. The Ultrabattery is a hybrid energy storage device which combines an asymmetric electrochemical supercapacitor in parallel with a lead-acid battery, designed to improve cycling and power performance.

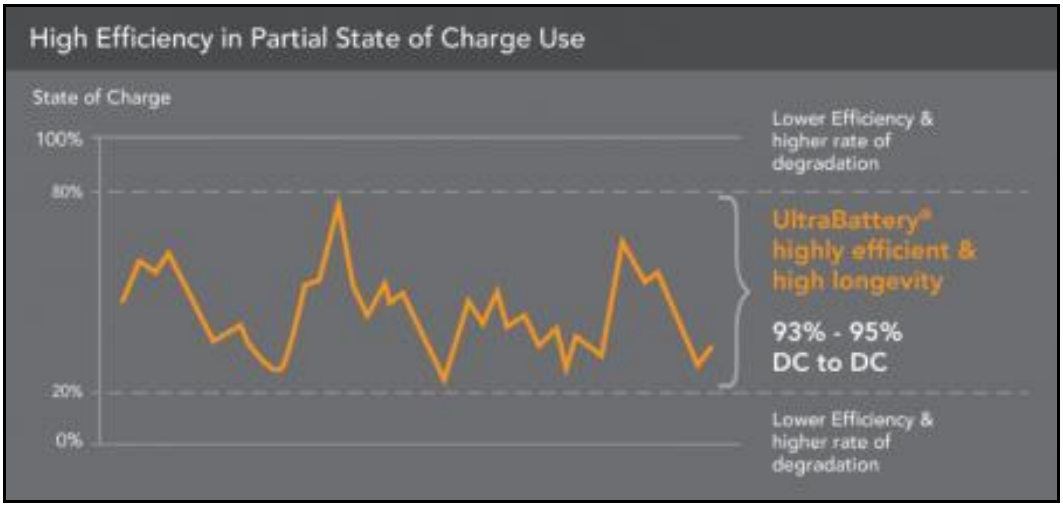

Figure 2. 8: Ultrabattery partial state high efficiency chart [26]

This technology avoids the upper and lower bands of charge in its normal operation, therefore improving efficiency and lasting longer. The Partial State of Charge (PSoC) technology avoids the effects of sulfation and electrolysis.

The ultrabattery has an entirely new set of performance enhancing features such as High Capacity Turnover and High Lifetime Capacity Turnover before Replacement. A higher capacity turnover indicates the battery provides more energy over its lifetime by energy throughput in relation to the capacity of the battery. Because it can be charged and discharged more often than conventional valve regulated lead-acid (VRLA) batteries, it can process much more energy in its lifetime, has a much longer life when used in variable power application, and can be charged and discharged more often over its lifetime than standard lead-acid batteries. In variable power applications, it has been shown in to exceed four or more times the capacity turnover of the competing best-performing conventional VRLA batteries [27].

2.5.2.1 Lower Lifetime Cost Per Kilowatt Hour

In variable power applications where batteries are put through multiple Partial State of Charge cycles per day the ultrabattery has been shown to last many times longer than a conventional VRLA battery. For this reason, and because it needs less frequent replacement

than conventional VRLA batteries, the ultrabattery has a lower lifetime cost per kilowatt hour, high efficiency and higher DC-DC converter efficiency.

A battery's DC-DC efficiency describes the amount of energy put into the battery by charging versus the amount of energy that is discharged by the battery to a load connected to it. During charging and discharging, some of the battery's stored energy is lost as heat, and some is lost to the process of electrolysis. Effectively, the lower the energy losses of a battery, then the more efficient it is [28].

The ultrabattery achieves a typical DC-DC efficiency of 93–95% in contrast to the typical 70% efficiency of VRLA batteries. Due to the reduced energy loss during PSoC operation, more energy is available to supply the load especially when performing variability management applications, such as grid regulation services or renewable ramp rate smoothing at 1C peak power in a Partial State of Charge (PSoC) regime.

2.5.2.2 Lower DC-DC Energy Losses

Conventional VRLA's operating at 80–100% SOC lose about five times more energy to heat and electrolysis than this battery; however DC-DC efficiency of this battery translates to lower DC-DC energy losses [29].

2.5.2.3 Fewer Refresh Cycles

In conventional VRLA batteries refreshing takes place at high voltages for an extended time to dissolve sulphate crystals that have accumulated on the negative electrode. The resulting electrolysis corrodes the positive electrode, thus shortening battery life. The ultrabattery needs refreshing far less often than conventional lead-acid batteries, and therefore lasts much longer.

2.5.2.4 Less Downtime Due to Refresh Cycles

A conventional VRLA battery that takes around 12 hours to refresh every fortnightly has a resulting downtime of 5% and is available for use only 95% of the time. It stays operational for longer than conventional lead-acid batteries, reducing the time spent offline

and increasing its economy. If refreshed once every 60 days, a battery has a downtime of less than 1%, and is therefore available for use 99% of the time.

The ultrabattery can operate in the Partial State of Charge range, and can therefore accept charge much more efficiently than conventional VRLA batteries.

2.5.2.5 Ultrabattery Test Results for Utility Cycling Applications

The Ultrabattery and VRLA battery with an absorbed glass matt (AGM) have been tested using a high-rate-partial-state-of-charge (HRPSoC) cycle profile designed to simulate the ancillary regulation services of a utility and a wind farm energy smoothing application. The test results show that the Ultrabattery cycled in excess of 15,000 HRPSoC cycles with less than 20% capacity loss and was able to cycle at the 4C 1 rate. The VRLA battery using this test procedure could only cycle at the 1C 1 rate, required a recovery charge at about 100 HRPSoC cycles, and at 1,100 HRPSoC cycles lost more than 20% of its capacity. In summary, the Ultrabattery was capable of about 13 times more HRPSoC cycles and more than 10 times the number of cycles between recovery charges compared to the VRLA battery. Based on the manufacturer's 2006 cost projections, the Ultrabattery should cost in the range of $220 for 1 kWh of energy storage [26].

There are a number of high value utility ancillary service applications for energy storage that range from regulation services to peak shaving/load levelling to power quality and improvements in reliability to deferments of new or upgraded T&D infrastructure.

The Ultrabattery is uniquely suited to the above applications because it was designed for HRPSoC cycling. The VRLA battery failure modes of water loss, negative plate sulfation, and grid corrosion are minimized in the Ultrabattery.

2.5.2.6 Test Results

In Figure 2.9 and 2.10 the voltage and capacity (Ah) data for the recovery charge and discharge on the Ultrabattery and absorbed glass matt (AGM) VRLA battery are presented. The Ultrabattery data is from before the first HRPSoC cycle, after 500 cycles, and after 16,740 HRPSoC utility cycles. At an initial capacity of 7.8 Ah, this battery exceeded the manufacturer's specified capacity of 6.67 Ah. After 500 HRPSoC pulse utility cycles, the

capacity increased to 8.1 Ah, an increase of 4%. The capacity after 16,740 cycles was 5.8 Ah, a loss of 26% [30].

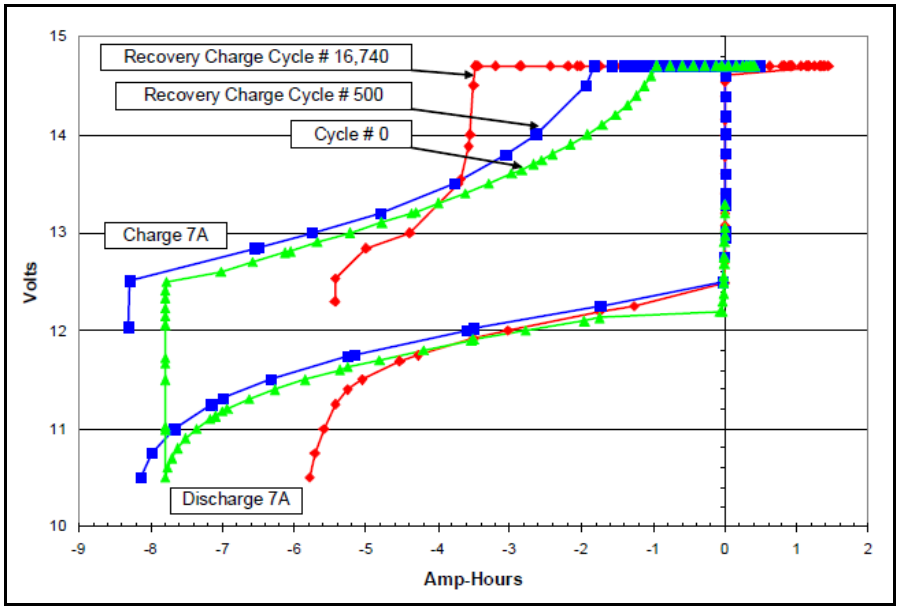

Figure 2. 9: **Ultrabattery Capacity Curve at 0, 500, and 16,740 HRPSoC Utility Cycles [31].**

As can be seen in Figure 2.8, the AGM VRLA battery also demonstrated an increase in voltage and time spent on taper charge, resulting in a similar shaped curve. In this case, the taper charge time increased from 3.5 to 6 hr at a 0.25C, 1 charge rate.

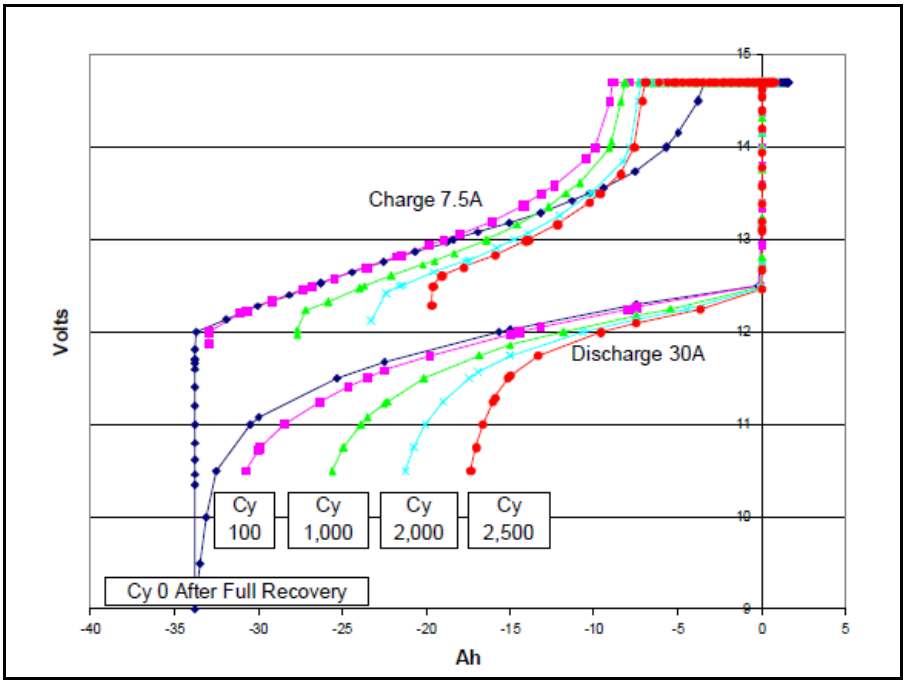

Figure 2. 10: VRLA Battery Capacity Curve at 0, 100, 1,000, 2,000 and 2,500 Utility HRPSoC Cycles [31].

The utility HRPSoC pulsed cycle test results are shown in Figures2.9, 2.10 and 2.11. There are a number of cycling characteristics that are unique to the Ultrabattery. These include the accelerated rise in the end of charge voltage after the first 1,000 cycle sequence (Fig. 2.10 and 2.11), the recovery of end of charge voltage after an extended rest period (~24 hr). If the battery was deep-cycled for an extra capacity measurement, then there would still be no reduction in the rise of end of charge voltage. The test termination with a rest period was repeated many times with the same improvement in end of charge voltage [31].

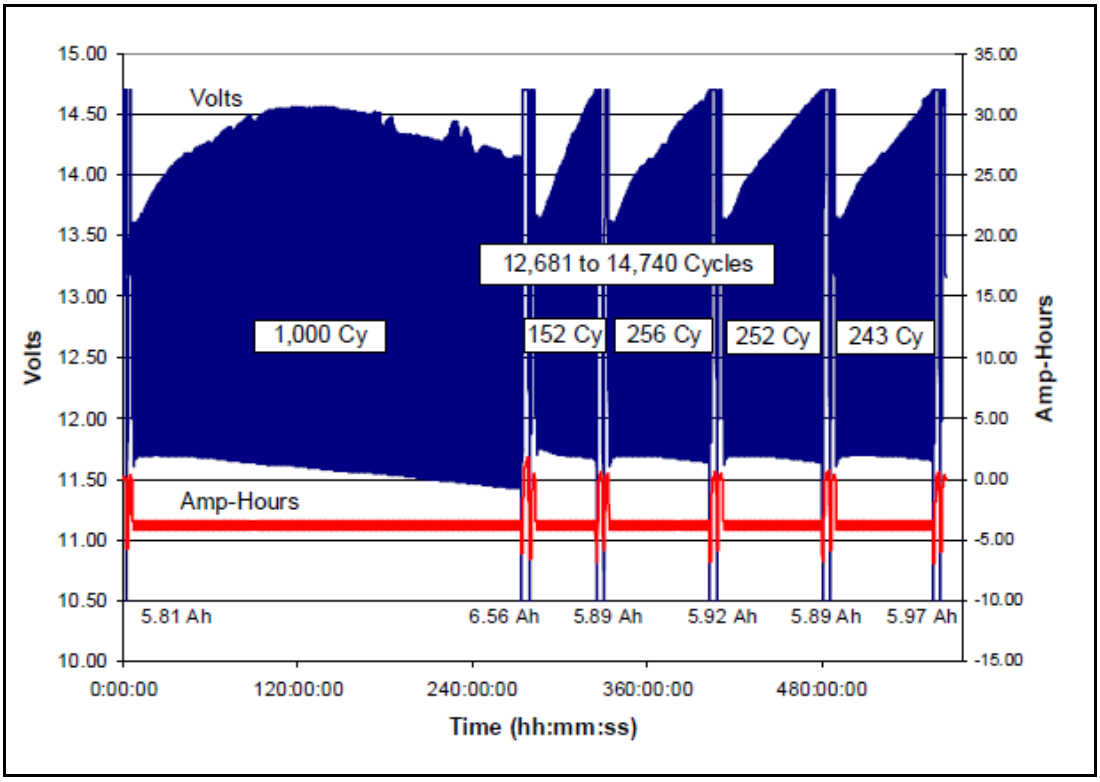

Figure 2. 11: Ultrabattery HRPSoC Utility Cycle Accelerated Rise [31].

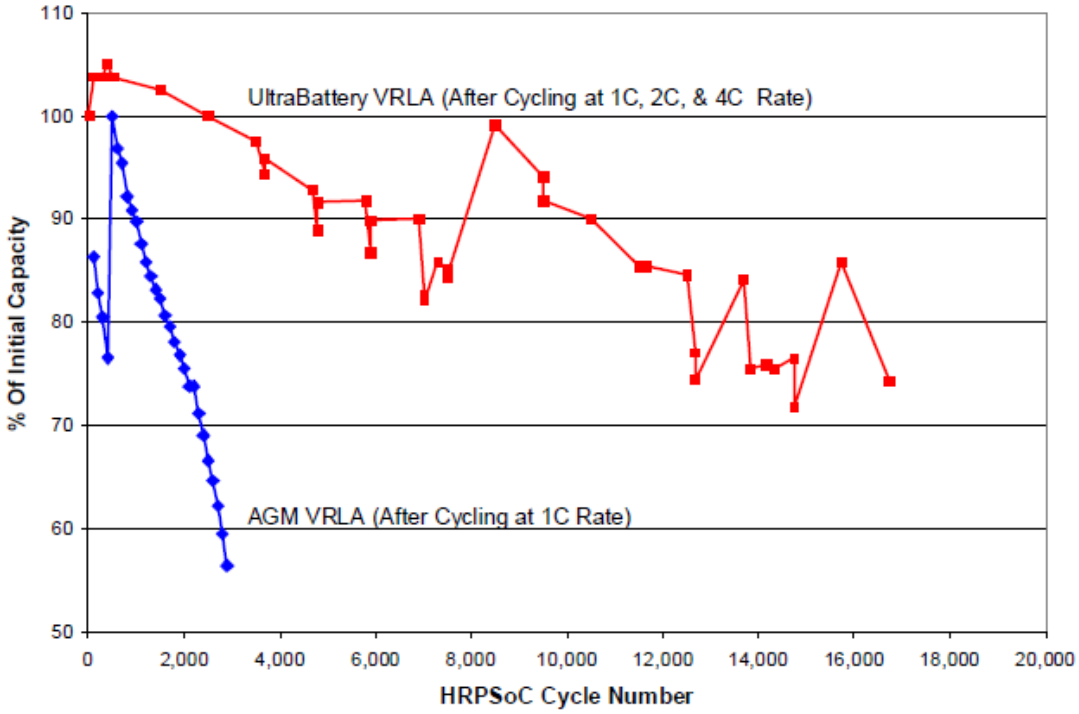

Figure 2. 12: Ultrabattery HRPSoC Utility Cycle Aging Effect [31]

2.5.3 Battery selection and system design involves many decisions and compromises

For selecting each battery system designers have to consider lifetime, deep cycle performance, tolerance to high temperatures and overcharge, and maintenance requirements. Batteries are first connected in series by connecting the negative terminal of one battery to the positive terminal of the next battery for as many batteries as are in the series string. For batteries of similar capacity and voltage connected in series, the circuit voltage is the sum of the individual battery voltages, and the circuit capacity is the same as the capacity of the individual batteries. Batteries are connected in parallel by connecting all of the positive terminals together and all of the negative terminals together [32]. The current of the parallel circuit is the sum of the currents from the individual batteries, the voltage across the circuit is the same as the voltage across the individual batteries, and the overall capacity is the sum of the capacities of each battery. It is generally recommended that batteries be connected in as

few parallel strings as possible. For PV systems with large capacity requirements, larger batteries allow configurations of one series string rather than several parallel strings.

Electrical codes and safety standards generally require batteries to be installed in an enclosure separated from controls or other PV system components. An enclosure may be insulated or may have cooling or heating mechanisms to protect batteries from extreme temperatures and it must be of sufficient size and strength to hold the batteries. Batteries should always be kept in a ventilated area because they can produce toxic, corrosive, and explosive mixtures of gases.

2.5.4 Overcurrent protection and disconnects

Battery systems must have proper DC rated over current protection and disconnects to protect system conductors and to isolate the battery bank from the rest of the system for testing and maintenance.

2.6 Inverters

An inverter is a device that converts DC power to AC power. Some inverters allow the flexibility to operate both AC and DC electrical loads. The solid-state inverters used in PV systems employ the latest in power electronics to produce AC power from a DC power source that is either a PV array or a battery bank. Static inverters change DC power to AC power using electronics and have no moving parts. Inverters used in PV systems are exclusively static inverters [33].

2.6.1 PV Inverters

Inverters for PV systems are broadly classified as either stand-alone or interactive in operation.

2.6.1.1 Stand-alone Inverters

Stand-alone inverters are connected to batteries as the DC power source and operate independently of the PV array and the utility grid. For stand-alone inverters, the electrical load is connected to the AC output, rather than the DC power source.

Listed below are the standards required for off grid inverter approval in Australia. There should also be a JAS-ANZ certificate of compliance to meet the Australian standards:

- AS 4777.2:2005
- AS 4777.3:2005
- AS/NZS 3100:2009
- IEC 62109-1
- IEC 62109-2
- AS 62040

The Australian Clean Energy Council will only accept certificates from one of the following JAS-ANZ accredited certifying bodies or state electrical regulator [34]:

- Australian Safety Approvals (ASA) (JAS-ANZ)
- Conformity Certification Services Pty Ltd (CCS) (JAS-ANZ)
- Electrical Safety Office (Qld)
- Energy Safe Victoria (ESV)
- ITACS (JAS-ANZ)
- Office of Fair Trading (NSW)
- SAA Approvals (JAS-ANZ)
- SGS Systems (JAS-ANZ)
- TUV Rheinland Australia (JAS-ANZ)

2.6.1.2 Utility-Interactive Inverters

Utility Interactive PV inverters are connected to and operate in parallel with the electric utility grid. Interactive inverters are loaded by the DC source, not the AC output, so AC loads do not directly impact the operation of the inverter. Interactive PV systems are interconnected with the utility at the distribution panel or on the supply side of service

entrance equipment. At night and during other low insolation periods when the electrical loads are greater than the PV system output the balance of power required by the loads is received from the electric utility.

All grid connected inverters connected to the SWIS are required to comply with the AS4777 standard which defines the requirements for disconnection during a grid fault. The inverter must detect a disturbance in the utility supply and island itself so that work may be carried out on the transmission line safely. The islanding detection techniques are generally classified into two categories, active and passive methods. Passive detection methodology is concerned with monitoring selected system parameters and will detect islanding when a certain disturbance is perceived. Active methods create some disturbance on the line which is then monitored to determine if the grid is still connected [34].

2.6.1.3 Bi-directional Inverters

Bi-directional inverters can operate in either an interactive or stand-alone mode. These inverters are connected to the battery bank like stand-alone inverters, while the PV array charges the batteries. When connected to an energized utility grid, bimodal PV systems operate in interactive mode, serving on-site loads or sending excess power to the grid while keeping the battery fully charged.

2.6.1.4 AC Module Inverters

An AC module is a PV module that outputs AC power through an interactive inverter attached in place of the normal DC junction box. AC modules are only permitted for interactive operation. Multiple AC module inverters are connected in parallel to form AC branch circuits.

2.6.2 Voltage Control Methods for Inverters

VC-VSIs are required wherever a utility grid or generator is not available. VSIs operated in a voltage control mode allow the output voltage to be carefully regulated to the desired magnitude and frequency. Comparing a reference sinusoid of the required output frequency to a triangular waveform creates the desired voltage sinusoid. The comparison of these two waveforms creates a succession of high and low signals of varying width, known as PWM. Varying the peak height of the reference sinusoidal

waveform controls the magnitude of the output voltage, known as the modulation index [35].

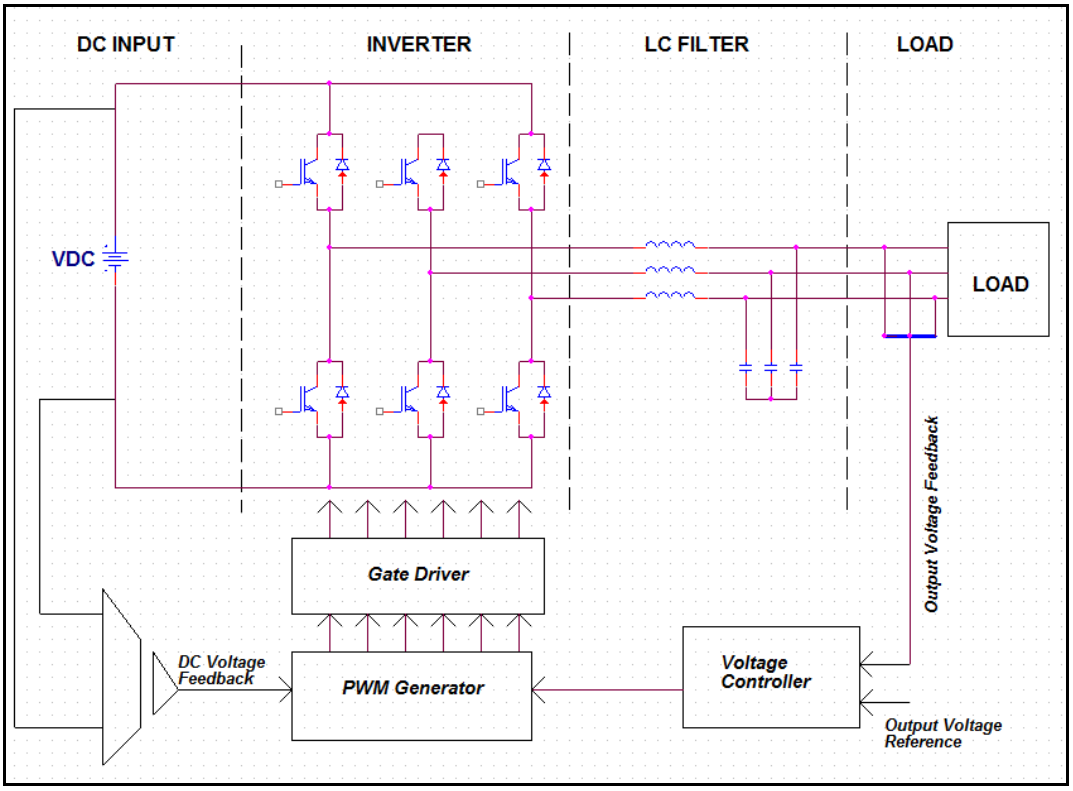

Figure 2. 13: VC-VSI Topology

2.6.3 Grid Connecting VC-VSI

Grid connecting a VC-VSI requires careful control of the voltage and phase of the inverter waveform with respect to the grid. A filter inductance is required to soften the effects of any instantaneous differences in phase during connection. A small mismatch in phase can create a large current flow in either direction. The grid connection inductor limits the rate of increase of change in current flow to or from the grid.

This technique of grid interfacing was used for some of the first PV installations in Western Australia such as the Kalbarri Wind Farm. With the increased safety requirements of islanding detection this method has become less popular. The grid inductor can also be quite large and be removed completely if modern current control techniques are used.

The VC-VSI grid connection method uses two parameters; the inverter voltage magnitude and the phase angle difference to control the active and reactive power flow to the grid. The expressions used to control the power flow are seen in figure 2.13 [36].

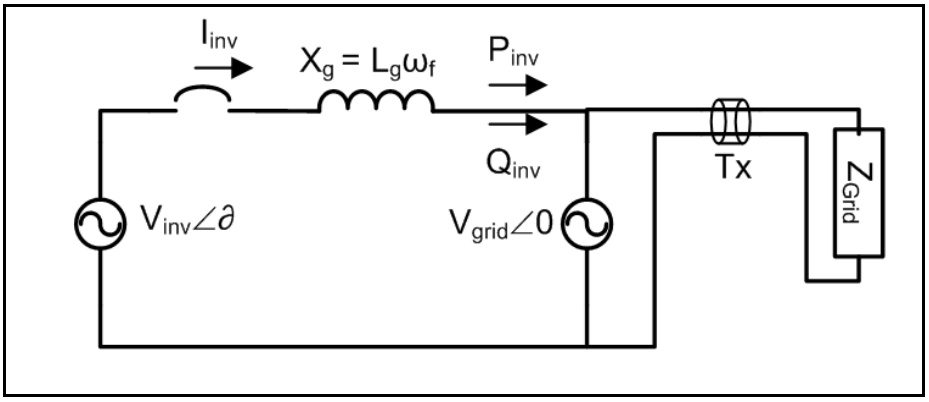

Figure 2. 14: VC-VSI grid connection diagram

Technically, this control method can be implemented with only a voltage sensing control loop which will measure the utility voltage and phase and compare it with the inverter's output voltage, Figure 2.14. However, this approach does not allow the output current to be instantaneously known, which makes MPPT on the DC side or short circuit protection difficult to implement. To resolve this issue, a faster output current loop is added, this allowing the instantaneous current and power be compared to an available DC reference value.

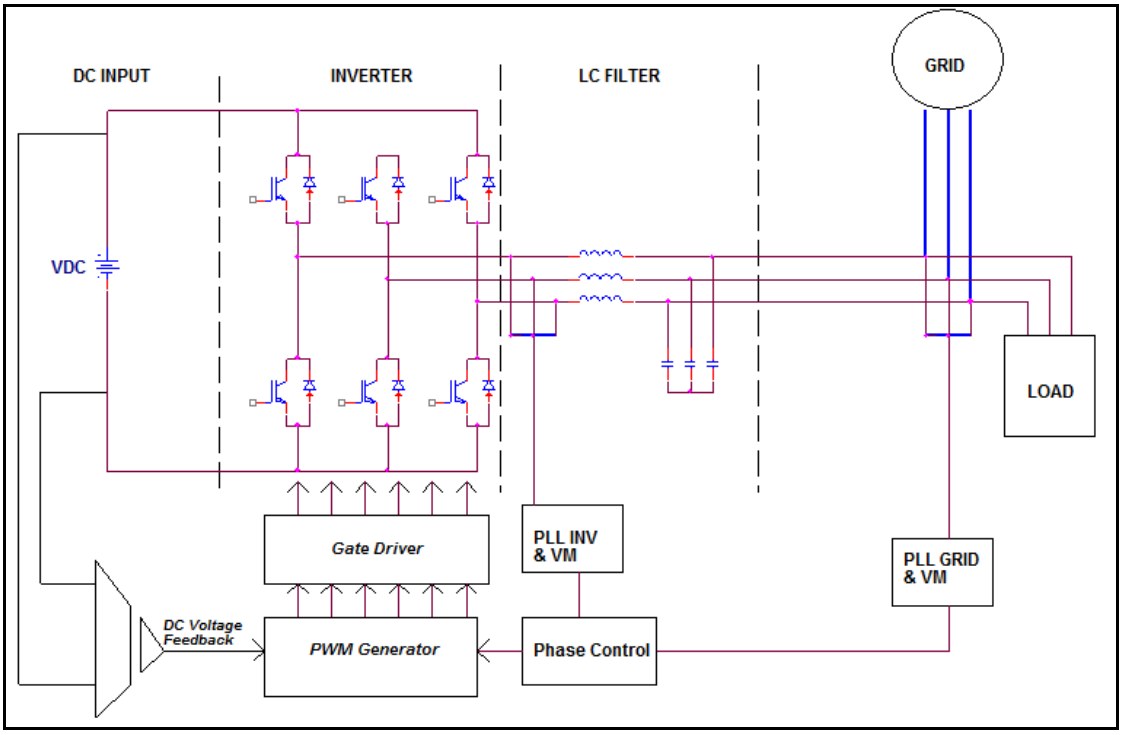

Figure 2. 15: Voltage control loop for phase difference

The difference in the grid and inverter voltage is seen across the grid inductor, which indirectly controls the inductor and grid current, (Figure 2.14). The main drawback of this technique is that the voltage active and reactive power supplied to the grid are proportional to both the voltage magnitude and phase. No single parameter can be changed to allow active or reactive power to be independently modified.

2.6.4 Current Control Methods for Inverters

The main method used to implement a grid connection for a VSI is to use a current control technique. All current control techniques require the sensing of the output voltage and current (Figure 2.15). The input voltage is measured to ensure that the crest of the AC waveform can be created. The output voltage is sensed and its phase is passed through a PLL, which is used to create a unity phasor template for the control system.

Multiplying the PLL unity reference signal with the magnitude of the desired current or power controls the desired active power transfer to the grid. Reactive power can be supplied to the grid by varying the phase angle of the current reference signal. The sum of the active and reactive waveform defines the template of the desired current waveform to be fed

to the grid. Figure 2.16 outlines this control strategy. The method to create the current waveform template is similar for all CC-VSI, however various different methods are used to drive the switches to force the current to follow the reference. The main advantage of this technique is that the active and reactive power can be controlled independently or decoupled. This ensures the inverter can provide reactive power support easily [37].

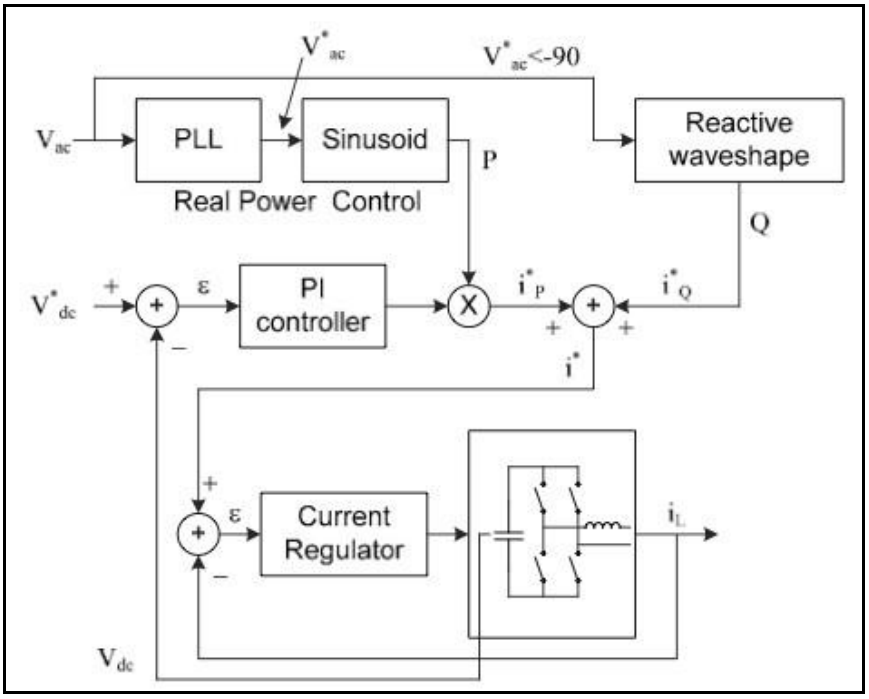

Figure 2. 16: Current control topology

Figure 2.15 shows the standard control topology of a CC-VSI where both active and reactive components can be controlled. All CC-VSI controllers must implement a PLL which is a control system employed to synchronize the inverter output current with the grid voltage. This ensures the active power output current template is locked in phase with the grid voltage. The output of the phase lock loop control block is actually a unity sinusoidal waveform template which creates the phase reference for the output current.

The unity signal from the voltage sensor is passed through a low pass filter to prevent any higher frequencies affecting the PLL. A PI controller is used to drive any error in the reference and grid phasers to zero. Some islanding detection methods use this as a limit. If the discrepancy is greater than a preset value the system will island. The output of the PI is added to a continuous cycling ramp from 0 to 360. The ramp represents the "ωt" while the PI output is the "x." The sum of these signals is fed to a SINE function which creates the desired unity

reference signal of "sin (ωt+x)." This waveform is multiplied by the available current to form the grid current reference waveform [38].

Many different methods have been used to drive H-bridge switches to create a current sinusoid that will follow the grid current reference. These methods can be broadly split into PI triangular carrier current control, hysteresis current control, ramp time current control and predictive current control. The two most commonly implemented techniques are the standard PI current control and hysteresis current control.

2.7 Power electronic topologies for solar applications

The requirements for a PV inverter are based upon the interconnection approach of the PV modules. These can be connected in series strings, then paralleled with blocking diodes to a single central inverter Figure 2.16(a); or each series string may have a grid connected inverter Figure 2.16(b), or each PV module may have its own inverter Figure 2.16(c). A central approach is generally adopted for larger scale three phase PV systems up to 250kW. This method exhibits high efficiency and reduced power electronic cost, but the MPPT is not optimal and there is no redundancy. Large MW level plants usually adopt a few of these systems in parallel. The series approach is usually utilized in systems up to 5kW single phase for roof top type installations. Each string has its own MPPT allowing optimal extraction of power and the loss of one inverter only deducts a single string's power from the system. The individual module approach is generally not adopted due to the increased power electronics components cost and low efficiency due to parasitic inverter losses [39].

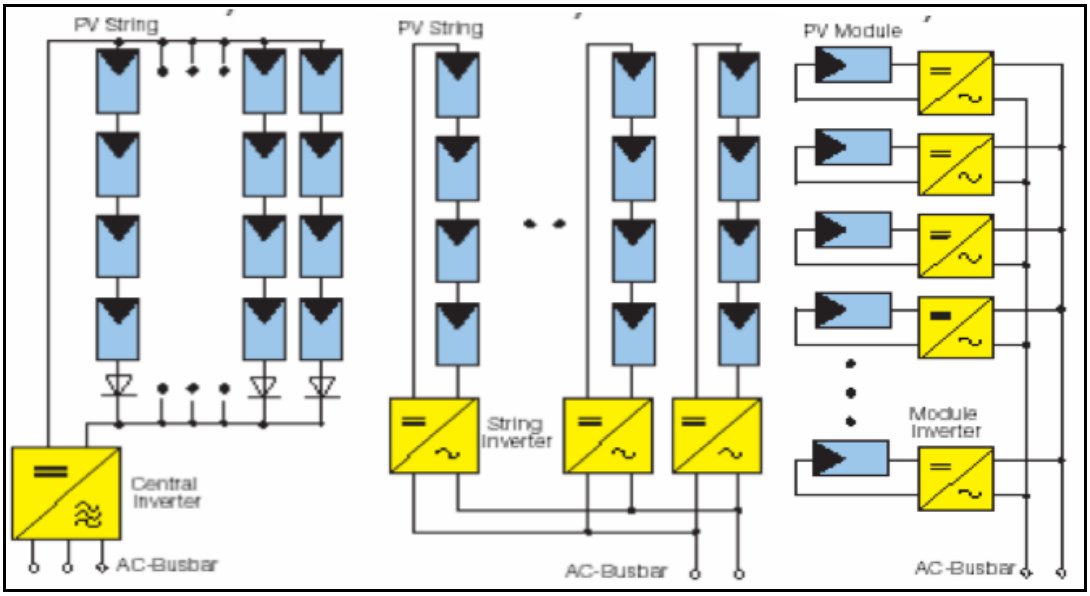

Figure 2. 17: PV inter connect topologies (a) Cent inverter (b) String inverter (c) Module inverter [40]

The PV power electronic topologies mainly rely upon the requirement of MPPT and galvanic isolation. These criteria depend on the grid connection requirements of the utility, which in Australia is covered by AS4777. Figure 3.18 shows the different possible design constraints.

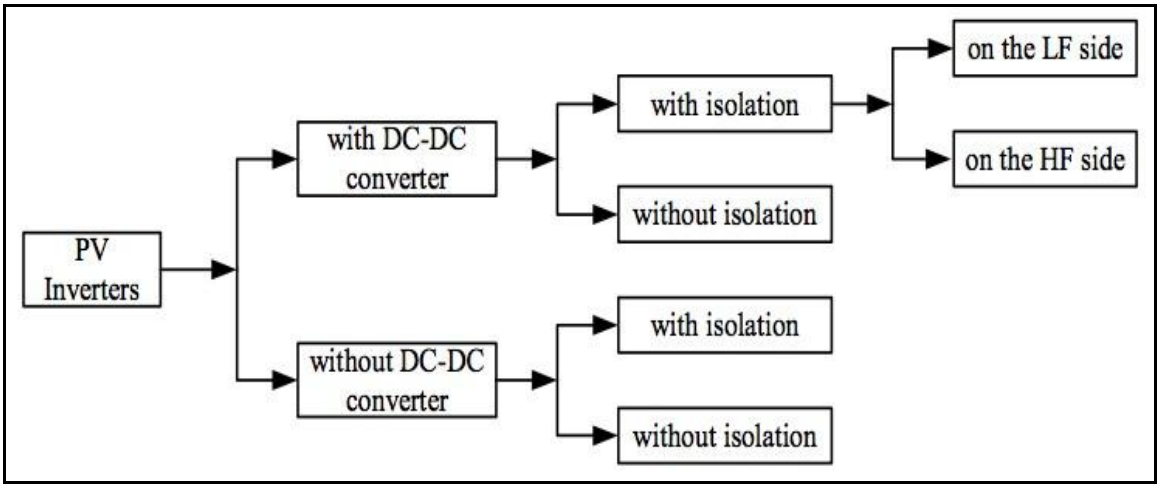

Figure 2. 18: PV power electronic design options [40]

The full bridge inverter (Figure 3.18), or CC-VSI, is the standard inverter topology adopted by almost all manufacturers. However this standard approach cannot perform MPPT

or provide isolation between the source and grid. It also depends on the PV string voltage generating a voltage high enough to recreate the crest of the AC grid voltage [40].

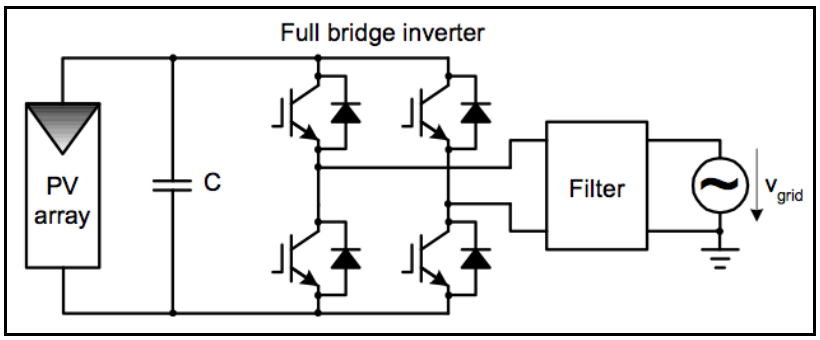

Figure 2. 19: Transformer less full bridge inverter [40]

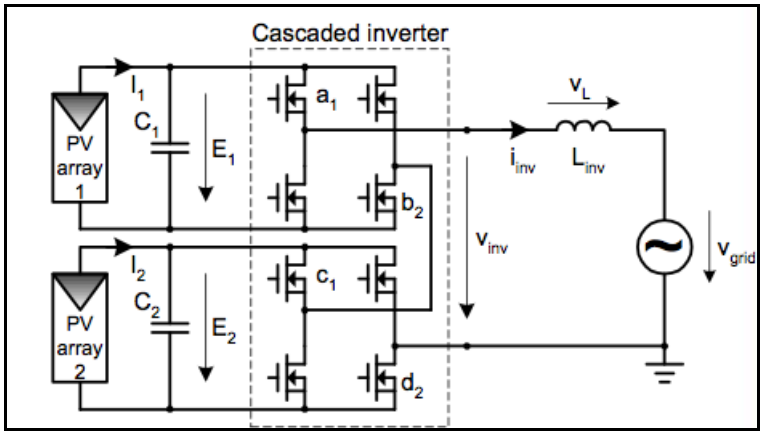

Figure 2. 20: Transformer less multilevel cascaded inverter topology [40]

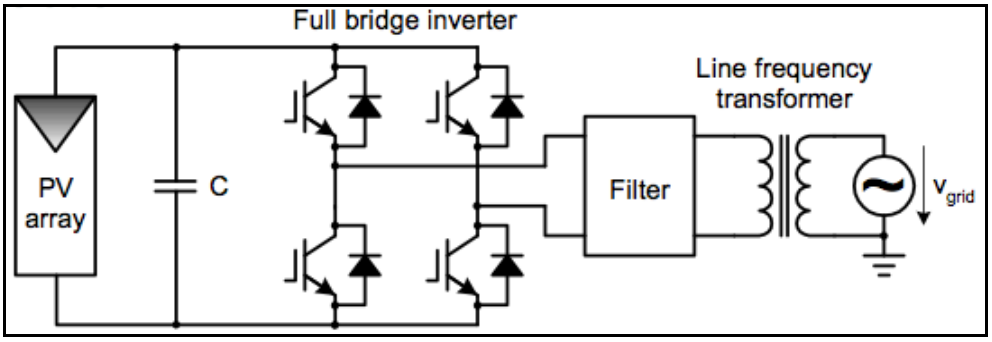

Figure 2. 21: Standard full bridge inverter with low frequency transformer [40]

Figure 2.20 presents a method which cascades the PV arrays on the DC side allowing the voltage to be increased and the PV operating point to be closer to the maximum voltage

point of the PV array. Figure 2.20 shows the typical inverter topology with a grid side low frequency transformer providing galvanic isolation. However the low frequency transformer introduces additional losses through winding resistance and magnetic hysteresis losses. Power Solutions Australia currently adopt this topology.

The front end converter can also be utilised as a switching converter to allow the inclusion of a high frequency transformer. The push pull front end converter has become very popular commercially as it keeps the transformer losses low while providing galvanic isolation. The switching of the front end converter can also be controlled to allow MPPT operation. Figure 2.21 shows this approach. SMA, Fronius, KACO and Leonics all use this topology in their standard grid connected, galvanically isolated inverter.

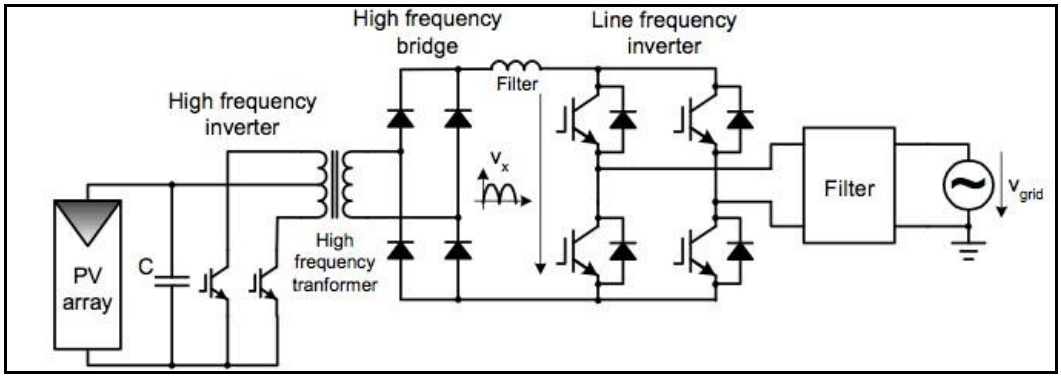

Figure 2. 22: Front end converter with high frequency transformer [40]

2.8 DC-DC Converters

A DC-DC converter is a device that changes DC power from one voltage to another. Many PV inverters use DC-DC converters to change the DC input from low voltage to high voltage prior to the power-inverting process. External DC-DC converters may be used on battery-based systems to deliver DC voltage at levels other than the nominal battery voltage.

2.9 Maximum Power Point Trackers (MPPT)

A maximum power point tracker (MPPT) is a device or circuit that uses electronics to continuously adjust the load on a PV device under changing temperature and irradiance conditions to keep it operating at its maximum power point. Stand-alone inverters do not directly operate or control the array, so they do not normally include MPPT circuits [41].

2.10 Inverter features and specifications

PV system inverters include a number of basic and optional features.

Inverters installed in PV systems are required to conform to certain standards for product listing and certifications. The principal inverter specification is the output power rating and in the case of stand-alone inverters, the power rating limits the power it can deliver to AC loads. For an interactive inverter, the output power rating limits the power it can handle at its DC input, which limits the size of the PV array. Thermal management in electronic inverters is still a major concern, and temperature is the primary limiting factor for inverter power ratings. Interactive inverters control high temperatures by limiting the array power delivered to the inverter. If the temperature or load limits are exceeded, inverters limit or disconnect their output. Most stand-alone inverters shut down or internally disconnect the AC output if load limits are exceeded. Inverter performance is strongly associated with operating voltages. Voltage ratings are given for the AC output and DC input circuits, and may apply to stand-alone and interactive inverters in different ways [42].

Inverter AC output interfaces with either the utility grid or with electrical loads and appliances, so inverter voltage ratings are consistent with normal utility voltage standards. For interactive inverters, AC voltage output must be maintained at -10% to +5% of the nominal system voltage. DC input voltage ratings are based on the operating characteristics of either a battery band (for stand-alone inverters) or a PV array (for interactive inverters). Small stand-alone inverters are designed to operate from nominal 12V lead-acid batteries, or multiples thereof. For interactive inverters, the DC input voltage requirements are more complex. There is a fixed relationship between the utility voltage and the array voltage that the inverter MPPT will track. Loads and systems are more sensitive to variations in frequency than voltage, so only a small variation is allowed from the nominal operating frequency [43].

Inverters are rated for operating and maximum allowable AC and DC currents, which are determined by the current-handling capabilities of the switching devices. For the DC side, current ratings limit the PV array or battery current that can be applied to the inverter. On the AC side, current ratings limit the AC load for stand-alone inverters and the AC current output for interactive inverters. Stand-alone inverters draw high DC input currents from low-voltage battery bands, especially at low battery voltages.

Inverters operating from batteries can deliver high surge and in-rush currents for short periods. Interactive inverters operating from PV arrays cannot produce surge current because they are loaded by the current-limited PV source.

High-frequency and high-voltage inverters are more efficient than lower-voltage inverters operating at low frequency. Inverter efficiency is primarily affected by the inverter load. In stand-alone inverters, the AC load defines the inverter load, and for interactive inverters, the PV array defines the load. Most interactive inverters maintain high efficiency over a wide operating range [44].

2.11 Protective Devices

Most inverters include devices to protect the inverter and connected equipment from damage from excessive temperatures, currents, or power levels. All interactive inverters must employ protective devices for the utility interface, based on the specified limits of grid operations [45].

2.12 Data and Control Interfaces

Most modern inverters incorporate microprocessors, and many provide features for data monitoring and communications. Interfaces may include displays and controls on the inverter itself, while others interface with remote units or computers. Inverter interfaces typically provide basic system information, including interconnection status, AC output voltage and power, DC input voltage, MPPT status, error codes, fault conditions, and other parameters. Inverter operation parameters are generally not field-adjusted, since this could affect critical safety features and operating limits. However, other power conditioning functions may allow operator control or adjustment, such as battery charger and charge controller settings and the operation and control of generators and other power sources, allowing flexibility for a variety of applications [46].

2.13 Schneider PV Shade Tolerant Maximum Power Point tracking

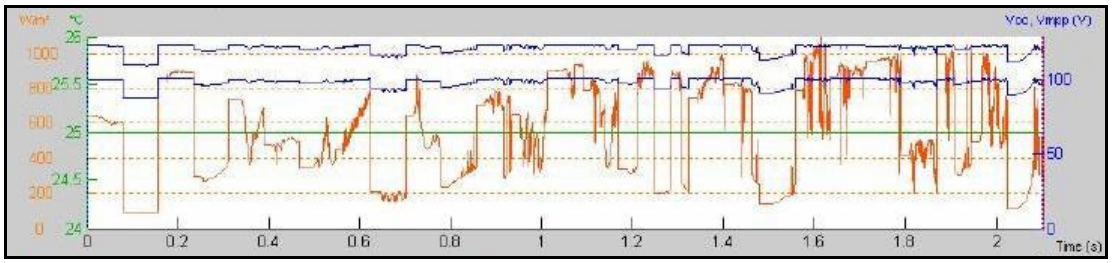

Figure 2. 23: MPPT continually changes with fast moving clouds [15]

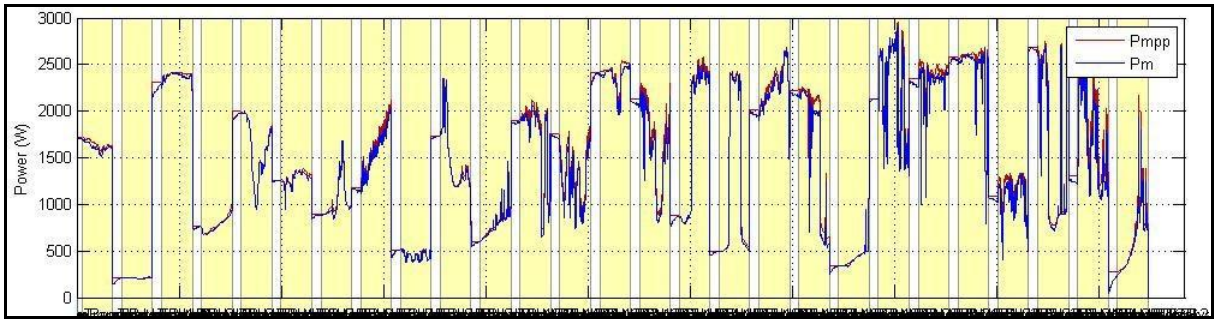

Figure 2. 24: MPPT algorithm adjusts to obtain maximum power [15]

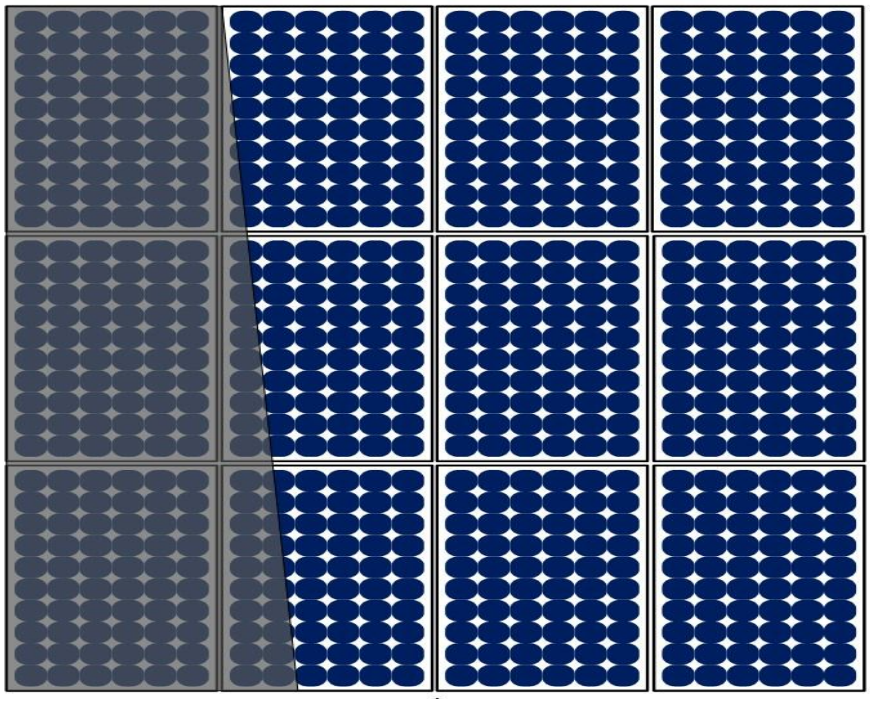

Figure 2. 25: Shaded Array Example [15]

Figure 2.23 shows the graph of MPPT changes with respect to the cloud and Figure 2.24 shows how the MPPT algorithm adjusts itself to obtain maximum MPPT through continual change in irradiance and temperature. The shaded array example of Figure 2.25 shows three uniformly shaded modules, three partially shaded modules and six non-shaded modules. It's sometimes thought that a small amount of partial array shade restricts the whole array disproportionally and that just a few shaded modules or cells can cause a "Christmas light effect" (when one light goes out they all go out). This limits the current and power output of the entire array. It's also thought that performing MPPT at the module level rather than the series string level mitigates this effect. However, this isn't necessarily true. The most informative way to understand how much power is available from a shaded array is to examine its I-V curve [15]. The series string I- V curve of the Figure 2.23 example is presented in Figure 2.24, and illustrates full current from the 24 non-shaded module sections (three sections per module), approximately 50% current from the one module section with no more than partial shading on any cell and, finally, the approximately 17% current from the 11 module sections that have at least one series cell restricted at 17% shade.

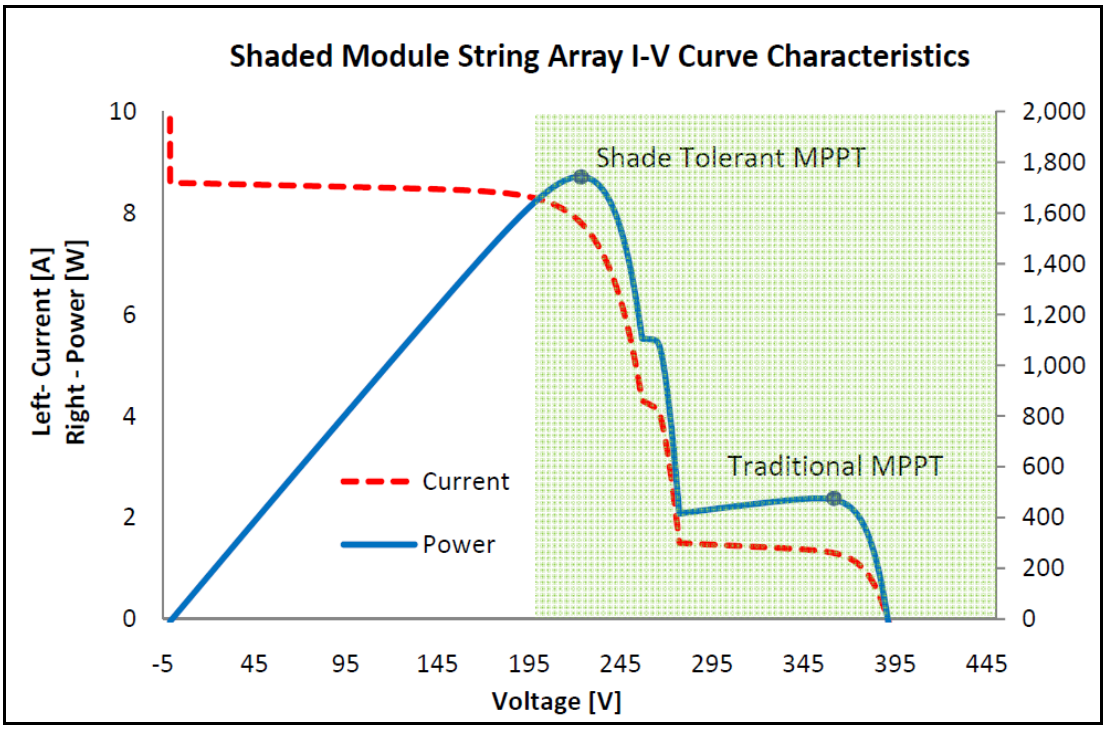

Figure 2. 26: Shaded Array String I-V curve [15]

Figure 2.25 shows the power available in the shaded array example. The maximum array power is available for harvest at approximately 1700W at 220V. However, there is

another localized power maximum at approximately 475W at 360V. A problem with this kind of shaded array I-V curve is that many traditional string inverters on the market may track the 475W localized maximum power "bump" on the right-hand side and not the global maximum of 1700W available at a lower voltage.

Operating at 360V also illustrates the Christmas light effect. If the inverter is forced to operate at 360V then this effect occurs where shading a small amount of the array will limit the current for the whole array.

However, if the inverter operates at a lower voltage the effect can be avoided as the shaded module sections are bypassed and the remaining array is allowed to operate at full current. For this reason, inverter operation at 220V is significantly more tolerant of the shaded array condition than at 360V.

Traditionally, non-shade-tolerant string-based maximum power point tracking has been acceptable since most PV arrays are homogenously irradiated most of the time. In fact, depending on how the shade evolves, the MPPT algorithm of the inverter may not get stuck on the right-hand bump. However, as technology progresses and more systems are being installed in urban situations, and increased emphasis is placed on system ROI, the MPPT performance and harvest efficiency are becoming more important to customers; especially for PV arrays that experience intermittent partial shading.

2.14 Shade-Tolerant String Inverter MPPT

The shade-tolerant solution for string inverters lies within the string inverter's MPPT tracking algorithm. The MPPT algorithm must take into account the entire MPPT voltage window in order to act on the presence of a global maximum. However, each time the MPPT control algorithm moves away from a local maximum power point to look for global maxima it is at some expense of the static MPPT harvest efficiency. Furthermore, if the entire MPPT voltage window isn't searched often enough, relatively rapid changes in shade may be missed [47].

Schneider Electric's proprietary shade-tolerant Fast Sweep string inverter MPPT technology allows for tracking of dynamically changing global power peaks with no significant decrease in traditional static and dynamic tracking and harvest efficiency. Part of the shade-tolerant solution is an ability to frequently scan the array I-V curve in a very short

amount of time and maintains industry-leading static and dynamic harvest efficiency over a wide range of shaded and non-shaded I-V and I-P curve scenarios, thus helping optimize PV system ROI (Return of Investment) [15].

2.15 Shade-Tolerant Micro-Inverter MPPT

Another shade-tolerant solution approach is to perform MPPT at the module level with micro-inverters. The assumption is that module-based MPPT inherently improves harvest efficiency and therefore PV energy yield, and that enough extra energy will be harvested to justify the premium cost for module-based MPPT technology, which then increases the overall system ROI [48].

When discussing shaded PV, partial module shade must not be ignored. It is virtually impossible to find a PV array that experiences only even shade on each module. The sun is constantly moving in the sky and shadows are dynamic. Even modules soiled with dirt and debris aren't often soiled in a uniform way. For these reasons it is necessary to further examine the I-V curve characteristics of a partially shaded module.

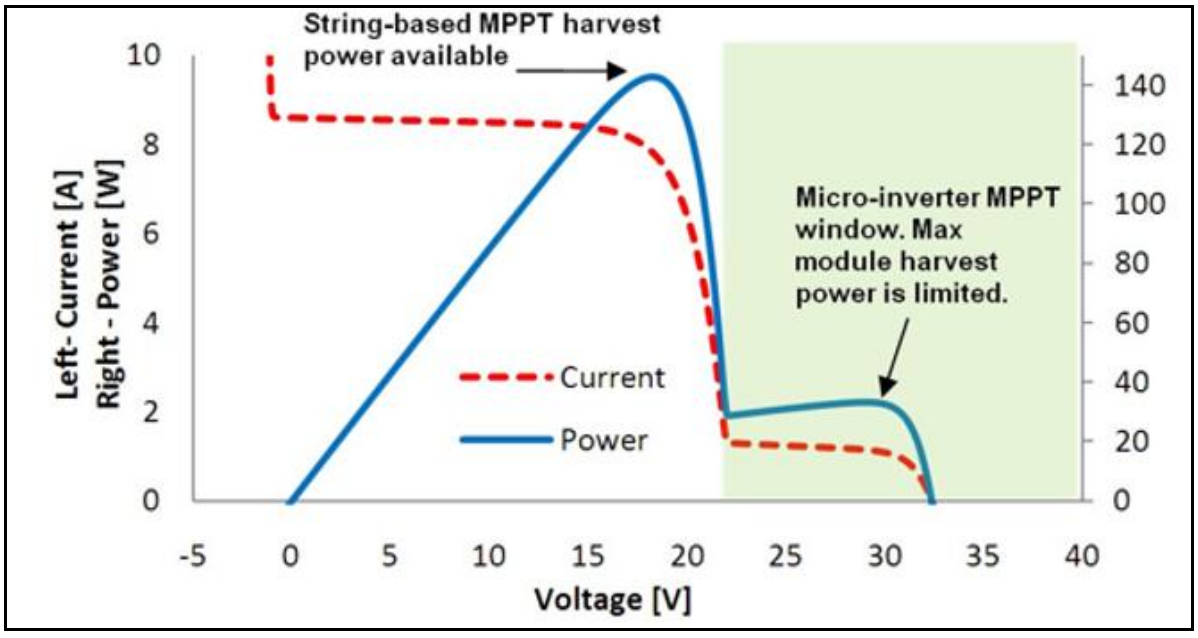

Figure 2. 27: Partial module shade IV curve [15]

Figure 2.26 illustrates the resulting I-V curve of a top-selling 60 cell silicon-based PV module with corner shading of 15%. Again, distinct global and local power maxima can be

observed due to the bypassed module section (it appears that the micro inverter also needs to be shade-tolerant of global and local maximum power bumps). However, upon closer examination, the micro- inverter's ability to harvest I-V curve energy is also inherently limited by its MPPT voltage window.

Micro-inverter designers have to make compromises on MPPT voltage windows to carefully balance efficiency and cost. Lower and wider voltage MPPT windows tend toward higher cost and/or less efficient designs. Manufacturers presumably have been forced to make design trade-offs sacrificing lower MPPT range for gains in the more noticeable efficiency, cost and maximum Voc metrics.

Conversely, a string inverter with shade- tolerant MPPT technology has a much better ability to operate at the true Vmp due to the extra range and flexibility of the string inverter's MPPT voltage window.

Figure 2.28 illustrates how the so-called "leaf problem" affects the I-V curve of the PV module. The leaf effectively blocks one module section completely and the resulting I- V curve is formed by the I-V characteristics of the remaining two module sections. Again, a MPPT voltage window of 22V will have trouble harvesting any of the approximately 150 available watts.

It's now possible to understand a significant challenge micro-inverters can have with common partial module shading conditions. Furthermore, even if micro-inverter MPPT windows were designed to go well below the sub-module section voltages – how would one know if they were engineered to be multi- maxima shade tolerant of partial module shading?

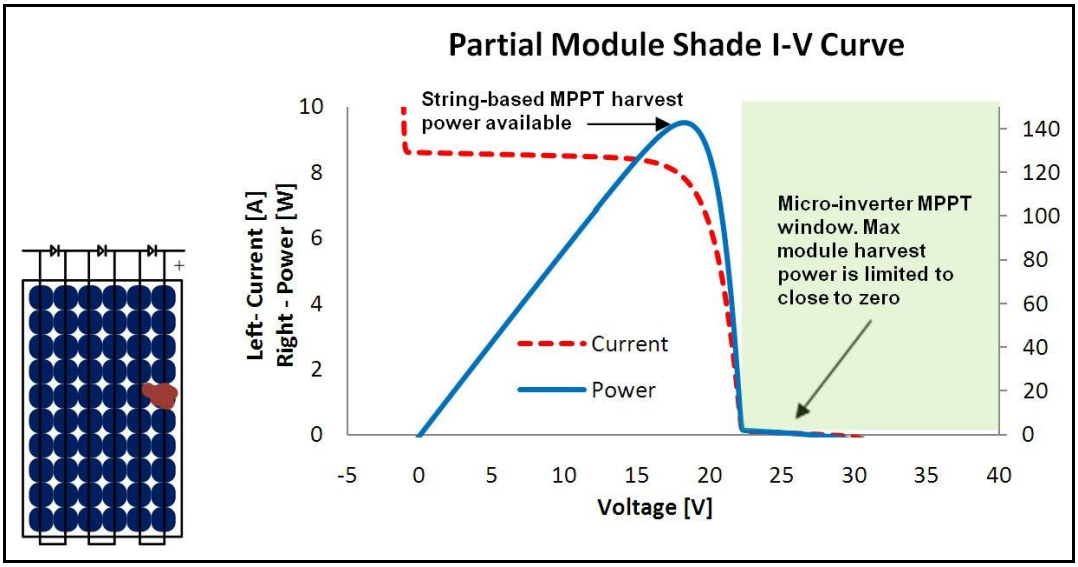

Figure 2. 28: Single cell opaque shade from a leaf or other material [15]

2.16 Shade-Tolerant Comparison: String Inverter vs. Micro-Inverter Energy Harvest

While it is possible to engineer examples of shaded arrays that optimize the benefits of micro-inverter technology, it is also possible to do the same with shade-tolerant string inverters. There will always be specific circumstances where each technology or approach will yield superior results. The reference example of Figure 2.24 wasn't selected as the best case for string inverters, but rather to include full module shade where module--based MPPT technologies work very well compared to string inverters.

As a final exercise, we can examine the power each approach can harvest from the shaded array example of Figure 2.24. The results for traditional string inverter, micro-inverter and shade-tolerant string inverter are found in Figure 2.27.

When operating with traditional non-shade tolerant string-based MPPT the string is operated at about 360V and 1.3A. Each module is operated at 1.3A and the individual module powers can be determined by looking at the I-V curve of each module. We can see that the increasingly shaded modules make a lesser power contribution. Total power harvested at the right-hand-side power maximum is 475W.

The micro-inverter architecture harvested power is the maximum power available within the micro-inverter allowable MPPT window of the I-V curve for each PV module.

Note the shaded modules all contribute some amount of power, but the partially shaded modules must operate above their 22V MPPT window which does not permit maximum module power harvest. The total micro-inverter energy harvest of 1599W is significantly higher than the 475W of the non-shade-tolerant string inverter.

The shade-tolerant string inverter operates at the global maximum power voltage (Vmp) of approximately 220V and at full current of the un-shaded module sections. The means that each partially shaded module section is bypassed allowing each other module section to operate at full current. The flexibility of the string-based MPPT window allows a significant number of module sections, in any location, to be bypassed before the Vmp is lower than the string inverter's MPPT window limit. This means the three completely shaded modules have -9W output due to forward biased bypass diode heating and the remaining three modules, each with 1 of 3 substrings now bypassed, operate at approximately 2/3 of the non-shaded power. In this situation of shade, the total power output of the shade-tolerant string inverter is actually higher than the micro-inverter approach [15].

The main difference between the two approaches is that micro-inverters are good at harvesting the 30W from the fully shaded modules but not at harvesting the available energy from the partially shaded modules. Conversely, the string inverter is not good at harvesting any energy from the fully shaded module sections but is much better at harvesting energy from the un-shaded module sections of the partially shaded modules. Considering the amount of partial module shade appearing in the field, this is a point worth understanding.

2.17 Methods of system integration and modelling

Computer modelling of power system components allows analysis of the interaction between components in various operating conditions. Modelling and simulation are essential in the design and operation process of a power system to ensure the power supply is reliable, safe in operation and financially viable. There are various mathematical modelling approaches used for analysing electrical power systems and hybrid power systems [49].

In electrical power system studies, system models are classified based on time constants and associated phenomenon. These models are summarized below:

- Steady-state models describe the equilibrium condition with negligible transient effects. These models are used to analyse the power balance at a particular operating point. All variables in steady-state models are assumed to be constant and there are no differential equations involved in steady state operation analysis.
- Long-term dynamics models are used to investigate the control of frequency and power in a time range of several minutes to several hours.

As for hybrid power systems, two broad categories of mathematical models have been identified and their features summarized below:

- Logistic models that are used to study system operation with a selected dispatch strategy and to predict long-term system performance. Logistic models are classified as time-series and probabilistic models. Time-series models have time constants in the range of minutes to hours, while statistical or probabilistic models have time constants in the order of months.
- Dynamic models that are used to analyse system stability and related to the dynamics of a local controller for a particular component in a system. Time constants of these models are in the range of milliseconds [50].

Table 2. 2: Classification of hybrid power system modelling

Models	Types	Purpose	Time constant scale
Logistic	• Time series • Probabilistic (Statistical) • Combination of time series and probabilistic	• Long-term performance predictions • Component sizing • Economic analysis	• Minutes to hours (for time series models) • Months (for probabilistic models)
Dynamic	• Dynamic mechanical • Dynamic mechanical/steady- state electrical • Dynamic mechanical/electrical	• System stability investigations • Power quality studies • Local controller designs	• milliseconds

Modelling approaches of hybrid power systems are prevalent and can be studied from general publications. Although the analytical performance model of conventional CSDG has long been in existence, very few analytical performance studies have been completed for VSDG. There is only one study made known to the author which investigates the operation of variable speed operation of diesel generators in hybrid power systems. The study showed that system architecture with variable speed diesel generator can provide benefits both in system operation and financial aspects [51].

The schematic diagram of basic solar systems and their integration are presented in figures 2.28, 2.29, 2.30 and 2.31. Solar PV, battery, and Diesel generators can be integrated in various methods by using proper converters and control units.

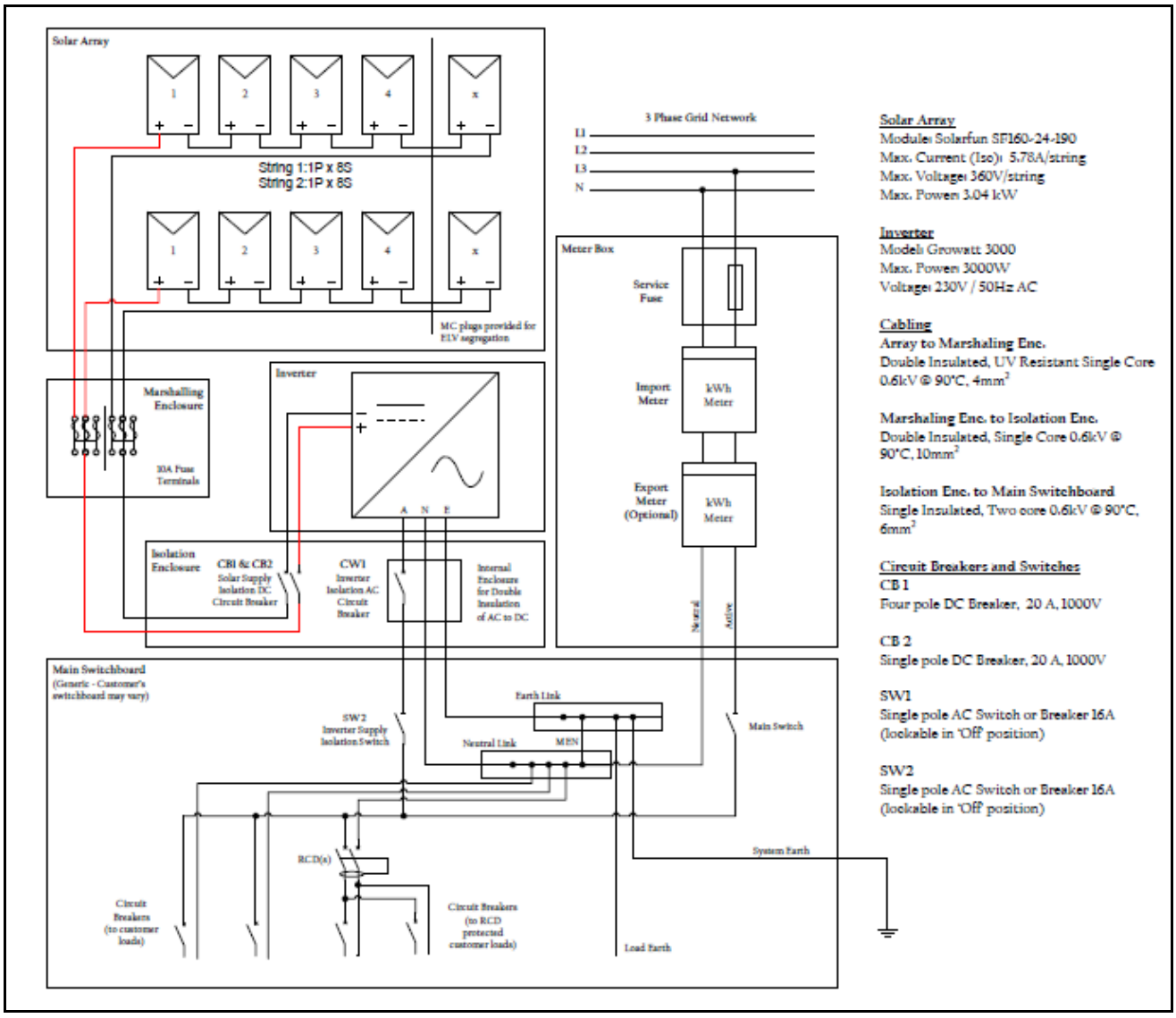

Figure 2. 29: Schematic diagram of typical grid connected system

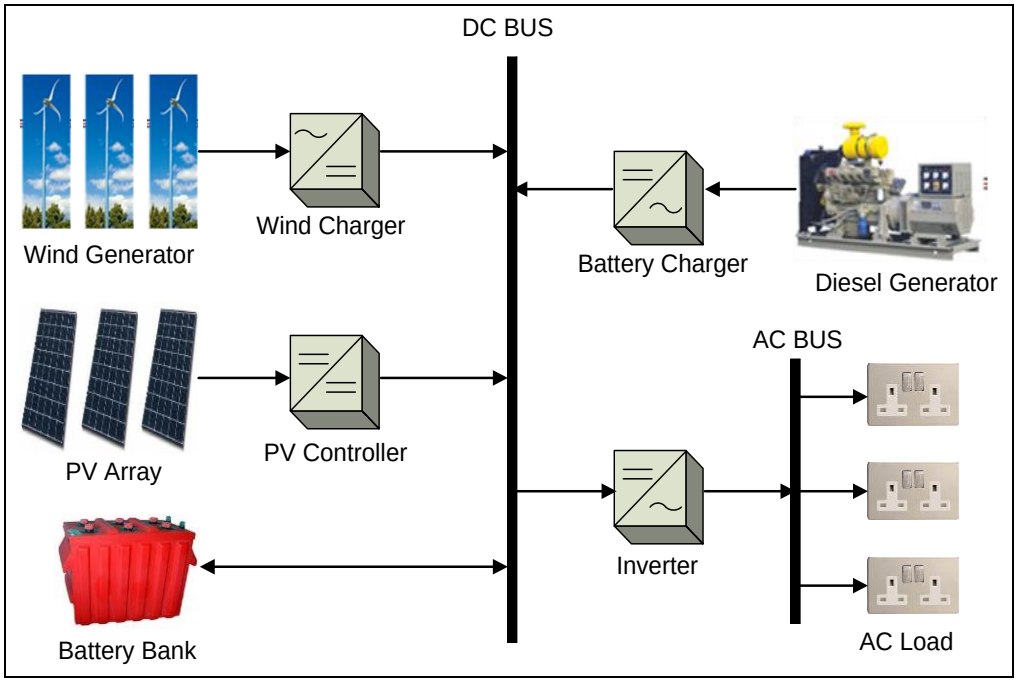

Figure 2. 30: Series hybrid power system configuration

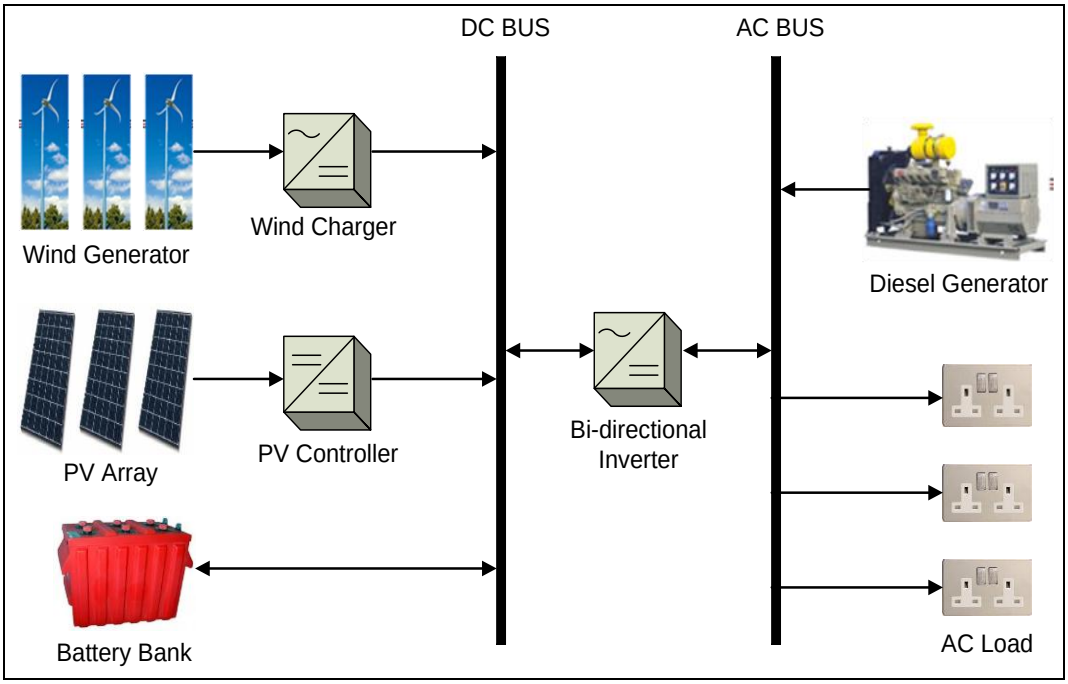

Figure 2. 31: Parallel hybrid power system configuration

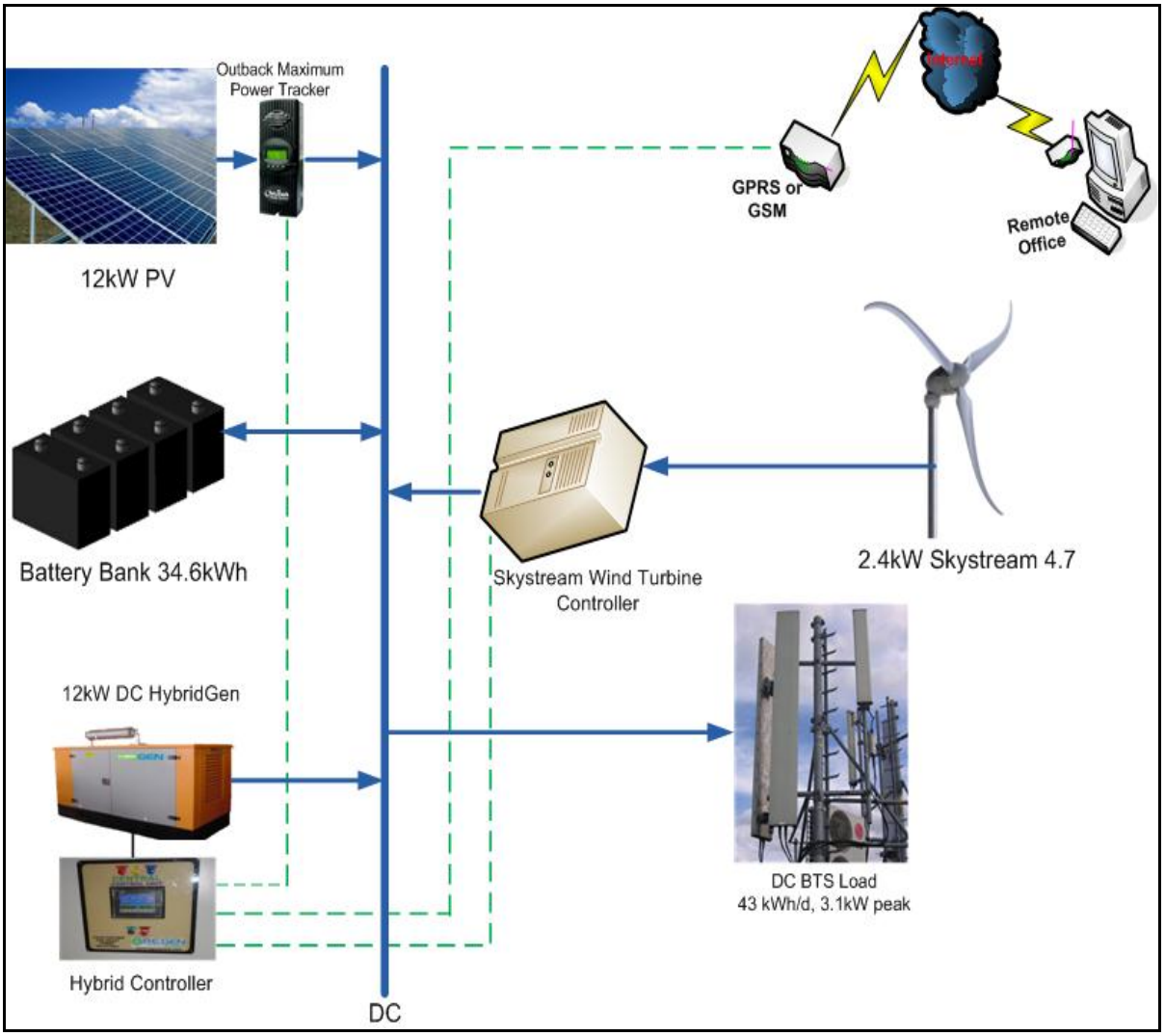

Figure 2. 32: Telecom BTS load only system

2.18 Summary

Firstly, the Ultrabattery has confirmed its ability to cycle well in a utility HRPSoC cycling environment compared to AGM VRLA batteries. Using the utility HRPSoC cycling profile at the 1C 1 to 4C 1 rate, the Ultrabattery cycle performance was about thirteen times greater (>15,000 cycles) than the AGM VRLA battery (1,100 cycles). The Ultrabattery was also able to cycle at a HRPSoC for more than ten times the number of cycles as compared to the AGM VRLA battery (1,000 vs. 100). The HRPSoC cycling also identified an aging effect and an accelerated end of charge voltage rise.

Secondly, various multi-function power electronic interfaces, which are applied to renewable energy sources have been explained and modelled. The main investigated

component is the inverter that converts the DC power for either PV to the same voltage and frequency of the utility. The chapter focuses on the control methods of the H-bridge single phase inverter; however, all the techniques shown may be applied to three phase systems.

Finally, the harvest efficiency challenges of partial PV array shading has been discussed Schneider Electric's shade-tolerant string inverter approach is shown to solve some of the challenges faced when obtaining maximum harvest efficiency of shaded module arrays with local maximum power "bumps" on their I-V curves. It has shown in a conservatively shaded array example that more shaded array energy harvest is possible with a shade-tolerant string inverter as compared to a micro-inverter.

2.19 References

[1] O. Edenhofer, R. Pichs-Madruga, Y. Sokona, E. Farahani, S. Kadner, K. Seyboth, *et al.*, "Summary for Policymakers: Climate Change 2014, Mitigation of Climate Change," IPCC, New York2014.

[2] L. Chia-Hung, H. Wei-Lin, C. Chao-Shun, H. Cheng-Ting, and K. Te-Tien, "Optimization of Photovoltaic Penetration in Distribution Systems Considering Annual Duration Curve of Solar Irradiation," *Power Systems, IEEE Transactions on*, vol. 27, pp. 1090-1097, 2012.

[3] J. Tabak, *Solar and Geothermal Energy*. New York: Facts On File, 2009.

[4] P. Hyeonah and K. Hyosung, "PV cell modeling on single-diode equivalent circuit," in *Industrial Electronics Society, IECON 2013 - 39th Annual Conference of the IEEE*, 2013, pp. 1845-1849.

[5] S. B. Kjaer, J. K. Pedersen, and F. Blaabjerg, "A review of single-phase grid-connected inverters for photovoltaic modules," *Industry Applications, IEEE Transactions on*, vol. 41, pp. 1292-1306, 2005.

[6] J. Traube, L. Fenglong, and D. Maksimovic, "Electric vehicle DC charger integrated within a photovoltaic power system," in *Applied Power Electronics Conference and Exposition (APEC), 2012 Twenty-Seventh Annual IEEE*, 2012, pp. 352-358.

[7] M. Kolhe, "Techno-Economic Optimum Sizing of a Stand-Alone Solar Photovoltaic System," *Energy Conversion, IEEE Transactions on*, vol. 24, pp. 511-519, 2009.

[8] J. Traube, L. Fenglong, D. Maksimovic, J. Mossoba, M. Kromer, P. Faill, *et al.*, "Mitigation of Solar Irradiance Intermittency in Photovoltaic Power Systems With Integrated Electric-Vehicle Charging Functionality," *Power Electronics, IEEE Transactions on*, vol. 28, pp. 3058-3067, 2013.

[9] Z. Wu and M. Yan, "Research on solar energy technologies for the ecological architecture," in *Strategic Technology (IFOST), 2011 6th International Forum on*, 2011, pp. 452-455.

[10] R. K. Jurgen, "Impact 2000: A place in the sun: Sponsored by Boston Edison as an energy-conservation experiment, this home in the suburbs was seen during its construction by public-television viewers across the United States," *Spectrum, IEEE*, vol. 22, pp. 64-68, 1985.

[11] M. Yamaguchi, "Effects of irradiation temperature on radiation damage in InP solar cells," *Journal of Applied Physics*, vol. 77, pp. 3679-3683, 1995.

[12] M. Imaizumi, R. D. Harris, R. J. Walters, J. R. Lorentzen, S. R. Messenger, J. G. Tischler, *et al.*, "Irradiation and measurement of solar cells at low intensity, low temperature (LILT) conditions," in *Photovoltaic Specialists Conference, 2008. PVSC '08. 33rd IEEE*, 2008, pp. 1-5.

[13] J. P. Dunlop, *Photovoltaic Systems*, 2 ed. Orland Park, Illinois: American Technical Publishers, INC, 2010.

[14] D. Sinha, A. B. Das, D. K. Dhak, and P. K. Sadhu, "Equivalent circuit configuration for solar PV cell," in *Non Conventional Energy (ICONCE), 2014 1st International Conference on*, 2014, pp. 58-60.

[15] A. Swinger. (December 2010, 08/12/2013). Photovoltaic String Inverters and Shade-Tolerant Maximum Power Point Tracking: Toward Optimal Harvest Efficiency and Maximum ROI.

[16] L. J. Caballero, P. Sanchez-Friera, B. Lalaguna, J. Alonso, Va, x, *et al.*, "Series Resistance Modelling of Industrial Screen-Printed Monocrystalline Silicon Solar Cells and Modules Including the Effect of Spot Soldering," in *Photovoltaic Energy Conversion, Conference Record of the 2006 IEEE 4th World Conference on*, 2006, pp. 1388-1391.

[17] A. Kajihara and T. Harakawa, "Model of photovoltaic cell circuits under partial shading," in *Industrial Technology, 2005. ICIT 2005. IEEE International Conference on*, 2005, pp. 866-870.

[18] A. Bilsalam, J. Haema, I. Boonyaroonate, and V. Chunkag, "Simulation and study of photovoltaic cell power output characteristics with buck converter load," in *Power Electronics and ECCE Asia (ICPE & ECCE), 2011 IEEE 8th International Conference on*, 2011, pp. 3033-3036.

[19] Y. Hishikawa, H. Shimura, and Y. Tsuno, "Influence of nonuniformity of irradiance within a cell on the accurate I–V curve measurement under 1 sun illumination," in *Photovoltaic Specialists Conference (PVSC), 2010 35th IEEE*, 2010, pp. 002684-002687.

[20] R. Arulmurugan and N. Suthanthira Vanitha, "Intelligent fuzzy MPPT controller using analysis of DC to DC novel buck converter for photovoltaic energy system applications," in *Pattern Recognition, Informatics and Mobile Engineering (PRIME), 2013 International Conference on*, 2013, pp. 225-231.

[21] Y. Zou, Y. Yu, Y. Zhang, and J. Lu, "MPPT Control for PV Generation System Based on an Improved Inccond Algorithm," *Procedia Engineering*, vol. 29, pp. 105-109, // 2012.

[22] A. K. Mahammad, S. Saon, and W. S. Chee, "Development of Optimum Controller based on MPPT for Photovoltaic System during Shading Condition," *Procedia Engineering*, vol. 53, pp. 337-346, // 2013.

[23] Syafaruddin, E. Karatepe, and T. Hiyama, "Performance enhancement of photovoltaic array through string and central based MPPT system under non-uniform irradiance conditions," *Energy Conversion and Management*, vol. 62, pp. 131-140, 10// 2012.

[24] S. Kazmi, H. Goto, O. Ichinokura, and G. Hai-Jiao, "An improved and very efficient MPPT controller for PV systems subjected to rapidly varying atmospheric conditions and partial shading," in *Power Engineering Conference, 2009. AUPEC 2009. Australasian Universities*, 2009, pp. 1-6.

[25] N.-K. C. Nair and N. Garimella, "Battery energy storage systems: Assessment for small-scale renewable energy integration," *Energy and Buildings,* vol. 42, pp. 2124-2130, 11// 2010.

[26] J. Wood, "Integrating renewables into the grid: Applying UltraBattery Technology in MW scale energy storage solutions for continuous variability management," in *Power System Technology (POWERCON), 2012 IEEE International Conference on*, 2012, pp. 1-4.

[27] J. Wood, "UltraBattery?? Cloud Energy Storage for the Grid: Positioning Data Center and Telecommunication Backup Resources as Smart Grid Assets That Support," in *Telecommunications Energy Conference 'Smart Power and Efficiency' (INTELEC), Proceedings of 2013 35th International*, 2013, pp. 1-5.

[28] B. B. McKeon, J. Furukawa, and S. Fenstermacher, "Advanced Lead-2013; Acid Batteries and the Development of Grid-Scale Energy Storage Systems," *Proceedings of the IEEE,* vol. 102, pp. 951-963, 2014.

[29] J. M. McAndrews, "Advanced technology that allows on-line discharge testing of VRLA or conventional cells and is invisible to the load," in *Telecommunications Energy Conference, 1992. INTELEC '92., 14th International*, 1992, pp. 200-204.

[30] J. Wood, "Integrating renewables into the grid: Applying UltraBattery Technology in MW scale energy storage solutions for continuous variability management," in *Power System Technology (POWERCON), 2012 IEEE International Conference on*, 2012, pp. 1-4.

[31] T. Hund, N. Clark, and W. Baca, "Ultrabattery Test Results for Utility Cycling Applications," presented at the The 18th International Seminar on Double Layer Capacitors and Hybrid Energy Storage Devices 12/08, 2008.

[32] "IEEE Guide for Selection, Charging, Test and Evaluation of Lead-Acid Batteries Used in Stand-Alone Photovoltaic (PV) Systems," *IEEE Std 1361-2003,* pp. 1-26, 2003.

[33] K. Feel-Soon, P. Sung-Jun, C. Su Eog, U. K. Cheul, and T. Ise, "Multilevel PWM inverters suitable for the use of stand-alone photovoltaic power systems," *Energy Conversion, IEEE Transactions on,* vol. 20, pp. 906-915, 2005.

[34] Solar Accreditation. (2014, 11/06/2014). *Australian Clean Energy Council: Inverter Standards*. Available: https://www.solaraccreditation.com.au/products/inverters.html

[35] K. De Brabandere, B. Bolsens, J. Van den Keybus, A. Woyte, J. Driesen, and R. Belmans, "A Voltage and Frequency Droop Control Method for Parallel Inverters," *Power Electronics, IEEE Transactions on,* vol. 22, pp. 1107-1115, 2007.

[36] T. Longcheng, L. Yaohua, L. Congwei, W. Ping, and L. Zixin, "Advanced voltage control methods for current source inverters with linear and nonlinear loads," in *Industrial Electronics, 2009. ISIE 2009. IEEE International Symposium on*, 2009, pp. 1534-1539.

[37] N. Uemura and T. Yokoyama, "Current control method using voltage deadbeat control for single phase utility interactive inverter," in *Telecommunications Energy Conference, 2003. INTELEC '03. The 25th International*, 2003, pp. 40-45.

[38] M. A. Rezaei, S. Farhangi, and G. Farivar, "An improved predictive current control method for grid-connected inverters," in *Power Electronic & Drive Systems & Technologies Conference (PEDSTC), 2010 1st*, 2010, pp. 445-449.

[39] E. Shimada and T. Yokoyama, "Current Control Method Using Voltage Deadbeat Control with Multi Sampling Pulse Compensation for Single Phas Utility Interactive Inverter with FPGA based Hardware Controller," in *Telecommunications Conference, 2005. INTELEC '05. Twenty-Seventh International*, 2005, pp. 369-374.

[40] F. Blaabjerg, R. Teodorescu, M. Liserre, and A. V. Timbus, "Overview of Control and Grid Synchronization for Distributed Power Generation Systems," *Industrial Electronics, IEEE Transactions on*, vol. 53, pp. 1398-1409, 2006.

[41] A. M. Nordin and A. M. Omar, "Modeling and simulation of Photovoltaic (PV) array and maximum power point tracker (MPPT) for grid-connected PV system," in *Sustainable Energy & Environment (ISESEE), 2011 3rd International Symposium & Exhibition in*, 2011, pp. 114-119.

[42] R. J. Bravo, R. Yinger, S. Robles, and R. Salas, "Evaluation of a residential solar PV inverter with advanced features for the U.S. market," in *T&D Conference and Exposition, 2014 IEEE PES*, 2014, pp. 1-5.

[43] Y. Yongheng, F. Blaabjerg, and W. Huai, "Low-Voltage Ride-Through of Single-Phase Transformerless Photovoltaic Inverters," *Industry Applications, IEEE Transactions on*, vol. 50, pp. 1942-1952, 2014.

[44] P. Hothongkham, S. Kongkachat, and N. Thodsaporn, "Analysis and comparison study of PWM and Phase-Shifted PWM full-bridge inverter fed high-voltage High-Frequency Ozone Generator," in *Power Electronics and Drive Systems (PEDS), 2011 IEEE Ninth International Conference on*, 2011, pp. 776-781.

[45] "IEEE Standard Test Specifications for Surge-Protective Devices (SPDs) for Use on the Load Side of the Service Equipment in Low Voltage (1000 V and less) AC Power Circuits," *IEEE Std C62.62-2010 (Revision of IEEE Std C62.62-2000)*, pp. 1-60, 2011.

[46] S. Morinaga, Y. Sugiura, N. Muto, H. Okuda, K. Nandoh, H. Fujii, *et al.*, "Microprocessor Control System with I/O Processing Unit LSI for Motor Drive PWM Inverter," *Industry Applications, IEEE Transactions on*, vol. IA-20, pp. 1547-1553, 1984.

[47] M. Boztepe, F. Guinjoan, G. Velasco-Quesada, S. Silvestre, A. Chouder, and E. Karatepe, "Global MPPT Scheme for Photovoltaic String Inverters Based on Restricted Voltage Window Search Algorithm," *Industrial Electronics, IEEE Transactions on*, vol. 61, pp. 3302-3312, 2014.

[48] N. Pragallapati and V. Agarwal, "Flyback configuration based micro-inverter with distributed MPPT of partially shaded PV module and energy recovery scheme," in *Photovoltaic Specialists Conference (PVSC), 2013 IEEE 39th*, 2013, pp. 2927-2931.

[49] S. Veerapen and R. T. F. Ah King, "Integrating distributed energy resources in the electrical grid considering resource variability for reliable power planning," in *IECON 2012 - 38th Annual Conference on IEEE Industrial Electronics Society*, 2012, pp. 1356-1361.

[50] S. Chakraborty, T. Ito, T. Senjyu, and A. Y. Saber, "Intelligent Economic Operation of Smart-Grid Facilitating Fuzzy Advanced Quantum Evolutionary Method," *Sustainable Energy, IEEE Transactions on*, vol. 4, pp. 905-916, 2013.

[51] G. F. Reed, L. A. Solomon, and B. M. Grainger, "Prototype development of a full-bridge isolated boost converter for solar photovoltaic systems integration," in *Innovative Smart Grid Technologies Conference Europe (ISGT Europe), 2010 IEEE PES*, 2010, pp. 1-6.

Chapter 3

3. Variable Speed DC Diesel Generator

3.1 Introduction

In electricity generation, an electric generator is a device that converts mechanical energy to electrical energy. A generator forces electric current to flow through an external circuit. The source of mechanical energy may be a reciprocating or turbine steam engine, water falling through a turbine or waterwheel, an internal combustion engine, a wind turbine, a hand crank, compressed air, or any other source of mechanical energy. Generators provide nearly all of the power for electric power grids [1].

Currently, generators consist of an engine connected directly to an alternator to produce electricity. Since the electricity produced must be at a fixed frequency (50 or 60 Hz), the engine must rotate at a constant speed (1500 or 1800 RPM), no matter what the power demand.

One way to save fuel in a generator is to operate the engine at variable speeds. Diesel engine speed is controlled solely by the amount of fuel injected into the engine by the injectors. Since a diesel engine is not self-speed-limiting, it requires both a means of changing engine speed (throttle control) and a means of maintaining the desired speed. The governor provides the engine with the feedback mechanism to change speed as needed and to maintain a speed once reached [2]. A governor is essentially a speed-sensitive device, designed to maintain a constant engine speed regardless of load variation. Governors used on diesel engines may be classified as ‘speed-regulating’ since they control engine speed by regulating fuel delivery to the cylinders. The major function of the governor is determined by the application of the engine. In an engine that is required to come up and run at only a single speed regardless of load, the governor is called a constant-speed type governor. If the engine is manually controlled, or controlled by an outside device with engine speed being controlled over a range, the governor is called a variable-speed type governor. If the engine governor is designed to keep the engine speed above a minimum and below a maximum, then the governor is a speed-limiting type [3-5].

This chapter reviews the operation of conventional constant speed diesel generators and their associated problems. Variable speed generators are also discussed, with particular reference to the types available, the developments of the last 5 years, and the advantages of

their use. A mathematical model for the control of variable speed diesel generators is developed, and the simulation of variable speed diesel generator as an entire system is done in Matlab/Simulink environment and Pspice software. Preliminary experimental results from the prototype are presented. Finally, the reactive power control strategies of variable speed diesel generator generation systems are explained.

3.1.1 Conventional Diesel Generators

The conventional method for electricity generation to meet the demand in remote areas relies on the use of constant speed diesel generator (DG) sets. In these systems, diesel engines drive synchronous generators at a near constant speed which depends on the specified frequency and the number of poles in the generator. Current diesel engine models cannot maintain the precise rotating speed required to generate the 50Hz or 60Hz power, hence the actual speed fluctuates around the demanded constant speed. Consequently, the output frequency of such a generator varies proportionately. This frequency variation may have a harmful effect on modern appliances such as computers and other sensitive equipment [6].

Real-world load profiles are dynamic in nature and may vary dramatically as a function of time. The peak demand typically occurs for only a few hours of the whole day. Thus, the DG sets normally have to be heavily over-sized in relation to the local load conditions and often operate under a light load state. In this scenario, the fuel economy of a DG set is poor, since not all of the fuel is burnt in the combustion process. Moreover, the unburned fuel dilutes the oil in the cylinders and causes harmful and destructive conditions of excessive wear in the cylinder walls, cylinder glazing and carbon build-up, which will negatively affect engine performance and result in premature engine failure. Thus, manufacturers insist that diesel engines should ideally run at least around 60-75% of their maximum rated load. Short periods of low load running are permissible providing the set is brought up to full load, or close to full load on a regular basis. In large installations, multiple DG sets of different capacity are employed to ensure the DG sets are running following the application and operating guidelines. However, the complexity of such a system is apparent. In the case of smaller applications, multiple generator set operation is not practical or economical, and the use of simple dump loads is common practice. Excess generated capacity is diverted to the dump load sized at approximately 30-40% of rated power, until the total load on the engine exceeds 60-80% [7-9].

Due to the inherent problems of constant speed minimum operating load and poor efficiency at low load, in this research the use of various types of variable speed diesel generator is proposed and developed. At low loads the revolution speed of the generator will be reduced ensuring that the engine is running optimally in terms of fuel economy. Furthermore, the problem of unburnt fuel build-up is avoided, since combustion is more complete at lower loads [10].

The demand for electricity in remote areas with relatively small isolated communities is increasing and high voltage gridline extension to these areas is prohibitive due to financial and technical constrains. Therefore, DG sets combining a diesel engine and a synchronous generator are widely used in these areas for power generation [11].

Fossil fuel prices continue to increase world-wide in response to the ever-increasing demand for this resource (Figure 3.1). Remote locations that must rely on off-grid power often have a good renewable source of energy. By utilizing this resource in remote areas, their consumption of fossil fuels, and hence their production of carbon pollution, can be reduced [10].

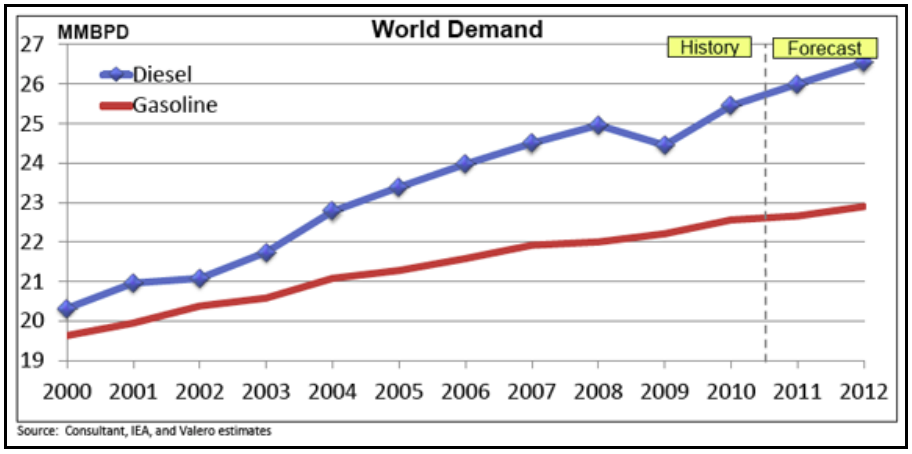

Figure 3. 1: Anticipated world growth in demand for gasoline and diesel [10]

3.1.2 Constant Speed Diesel Generator(s)

Conventional diesel generators used for power generation run at a constant speed to produce the constant voltage and constant frequency AC output required by common appliances [11]. Figure 3.2 shows the structure of a conventional diesel generator. It consists of a diesel engine and a synchronous generator. The diesel engine must run at a synchronous speed so that the output voltage has both a constant amplitude and a constant frequency. The constant rotating speed of a diesel engine under different power requirements is achieved

through the use of a fuel distributor, which controls the diesel intake. A voltage regulator is used to adjust the flux of the synchronous generator so that a constant voltage is produced. Thus, for a conventional diesel generator, the diesel engine realizes frequency control, while the synchronous generator controls output voltage amplitude [12-14].

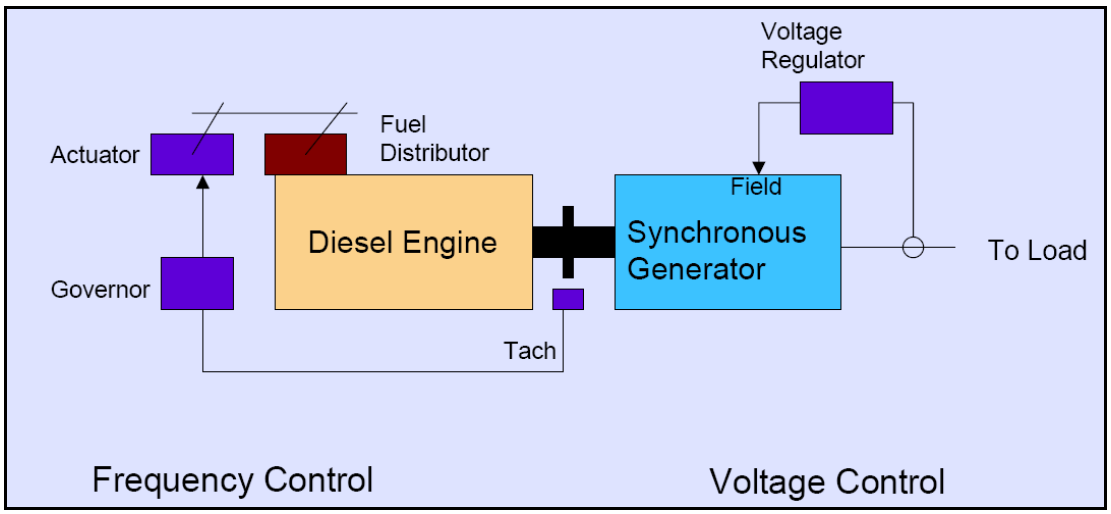

Figure 3. 1: Conventional Diesel Generator Configuration [15]

The typical load pattern for remote area power supplies is characterized by a small to medium base load, with periods of higher electricity demand during the day. The peak demand for electricity is typically observed in the evening for several hours. Since diesel generators providing power to remote communities are normally sized for peak loads, the average load is often as low as 30% of capacity, resulting in very poor fuel economy. Typical fuel efficiency characteristics for a 50kW DG is show in Figure 3.3 [15-17].

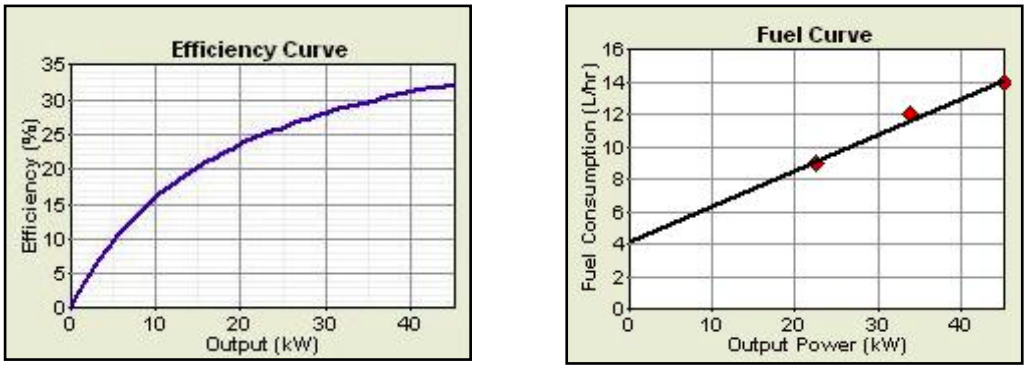

Figure 3. 2: Typical fuel efficiency characteristics for a 50kW DG [18]

In remote areas, diesel fuel is more expensive due to the high cost of transportation. The lifetime fuel expenditures are often ten times the purchase cost of a diesel generator.

In large installations, the problem of under-loading engines is overcome by employing multiple DG sets running at constant speed which are brought on line or shut down as the load demand increases or decreases so as to operate with high capacity factors at all times. However, in smaller applications, multiple DG set operation is not practical or economical, and the use of simple dummy loads is common practice. The "dump loads" deliberately dissipate energy when useful demand is low, thus loading the engine generator to a sufficient level. Another solution is to use two generators: a smaller generator and a larger generator, as shown in Figure 3.4. When the load is light, the smaller generator is used. As the load is increased the larger generator is started and the load is manually transferred to it [19].

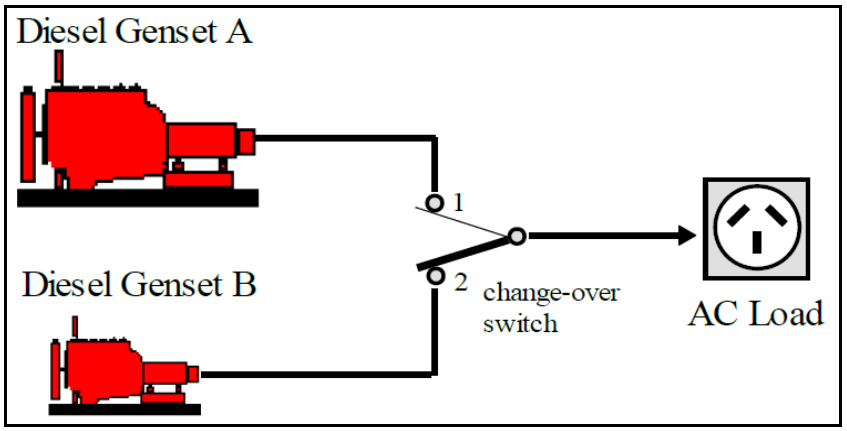

Figure 3. 3: Multiple DG sets for large installation

3.2 Diesel generators integrated with renewable energy sources.

In order to overcome the problems caused by light loading, diesel battery hybrid energy systems that combine renewable and conventional energy sources with batteries for energy storage have been developed. A sample configuration of a PV- diesel battery hybrid system is shown in Figure 3.5. These systems provide sufficient storage to allow the load to be shifted and ensure that the generator is always substantially loaded [20, 21]. However, their use is inhibited by the high cost of batteries (both initial and replacement), the loss of energy in the batteries and inverters, and the cost of managing and maintaining the system.

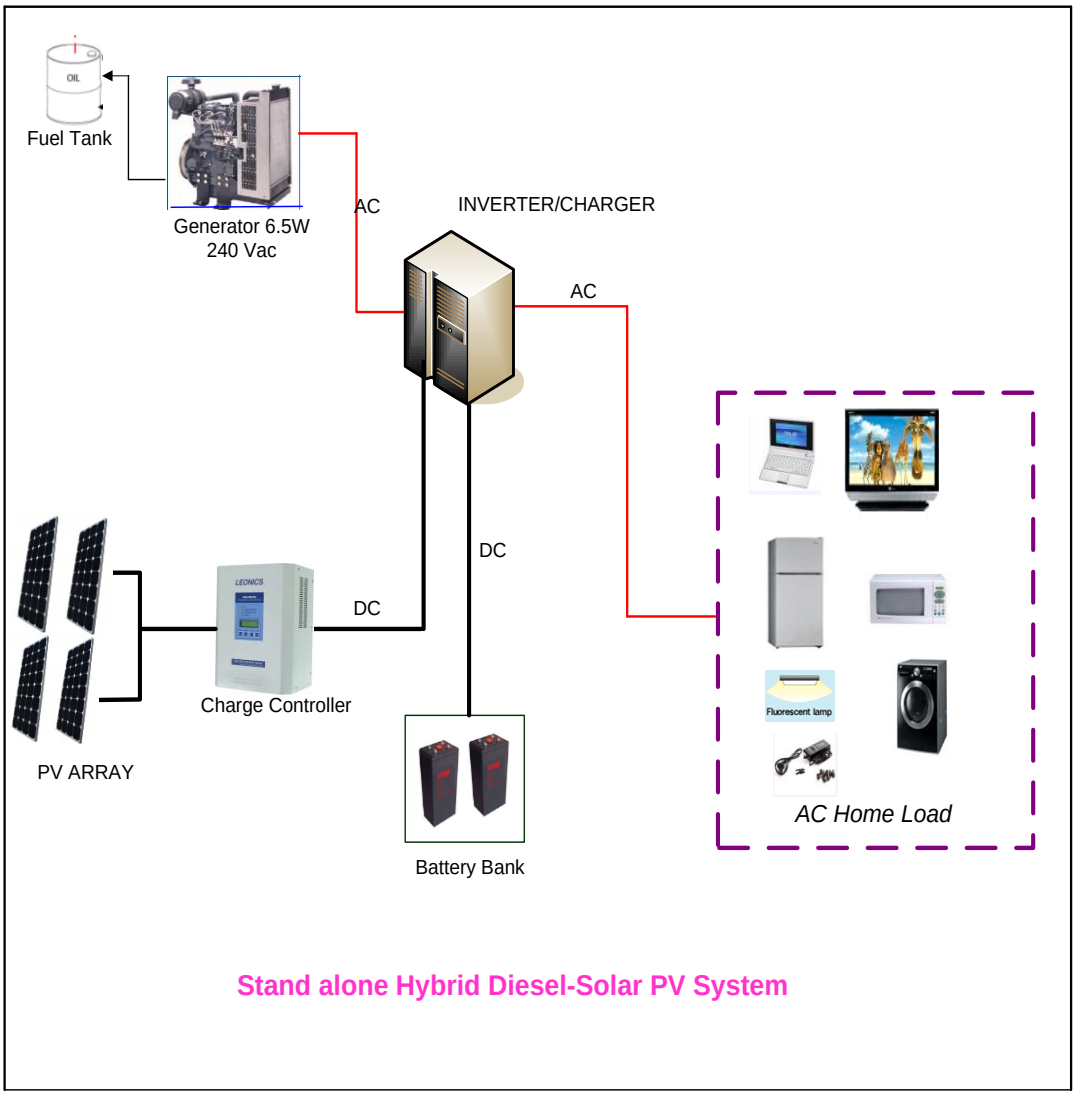

Figure 3. 4: Standalone Hybrid Diesel-Solar PV System

A decentralized distribution generation system (DDGS) that integrates renewable energy generation can be created to offset the cost of diesel produced electricity and supply cleaner energy. Renewable energy sources, such as photovoltaic (PV), wind energy, or small-scale hydro, provide a realistic alternative to engine driven generators for electricity generation in remote areas [22, 23]. Indeed, DDGS have been shown to significantly reduce the total life cycle cost of electric power supplies in many situations while maintaining power quality at an adequate level [24, 25]. One disadvantage of the DDGS is that the average efficiency of the conventional DG may be further compromised by the inclusion of a renewable energy source, since the load to the generator would be further reduced.

3.2.1 The variable speed diesel power generation concept

One way to avoid the fuel economy and maintenance problems associated with conventional diesel generators would be to operate the system at variable speed thus improving efficiency at part-load. The variable speed diesel generator is able to run at variable speed by using power electronic converters to change the VVVF (Variable Voltage Variable Frequency) produced by the generator to the constant voltage and frequency of the grid. In this way, the engine can be operated at the most efficient speed according to the imposed load [26-28].

3.2.2 Decentralized distributed generation system

In a decentralized distributed generation system (DDGS) power is generated by utilizing energy sources located close to the demand location. The DDGS may consist of any autonomous electricity generating system including both primary and secondary load diesel generators combined with a renewable energy source combining renewable energy sources and conventional generators [18, 29].

Although the use of renewable energy sources such as solar and wind power technology is attractive, their power output is often dependent on weather conditions. For this reason, a novel design approach for DDGS using a standard design with battery storage and a variable speed diesel generator, is proposed. In such a system, any excess energy could be stored in batteries and discharged at a set rate, with the batteries recharged as necessary by the diesel generator [30, 31].

The lifetime of a conventional battery is typically not more than ten years under optimal conditions. Their inclusion in a DDGS would provide a weak link, since a lifetime of at least 20 years is required for a remote area DDGS to be cost-effective. Furthermore, the lifetime rating of lead acid batteries, which to date would be the battery of choice for such a system, is influenced by the ambient temperature. Generally, lead-acid battery life time is halved by raising the average ambient temperature by 10 °C. The effective use of these batteries in a DDGS in a hot region would require an air-conditioned battery room. Variable speed diesel generator technology inclusion in a DDGS would circumvent this problem.

3.2.3 DC Variable Speed Generators

The DC genset comprises a variable-speed diesel engine coupled to an alternator that is specifically configured to directly connect to a battery bank (more often acting as a buffer). An external DC/AC inverter is employed when AC power is desired.

In a DC genset, the engine operates at a variable-speed similar to that of a variable-speed AC genset. The reason for this is twofold. Firstly, the standard nominal voltages of 48V in both fields of application are common. Secondly, the prime movers, which are IC engines in both cases, have a variable- speed character with comparable operating speed range (~700 – 3000rpm for large diesel vehicle engines like those of buses and trucks, and ~1000 – 3600rpm for variable speed genset diesel engines).

A number of electrical machine technologies can be used in DC alternators, namely: induction (asynchronous) machines (IM or AM), permanent magnet synchronous machines (PMSM), wound rotor synchronous machines (SM), and switched- reluctance machines (SRM).

The PMSM is generally considered to be the most efficient of these, to have the highest power density, and to require the least maintenance. However, the PMSM is also the most expensive, due to the high cost of the magnets that are required as power electronic converters for regulating output voltage. A more economical version of this system is the permanent magnet hybrid homopolar (PMHH) that requires a minimum of power electronics.

The wound rotor SM, with its simpler circuit design that facilitates voltage design, is considered to be cheaper than the PMSM. However, this system is also less efficient, has a lower power density, and needs higher maintenance when the brush-type design (cheaper solution) is used [30-32].

The IM (or AM) is also generally cheaper than the PMSM. This system requires power electronic converters (with bi-directional power flow capability) in combination with a battery source and/or large capacitors when used in stand-alone (non-grid fed) application. It is currently one of the candidate machines employed in the integrated starter-generator (ISG) application. Due to the low power density of the conventional squirrel cage-rotor design for the IM, alternative machine (rotor) designs that are compact enough to be integrated under-the-bonnet (under-the-hood) are needed for application in vehicles.

The alternators used in most DC gensets are based on PM technology and use either conventional PMSM with DC/DC converter or PMHH technology. DC gensets, though relatively new, are already popular in marine and remote land applications because of their ability to quickly recharge batteries due to their high DC current output capability compared to grid connected or conventional AC genset powered battery charger rectifiers. This configuration is shown in Figure 3.6 [33-35].

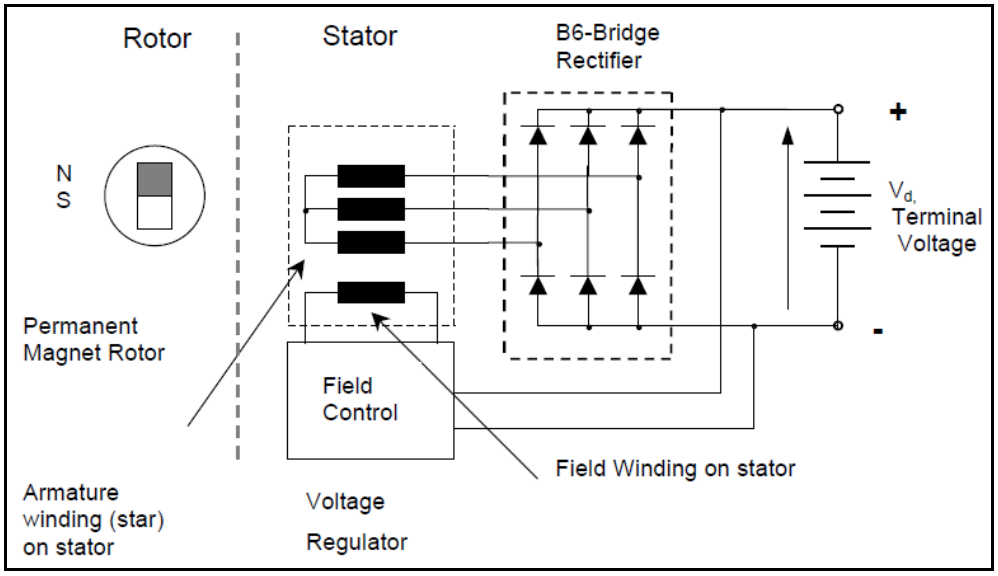

Figure 3. 5: Permanent magnet hybrid homopolar (PMHH) DC alternator [34]

The conversion of DC power into AC represents an extra power conversion step. However, the efficiency of a good PM alternator together with rectifier (75 – 85%) and an inverter (90 – 94%) is comparable to the efficiency of a good synchronous or induction machine AC genset (70 – 80%). The major source of inefficiency in a DC generator/inverter combination system is in the battery charge/discharge cycle. A battery is only about 80% (and sometimes as low as 40%) efficient, depending on the age of the battery and the charge cycle method.

3.2.4 Fuel Saving by Variable Speed Operation

The factors that affect the fuel efficiency of variable speed operation diesel generators include: diesel engine fuel consumption as a function of load demand and engine speed, the chosen speed versus engine torque relationship, the power conversion efficiency, and the relationship between the performance characteristics of VSDG and the load profile. To maximize fuel efficiency subject to limitations of engine and generator characteristics, the engine speed should be determined by best speed torque relationship, which can be done with system performance maps. Once the system performance map is designed, variable speed systems would provide the most fuel savings where the average load is much less than the peak capacity of power system [18, 36].

3.2.5 Diesel generator fuel efficiency

Diesel generator fuel efficiency is directly proportional to the efficiency at which fuel is burned to produce electrical power. The net fuel conversion efficiency is based on a combination of mechanical efficiency, generator efficiency and thermal efficiency. Mechanical and generator efficiencies increase when the load of the generator is increased, and the operation speed is decreased. In contrast, thermal efficiency, that is the conversion efficiency of the chemical energy in the fuel into work in the cylinder, is roughly constant with load and speed. Lower fuel inputs result in lower pressures and proportionately less work in the cylinder, as well as lower temperatures and proportionately less heat transfer and exhaust energy loss. The approximate fuel consumption of common diesel generators is presented in Table 3.1 [37, 38].

Table 3. 1: Approximate fuel consumption chart of common diesel generators [38].

Generator Size (kW)	1/4 Load (gal/hr)	1/2 Load (gal/hr)	3/4 Load (gal/hr)	Full Load (gal/hr)
20	0.6	0.9	1.3	1.6
30	1.3	1.8	2.4	2.9
40	1.6	2.3	3.2	4.0
60	1.8	2.9	3.8	4.8
75	2.4	3.4	4.6	6.1
100	2.6	4.1	5.8	7.4
125	3.1	5.0	7.1	9.1
135	3.3	5.4	7.6	9.8
150	3.6	5.9	8.4	10.9
175	4.1	6.8	9.7	12.7
200	4.7	7.7	11.0	14.4
230	5.3	8.8	12.5	16.6
250	5.7	9.5	13.6	18.0
300	6.8	11.3	16.1	21.5
350	7.9	13.1	18.7	25.1
400	8.9	14.9	21.3	28.6
500	11.0	18.5	26.4	35.7
600	13.2	22.0	31.5	42.8
750	16.3	27.4	39.3	53.4
1000	21.6	36.4	52.1	71.1
1250	26.9	45.3	65.0	88.8
1500	32.2	54.3	77.8	106.5
1750	37.5	63.2	90.7	124.2
2000	42.8	72.2	103.5	141.9
2250	48.1	81.1	116.4	159.6

A typical fuel consumption characteristic of diesel engine is shown in Figure 3.7 and in Figure 3.8 the fuel consumption of a variable speed diesel generator is shown. The diesel engine can be operated at the speed window between ω_{dmin} and ω_{dmax}. In order to output 50Hz frequency voltage, the engine in a conventional 4-pole diesel generator has to run at a fixed speed of 1500rpm. The blue line represents the fixed speed power curve of diesel engine. Curves of Kmax, K1, K2, K3, K4 represent the fuel efficiency.

For fixed speed operation, the higher power the output, the higher fuel efficiency that will be achieved. Fuel consumption almost increases linearly with load. Thus, for heavy load operation, the fuel efficiency is close to maximum, whereas in light load operation, the fuel efficiency becomes poor. Moreover, the fuel cannot be fully burnt at synchronous speed under a light load, resulting in excessive maintenance problems, or even engine damage. If the engine speed could be adjusted to follow the optimum fuel efficiency curve according to power demand, then fuel consumption would be reduced. As Figure 3.7 shows, to produce the same power, Pd, for constant speed operation, the fuel efficiency is K4. If the engine speed is reduced to $\omega_{dmin,}$ the operation point would shift to point F2 that represents higher fuel efficiency. Thus, using the same diesel engine, variable speed operation can achieve higher fuel efficiency that results in producing more power than constant speed operation [39].

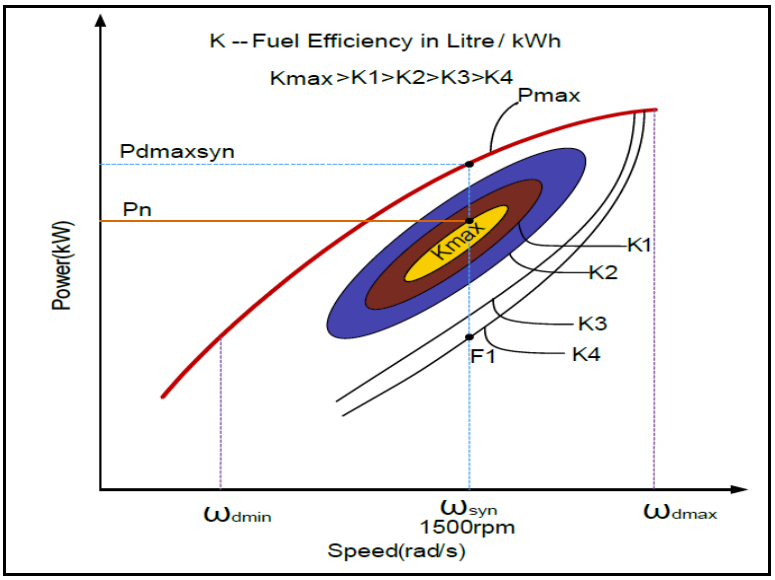

Figure 3. 6: Power and specific fuel efficiency of diesel engine driving synchronous generator [39]

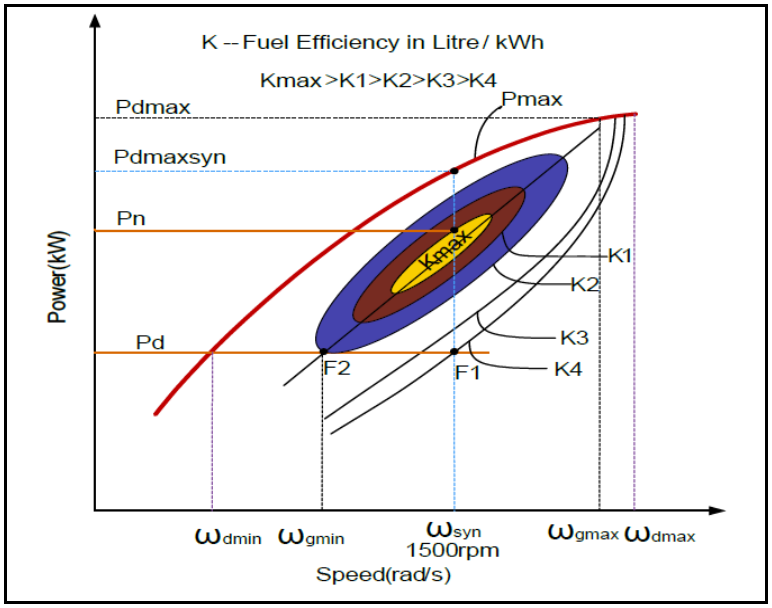

Figure 3. 7: Power and specific fuel efficiency of the diesel engine driving variable speed generator [39]

3.2.6 Diesel engine performance maps

The exact fuel savings obtained by operating the diesel engine at variable speeds depend on the relationships between the system speed and power, and between the load profile and system characteristics. Diesel engine performance maps provide the basis for determining the most fuel-efficient speed-power relationship given a specific diesel engine and generator. Performance maps typically plot fuel efficiency, expressed as fuel consumption per delivered unit of energy, for example Litre/KWh, versus engine speed and load.

Figure 3.9 shows the diesel generator performance map for the 15kW diesel generator tested at Regen Power Pty Ltd. Each line represents generator operation when a constant volume of fuel was delivered per kWh, and is shown as a function of delivered generator power and speed. The system did not include any electronic power conversion. Standard operation for this constant speed system places the diesel generator operating points along the vertical 1500 rpm line between 2 and 16 kW. Such operation results in specific fuel consumption of no less than 0.416Liter/kWh, which is near rated output power, but not near the most efficient point of the system. The impact of weather conditions on the performance of such a diesel generator was not specifically investigated for this dissertation. However, the

performance characteristics of the diesel engine would vary significantly with change in ambient conditions.

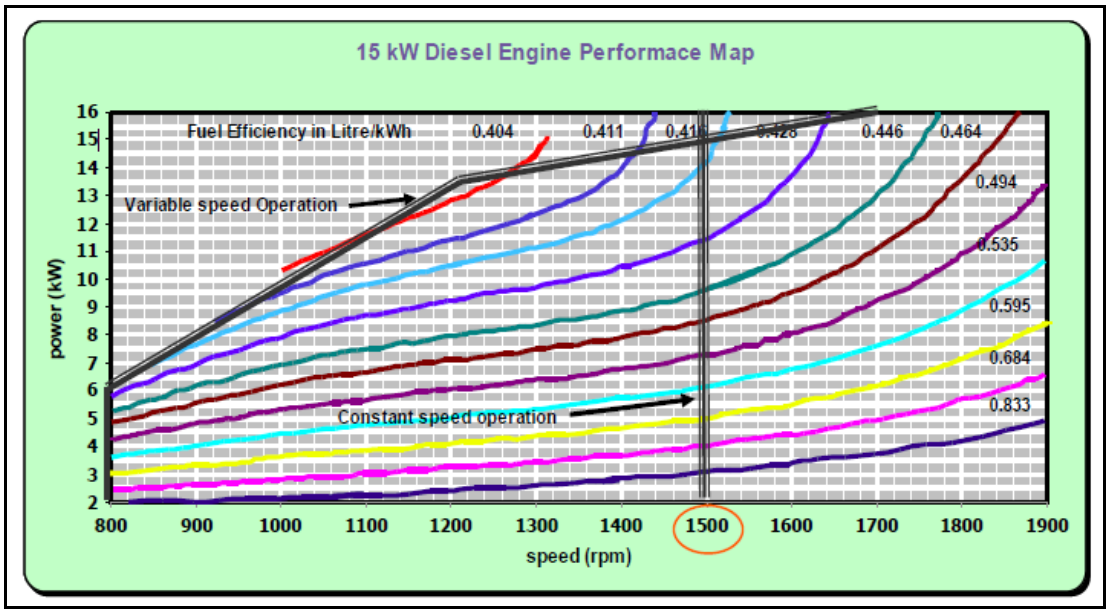

Figure 3. 8: Diesel Engine Performance Map

From the diesel generator performance map and converter efficiency map, a performance map for power delivered from the power electronics as a function of speed and delivered power can be derived. Figure 3.10 illustrates such a map for the 15 kW variable speed system.

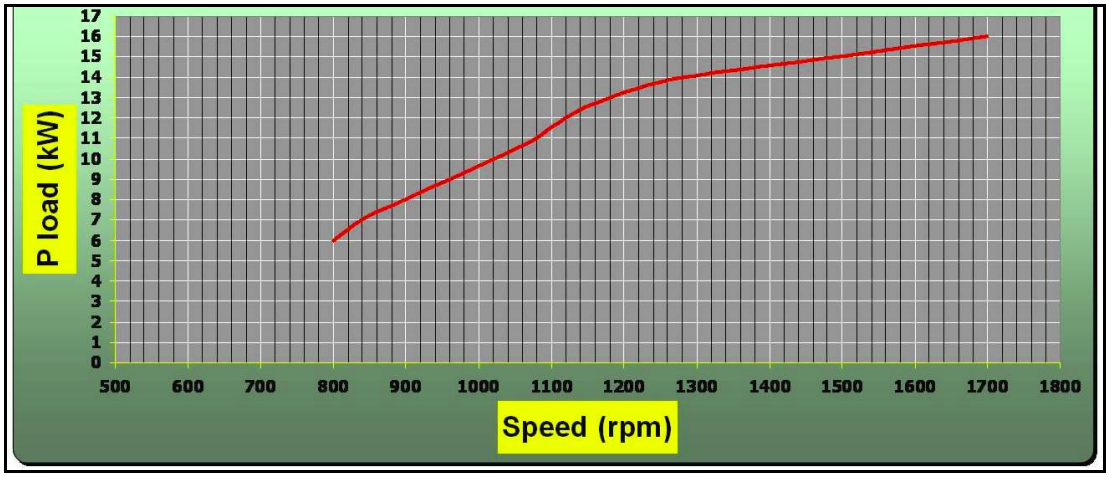

Figure 3. 9: 15 kW Diesel Engine Performance Map

Figure 3.10 shows Power Output Vs Optimum Shaft Speed for a 15kW Diesel Engine. As can be seen by comparison with the previous two figures, such variable speed

operation would vastly reduce fuel consumption. Constant speed operation has a minimum specific fuel consumption of 0.416Liter/kWh at 15 kW, which increases as the load decreases. With the variable speed system specific fuel consumption would remain below 0.416Liter/kWh even if the power was reduced to 6 kW (40% of rated system capacity).

3.2.7 VSDG fuel consumption vs. Generator Output

The choice of the power-speed relationship for variable speed operation determines the system fuel consumption as a function of delivered power. Table 3.2 illustrates the expected improvement in fuel consumption using the variable speed operation defined in Figure 3.9 and Figure 3.10 for the 15 kW diesel generator set.

Table 3. 2: Variable Speed Fuel Efficiency vs. Fixed Speed Fuel Efficiency Power

Power Output (kW)	Variable Speed Point of operation	Fixed Speed Point of operation	Variable Speed Fuel Consumption (mL/min)	Fixed Speed Fuel Consumption (mL/min)	% Fuel Savings in VSDG
2	958	1500	20	38	47
4	1042	1500	26	44	41
6	1083	1500	40	59	32
8	1083	1500	46	61	25
10	1083	1500	58	77	25
11	1125	1500	67	86	22
12	1208	1500	71	93	24
14	1375	1500	92	104	12
15	1500	1500	120	120	0

3.2.8 Long Term variable speed diesel generator fuel savings

The most fuel efficient speed-power relationship in a VSDG is determined by the engine, generator, and power converter characteristics, but ultimate fuel savings depend on the relationship between the end use load profile and the variable speed system characteristics.

Figure 3.11 shows a typical fuel efficiency curve of a diesel engine in variable speed and constant speed operation, where it shows that VSDG provides fuel savings, especially at low engine loads, in spite of the power converter losses. At high load, inverter losses make a variable speed system no more efficient than a constant speed system. Thus, for single diesel systems, variable speed systems are most applicable where the peak power system capability is large compared to the average load. Such systems might include systems sized for future

expansion, or sized for peak seasonal loads with a much smaller average load. In multiple diesel systems only one diesel engine needs to be a variable speed DG set. The others could operate at a fixed high load for high efficiency while the variable speed diesel load could fluctuate over its range, providing significant savings.

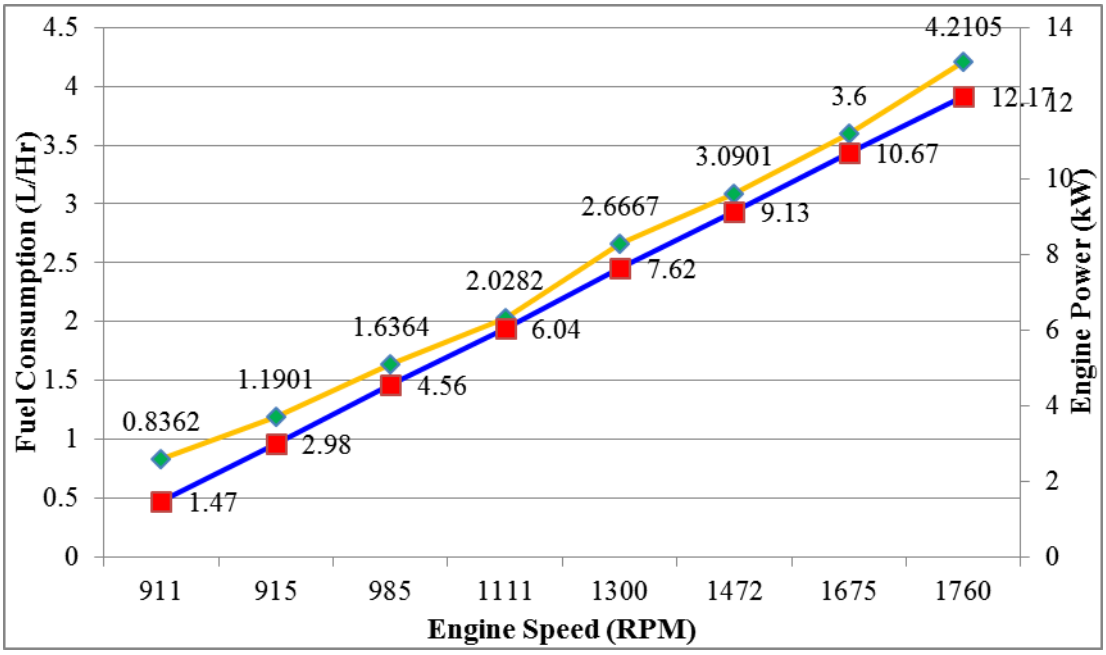

Figure 3. 10: Typical fuel efficiency curve of a diesel engine in variable speed

3.2.9 Adjusting engine speed to power demand

Operating a Genset at fixed speed (1500 or 1800 RPM) is similar to having a car stuck in 3rd gear at 30 mph. When climbing a hill (high power demand) it would be more efficient in a lower gear (e.g. 2nd) at a higher rev. Conversely, when going downhill (low power demand) it would be more appropriate to be in overdrive to save fuel. This is the basic idea behind variable speed Gensets. As an additional example, suppose a Genset is powering a fishing camp. At night, everyone is asleep so power demand is very low. In this case, the engine will slow down to save fuel (and reduce noise). In the morning, when power demand is high, the engine speed can be increased to meet the increased power demand.

There are a number of Genset applications for which power demand varies greatly that can benefit from an adjustable Genset. Examples of such applications are: sporting camps where demand varies as visitors come and go; cooking facilities on oil, gas and mineral exploration sites; construction sites where demand fluctuates night and day; remote

houses, cabins and villages; trucks or railway cars that carry refrigerated cargo; and telecom towers with air conditioning units that start and stop.

3.2.10 Fuel savings

A variable speed Genset saves fuel in two ways. First, running the engine at its most efficient speed for a given power demand allows for considerable fuel savings. Second, a variable speed Genset can use a smaller engine than a fixed speed Genset of the same power rating. A smaller engine for the same job means additional fuel savings.

3.2.11 Reduced noise and prolonged engine life

Almost all the noise produced by a Genset is due to the engine and its revolution speed. When the engine speed is reduced, noise is also greatly reduced, which means that in power saving mode, when the engine is at a low speed, a variable speed Genset is much quieter.

Variable speed Gensets can prolong engine life in two ways. First, moving parts in an engine are subjected to one "load cycle" every time the engine rotates. A reduction in speed results in a reduction of the number of load cycles to which mechanical components are subjected and an extension to engine life. Secondly, a common problem in engines called bore glazing or wet stacking is eliminated. Bore glazing usually occurs when an engine runs too cold and combustion is inefficient. This happens in fixed speed Gensets when operating at low load, as when the engine runs colder, deposits form on the cylinder walls of the combustion chamber. When the engine is continuously at its most efficient point, as is the case with variable speed Gensets, it remains hot and bore glazing is greatly reduced and/or eliminated.

3.3 Hybrid Generator

Modelling approaches of hybrid power systems are prevalent and can be studied from general publications. Although the analytical performance model of conventional CSDG has long been in existence, such data is not readily available for VSDG. In the only published study prior to these dissertation, in which the operation of variable speed operation of diesel generators in hybrid power systems was investigated, the system architecture using a variable speed diesel generator provided benefits both in system operation and financially [40].

Discussion on VSDG model for system performance analysis is carried out in this chapter along with modelling of the other components. Fuel consumption characteristics of

CSDG and VSDG that were used for simulation are shown in Figure 3.12 and Figure 3.13 respectively. From the graph in Figure 3.12 fuel consumption of the CSDG is 0.96L/hr during no load operation while there is only 0.67 L/hr for the VSDG. This shows that VSDG consumes approximately 30% less fuel when compared to the CSDG in a similar operating condition. Also, it can be seen that VSDG has higher fuel efficiency than the conventional CSDG, especially during low load operation. With these characteristics, it is anticipated that in terms of fuel consumption, the hybrid power system that has a VSDG will outperform a system that is using CSDG.

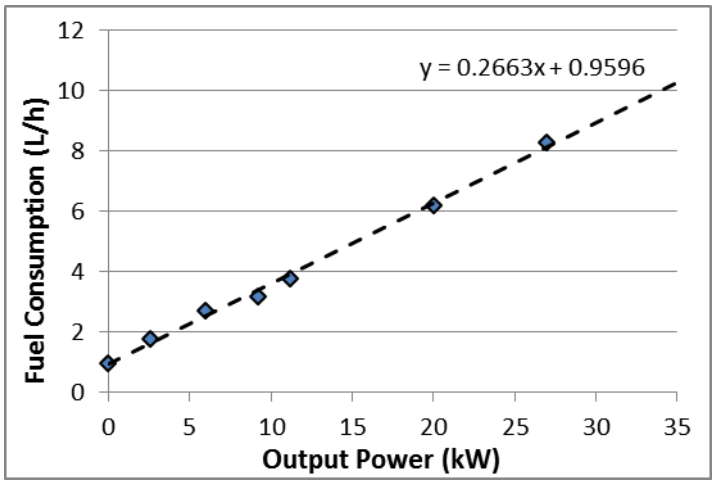

Figure 3. 11: **Fuel consumption versus power production of a CSDG [41]**

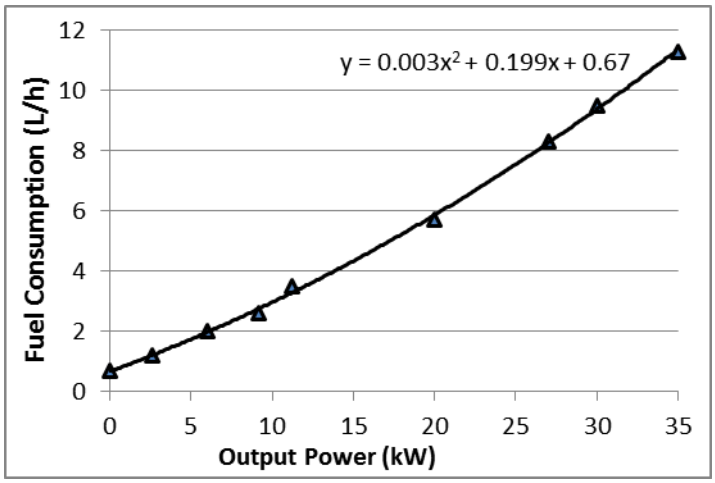

Figure 3. 12: Fuel consumption versus power production of a VSDG [41]

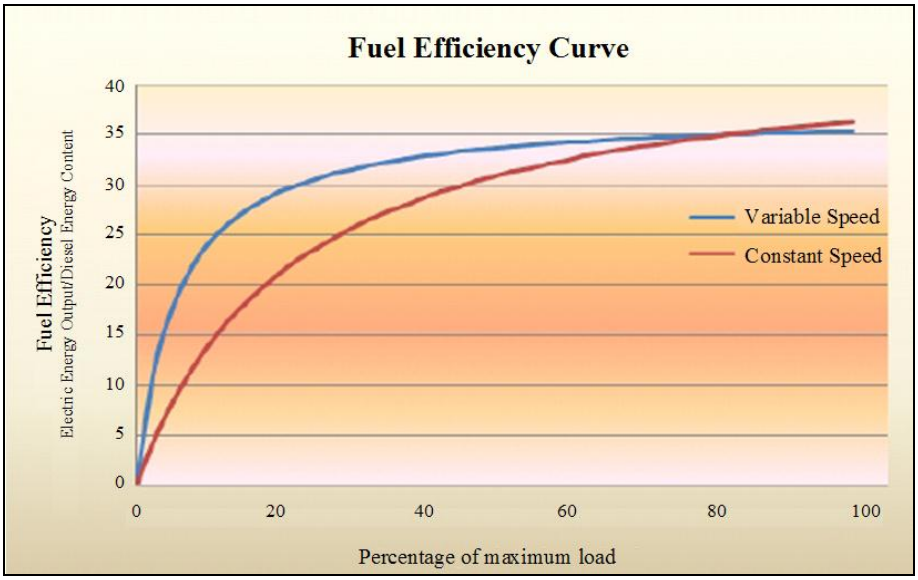

Figure 3. 13: Fuel efficiency in variable speed and constant speed engines [41]

Analytical performance models of hybrid power system in the following sections were used for system-level simulation to compare the operation of systems with different types of diesel generators. Dynamic and fast response operation conditions were not investigated. Simulations of the systems were based on the following assumptions:

- System operations were in steady state;
- Power supply and demand were balanced in each simulation time step;
- System operations were continuous (events such as breakdowns or maintenance were disregarded);
- Renewable resources and load demand remained constant within a simulation time step.

The selection of an appropriate simulation tool for analyses of the hybrid power system performance was critical. Although HOMER is recognized as the most commonly used software for hybrid power systems simulation for the purpose of general logistic performance analyses, it is better to use Matlab and PSpice.

The versatile simulation environment provided by PSpice MATLAB/Simulink was well suited to this research study. All system components were modelled using this simulation tool and the simulation results were validated through comparison with the results provided by the benchmark simulation tool. Ideally, the validation of component models should involve empirical data obtained from several system configurations and different modes of operation. Unfortunately, detailed validation is a demanding and time consuming

activity which is beyond the scope of this thesis. Also, data from systems with different configurations is not always available. Thus, the electrical simulation results of HOMER were used for model comparison, evaluation and validation. While this approach requires additional effort for developing all system component models in Simulink, its flexible simulation environment is propitious as it provides unrestricted possibilities to explore the proposed power management strategies. The interactive MATLAB workspace can facilitate the data transfer between different software tools. In addition, the ready-to-use blocks available in Simulink tool-boxes have eased the complex programming for the component models [42].

3.3.1 DC Variable Speed Diesel Generator Operation

DCVSDG is smartly controlled and manages the cyclic energy flow between the generator, renewable energy sources, battery bank and load in order to minimise the fuel consumption while providing reliable power to the load.

The Charge–Discharge Cycle is as follows: -

- **Charging Cycle**

The VSDG starts up when it senses that the Battery Bank state of charge (SOC) has reached the lower bound of its pre-set level. During the charging cycle, the VSDG runs at the optimum speed to support the Load as well as supplying a charge current to the Battery Bank. The maximum charge current that can be supplied is normally 0.1C for Lead-Acid Batteries (10% of the Battery Bank capacity). For example, for a 600Ah Battery Bank, this equates to a charging current of about 60A. This requires the VSDG to supply 3kW to the Battery Bank. When this is added to the Load, then it can be seen that the VSDG must supply around 5kW (for 1.5kW – 2kW Load) during the charge cycle. The Charge Cycle continues until the Battery Bank is full, when the charge current will be reduced to 0.01C, and the VSDG automatically turned off.

- **Discharging Cycle**

The Battery Bank will now supply the Load until it has discharged to the pre-configured SOC. Generally, the best lifespan vs cost trade-off is to discharge to 50% SOC. Consequently, there is a direct correlation between the depth of discharge and the number of cycles that a battery bank will perform before degrading. To illustrate this point, 50% of 600Ah is 300Ah which equates to 14.4kWh at 48VDC. For a

1.5kW Load this equates to 9.6 hours. So the discharge cycle is around 9.6 hours. When the Battery Bank reaches 50% DOD the VSDG will start and the Charge Cycle begins again.

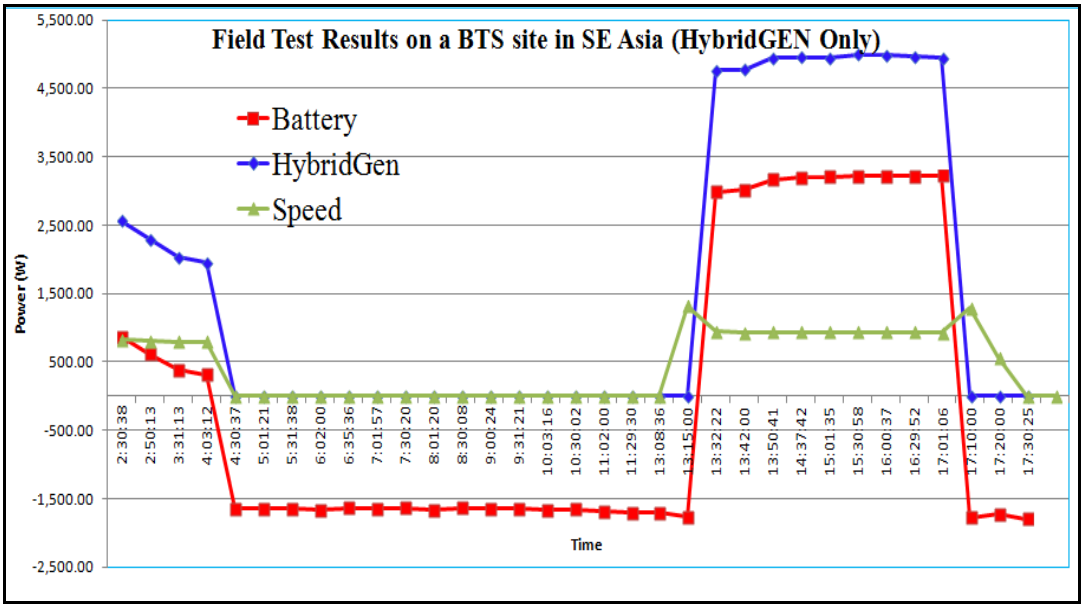

Figure 3. 14: BTS with VSDG Only

During the charge cycle, while renewable energy is generated, the current demanded by the Battery Bank from the VSDG is reduced and may even be nil. At this point, the VSDG only supports the Load and possibly a fraction of the charge current of the battery bank. The reduction in VSDG fuel consumption is dependent on the amount of renewable energy that is supplied.

During the Discharge cycle the VSDG is turned off. The Load is 100% supported by discharging the Battery Bank. All energy supplied by the renewable energy sources goes towards charging the Battery Bank. So, while the Battery Bank is being discharged, it is also being charged. If the renewable energy supplied is greater than the Load demand then the Battery Bank will receive net charging. If the renewable energy supplied is the same as the Load then the Battery Bank will maintain its SOC until the renewable energy reduces, at which point it will begin discharging. If the renewable energy supplied is less than the Load then the Battery Bank will net discharge, but at a slower rate than normal.

In all of the above cases, the net effect is that the discharge cycle period (the time that VSDG is switched off and not consuming any fuel) is extended. Each hour that this period is extended is an additional hour without diesel consumption. The length of the extended

discharge period depends entirely on the capacity of the renewable energy source, and the wind and sun resources available at the site.

It should be noted that the maximum charge current for most lead acid batteries is 0.1C. Thus, in order to achieve optimal RE capture, we should avoid sizing renewable energy sources greater than this value. For a 600Ah Battery Bank, this equates to limiting renewable energy current generated to 60A.

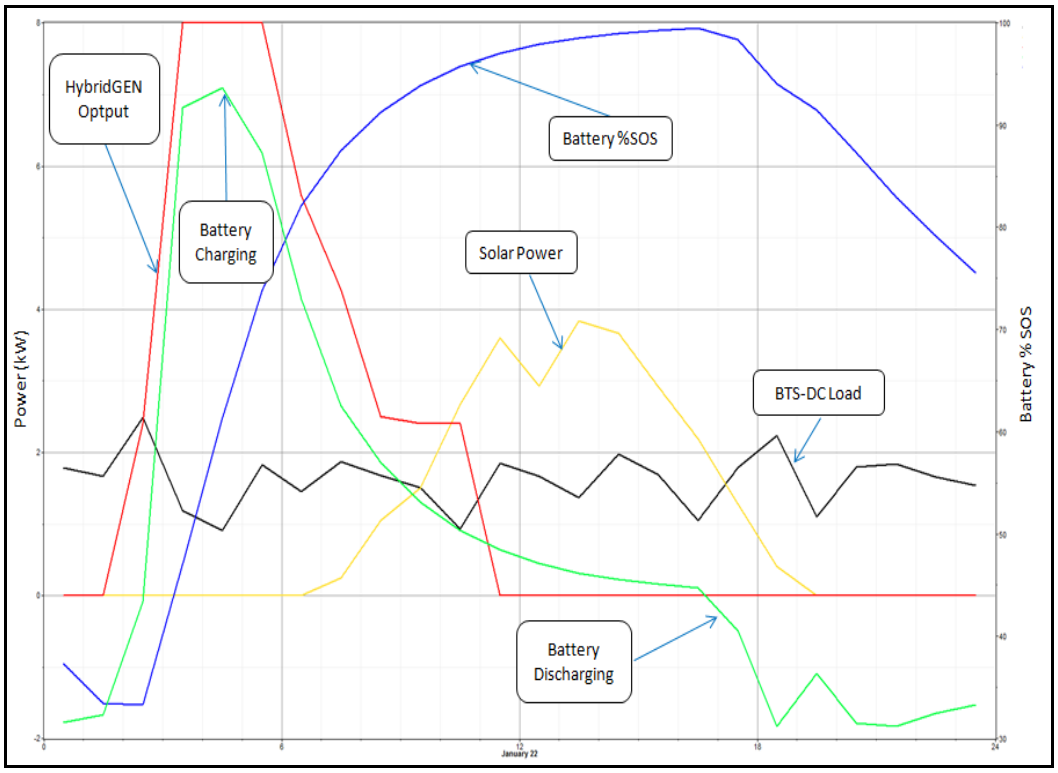

Figure 3. 15: Battery state of Charge and power

3.3.2 Variable Speed Diesel Generator

This DC VSDG is designed as a Perkins Engine coupled to a Standard AC Alternator at 50Hz. This is connected to the systems power electronics, ie a diode rectifier and LC filter unit, to change the output alternator AC to 48V DC output. The VSDG is then, in turn, connected to a battery bank and a constant load that have both been selected to meet customer requirements. The battery bank and the load are connected to the system through an Over Ground (OG) box. The block diagram in Figure 3.17 illustrates the VSDG.

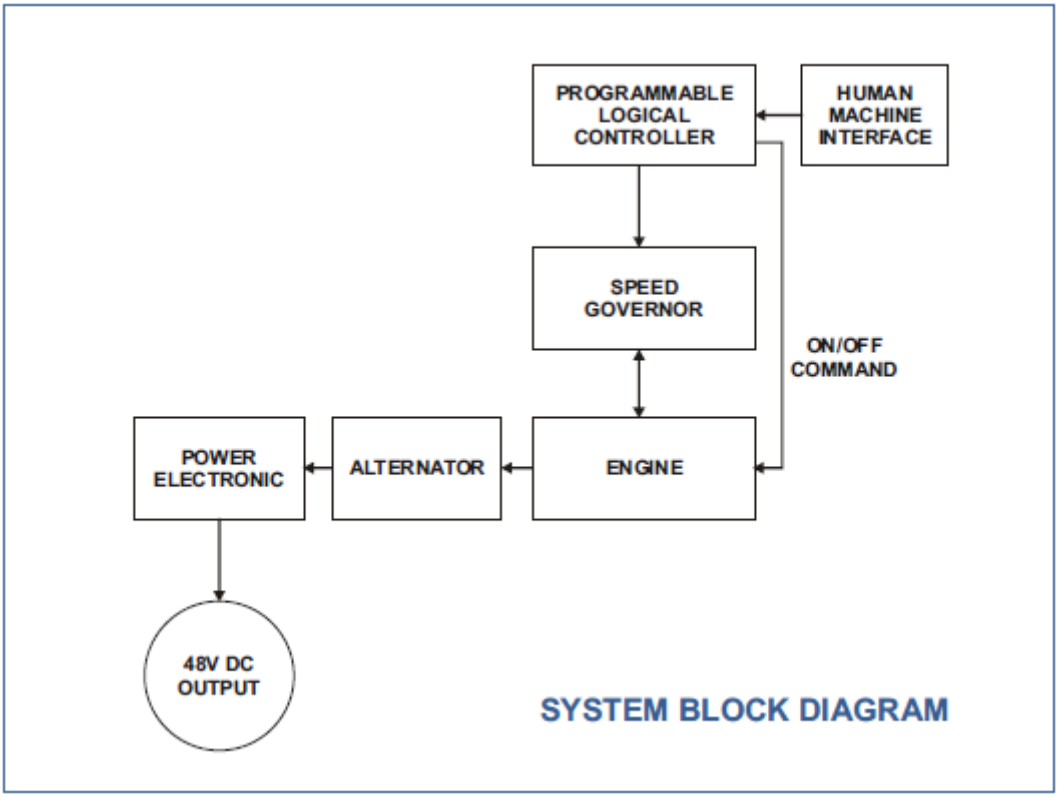

Figure 3. 16: VSDG System Block Diagram

3.3.3 How the system works

The VSDG works by connecting a desired customer sized battery bank to the system with a desired customer sized load. Once both of these have been connected to the system, the customer can enter these into the programmable parameters.

The system works as a two-step cycle system. When the battery bank state of charge is 100 percent, the DC generator will automatically stop running and send a signal to the power electronics for the battery bank to supply the load. When the battery bank state of charge is at its programmable battery depth of discharge level, the generator will automatically start running and send a signal to the power electronics for the generator to charge the battery bank to 100 percent state of charge and supply the load.

The power electronics used in the application can be programmed manually, according to the specific requirements. On receipt of this information, the electronic Logical Controller can operate the engine and alternator accordingly. The Battery Bank and the Load are connected so that all components operate together efficiently when renewable energy sources – solar photovoltaic panels and wind generators are combined with the system.

3.3.4 Generator Electrical System

The DC Generator uses power electronics to convert variable voltage, variable frequency AC output from the generator to the nominal battery voltage (48V). The diagram presented in Figure 3.16 shows the generator main loop circuit diagram including the power electronics used to transform the output current and voltage.

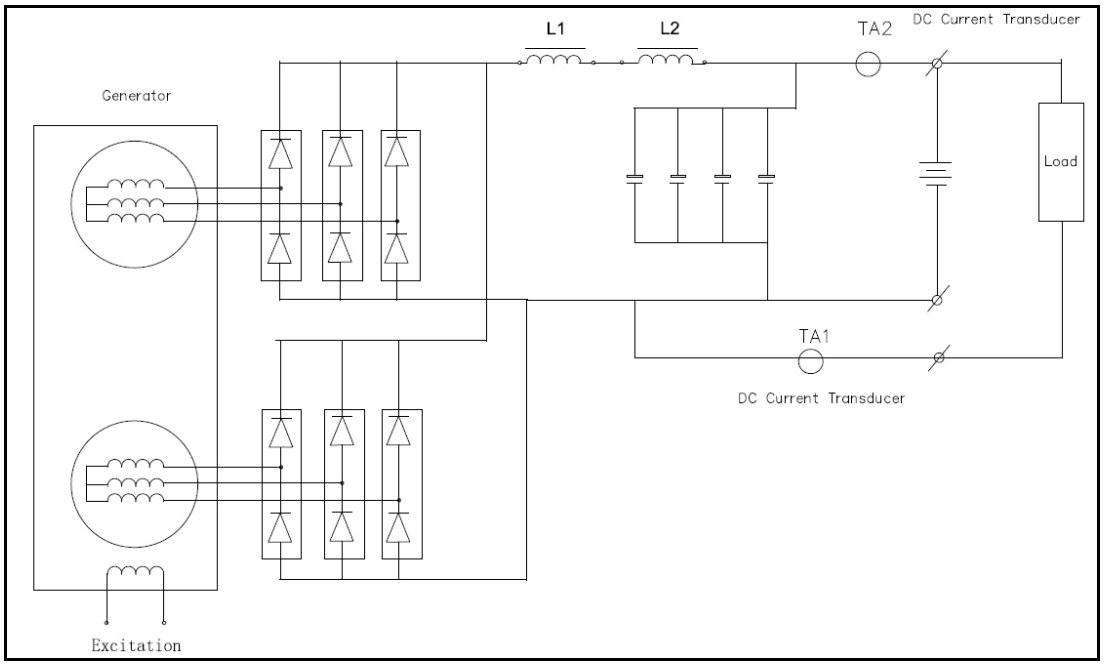

Figure 3. 17: Generator main loop circuit diagram

On the left-hand-side of the diagram, each of the 3-phase outputs from the stator of the alternator are connected to a pair of thyristor in series. A thyristor is a solid state semiconductor device with four layers of alternating N and P type material. In the VSDG they act as bistable switches, conducting when their gate receives a current trigger and continuing to conduct while they are forward biased (that is, while the voltage across the device is not reversed). Thus, they emulate the more basic function of a diode, allowing current in one direction only.

The circuit arrangement of each alternator output phase connected to a pair of thyristor forms a 3-phase bridge rectifier (or 6 pulse bridge) which performs full wave rectification, as shown below. The far right-hand-side of the main loop circuit diagram shows the connections

to the main battery bank and the load. The current transducers measure the current drawn by the load and the battery, respectively, and this data is used for monitoring and control.

This diagram illustrates the inside of the control panel and the components which makes up the control system for the DC VSDG. The General Packet Radio Service (GPRS) module collects data from the Human Machine Interface (HMI) on-board the VSDG through serial ports (RS485). The transfer is done using HMI-established protocols. The system uses two protocols: MODBUS RTU and Free port communication. The GPRS module will then send the data through serial ports to the GPRS public network. Users can receive and transform data at the server side.

3.4 Diesel Generator Model Representation

An analytical performance model for the diesel generator was developed based on the power versus fuel consumption characteristics or measurements in datasheets provided by the manufacturer. Figure 4.17 show the models of diesel generator and controller in *Simulink*. Diesel generator fuel consumption characteristics were modelled using mathematical functions; characteristic of CSDG was represented by linear function and characteristic of VSDG was represented by polynomial function.

3.5 Long-term Performance Analysis of Various Off-grid Hybrid Power Systems

This section compares and discusses the long-term performance for three categories of off-grid power systems:

- Diesel-only systems;
- Hybrid power systems without battery;
- Hybrid power systems with battery;

Since it was not the intention of this research to create new tools for each and every analysis of different system configurations, the simulation of long-term performance for three different off-grid hybrid power systems was carried out using the Matlab, PSpice and HOMER simulation software package [43]. Diesel generators with same power ratings were used for each category. PV generator size was identical for both the hybrid power system configurations and those with an integrated PV generator. The PV generator size selected for the study provided approximately 20% of the annual renewable energy.

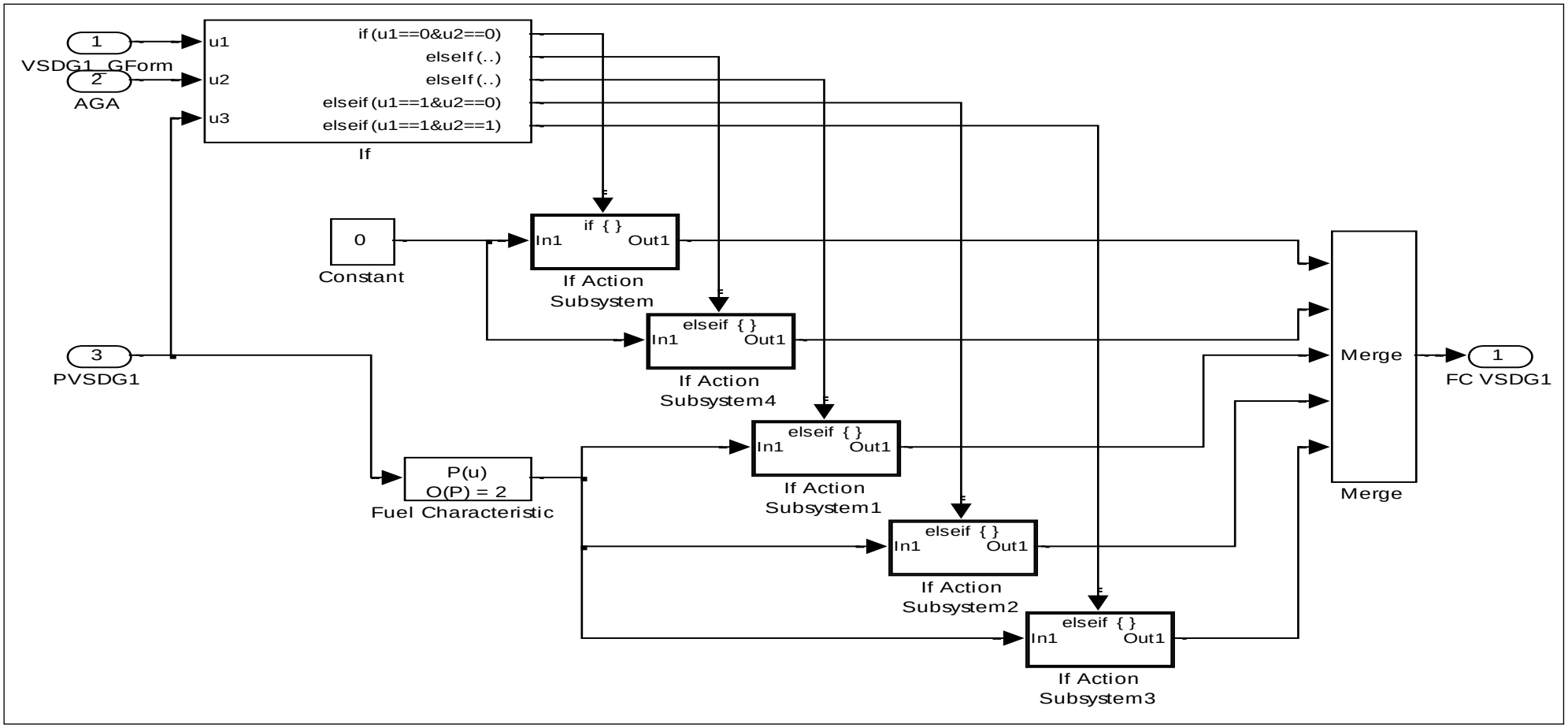

Figure 3. 18: Simulink model of diesel generator

Simulation results are tabulated in Table 3.3. The costs of electricity calculated were between AUD $0.30 to AUD $0.50. These values are comparable to the off-grid hybrid power system tariffs for Broome, Western Australia. From the results, it can be seen that diesel generator-only systems have the lowest initial capital costs. However, these systems have the highest fuel consumptions. The fuel costs indicated in the table are calculated based on the local diesel price in Broome, Western Australia of A$1.79.

For the environmental simulation results of the hybrid power systems, six types of pollutants were included in the HOMER simulation results: Carbon Dioxide (CO_2), Carbon Monoxide (CO), Unburned Hydrocarbons (UHC), Particulate Matter (PM), Sulfur Dioxide (SO_2) and Nitrogen Oxides (NO_x). In the absence of a renewable energy generator, the diesel-based systems produced high pollutant emissions. Retrofitting the CSDG-only and VSDG-only systems with PV generator reduced the primary polluting gas, CO_2, by 10% to 20%. The CO_2 emission in the PV-CSDG system was 10% higher than the PV-CSDG-Battery system. As for the PV-VSDG systems, with or without battery, the difference in CO_2 emissions between the configurations was negligible. The obvious environmental benefits of these four hybrid power systems did not provide sufficient justification for their use in off-grid power systems for remote locations. Therefore, the economic aspects of the systems were investigated in more detail.

The decision to implement a hybrid power system by off-grid owners is largely influenced by the initial cost of such a system and the long-term operating costs. Selection of a hybrid power system with a battery increases the initial investment by 70-75%, and also increases the annual operating costs, in comparison to a battery-free system.

Table 3. 3: Economic, environmental and electrical performance of various off-grid power system configurations

Parameter	CSDG-only	VSDG-only	PV-CSDG	PV-VSDG	PV-CSDG-Battery	PV-VSDG-Battery
Economic						
Initial capital cost	37,000	46,000	249,000	263,000	457,000	473,000
Operating cost (AUD$/year)	55,973	53,715	52,234	46,470	54,903	54,375
Total net present cost	755,520	736,663	939,722	876,043	1,173,845	1,177,091
Cost of electricity (AUD$/kWh)	0.309	0.301	0.384	0.358	0.480	0.481
Annual fuel consumed (L)	61,714	59,823	54,897	48,332	49,785	48,243
Annual fuel cost	71,588	69,394	63,680	56,065	57,750	55,962
Environmental						
CO_2 (kg/year)	162,513	157,533	144,562	127,275	131,099	127,040
CO (kg/year)	401	389	357	314	324	314
UHC (kg/year)	44.4	43.1	39.5	34.8	35.8	34.7
PM (kg/year)	30.2	29.3	26.9	23.7	24.4	23.6
SO_2 (kg/year)	326	316	290	256	263	255
NO_x (kg/year)	3,579	3,470	3,184	2,803	2,888	2,798
Electrical						
RE penetration (%)	0	0	19	20	20	20
Diesel Production (%)	100	100	81	80	80	80
Excess Production (%)	0.09	0	6.84	0.04	0.3	0.4

A quick comparison of the system configurations can be performed using the simple payback time (SPBT) as give in Equation (4.1)[44, 45]. As the SPBT does not account for the variation of system costs from one year to another [43, 46] , it can only be used as a guideline along with the details given in Table 3.3 for system configurations assessment.

$$SPBT = \frac{Excess\ cost\ of\ power\ system}{Rate\ of\ saving} \qquad (3.1)$$

Among the hybrid power system configurations, the PV-VSDG system without battery appears to provide the most balance between economic and environmental benefits. This system has the lowest annual operating cost, the lowest cost of electricity compared to the other three hybrid power system alternatives, as well as the lowest simple payback time (SPBT).

3.6 Fundamental Power Management Strategies

The core component for the power management of both Diesel Generator-only (DG) and hybrid PV-Diesel Generator (PV-DG) systems is the supervisory controller, which is responsible for ensuring reliable power supply in spite of variations in renewable sources or the load demand, while maintaining diesel generator operation within the prescribed power rating. The system level power management strategy, also known as dispatch and control strategy, involves starting and stopping the dispatchable components such as diesel generators and dump loads[47] .

3.6.1 Power Management for Photovoltaic-Diesel Generator System

The overall power management strategy for a system with an integrated renewable energy generator is depicted in Figure 3.20. The renewable energy source has the highest priority to supply the primary load demand. The net load, NL, is defined by the difference between the output from the renewable energy generator power supply and the primary load demand:

$$NL = P_{Load,pri} - P_{PV,inv} \qquad (3.2)$$

At any instant, when there is excess power after meeting the load requirements, i.e: NL < 0, the grid-form generator will operate at minimum allowable loading and the surplus power generated in the system drain through the dump load. In contrast, whenever there is shortage of power where the NL is greater than the minimum loading but lower than the rated

value of the grid-form generator, the grid-form power generation will meet the NL. If the NL exceeds the grid-form generator's power rating, the grid-feed generator will be activated to supplement the power supply.

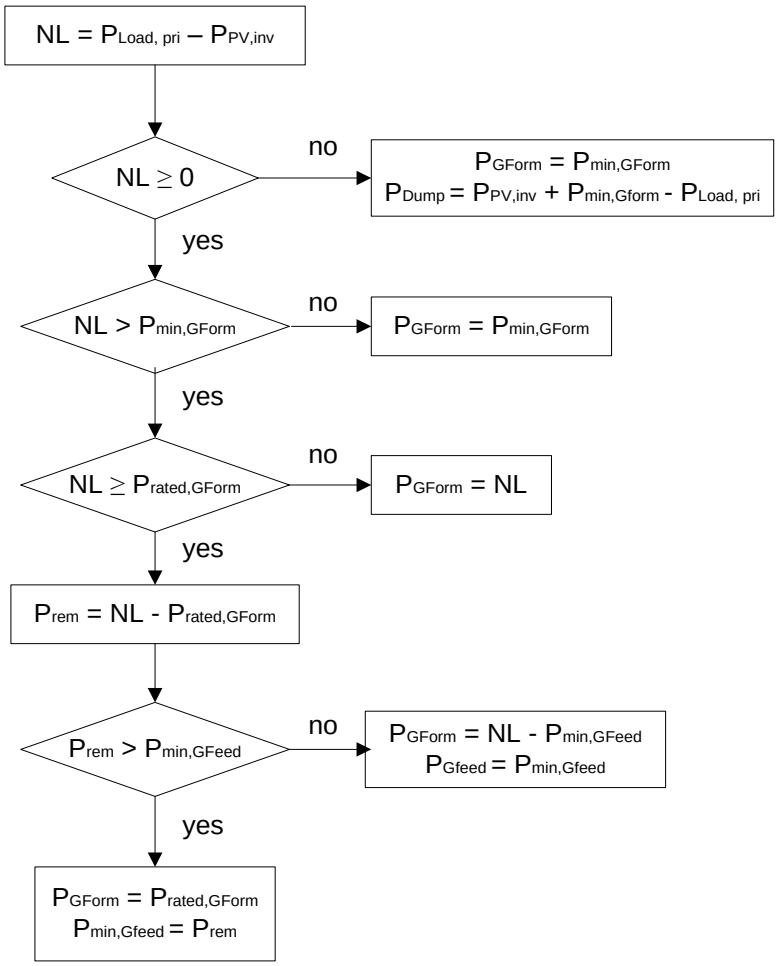

Figure 3. 19: Power management algorithm for the PV-Diesel hybrid power system

Basically, a PV-Diesel hybrid power system has two distinct daily operating conditions, i.e.: system operation without contribution from the PV generator during night time and system operation with contribution from the PV generator during day time. For many locations, contribution from PV generator between 6 a.m. to 6 p.m. is significant and a high fraction of the load demand can be supplied by the renewable energy during this period. Apart from these conditions, there are other possible system operating modes. Figure 3.21 shows typical operation modes (OM) of a PV-Diesel hybrid power system. A synthesized load demand profile is used to demonstrate the changes of daily operation modes. There are six operation modes in total and they are described as below:

- OM1: The primary load demand is supplied by the diesel generator only, P_{dg}, when there is no PV power (P_{pv}) available.
- OM2: Low PV power is available; the net load demand is supplied by the diesel generator.
- OM3: High PV power is available; the PV power has exceeded the primary load demand ($P_{load,pri}$). The diesel generator is operating at its minimum loading and the excess power produced is dumped (P_{dump}).
- OM4: High PV power is available; the deferrable load is activated. The PV power is sufficient to meet the primary load and charge the battery (P_{bat}). The diesel generator is not operating.
- OM5: Low PV power is available; the deferrable load is kept activated. The PV power is insufficient to meet the primary load and deferrable load demand. The diesel generator has to supply the net load and the deferrable load.
- OM6: No PV power is available; the deferrable load remains activated. The diesel generator supplies the total load demand of the primary and deferrable loads.

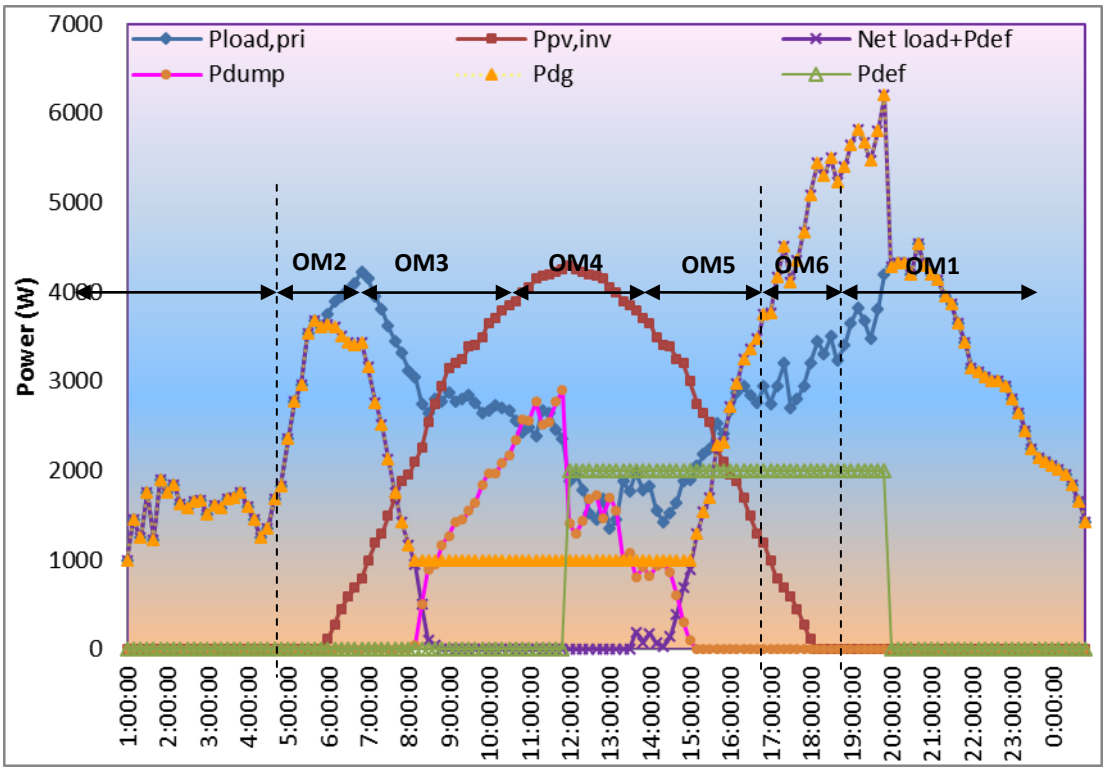

Figure 3. 20: Operation of a PV-diesel hybrid power system

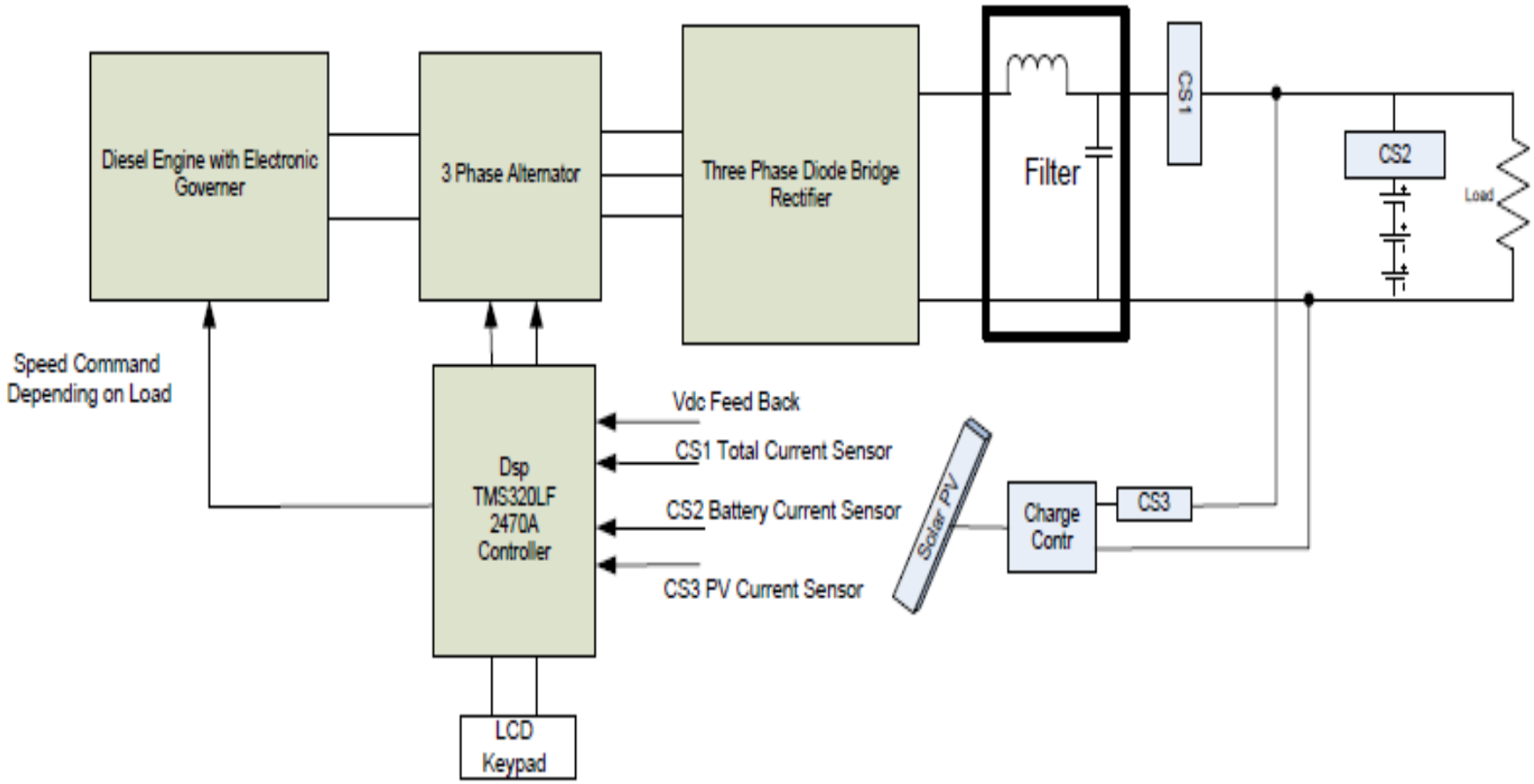

Figure 3. 21: Schematic diagram of off-grid PV-VSDG hybrid power system

3.7 Summary

This chapter covered the theoretical analysis, modelling and simulation of the variable speed diesel generator using various generation technologies. The prototype was built up and the experimental results presented. The simulation results using MATLAB/Simulink validate the use of VSDG to realize variable speed operation for diesel engine. The use of different vector control algorithms for different operation modes showed that such a system could provide acceptable power quality. The experimental results also show that the variable speed system produced high quality DC voltages independent of diesel engine speed.

In many remote areas, decentralized distributed generation systems (DDGS) are commonly used for increasing the capacity and reducing diesel fuel consumption. The renewable energy power generation such as PV array integrated with the conventional diesel generator to supply local load. Unfortunately, the introduction of the renewable energy sources resulted in longer time periods of low load diesel operation. By applying VSDG in decentralized distributed generation systems, the problem caused by the conventional diesel generator could be avoided. Three innovative configurations of decentralized distributed generation systems were proposed. One configuration for small power usage, one configuration for medium size power demand and the third configuration of integrating with utility scale to supply power during the short transient duration when load changes.

Conventional constant speed diesel generators supplying electric power to remote areas have the problems of low efficiency, cylinder glazing and carbon build-up due to their poor performance in long term light-load operation. The combination of a conventional diesel generator, battery bank, and/or another type of renewable energy source to form a hybrid power system can maintain a diesel generator that operates at a substantial load level, but encounters the problem of high capital cost and maintenance costs due to the included battery bank.

Variable speed operation for a diesel engine can save significant amounts of fuel, especially at times when the average load demand is much smaller than the peak load. Performance maps should be used to determine the best speed power relationship. Different variable speed diesel generator types were reviewed and a novel variable speed diesel generator proposed. The detailed integration of the variable speed generator in various load conditions and its benefits will be covered in the next three chapters.

3.8 References

[1] A. K. Srivastava, A. A. Kumar, and N. N. Schulz, "Impact of Distributed Generations With Energy Storage Devices on the Electric Grid," *Systems Journal, IEEE,* vol. 6, pp. 110-117, 2012.

[2] J. Y. Chen and C. V. Nayar, "A direct-coupled, wind-driven permanent magnet generator," in *Energy Management and Power Delivery, 1998. Proceedings of EMPD '98. 1998 International Conference on*, 1998, pp. 542-547 vol.2.

[3] F. Chun-Che, W. Buntoon, and C. V. Nayar, "An investigation on the characteristics and performance of a PV-diesel hybrid energy system for teaching and research," in *TENCON '02. Proceedings. 2002 IEEE Region 10 Conference on Computers, Communications, Control and Power Engineering*, 2002, pp. 1962-1965 vol.3.

[4] F. Chun-Che, W. Rattanongphisat, and C. Nayar, "A simulation study on the economic aspects of hybrid energy systems for remote islands in Thailand," in *TENCON '02. Proceedings. 2002 IEEE Region 10 Conference on Computers, Communications, Control and Power Engineering*, 2002, pp. 1966-1969 vol.3.

[5] P. Y. Lim and C. V. Nayar, "Photovoltaic-variable speed diesel generator hybrid energy system for remote area applications," in *Universities Power Engineering Conference (AUPEC), 2010 20th Australasian*, 2010, pp. 1-5.

[6] P. Y. Lim and C. V. Nayar, "Control of Photovoltaic-Variable Speed Diesel Generator battery-less hybrid energy system," in *Energy Conference and Exhibition (EnergyCon), 2010 IEEE International*, 2010, pp. 223-227.

[7] S. V. Mathews, S. Rajakaruna, and C. V. Nayar, "Design and implementation of an offgrid hybrid power supply with reduced battery energy storage," in *Power Engineering Conference (AUPEC), 2013 Australasian Universities*, 2013, pp. 1-6.

[8] C. Nayar, M. Tang, and W. Suponthana, "A case study of a PV/wind/diesel hybrid energy system for remote islands in the republic of Maldives," in *Power Engineering Conference, 2007. AUPEC 2007. Australasian Universities*, 2007, pp. 1-7.

[9] C. Nayar, M. Tang, and W. Suponthana, "Wind/PV/diesel micro grid system implemented in remote islands in the Republic of Maldives," in *Sustainable Energy Technologies, 2008. ICSET 2008. IEEE International Conference on*, 2008, pp. 1076-1080.

[10] C. V. Nayar, "Control and interfacing of bi-directional inverters for off-grid and weak grid photovoltaic power systems," in *Power Engineering Society Summer Meeting, 2000. IEEE*, 2000, pp. 1280-1282 vol. 2.

[11] F. Qiang, L. F. Montoya, A. Solanki, A. Nasiri, V. Bhavaraju, T. Abdallah, *et al.*, "Microgrid Generation Capacity Design With Renewables and Energy Storage Addressing Power Quality and Surety," *Smart Grid, IEEE Transactions on,* vol. 3, pp. 2019-2027, 2012.

[12] M. Arriaga, C. A. Canizares, and M. Kazerani, "Renewable Energy Alternatives for Remote Communities in Northern Ontario, Canada," *Sustainable Energy, IEEE Transactions on,* vol. 4, pp. 661-670, 2013.

[13] K. V. Bhadane, M. S. Ballal, and R. M. Moharil, "Investigation for Causes of Poor Power Quality in Grid Connected Wind Energy - A Review," in *Power and Energy Engineering Conference (APPEEC), 2012 Asia-Pacific*, 2012, pp. 1-6.

[14] W. Chengshan, L. Mengxuan, and G. Li, "Cooperative operation and optimal design for islanded microgrid," in *Innovative Smart Grid Technologies (ISGT), 2012 IEEE PES*, 2012, pp. 1-8.

[15] S. Gopalan, V. Sreeram, H. Iu, and Y. Mishra, "An improved protection strategy for microgrids," in *Innovative Smart Grid Technologies Europe (ISGT EUROPE), 2013 4th IEEE/PES*, 2013, pp. 1-5.
[16] V. Gevorgian, M. Singh, and E. Muljadi, "Variable frequency operation of a HVDC-VSC interconnected type 1 offshore wind power plant," in *Power and Energy Society General Meeting, 2012 IEEE*, 2012, pp. 1-8.
[17] C. Kayser-Bril, C. Liotard, N. Maizi, and V. Mazauric, "Power Grids on Islands: from Dependency to Sustainability?," in *Energy 2030 Conference, 2008. ENERGY 2008. IEEE*, 2008, pp. 1-7.
[18] D. H. Wang, C. V. Nayar, and C. Wang, "Modeling of stand-alone variable speed diesel generator using doubly-fed induction generator," in *Power Electronics for Distributed Generation Systems (PEDG), 2010 2nd IEEE International Symposium on*, 2010, pp. 1-6.
[19] B. L. Schenkman, D. G. Wilson, R. D. Robinett, and K. Kukolich, "PhotoVoltaic distributed generation for lanai power grid real-time simulation and control integration scenario," in *Power Electronics Electrical Drives Automation and Motion (SPEEDAM), 2010 International Symposium on*, 2010, pp. 154-157.
[20] F. Yang, V. Rimali, M. Tang, and C. Nayar, "Design and Implementation of stand-alone smart grid employing renewable energy resources on Pulau Ubin Island of Singapore," in *Electromagnetic Compatibility (APEMC), 2012 Asia-Pacific Symposium on*, 2012, pp. 441-444.
[21] O. M. Zoubeidi, A. A. Fardoun, H. Noura, and C. Nayar, "Hybrid renewable energy solution for safari camps in UAE," in *Energy Conference and Exhibition (EnergyCon), 2010 IEEE International*, 2010, pp. 244-249.
[22] Y. Makarov, D. Pengwei, M. C. W. Kintner-Meyer, J. Chunlian, and H. Illian, "Optimal size of energy storage to accommodate high penetration of renewable resources in WECC system," in *Innovative Smart Grid Technologies (ISGT), 2010*, 2010, pp. 1-5.
[23] F. Qiang, A. Nasiri, V. Bhavaraju, A. Solanki, T. Abdallah, and D. C. Yu, "Transition Management of Microgrids With High Penetration of Renewable Energy," *Smart Grid, IEEE Transactions on*, vol. 5, pp. 539-549, 2014.
[24] D. Renchang, J. D. McCalley, D. C. Aliprantis, V. Ajjarapu, T. Das, W. Di, *et al.*, "Hierarchical control for hybrid wind systems," in *North American Power Symposium (NAPS), 2009*, 2009, pp. 1-6.
[25] J. A. Sanchez, N. Moreno, S. Vazquez, J. M. Carrasco, E. Galvan, C. Batista, *et al.*, "A 800 kW wind-diesel test bench based on the MADE AE-52 variable speed wind turbine," in *Industrial Electronics Society, 2003. IECON '03. The 29th Annual Conference of the IEEE*, 2003, pp. 1314-1319 Vol.2.
[26] A. R. Cooper, D. J. Morrow, and D. J. McGowan, "Recreating the mechanical response of a diesel generator set using a variable speed DC drive," in *Universities Power Engineering Conference, 2008. UPEC 2008. 43rd International*, 2008, pp. 1-5.
[27] Y. Hu, M. McCormick, L. Haydock, M. Cirstea, and G. A. Putrus, "Advanced hybrid variable speed controller for stand-alone diesel engine driven generator systems," in *Power System Technology, 2002. Proceedings. PowerCon 2002. International Conference on*, 2002, pp. 711-715 vol.2.
[28] L. Joon-Hwan, L. Seung-Hwan, and S. Seung-Ki, "Variable Speed Engine Generator with Super-Capacitor; Isolated Power Generation System and Fuel Efficiency," in *Industry Applications Society Annual Meeting, 2008. IAS '08. IEEE*, 2008, pp. 1-5.

[29] D. Katsis, P. Wheeler, J. Clare, and P. Zanchetta, "A three-phase utility power supply based on the matrix converter," in *Industry Applications Conference, 2004. 39th IAS Annual Meeting. Conference Record of the 2004 IEEE*, 2004, pp. 1447-1451 vol.3.

[30] D. Katsis, P. Wheeler, J. C. Clare, L. Empringham, and M. Bland, "A utility power supply based on a four-output leg matrix converter," in *Industry Applications Conference, 2005. Fourtieth IAS Annual Meeting. Conference Record of the 2005*, 2005, pp. 2355-2359 Vol. 4.

[31] J. Leuchter, V. Refucha, Z. Krupka, and P. Bauer, "Dynamic Behavior of Mobile Generator Set with Variable Speed and Diesel Engine," in *Power Electronics Specialists Conference, 2007. PESC 2007. IEEE*, 2007, pp. 2287-2293.

[32] J. Panqiu, Z. Hong, X. Limei, L. Xuesheng, Z. Peidong, and Z. Shufeng, "Research on a novel hybrid power system," in *Mechatronics and Automation (ICMA), 2012 International Conference on*, 2012, pp. 2494-2498.

[33] L. Seung-Hwan, Y. Jung-Sik, L. Joon-Hwan, and S. Seung-Ki, "Design of Speed Control Loop of A Variable Speed Diesel Engine Generator by Electric Governor," in *Industry Applications Society Annual Meeting, 2008. IAS '08. IEEE*, 2008, pp. 1-5.

[34] P. A. Stott, M. A. Mueller, V. D. Colli, F. Marignetti, and R. Di Stefano, "DC Link Voltage Stabilisation in Hybrid Renewable Diesel Systems," in *Clean Electrical Power, 2007. ICCEP '07. International Conference on*, 2007, pp. 20-25.

[35] T. A. Theubou, R. Wamkeue, and I. Kamwa, "Control of grid-side inverter for isolated wind-diesel power plants using variable speed squirrel cage induction generator," in *IECON 2012 - 38th Annual Conference on IEEE Industrial Electronics Society*, 2012, pp. 4304-4309.

[36] T. Waris and C. V. Nayar, "Variable speed constant frequency diesel power conversion system using doubly fed induction generator (DFIG)," in *Power Electronics Specialists Conference, 2008. PESC 2008. IEEE*, 2008, pp. 2728-2734.

[37] P. Zanchetta, P. Wheeler, L. Empringham, and J. Clare, "Design control and implementation of a three-phase utility power supply based on the matrix converter," *Power Electronics, IET*, vol. 2, pp. 156-162, 2009.

[38] Diesel Service Supply. (15/04/2014). *Approximate Diesel Fuel Consumption Chart*. Available: http://www.dieselserviceandsupply.com/Diesel_Fuel_Consumption.aspx

[39] W. Koczara, G. Iwanski, and Z. Chlodnicki, "Adjustable speed generation system for wind turbine power quality improvement," in *Industrial Electronics, 2009. IECON'09. 35th Annual Conference of IEEE*, 2009, pp. 4543-4547.

[40] J. F. Manwell, W. A. Stein, A. Rogers, and J. G. McGowan, "An investigation of variable speed operation of diesel generators in hybrid energy systems," *Renewable Energy*, vol. 2, pp. 563-571, 1992.

[41] Regen Power Pty. Ltd. (Jan.). *Hybrid renewable energy penetration micro-grid power system using a variable speed constant frequency generator*. Available: http://www.dailylife.com.sg/HybridGen%20Writeup%20ver3.pdf

[42] R. Pena, R. Cardenas, J. Clare, and G. Asher, "Control strategy of doubly fed induction generators for a wind diesel energy system," in *IECON 02 [Industrial Electronics Society, IEEE 2002 28th Annual Conference of the]*, 2002, pp. 3297-3302 vol.4.

[43] "HOMER help file - HOMER v2.68 beta," ed: National Renewable Energy Laboratory, 2009.

[44] R. W. Wies, R. A. Johnson, A. N. Agrawal, and T. J. Chubb, "Simulink model for economic analysis and environmental impacts of a PV with diesel-battery system for remote villages," *IEEE Transactions on Power Systems*, vol. 20, pp. 692-700, 2005.

[45] A. A. Setiawan, "Development of a modular AC coupling minigrid hybrid system for sustainable power supply in remote areas and disaster response and reconstruction," Electrical and Computer Engineering, Curtin University of Techonology, 2009.
[46] W. Short, D. J. Packey, and T. Holt, "A Manual for the Economic Evaluation of Energy Efficiency and Renewable Technologies," National Renewable Energy Laboratory, Colorado, U.S.1995.
[47] D. Barley and B. Winn, "Optimal dispatch strategy in remote hybrid power systems," *Solar Energy*, vol. 58, pp. 165-179.

Chapter 4

4. Design and Implementation of a Small Scale Remote Area Power Supply System

4.1 Introduction

Remote areas in Australia are mostly powered by conventional diesel generators (DG). Difficulties associated with the use of DG include the increasing cost of diesel, the transportation of diesel over long distances, and the increased fuel consumption and maintenance costs associated with running a DG under a low load [1].

In this chapter, the design and implementation of an innovative solar diesel hybrid power system in one of the most remote desert locations in Western Australia is described. The design objective was to minimize costly battery energy storage by using an innovative variable speed diesel generator. Diesel fuel saving was achieved by running the DG in variable speed mode as well as managing the operation of the generator. PSpice [2] and HOMER [3] software's were used to model and simulate various battery and PV sizes, which allowed selection of the optimal battery size.

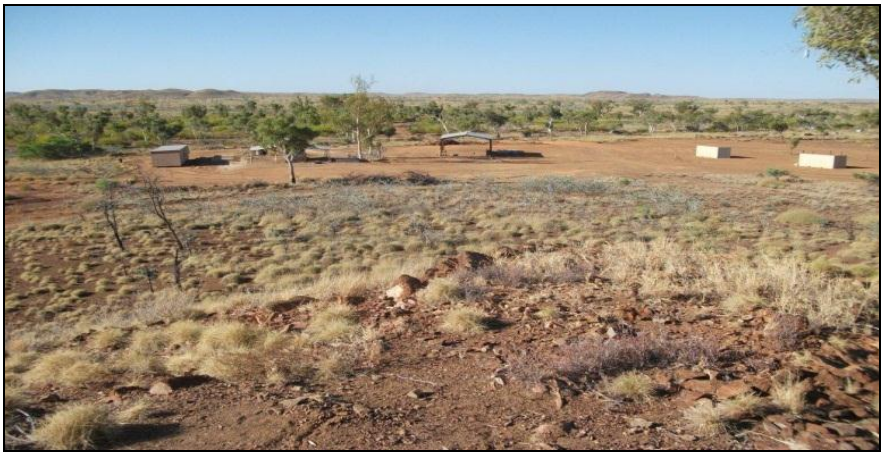

Figure 4. 1: Meentheena Veterans Camp, Marble Bar

The Veterans Retreat (Figure 4.1) Meentheena Cattle Station is located about 75 km from Marble Bar. Local advertising emphasizes two of the major problems associated with

providing power at this site. Firstly the remoteness- this location is part of the largest shire in the world, the East Pilbara, and secondly, the ambient temperature- this locality is also known as the hottest place in Australia (Figure 4-3).

Simulations of two configurations of off-grid hybrid power systems under different power management strategies are presented. The developed models of system components that have been verified using HOMER are applied to simulate hypothetical PV-CSDG and PV-VSDG systems. Simulations are based on weather and load demand data for the location stated in Chapter 4. All simulations are done using synthesized time series for 365 days. Simulation time-step is set to one minute to emulate the practical system with randomness of load demand. System power balance was confirmed by computation at each simulation time step. The prediction algorithm is written in the MATLAB [4] programming language [5-7] and is saved in m-file format.

Figure 4. 2: Largest Shire of East Pilbara

Figure 4. 3: Hottest town in Australia

4.2. Power Demand and Resource Data Analysis

4.2.1. Load Profile

The effect of occupancy on the load profile at the Veterans Retreat was difficult to predict due to the remoteness of the location. However, it was possible to formulate the daily and seasonal variations in electrical demand (Figure 4.4) after consultation with the management.

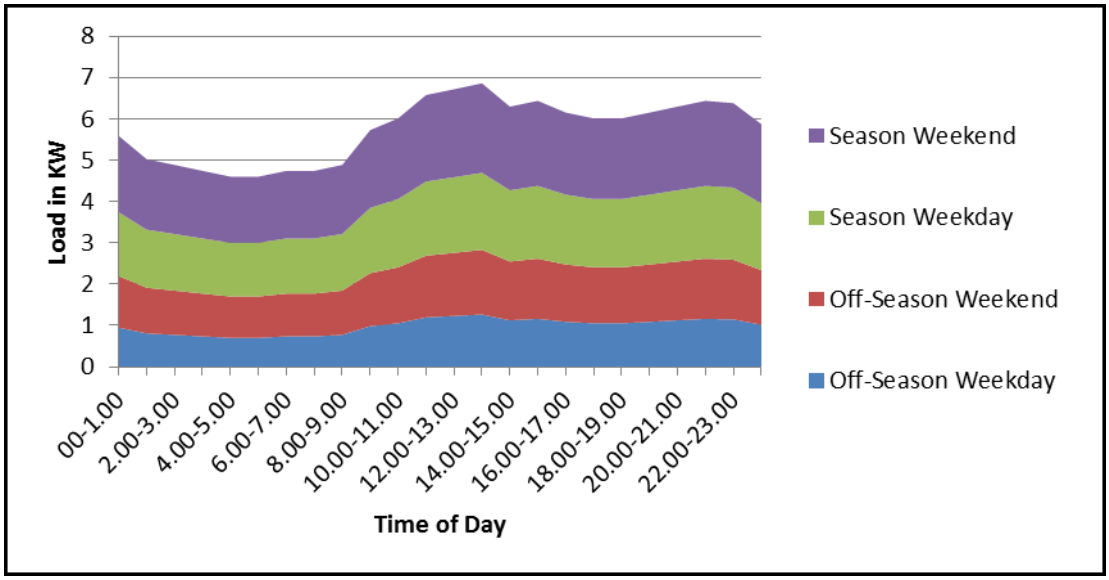

Figure 4. 4: Load profile of the proposed off-grid hybrid renewable energy system

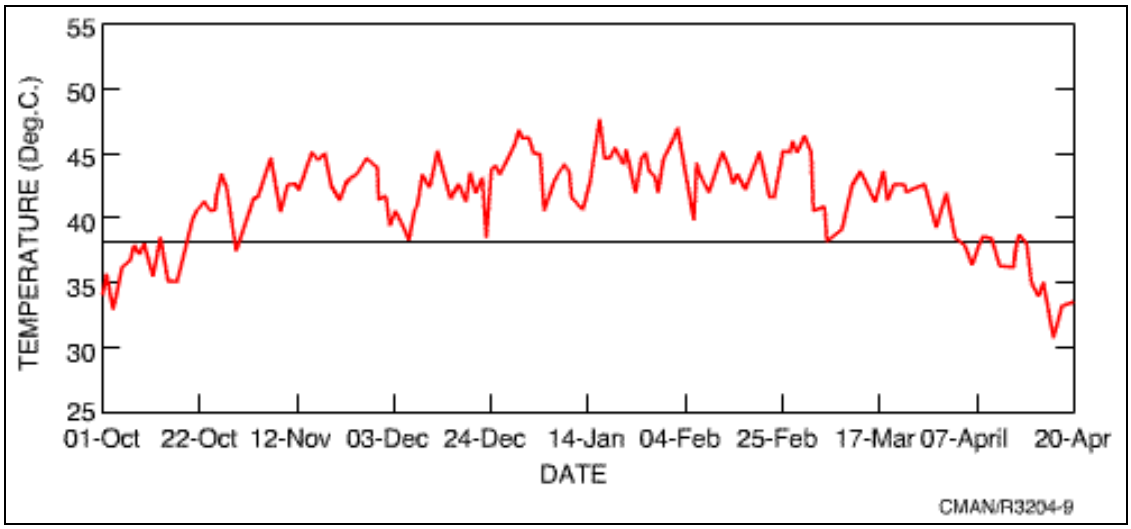

Figure 4. 5: Marble Bar longest hot days recorded [8]

4.2.2. Resource Data Analysis

Marble Bar is located in the Pilbara region of Western Australia 22^{o} south of the equator. Therefore it receives an abundant supply of solar radiation throughout the year and temperatures above 37.8°C are common. On average, Marble Bar experiences about 154 such days every year [4]. This region actually holds the world record for the longest sequence of days above 37.8° C. The temperature, measured under standard exposure conditions, touched or exceeded 37.8°C every day from 31 October 1923 to 7 April 1924, a total of 160 days (Figure 4.6).

Climate data for Marble Bar, Western Australia													
Month	Jan	Feb	Mar	Apr	May	Jun	Jul	Aug	Sep	Oct	Nov	Dec	Year
Record high °C (°F)	49.2	48.3	46.7	45	39.5	35.8	35	37.2	42.6	45.6	47.2	48.3	49.2
	-120.6	-118.9	-116.1	-113	-103.1	-96.4	-95	-99	-108.7	-114.1	-117	-118.9	-120.6
Average high °C (°F)	41	39.8	39	36	30.7	27.1	26.8	29.6	33.9	37.6	40.5	41.6	35.3
	-105.8	-103.6	-102.2	-96.8	-87.3	-80.8	-80.2	-85.3	-93	-99.7	-104.9	-106.9	-95.5
Average low °C (°F)	26.1	25.7	24.8	21.4	16.6	13.2	11.7	13.3	16.7	20.3	23.6	25.5	19.9
	-79	-78.3	-76.6	-70.5	-61.9	-55.8	-53.1	-55.9	-62.1	-68.5	-74.5	-77.9	-67.8
Record low °C (°F)	18.9	13.9	15	10	5.6	1.1	2.2	3.9	5.6	10	14.4	17	1.1
	-66	-57	-59	-50	-42.1	-34	-36	-39	-42.1	-50	-57.9	-62.6	-34
Precipitation mm (inches)	76.3	87.8	56.7	21.9	23	23	12.6	6.4	0.9	3.8	9.1	39.6	361.7
	-3.004	-3.457	-2.232	-0.862	-0.906	-0.906	-0.496	-0.252	-0.035	-0.15	-0.358	-1.559	-14.24
Source: Australian Bureau of Meteorology[6]													

Figure 4. 6: Shows the monthly average solar radiation data for this area [8].

The warm weather and near constant sunshine of Marble Bar make it an ideal location for the solar power generation, even in winter. According to data obtained from the NASA

Surface Meteorology [5] and Solar Energy data base, the area receives annual average solar radiation of kWh/m2/day. Table 5.1 shows the yearly average high and low climate data obtained from Australian Bureau of Meteorology.

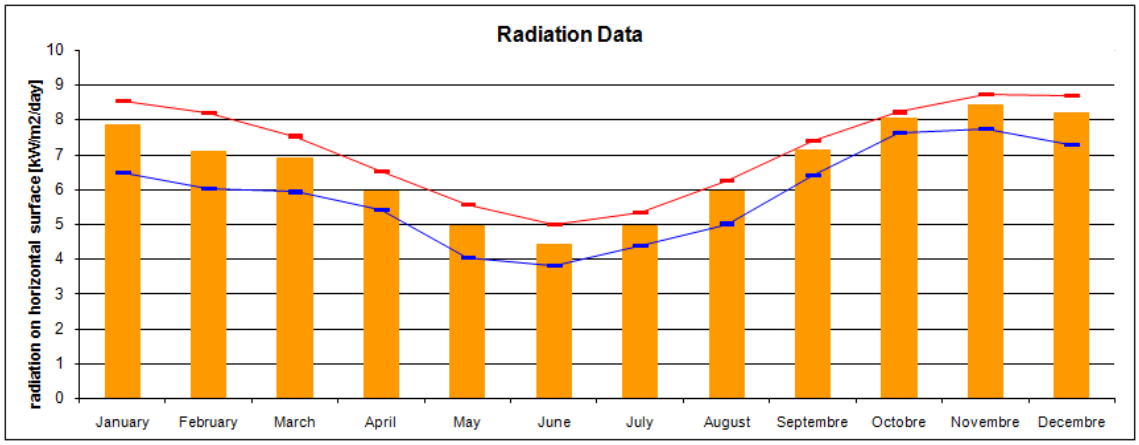

Figure 4. 7: Location radiation data

4.3. Hybrid System Design and Modelling

4.3.1. Design

The solar hybrid power system that was proposed for Veterans Retreat was unique because it required the integration of a variable speed diesel generator and photovoltaic panels in order to meet the electrical demand.

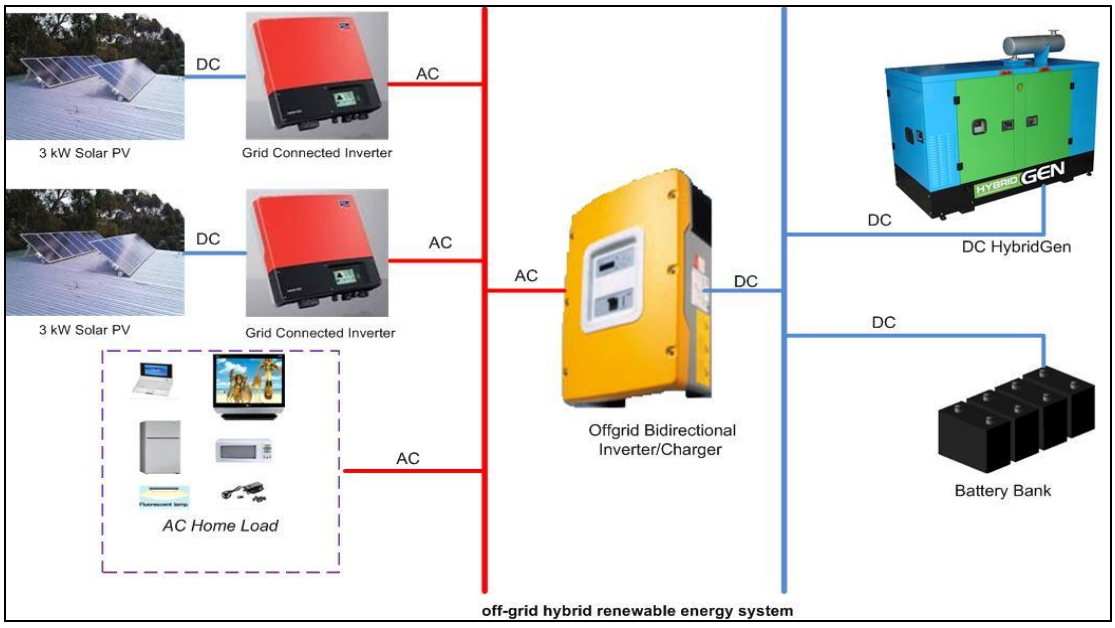

Figure 4. 8: System configuration

Figure 4.8 shows a schematic diagram of the proposed system. In this system the load is met from PV, diesel or the battery. The formulae given in Table 4.1 show the contribution from the various sources meeting the load. It should be noted that the sizing of the PV modules will be affected by ageing factors, resulting in a decrease in efficiency, and the accumulation of dirt, which would reduce productivity.

Table 4. 1: Formulas used for design

<table>
<tr><td colspan="2">Assuming the components' efficiencies:
$\eta_{inv} = 0.9$; $\eta_{rec} = 0.9$; PV Derating Factor = 0.9; $\eta_{Batt} = 0.85$</td></tr>
<tr><td>Generator</td><td>Power received at the load (%)</td></tr>
<tr><td rowspan="2">PV</td><td>Direct supply:
Efficiency of PV
$\eta_{pv,direct} = \eta_{inv} \times$ PV Derating Factor
$P_{pv,direct} = \eta_{pv,direct} \times P_{pv} \approx 0.81 \times P_{pv}$</td></tr>
<tr><td>Indirect supply/Cycled through battery:
$\eta_{pv,indirect} = \eta_{inv} \times$ PV Derating Factor $\times \eta_{Batt}$
$P_{pv,indirect} = \eta_{pv,indirect} \times P_{pv} \approx 0.69 \times P_{pv}$</td></tr>
<tr><td rowspan="2">Diesel</td><td>Direct supply:
$P_{diesel,direct} = P_{diesel}$</td></tr>
<tr><td>Indirect supply/Cycled through battery:$\eta_{diesel,indirect} = \eta_{rec} \times \eta_{Batt} \times \eta_{inv}$
$P_{diesel,indirect} = \eta_{diesel,indirect} \times P_{diesel} \approx 0.69 \times P_{diesel}$</td></tr>
<tr><td colspan="2">a. A derating factor is to account for the decreased efficiency due to dirt on the surface and the ageing of PV module.[9]
b. P_{pv} is the electrical power output from the PV module with the solar cell efficiency taken into account.</td></tr>
</table>

Calculation of the sun path diagram is important in photovoltaic system design. It is used not only for predicting the position of the sun, but also for predicting the shading pattern

of the designated area. According to Masters [10], the sun path diagram can be plotted by calculating the "altitude angle, β" and the "azimuth angle, Φs" to determine the sun location. In predicting the shadow pattern, natural and man-made obstructions should be sketched on the diagram, so that the loss of insolation can be calculated roughly. The Veterans Retreat location was free from all possible types of shadow. However, since it was decided to install the panels on the flat roof of the available shipping containers, the shadow calculation was required for placing the modules on frames with a tilt angle of 22 degrees.

Altitude angle β and azimuth angle Φs can be calculated by the following two equations:

$$\sin \beta = \cos L.\cos \delta.\cos H + \sin L.\sin \delta \qquad (4.1)$$

$$\sin \emptyset_s = \frac{\cos \delta . \sin H}{\cos \beta} \qquad (4.2)$$

and if $\cos H \geq \frac{\tan \delta}{\tan L}$, $|\varphi s| \leq 900$ otherwise $|\varphi s| > 900$

Both angles depend on the "latitude, L", "hour angle, H" and "the number of days, n". For the calculation of sun declination number of days has to be considered and for this project, all the calculations are made for the 15th day of each month of the year. Table 4.2 shows the numbers of days (D) of the 15th day of each month (M) from January 1st.

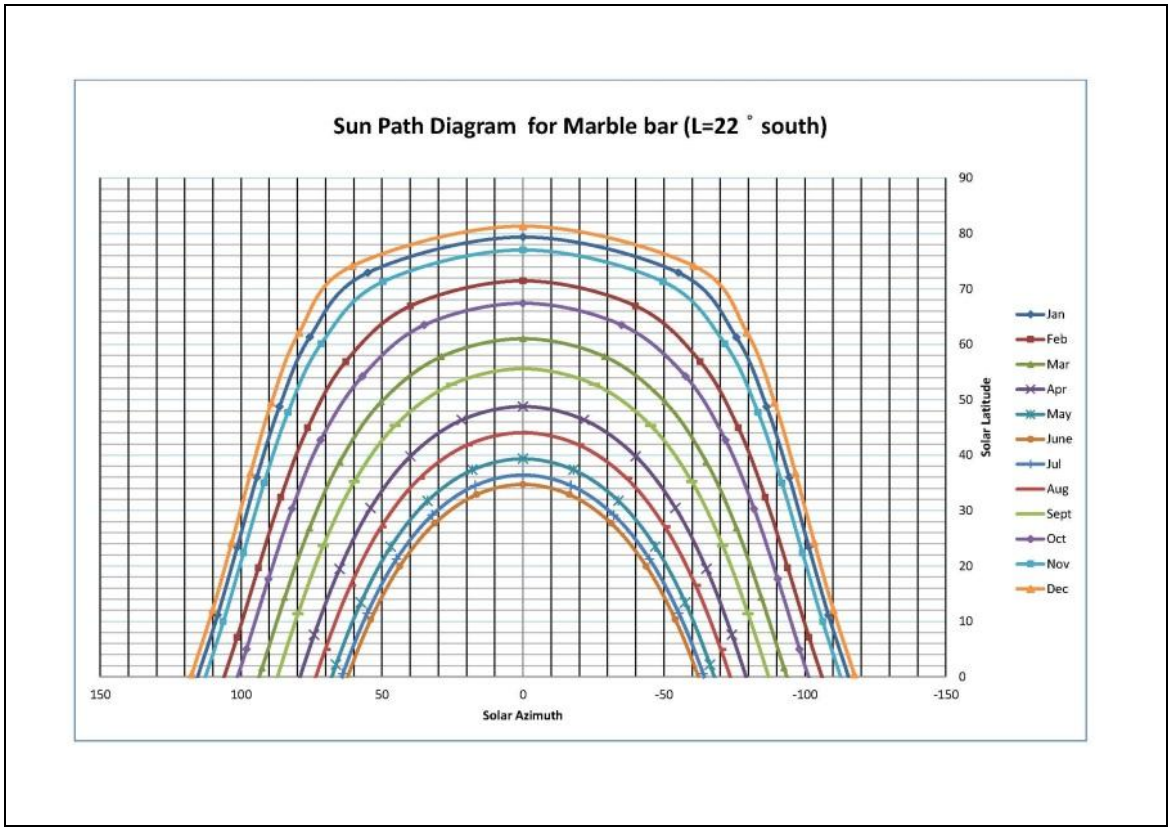

Figure 4. 9: Sun path Diagram for L= -22

Table 4. 2: Day Numbers for 15th Day of Each Month

Month and date	Jan. 15	Feb. 15	Mar. 15	Apr. 15	May 15	June 15	July 15	Aug. 15	Sept. 15	Oct. 15	Nov. 15	Dec. 15
day	15	46	74	105	135	166	196	227	258	288	319	349

Based on the data for β and φs provided in the tables, the sun path diagram for Veterans Retreat was drawn, and is presented in from Figure 4.8.

For this particular installation, the shadow effect from another panel or array was an important parameter to consider. This is because shadow from another panel would decrease the insolation on the photovoltaic module and also decrease the output power from the system. In order to minimize the shadow effects due to other modules, maximum shaded area for each array had to be calculated. Therefore we should allocate space on both north to south

and east to west for each array. Figures 4.10 and 4.11 illustrate the elements that should be calculated to minimize the shadow effect.

Calculations for the total length of shadow from "north to south", DNS", and "east to west, DEW" are different for each mounting. Of the three mounting techniques considered, the fixed angle option had the simplest calculation for its DNS and DEW. For fixed angle mounting, the DNS is the following:

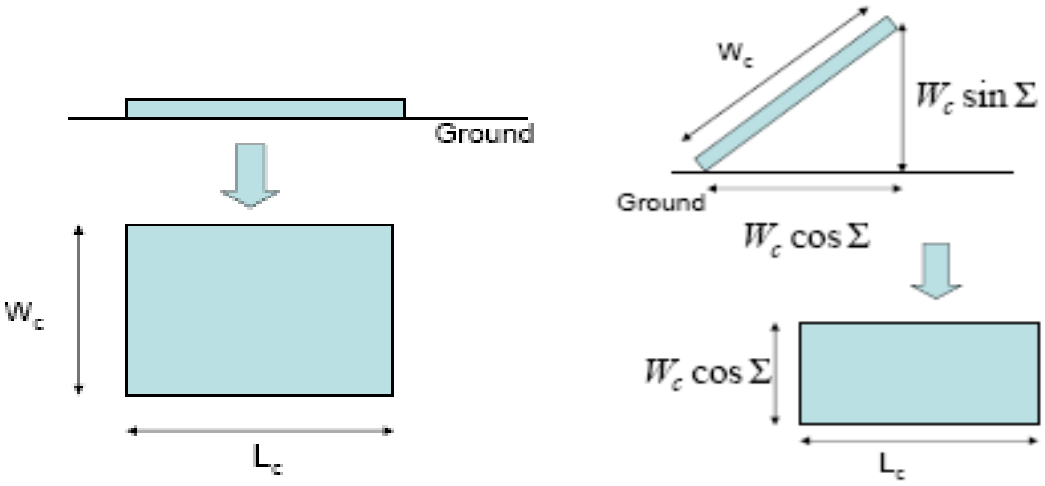

Figure 4. 10: Shadow Space for Each Module

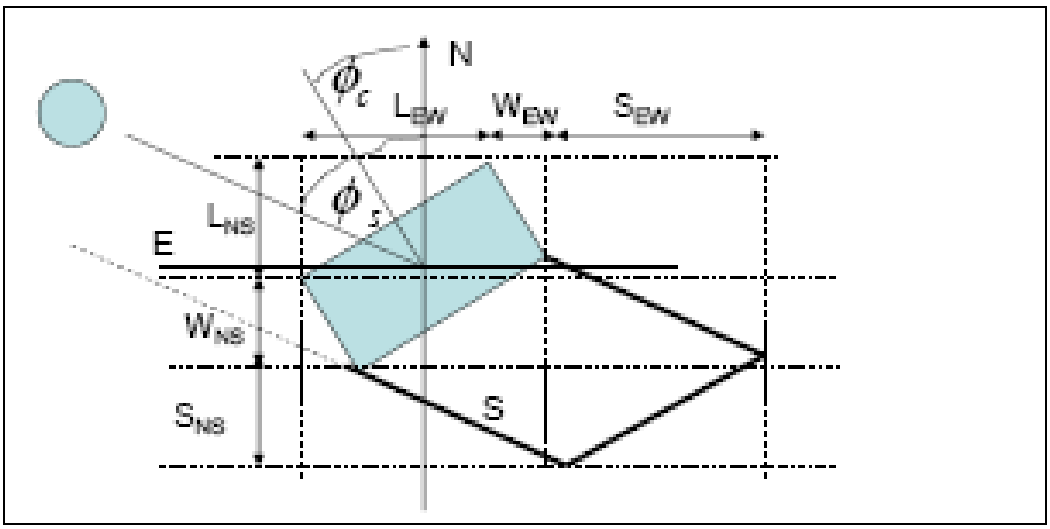

Figure 4. 11: Shadow Space for array

Array's shadow in "North-South, N-S" direction:

The total length in N-S direction occupied by the array and the shadow is

$$D_{NS} = L_{NS} + W_{NS} + S_{NS} \quad (4.3)$$

$$= L_c \sin \emptyset_c + W_c \cos \sum \cos \emptyset_c + \frac{W_c \sin \Sigma}{\tan \beta} \cos \emptyset_s \quad (4.4)$$

Array's shadow in the "East-West, E-W" direction:

The total length in E-W direction occupied by the array and the shadow is

$$D_{EW} = L_{EW} + W_{EW} + S_{EW}$$

$$L_c \cos \phi_c + W_c \cos \sum \sin \emptyset_c + \frac{W_c \sin \Sigma}{\tan \beta} \sin \emptyset_s \quad (4.5)$$

Possible maximum values of the above two lengths should be used in assigning the area per array.

If the arrays are facing the equator (North or South), and are tilted up by a fixed angle,

$\phi_c = 0$

$$D_{NS} = W_c \left(\cos \Sigma + \sin \Sigma \left(\frac{\cos \phi_s}{\tan \beta} \right) \right) \quad (4.6)$$

This length is maximum where $\left(\frac{\cos \phi_s}{\tan \beta} \right)$ is maximum.

$$D_{EW} = L_c + W_c \sin \Sigma \left(\frac{\sin \phi_s}{\tan \beta} \right) \quad (4.7)$$

This length is maximum where $\left(\frac{\sin \phi_s}{\tan \beta} \right)$ is maximum.

From the diagrams Figure 4.12 and Figure 4.13 potential shadow from arrays have been calculated from the maximum values for DNS and DEW for each mounting angle. This value was used in allocating space per module for each mount. Fixed angle mounting was selected for the Veterans Retreat project due to the additional costs involved and space required for tracking.

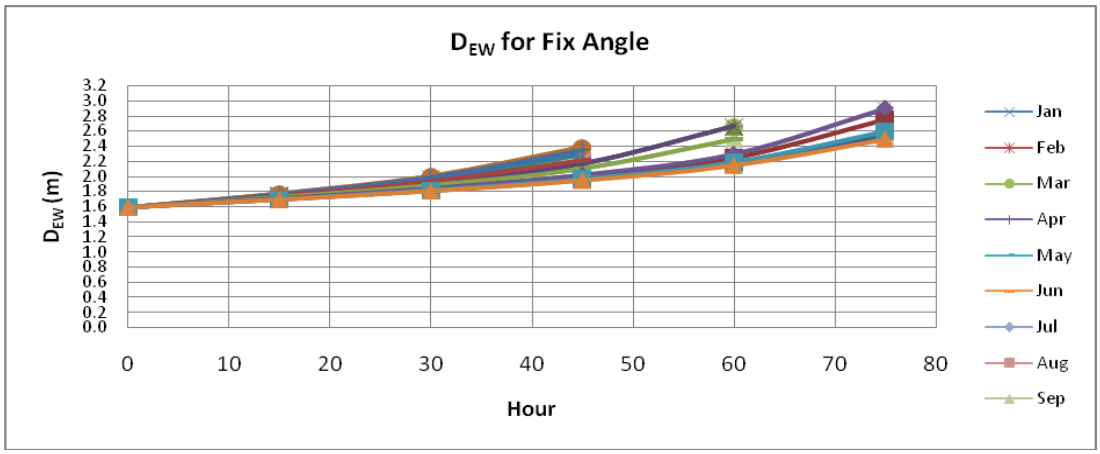

Figure 4. 12: DEW for Fix Angle

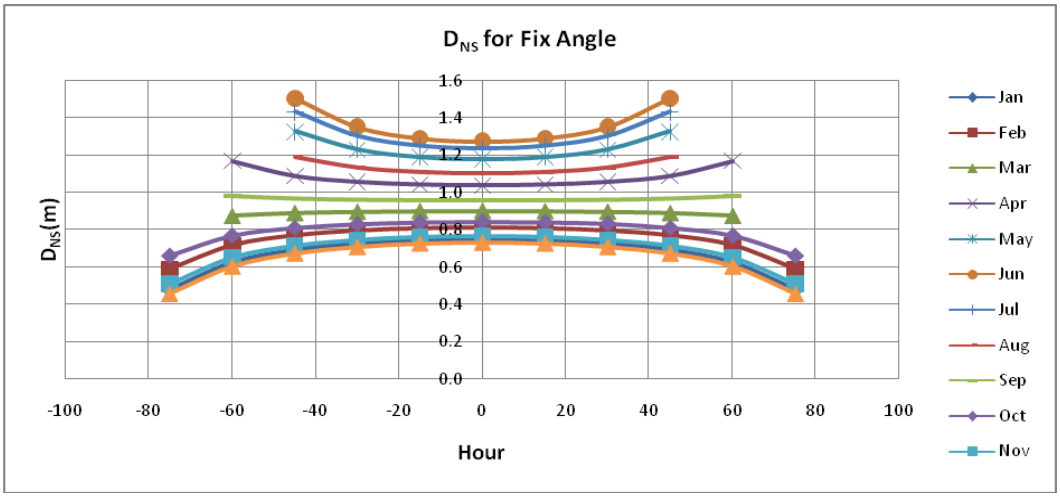

Figure 4. 13: DNS for Fix Angle

Table 4. 3: Maximum value for DNS and DEW for Each Mounting

Shadow direction	Fix angle (m)
D_{EW}	2.9026
D_{NS}	1.5036
Area (m^2) =	4.3642

4.3.2. Selection of module

String Ah/day = Insolation (h/day @ 1-sun) x IR (A) x Coulomb x De-rating Selection of module

String Ah/day = Insolation (h/day @ 1-sun) x IR (A) x Coulomb x De-rating

Strings in parallel = $\frac{Design-month\_load(Ah/day)}{Ah/day\_per\_module\_in\_design\_month}$

Modules in series = $\frac{System\_voltage(V)}{Nominal\_module\_voltage(V)}$

Total storage capacity = Usable storage capacity (Ah)

(Ah @ C/20, 25ºC) (MDOD) × (T, DR)

Minimum storage capacity (Ah) required = $\frac{Max\,load\,Power\,(W)X\,5h}{Sy\,Voltage\,(V)X\,Max\,Depth\,of\,Discharge}$

Number of batteries in series = $\frac{System\,Voltage}{Nom\,Battery\,Voltage}$

Number of strings of batteries in parallel = $\frac{Total\,Storage\,Capacity\,(Ah)}{Capacity\,of\,a\,single\,battery\,(Ah)}$

4.3.3. Selection of Inverter

Total DC load, Z_{DC} = dc load (Wh/day) + $\frac{ac\_load(Wh/day)}{Inverter\_efficiency}$

$$Z_{DC}=\frac{Z_{AC}}{\eta_{INV}} \qquad (4.8)$$

Total Ampere-hour dc load (@ system voltage), $A.h_{DC}=\frac{Z_{DC}}{V_{INV}}$ (4.9)

Design month Load (Ah/day) = Design month fraction X Total load (Ah/day)

Using the above insolation data, July (2.41kWh/m2) is the worst insolation month of the Year

Design Month Solar fraction taken as 60%

Design month Load (Ah/day) = Design month fraction X Total load (Ah/day)

Module de-rating factor taken as 90%

4.3.4. Diesel Generator Sizing

A generator should be able to replenish the batteries in a reasonable amount of time, but not faster than at a C/5 rate.

Generator size (W) = $\frac{Total\ Stog\ Capacity\ (Ah)\ X\ System\ Voltage\ (V)}{Charge\ time\ (9h)\ X\ Charger\ efficiency}$

Generator (kWh/yr) = $\frac{dcload\left(\frac{Wh}{day}\right) X\ 365\ X\ (1-Annual\ solar\ fraction)}{Charger\ eff\ X\ 1000\ (\frac{W}{kW})}$

4.4. System Components

4.4.1. Photovoltaic (PV) Generator Off-Grid Inverter

A photovoltaic module will produce its maximum current when there is essentially no resistance in the circuit. In its simplest form, this requires a short circuit between its positive and negative terminals. Standard sunlight conditions on a clear day are assumed to be 1000 watts of solar energy per square meter (1000 W/m2). This is sometimes called "one sun," or a "peak sun." Less than one sun will reduce the current output of the module by a proportional amount. For example, if only one-half sun (500 W/m2) is available, the amount of output current is roughly cut in half. Thus, the brightness affects the current output only. The greater the temperature, the smaller the open-circuit voltage. Higher module temperatures will reduce the voltage by 0.04 to 0.1 volts for every one Celsius degree rise in temperature [11]. This is why modules should not be installed flush against a surface. Air should be allowed to circulate behind the back of each module so its temperature does not rise and reducing its output.

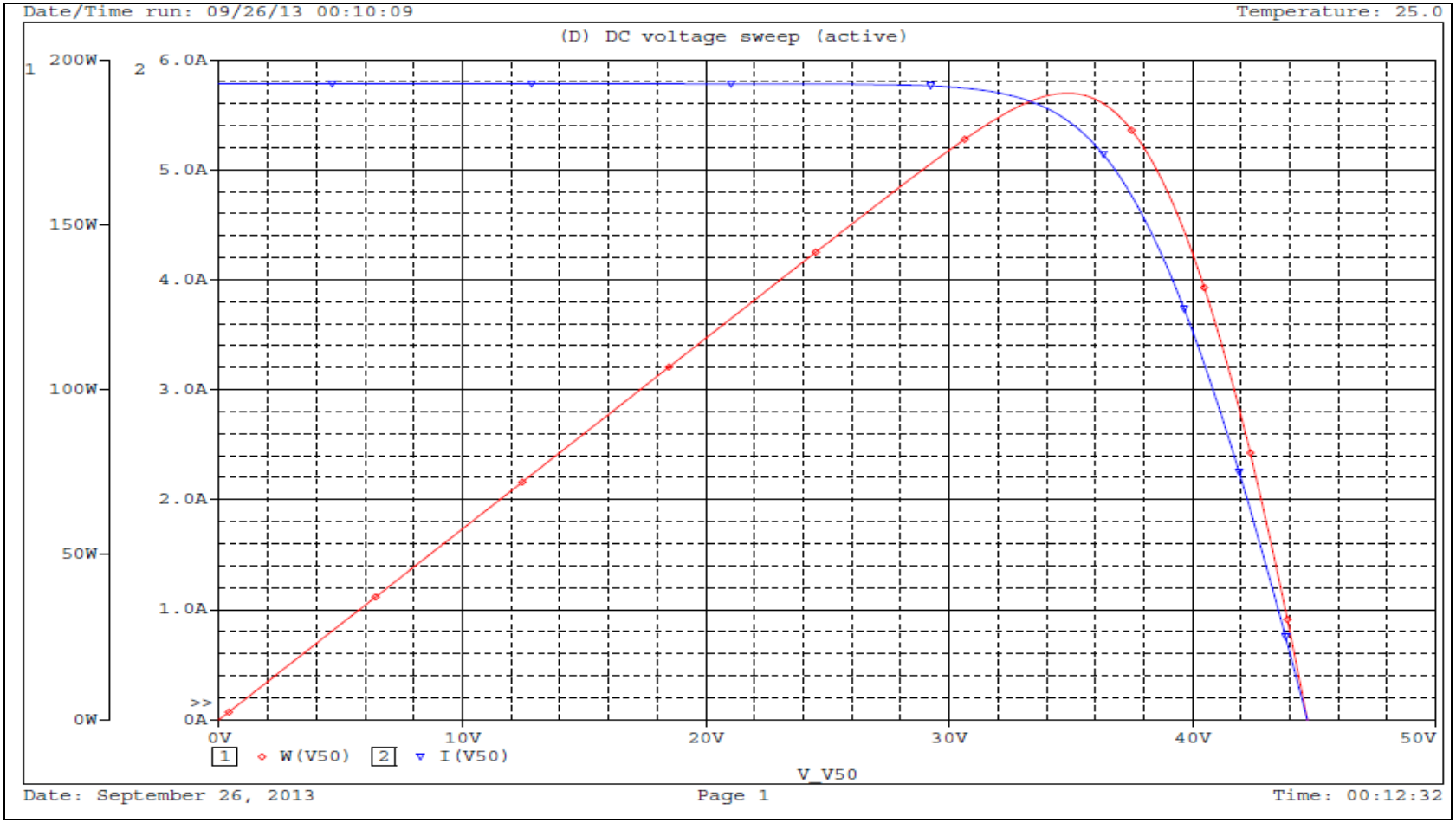

Figure 4. 14: Module Characteristic

A maximum power point tracker (or MPPT) is a high efficiency DC to DC converter which functions as an optimal electrical load for a photovoltaic (PV) cell, most commonly for a solar panel or array, and converts the power to a voltage or current level which is more suitable to whatever load the system is designed to drive.

PV cells have a single operating point where the values of the current (I) and Voltage (V) of the cell result in a maximum power output. These values correspond to a particular resistance, which is equal to V/I as specified by Ohm's Law. A PV cell has an exponential relationship between current and voltage, and the maximum power point (MPP) occurs at the knee of the curve, where the resistance is equal to the negative of the differential resistance (V/I = -dV/dI). Maximum power point trackers utilize some type of control circuit or logic to search for this point and thus to allow the converter circuit to extract the maximum power available from a cell [12].

Battery-less grid-tied PV inverters utilize MPPTs to extract the maximum power from a PV array, convert this to alternating current (AC) and sell excess energy back to the operators of the power grid. MPPT charge controllers are also desirable for off-grid power systems to make the best use of all the energy generated by the panels.

Studies of photovoltaic systems in outdoor conditions require a precise knowledge of the system details of the system. With the help of the simulation model, the energy output of photovoltaic systems can be predicted in different weather conditions. The world’s highest efficiency PV cells in use are the flat-plate modules, which have a production average efficiency of 22.4%. Figure 4.13 illustrates a typical solar PV module characteristic.

4.4.2. Off-Grid Inverter

It is customary practice to select an inverter for a system based on its capacity to handle peak load. For the Veterans Retreat system, a 5kW off-grid inverter was considered capable of covering all load combination permutations. In Fig. 4.15 the general shape of the inverter efficiency curve illustrated.

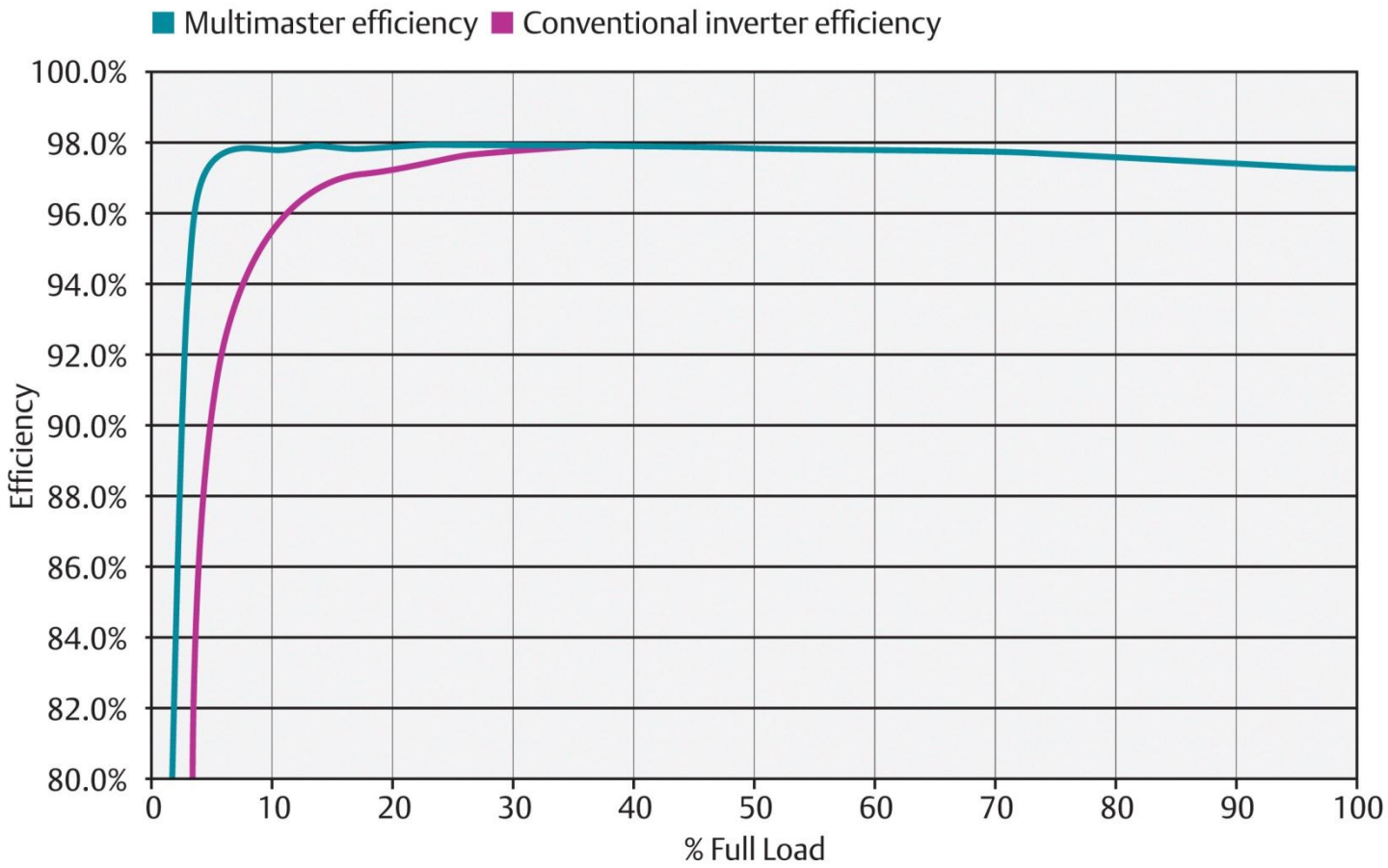

Figure 4. 15: Efficiency curve of inverter

Most of the electrical equipment (refrigerator, microwave oven, air conditioner, lights, cooktop, washing machine) that would be used at the Veterans Retreat has an individual power ratings below 400W. A refrigerator (and by inference, any other item) with a 400 W rating could be kept in continuous operation by a 5 kW inverter, and use less than 10% of the inverter rating. Since it is somewhat difficult to find the optimum rating for the inverter in this situation, the inclusion of two 3kW grid connected inverter units to take care of the day time peak load by AC Coupling to the system was proposed.

4.4.3. Grid-interactive Inverter

Factors that influence the selection of an inverter for a specific installation site include: the energy output of the array, the requirement to match the allowable inverter string configurations with the size of the array in kW, and the size of the individual modules within that array, and whether the system will require one central inverter or multiple (smaller) inverters.

The solar PV array must be matched to the voltage window of the grid connected inverter and therefore the final array configuration will be dependent on the inverter selected and the allowable operating voltage window. The temperature of the solar cells regulates the solar PV power output. Mono or poly crystalline solar modules power output vary around 0.5% per centigrade [13].

$$f_{temp} = 1 + \left[\gamma \times (T_{cell-eff} - T_{STC})\right] \qquad (4.10)$$

where,

f_{temp} = temperature de-rating factor, dimensionless

γ = power temp co-efficient per centigrade

T cell.eff = average daily cell temperature, in °C

As stated earlier, the output voltage of a module is affected by cell temperature changes in a similar way as the output power. The PV module manufacturers will provide a voltage temperature co-efficient that is generally specified in V/°C (or mV/°C), or alternatively as a % of Voc.

To ensure that the output voltages of the array do not fall outside the range of the inverter's DC input operating voltages, the minimum and maximum day time temperatures for that specific site are required.

On a hot, sunny, summer module voltage will be much higher and because of the higher temperature, the voltage of solar PV module will reduce. In contrast, on a cool winter day the voltage of the solar module will increase. Therefore, the dependence of the actual PV array voltage on ambient conditions must be considered in the design of any system. Equation 12 can be adapted to determine the maximum power point voltage at a specified temperature.

$$V_{mp\_cell\_eff} = V_{mp\_STC} - [\gamma_v \, x \, (T_{cell\_eff} - T_{ST}) \qquad (4.12)$$

Where,

V *mp_cell_eff*= Maximum Power Point Voltage at effective cell temperature, volts

V *mp_stc*= Maximum Power Point Voltage at STC, volts

γ_v = voltage temperature co-efficient, V per °C

T cell_eff= cell temperature at specified temperature, in °C

T stc= cell temperature at STC, measured in °C

Though formula 11 defines the effective cell temperature - it is vital that the array voltage always above the minimum inverter specification. The string voltage must be higher than the minimum voltage operating window of the inverter at expected higher temperature. The daytime ambient temperature in selected areas can reach, or exceed 45°C. In these cases, a maximum effective cell temperature of 70°C or above required.

The minimum number of modules in the string can be determined by the following equation.

$$N_{\min\_per\_string} = \frac{V_{inv\_min}(V)}{V_{\min\_mpp\_inv}(V)} \qquad (4.13)$$

where,

V_{inv_min} = the minimum inverter input voltage

$V_{min\_mpp\_inv}$= the effective minimum MPP voltage of a module at the inverter at maximum effective cell temperature

At the winter season minimum day time temperature, especially sunny early morning, the open circuit voltage of the array should be less than the maximum voltage of the inverter. Hence, the lowest daytime temperature for the area is used to determine the maximum Voc. This is calculated by the following equation.

$$V_{max\_oc} = V_{oc\_STC} - [\gamma_v \, x \, (T_{min} - T_{STC}) \qquad (4.14)$$

Where,

V max_oc= Open Circuit Voltage at minimum cell temperature, volts

V oc_STC= Open Circuit Voltage at STC, volts

γ_v = voltage temperature co-efficient, V/°C

T_{min} = expected min. daily cell temperature, °C

T_{STC}= cell temperature STC, °C

The maximum number of modules in the string,

N max_per_string, is determined by the following equation

$$N_{max\_per\_string} = \frac{V_{inv\_max}(V)}{V_{oc\_max}(V)} \qquad (4.15)$$

When selecting the number of modules to be included in a string, it is important to ensure that the output voltage of the array is always within the voltage operating window of the inverter. The above formula has been used to determine the effect of temperature, both maximum and minimum daytime, on the output voltage of the array selected for installation at Veterans Retreat.

4.4.4. Battery Bank

There is no definitive guide for choosing battery size and operating strategies for a hybrid system. Factors that make up the design criteria (or rules–of–thumb) generally depend on the nature of sources and loads, and include:

1. Load energy consumption analysis
2. Allowed depth of discharge (DOD)
3. Number of days of autonomy
4. System efficiencies or losses (e.g. battery, wiring, and power conversion)
5. Operating temperature

6. Allowed maximum battery weight
7. Recommended charging rate (or battery charge acceptance rate)

In view of these factors, the following criteria were investigated in the search for an optimum battery bank size.

- High Temperature Effect on Lead Acid,
- Battery at 50% DOD in VRLA Tubular Gel Cells.

Table 4. 4: Lead Acid Battery Problems

Temperature (^{0}C)	50% DOD Cycles
25	3,300
30	2,500
35	1,800 (~5years)
40	1,350
45	1,000 (3 years)

4.4.5. Variable Speed Diesel Generator

Although diesel generators are a well-established technology fundamental problems with their operation still exist. At full load and at constant speed, diesel generators run at maximum efficiency, but at Veterans Retreat daily and seasonal load variation will make low loading of the diesel generators unavoidable.

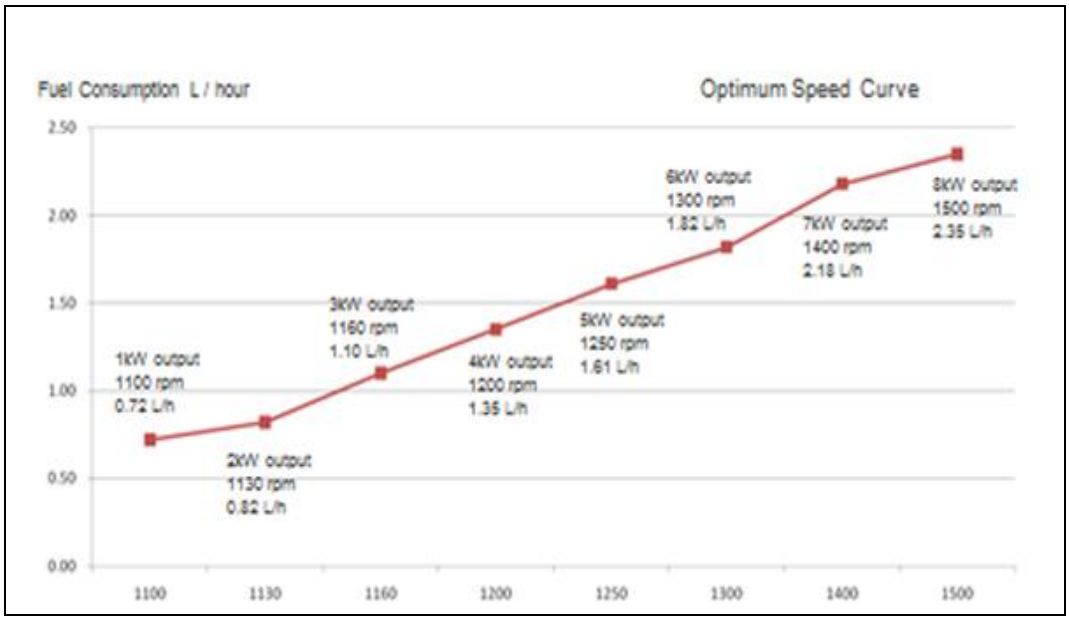

Figure 4. 16: VS Diesel Generator Fuel Consumption

Reduction in fuel consumption can be accomplished by running the engine at the most efficient speed for a given power demand. Figure 4.16 shows that the fuel consumption of a 8kW generator can vary from 1 litre per hour to 2.35 litre per hour. At full capacity it only takes around 3 litres per hour, demonstrating that the generator runs on minimum fuel.

The engine can also be run at much lower loads without the detrimental consequences that may result from constant speed operation. The engine performs fewer rotations per minute and consequently there is less combustion than that occurring in a constant speed operation at the same load. As a result, the combustions are fuller, the build-up of unburnt fuel is alleviated and the engine exhaust is less polluting. The operating set points can also be augmented to make engine pollution the most important criteria.

Table 4. 5: Variable Speed Specs

Variable Speed Generator Specs		
Parameters	**Units**	**Range**
General		
Output Power	kW	8
Output V - DC(settable range)	V	44-56.5VDC
Output Current (Max)	A	145
DG Start Battery	V	12V 80Ah
Operating Temperature Range	Degree Celsius	≤45
Output Voltage Ripple With battery	Milli Volts	Less than 20
Engine		
Make	Perkins	-
Model number	403D-15G	-
Operating speed	RPM	1100 to 1500 rpm
No. of cylinders	-	3
Alternator		
Make	Stamford	-
Model number	P1044H	-

A genset with a maximum electrical prime power rating of 8kW at maximum speed was selected for installation at Veterans Retreat. Altitude de-rating is included in the analysis. Under variable speed operation, the power output varies in the range 2.5 - 8kW. Figure 4.16 shows the fuel consumption chart and Figure 4.17 describes the circuit diagram of the variable speed diesel generator. Additionally, since this generator employs two or more different sources of energy, it provides the user with a highly reliable energy source, in comparison to single-source systems such as a stand-alone diesel generator or a stand-alone PV or wind systems.

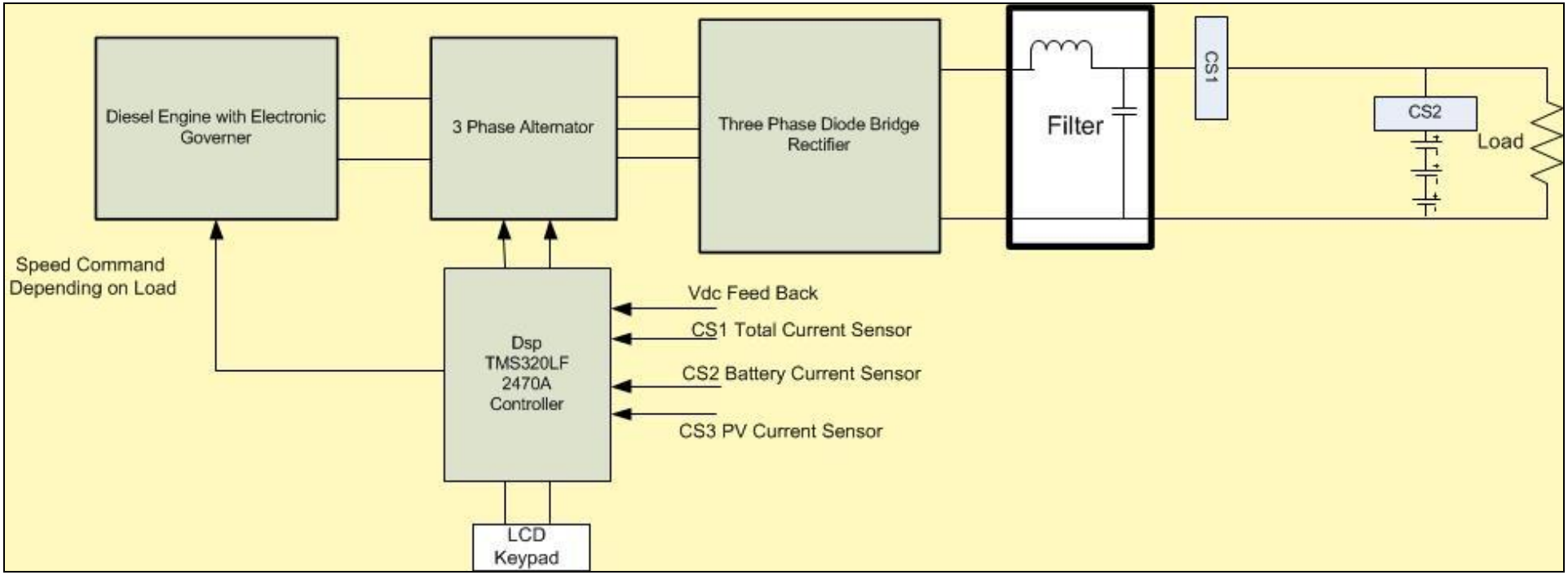

Figure 4. 17: Variable Speed Generator Circuit Diagram

4.4.6. System Description

The off-grid energy system at Veterans Retreat consists of solar photovoltaic (PV) modules, a grid connected inverter, an off-grid inverter, a battery and the Variable Speed Diesel Generator (Fig. 4.18). The generator will operate in variable speed fuel efficient mode to charge the battery bank. The output of the battery bank is connected to a single phase sine wave off grid inverter. During the day, the PV modules will supply the load and or charge the battery. The hybrid power source system consists of the following components:

- Solar PV panels (Mono / Poly).
- A variable speed diesel generator.
- A conversion system shall include inverting capability at 240 V, 50Hz.
- A storage system shall consist of 2V Valve Regulated Lead Acid (VRLA) batteries.
- The system will be fully integrated and automated in such a way that the diesel power generator automatically switches on and off when renewable energy power is unavailable or when battery energy is below or above the specified charge capacity. This way, the ampere-hour storage size of the battery bank can be kept at a minimum value.
- A single controller manages the complete power system seamlessly selecting the appropriate power source for lowest operating expenses by constantly monitoring load demand and battery charge.
- The PV/Diesel hybrid power system makes use of the solar PV energy to produce electricity that can be supplemented by the diesel generator when needed. The unit will have three management control components:

a) An Engine Management Controller
b) A Battery Management Controller
c) A Battery Charge Controller to charge the battery by running the engine at “optimum speed” at which the fuel consumption is the minimum.

The engine speed is automatically controlled based on the state of charge of the battery. The components and its program settings are identified to arrive at building an efficient system and taking into consideration the cost of energy and the dependency on diesel generator. When load increases and battery energy is not sufficient to support the load, the generator begins to produce power. Once the generator starts running it assesses the power requirement and then adjusts the speed according to the load and the demand of

the battery charge. This reduces speed and saves precious fossil fuel. This generator can run and produce constant voltage and frequency at variable speeds and also promptly available on load demand, we could design a system with minimal battery capacity.

By reducing the battery capacity we could reduce the capital cost and increase overall system efficiency by reducing battery charge and discharge losses. The engine stops after the battery is fully charged or when load demands are at the minimum. At this stage battery will support the demand for power. By setting up a hybrid system in this topology we were able to avoid the traditional disadvantages of a constant speed diesel generator. The system reduces the fuel consumption by diesel engine run time reduction resulting of battery usage.

The system for Veterans Retreat will have 3 modes of operation:

a) During Day Time

The energy from the PV modules shall supply the load and charge the battery on a priority basis. When the engine is running, it will meet any shortfall in energy, and the inverter convert the DC power from the solar PV/battery to AC power for the load.

b) During Night Time

The load power shall be met by running the engine at optimum speed. Depending upon the battery capacity, the engine will be switched on or off automatically.

c) Variable Speed Mode

In the variable speed mode, the engine essentially runs at variable speed depending on the state of charge of the battery which takes into account the power being supplied by the solar. The load is continuously supplied via the inverter.

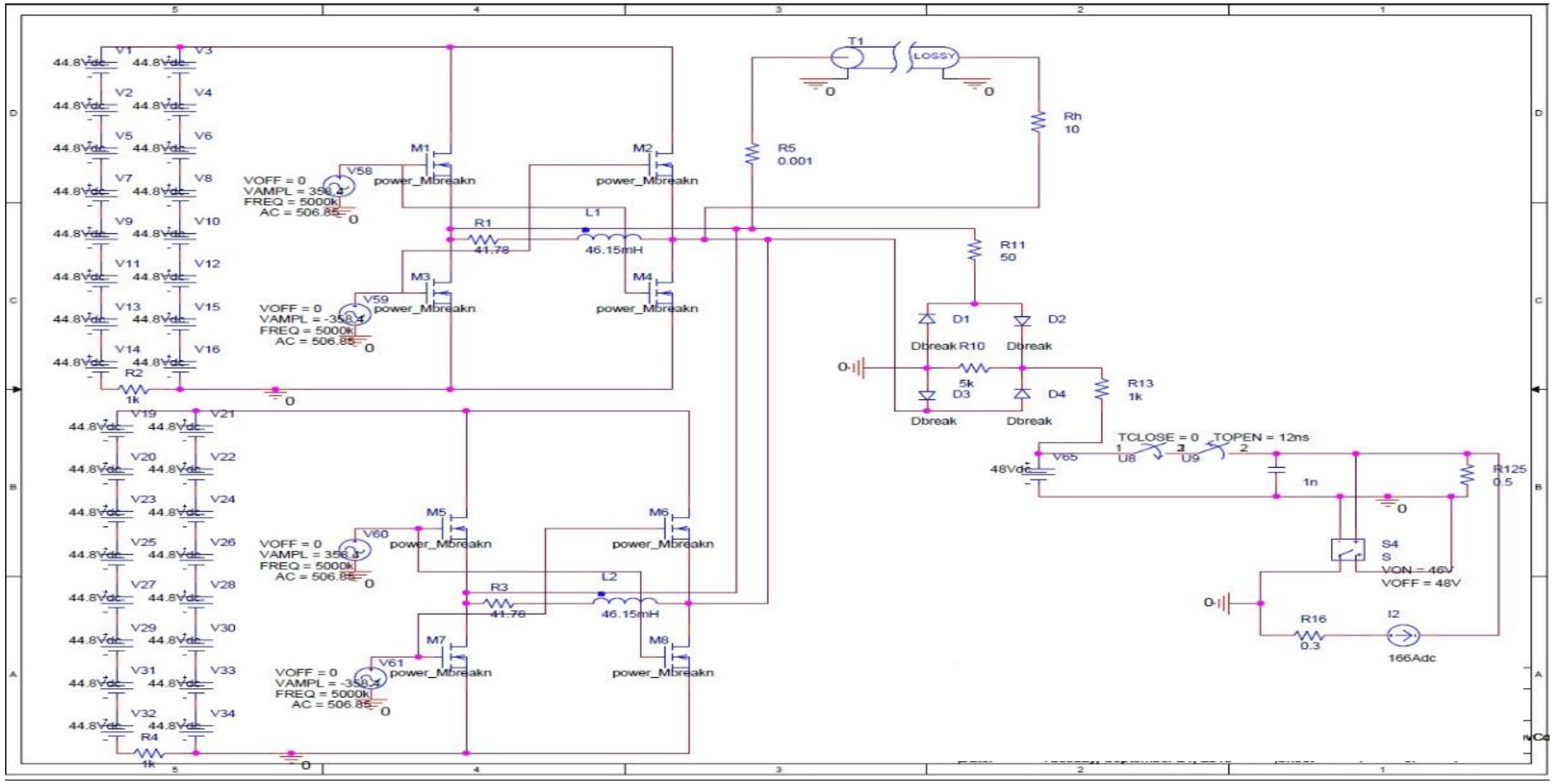

Figure 4. 18: Hybrid System Equivalent Diagram

4.5. System Modelling Using Homer and Pspice Simulations

Simulations were conducted using HOMER software; a product of National Renewable Energy Lab, a division of the U.S. Department of Energy. Based on the load profile at the site and the system components available in the market, a number of different sizing options were compared using Homer software for the optimization of economic, environmental and durability. Table 4.6 illustrates the best option out of over a thousand available combinations, based on the above mentioned factors.

Table 4. 6: System Simulation Table

PV (kW)	DCHyG (kW)	GEL 2V8..	Conv. (kW)	Initial Capital	Operating Cost ($/yr)	Total NPC	COE ($/kWh)	Ren. Frac.	Diesel (L)	DCHyG (hrs)
6	8	24	5	$ 61,500	2,443	$ 92,736	0.879	0.82	641	288
5	8	24	5	$ 58,000	2,725	$ 92,838	0.880	0.74	872	388
10	8	24	5	$ 75,500	2,038	$ 101,550	0.963	0.95	248	112
6	8	24	10	$ 69,000	2,593	$ 102,153	0.969	0.82	641	288
5	8	24	10	$ 65,500	2,875	$ 102,255	0.970	0.74	872	388
10	8	24	10	$ 83,000	2,188	$ 110,968	1.052	0.95	248	112
6	8	24	15	$ 76,500	2,743	$ 111,571	1.058	0.82	641	288
5	8	24	15	$ 73,000	3,025	$ 111,673	1.059	0.74	872	388
15	8	24	5	$ 93,000	2,001	$ 118,579	1.125	0.99	72	32
10	8	24	15	$ 90,500	2,338	$ 120,385	1.142	0.95	248	112
6	8	24	20	$ 84,000	2,893	$ 120,988	1.147	0.82	641	288
5	8	24	20	$ 80,500	3,175	$ 121,090	1.148	0.74	872	388
15	8	24	10	$ 100,500	2,151	$ 127,996	1.214	0.99	72	32
10	8	24	20	$ 98,000	2,488	$ 129,803	1.231	0.95	248	112
	8	24	5	$ 40,500	7,473	$ 136,029	1.290	0.00	3,318	1,459
15	8	24	15	$ 108,000	2,301	$ 137,414	1.303	0.99	72	32
20	8	24	5	$ 110,500	2,171	$ 138,252	1.311	1.00	36	16
	8	24	10	$ 48,000	7,623	$ 145,446	1.379	0.00	3,318	1,459
15	8	24	20	$ 115,500	2,451	$ 146,831	1.392	0.99	72	32
20	8	24	10	$ 118,000	2,321	$ 147,670	1.400	1.00	36	16

Table 4.7 shows the different options for system sizing that were compared through Homer simulations to arrive at the solution with minimised battery storage. For better understanding and clarity four possible types of electric systems were simulated. The former two options are hybrid systems while the latter two are conventional systems.

Table 4. 7: System Sizing

Description	Hybrid System		Hybrid without battery		Conventional system with no Solar PV		Conventional System	
	Value	Units	Value	Units	Value	Units	Value	Units
Solar PV Size	6	kW	10	kW	0	kW	0	kW
Batteries	800	Ah	0	Ah	800	Ah	0	Ah
Battery Voltage	48	V	0	V	48	V	0	V
Inverter Size	5	kW	5	kW	5	kW	0	kW
DC HybridGen	8	kW	8	kW	8	kW	0	kW
Diesel Generator	0	kW	0	kW	0	kW	15	kW
Initial Capital	$61,500.00	$	$62,500.00	$	$40,500.00	$	$15,000.00	$
Operational Cost	$2,443.00	$/yr	$12,374.00	$/yr	$7,473.00	$/yr	$28,070.00	$/yr
Total Net Present Cost	$92,736.00	$	$220,679.00	$	$136,029.00	$	$373,825.00	$
Cost of Energy	$0.88	$/kWh	$2.093	$/kWh	$1.29	$/kWh	$3.545	$/kWh
Renewable Fraction	0.82		0.74		0		0	
Diesel	641	L	4,824	L	3,318	L	20,367	L
Carbon Emission	1,689	kg/yr	12,704	kg/yr	8,737	kg/yr	53,632	kg/yr

- Option 1 consists of 6kW of Solar PV, 6kW grid connected inverter, and 5kW off grid Inverter, 800AhStorage battery and 8kW Variable speed Diesel Generator.
- Option 2 consist of 10kW of Solar PV, 6kW grid connected inverter, 5kW off grid Inverter, 8kW Variable speed Diesel Generator.
- Option 3 consists of 5kW Inverter, 800Ah Storage battery and 8kW Variable speed Diesel Generator. No Solar PV and the Diesel Generator is only running for 9 hrs (4pm to 1am) per day.
- Option 4 consists of a 15kW Diesel Generator only.

4.6. Results

Option 1 was selected for Veterans Retreat for several reasons:

- Due to limited external funding, finance had to be raised from internal accruals and private donations.
- The roof area on the makeshift transportable buildings (Donga) limited the size of the Solar PV system to only 6 kW.
- Visitors to the Retreat are irregular and seasonal, and despite consultation with the management, the load profile and energy requirements were only an estimate.

A detailed analysis of the monthly electrical output at Veterans Retreat is presented in Figure 4.19. In all months apart from June, PV provided more than half of the power output. On a yearly basis, 82% of the electrical output was sourced from PV. This ‘selective’ use of

the solar option was achieved by running the generator in variable speed mode as well as controlling its start/stop operation. During the winter months (June-August), the generator runs automatically during the early morning and early evening hours. Despite this, the average running time of the generator remained less than 300 hours per annum, effectively increasing its lifespan and lowering its maintenance requirements.

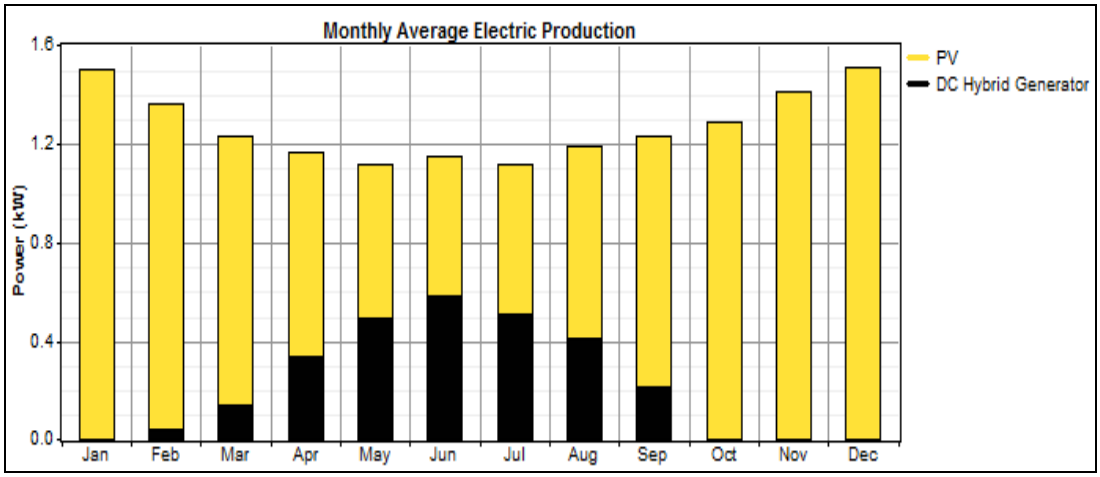

Figure 4. 19: Monthly Electricity Output

In Figure 4.20 the candlestick chart gives the variable speed diesel generator running time in an annual basis. During the winter months (June– August) the generator runs automatically during the early morning and early evening hours. The analysis shows the average running time of the generator is less than 300 hours per annum effectively increasing the lifespan and lowering maintenance compared to a conventional constant speed generator.

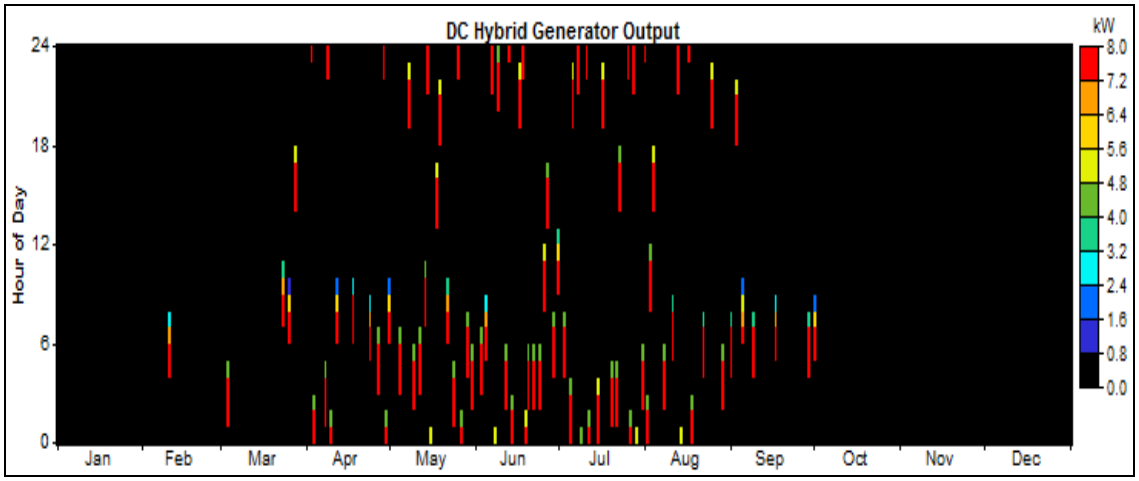

Figure 4. 20: DC Hybrid Generator Output

Figures 4.21 and 4.22 shows the performance of the battery (state of charge) on a yearly basis. During the summer months of October to February, the battery remains fully charged, while for the remainder of the year it undergoes several charge and discharge cycles. The battery is never discharged below 80 percent of state of charge because of the automatic setting of the generator. The battery bank consists of 24 numbers of 2V, 800Ah battery cells and all batteries are connected in series to get 48V DC. The analysis shows that the battery life exceeds 7 years.

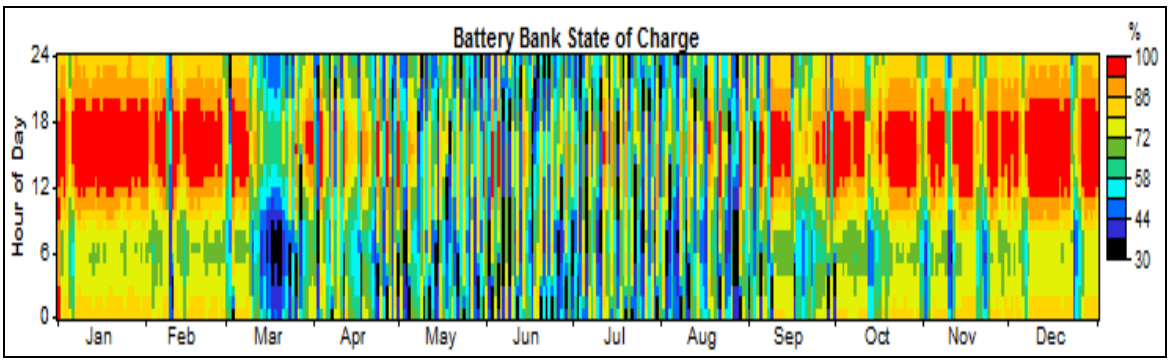

Figure 4. 21: Battery Bank – State of Charge

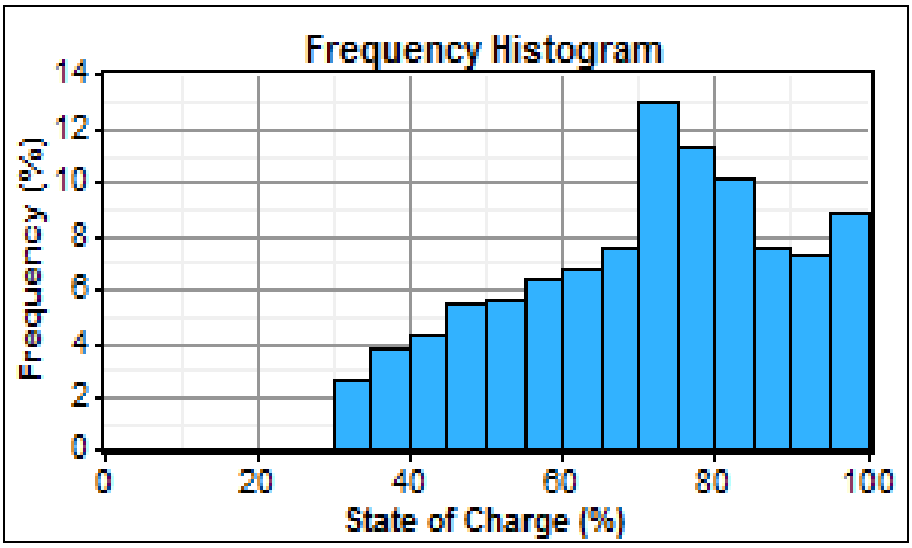

Figure 4. 22: Battery Frequency Histogram

Figure 4.23 illustrates the one day operation of the system in January. AC primary load, PV Power, variable speed generator power and battery state of charge are indicated on system performance hourly data.

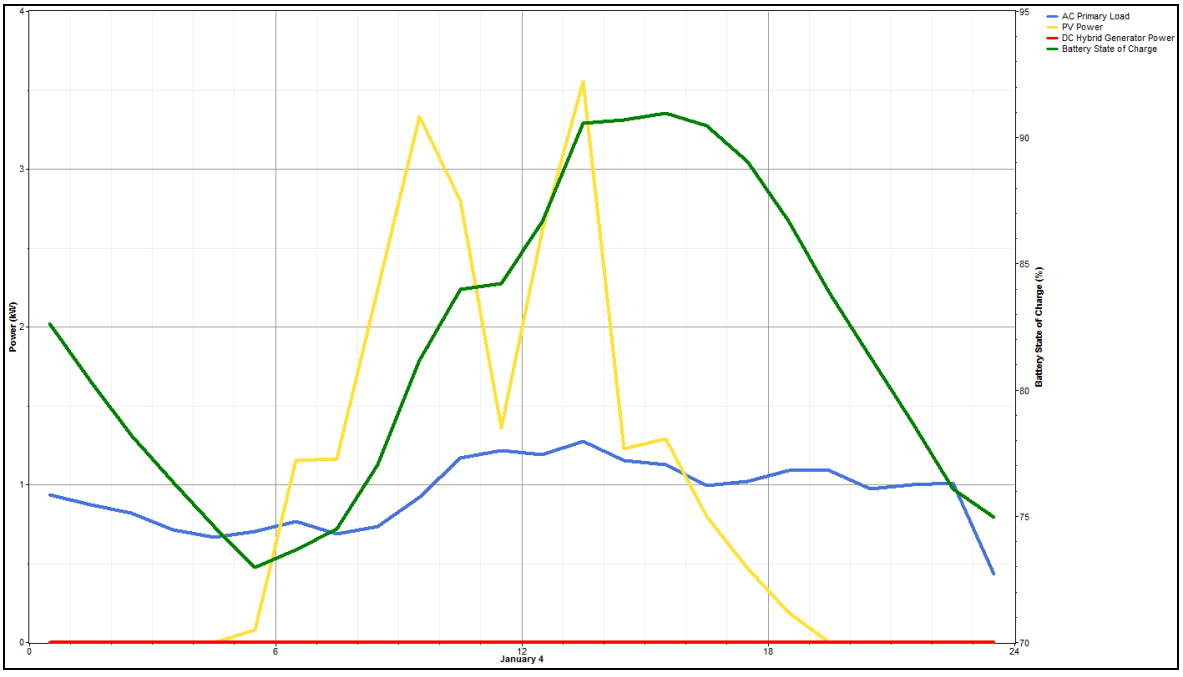

Figure 4. 23: System Performance Hourly data for Jan 1st

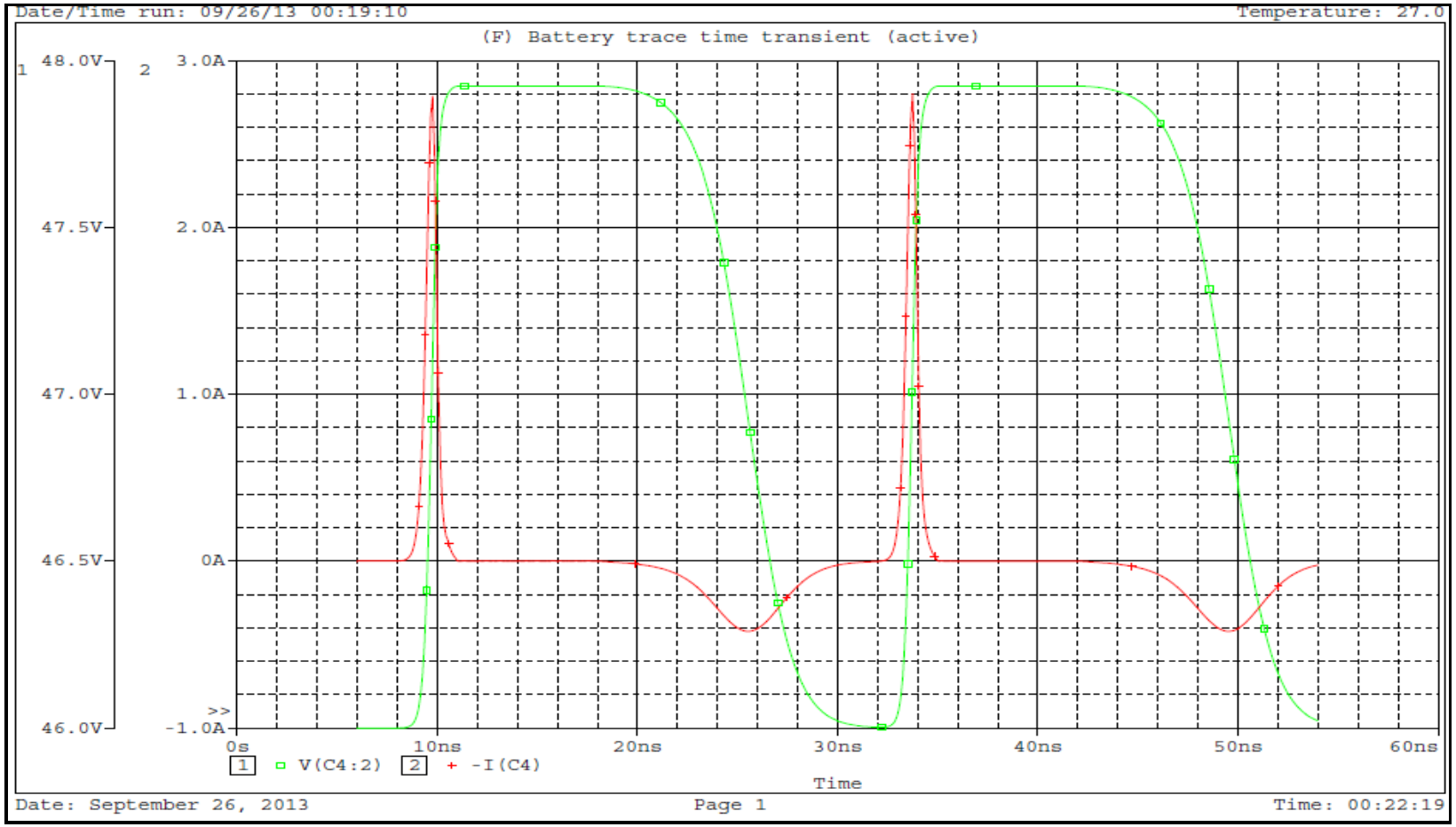

Figure 4. 24: Battery Bank State of Charge

Figure 4.24 indicates the battery bank state of charge graph which is modelled using the PSpice circuit analysis program (Figure 4.17). The system was installed at Veterans Retreat in April 2012. Figure 4.25 shows photos of the generator, solar panels on the roof, grid interactive inverter and the battery bank inside the air-conditioned sea container.

Figure 4. 25: System after installation and commissioning

4.7. Summary

In this chapter, the development of an innovative solar hybrid energy system incorporating a variable speed diesel generator with minimum battery storage has been presented. Simulation and experimental results confirmed that the combination of generator, battery and photovoltaic was ideally suited for remote community applications. Indeed, the Veterans Retreat system has been working satisfactorily for more than 20 months. Renewable energy generator size was a critical factor in the hybrid power system for two reasons. Firstly, it affected the ability of the system to operate in an efficient, cost-effective manner, and secondly, it affected the selection of power converter. The inclusion of a VSDG in an off-grid hybrid power system, with the predictive control algorithm in the supervisory controller, increases total system capital costs by only a small amount, and can be offset by the savings in battery replacement. Therefore, the off-grid PV-VSDG hybrid power system with advanced power management capability has great potential in the market for off-grid power generation.

4.8. References

[1] S. V. Mathews, S. Rajakaruna, and C. V. Nayar, "Design and implementation of an offgrid hybrid power supply with reduced battery energy storage," in *Power Engineering Conference (AUPEC), 2013 Australasian Universities*, 2013, pp. 1-6.

[2] J. Yuncong, J. A. Qahouq, and M. Orabi, "Matlab/Pspice hybrid simulation modeling of solar PV cell/module," in *Applied Power Electronics Conference and Exposition (APEC), 2011 Twenty-Sixth Annual IEEE*, 2011, pp. 1244-1250.

[3] I. Prasetyaningsari, A. Setiawan, and A. A. Setiawan, "Design Optimization of Solar Powered Aeration System for Fish Pond in Sleman Regency, Yogyakarta by HOMER Software," *Energy Procedia*, vol. 32, pp. 90-98, // 2013.

[4] K. A. Cook, F. Albano, P. E. Nevius, and A. M. Sastry, "POWER (power optimization for wireless energy requirements): A MATLAB based algorithm for design of hybrid energy systems," *Journal of Power Sources*, vol. 159, pp. 758-780, 9/13/ 2006.

[5] *MATLAB 7 Getting Started Guide*. Natick, MA: The Math Works, Inc., 2008.

[6] *MATLAB 7 Programming Fundamentals*. Natick MA: The Math Works, Inc., 2008.

[7] *MATLAB 7 Programming Tips*. Natick MA: The Math Works, Inc., 2008.

[8] A. G. B. o. Meteorology. Marble Bar heatwave, 1923-24 [Online]. Available: http://www.bom.gov.au/lam/climate/levelthree/c20thc/temp1.htm

[9] G. M. Masters, *Renewable and efficient electric power systems*. Hoboken, New Jersey: John Wiley & Sons, Inc., 2004.

[10] G. M. Masters, "Renewable and efficient electric power systems," 2004.

[11] X. Wang and H. Liang, "Output Characteristics of PV Array under Different Insolation and Temperature," in *Power and Energy Engineering Conference (APPEEC), 2012 Asia-Pacific*, 2012, pp. 1-4.

[12] B. A. S. Davis and S. Brewer, "A unified approach to orbital, solar, and lunar forcing based on the Earth's latitudinal insolation/temperature gradient," *Quaternary Science Reviews*, vol. 30, pp. 1861-1874, 7// 2011.

[13] NREL. (2014). *Homer Energy*. Available: http://www.homerenergy.com/HOMER_2.html

"Every reasonable effort has been made to acknowledge the owners of copyright material. I would be pleased to hear from any copyright owner who has been omitted or incorrectly acknowledged."

Chapter 5

5. Design and Implementation of a Medium Scale Mini-Grid Remote Area Power Supply System

5.1 Design Example for a Large De-centralized Remote Application Power System

5.1.1 Eco Beach Project Overview

This chapter refers to the 120 kW, fully hybrid renewable power system set up at the Eco Beach Wilderness Resort in Western Australia. The feasibility study conducted by Regen Power in 2008 formed the basis of this project. Regen Power completed the design, installation and commission of the power system at the resort in 2009.

The installed power system consisted of 24 x 2kW PV arrays, a 120kW central bi- directional inverter with a 360V, 1500Ahr battery bank and 4 x 50kW diesel generators. Every villa was equipped with a power monitoring device, which tracked the energy generated and the actual energy consumed in the villa, and allowed energy conscious guests to audit their use [1].

Figure 5. 1: Eco Beach Layout

The photograph in Figure 5.1 provides a 'hawk's eye view' of the entire Eco Beach Resort and surroundings. The villas are seen on the right near the coast and in the

centre of the photograph with the tin roofs. Each villa has a 2kW PV array installed on its roof. The maximum load was consumed by Jack's Bar, situated in the centre by the coast. The power station is located inland, and on the left, away from the villas to minimise noise disturbance for the guests. Two major requirements for the design were to minimize the use of diesel fuel as it is an eco-tourist resort, and to switch off diesel use at night to ensure that the guests could enjoy the natural night sounds. Therefore, an inverter based system would be required with maximum solar penetration and a large battery bank to carry the load throughout the night [2].

This system has been running for the past five years and the eco resort is content with the outcome. Only two incidents have disrupted operation. In the first, the batteries were damaged and the system failed, but the battery manufacturer accepted responsibility and replaced the battery bank. In the second, the complete system was damaged because of lightning and thunder storm and the complete battery system was replaced through insurance. Due to the popularity of the resort, occupancy rate has increased and the initial connected load is also increasing. Considering the fact that solar PV prices have come down, we proposed an addition of a 60-80kW PV system on the power plant roof and also one variable speed generator to charge the battery whenever required. By using this new technology, the usage of 4 diesel generator can be reduced and also save 30% of fuel; thus saving operating cost considerably and at the same time save the environment and reduce the noise pollution as well [3-6].

The annual climate graph for the resort is presented in Figure 5.2.

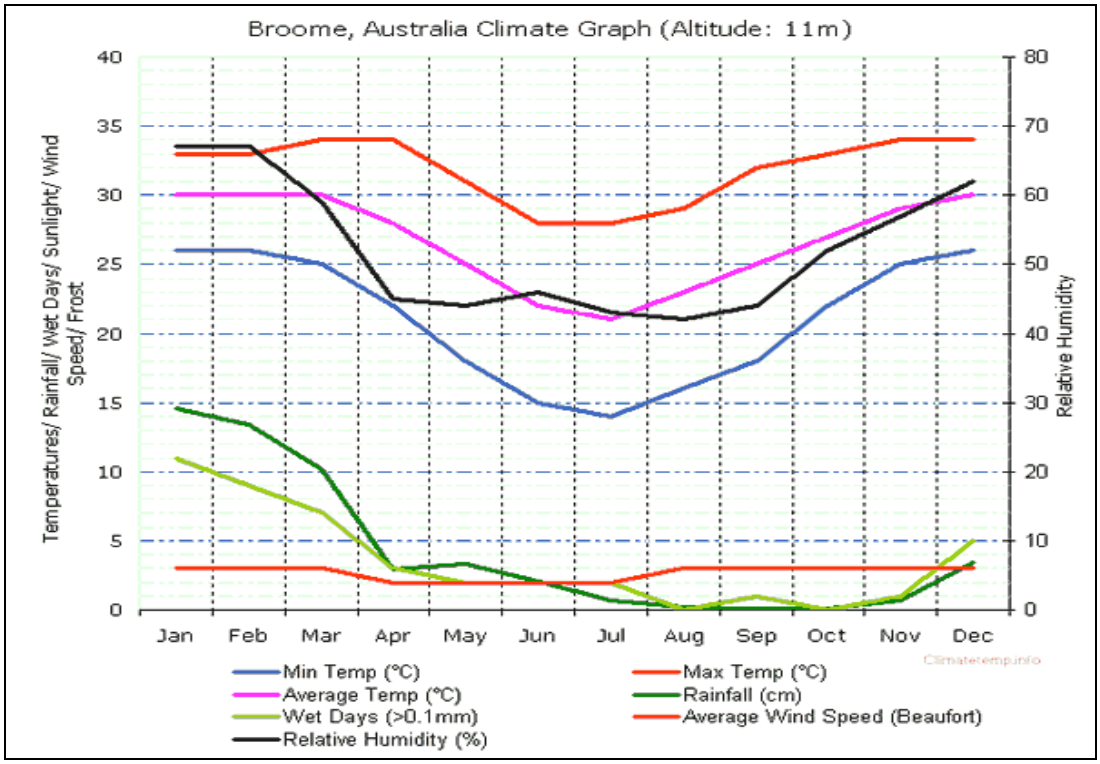

Figure 5. 2: **Broome Climatic Graph [7]**

Table 5.1 shows the power level and energy consumption at the resort for the years 2012. From this analysis an absolute peak load of 120kW was expected with a surge not greater than 150kW and an energy requirement of up to 600kWh per day. However, due to an increase in the number of guests in the past few years, the high seasons system load and peak load have almost reached to 120kW. Scaling values based upon resort occupancy were factored in to create seasonal and monthly load profiles. These were entered into HOMER and can be seen in Figure 5.3.

	Baseline	Scaled
Average (kWh/d)	555	555
Average (kW)	23.1	23.1
Peak (kW)	97.5	97.6
Load factor	0.237	0.237

Figure 5. 3: Eco System Loads

A frequency analysis of the load profile over a year was carried out in HOMER [5] and the system loading was expressed as a probability distribution (Figure 5.3). In this way, the generator size for the system could be optimised. Due to the noise restrictions at night in the resort, we had to use a bi-directional central inverter, which allowed the system to operate in VC-VSI and CC-VSI modes. This CC-VSI feeding functionality allows an inverter to cover small scale changes in load profile hold the DGs at a constant optimal load, in this case 80%. Since the generators were never lightly loaded or transiently overloaded, their operational lifetime was extended. As Jack's Bar provided the major system load the system was programmed for the generators to run between 5am and 8am and from 6pm to 9pm.

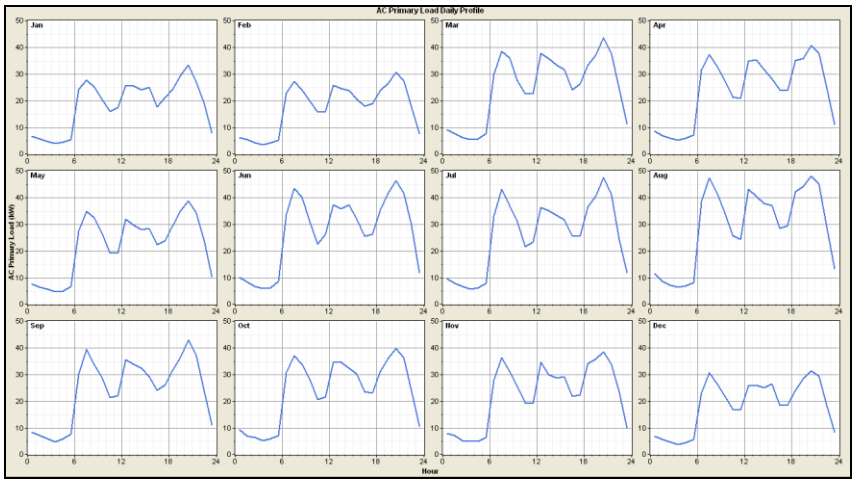

Figure 5. 4: **Predicted daily load profile per month**

5.2 System proposal and modelling

In the proposed system, the generator run time will be reduced by 20% through the inclusion of a variable speed generator. A further reduction of 20% will be achieved by the addition of 60kW of solar panels. The diesel generators will still be operated at times of peak load and simultaneously charge the batteries. However, the majority of the energy required to charge the batteries will be provided by the solar PV and the variable speed generator. It should not be necessary to run the generators solely to charge the batteries, except during uncontrollable situations such as unusual weather conditions or very high guest numbers.

Figure 5.4 shows that for the majority of the system's operation, the load will remain below 50kW, only reaching 80-100kW on a few occasions. If this occurs during a sunny day,

the majority of the load required can be met from the solar, and the remainder from the battery. So, even in this scenario, diesel generator use would be minimal. If the load was to increase because of high demand for the current facilities or as a result of expansion of the site, then consumption could increase by 20-30%. In these situations, a load of 80-100kW would be about 6%. The system would still be able to operate using energy from the solar PV, batteries and variable speed generator support [8-11].

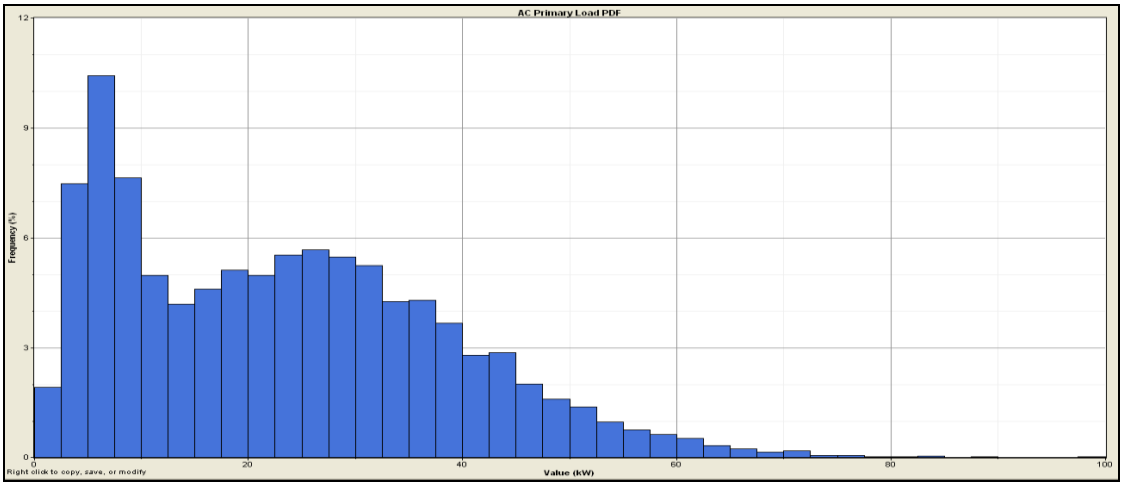

Figure 5. 5: System load frequency distribution

The solar irradiation and ambient temperature data were collected from BoM [12] ground irradiation data at Broome Airport, some 80km away. This information was entered into HOMER to create the expected monthly variations in energy yield.

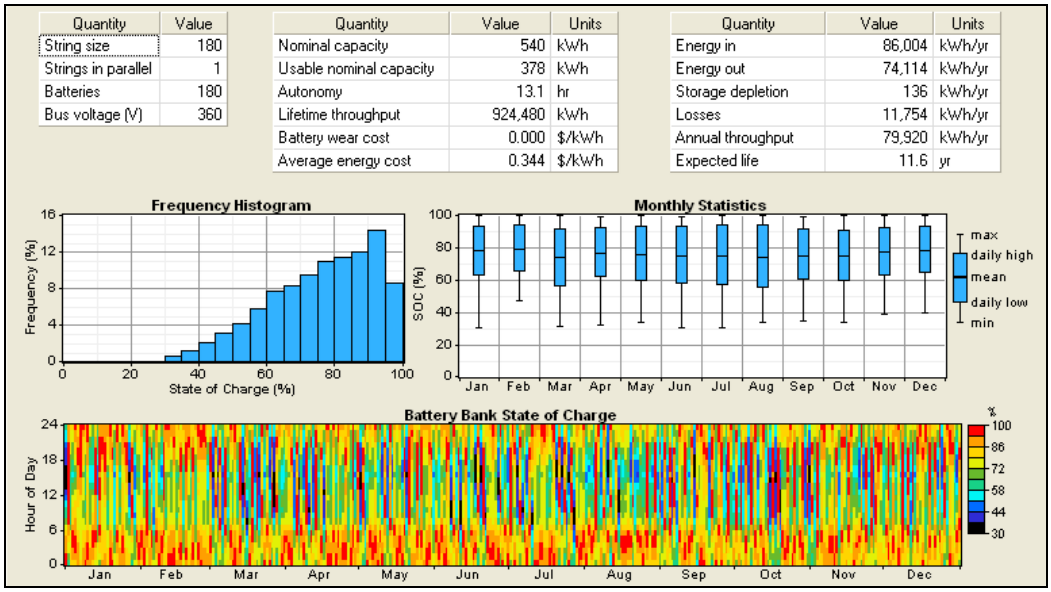

Figure 5. 6: **HOMER battery cycle analysis**

HOMER allows an annual battery cycling analysis to be easily simulated, as given in Figure 5.5. The expected battery lifetime is 11.6 years with an annual battery output of 80MWh. The battery SOC should never fall below 30 with it nominally operating between 60 and 95%. The lowest annual SOC is expected in the middle of the year, between April and August, when the occupancy and loads are the highest and the solar irradiation levels are low [13].

In reality, the lifetime of any battery is ultimately decided by its manufacturer and quality. In this project the battery banks have already been replaced twice. Immediately after the system was commissioned irregularities in battery operation were noticed, and after close monitoring it was concluded that 4 batteries were damaged. These batteries were replaced by the manufacturer. However, the batteries continued to perform well below the expected optimum level. Studies conducted by the engineers and their team demonstrated a defect in manufacturing, and within 6 months, all 180 batteries were replaced by the manufacturer, and the system began to function properly.

In 2011, a big thunderstorm and lightning hit the Eco beach resort, completely damaging the electric cabling & control system, communication and C-Bus system. Some components of the hybrid power system such as the inverters, generator and solar PV, continued to work well, but the battery bank did not. Figure 6.6 shows the extent of the damage to the individual villa monitoring and control system.

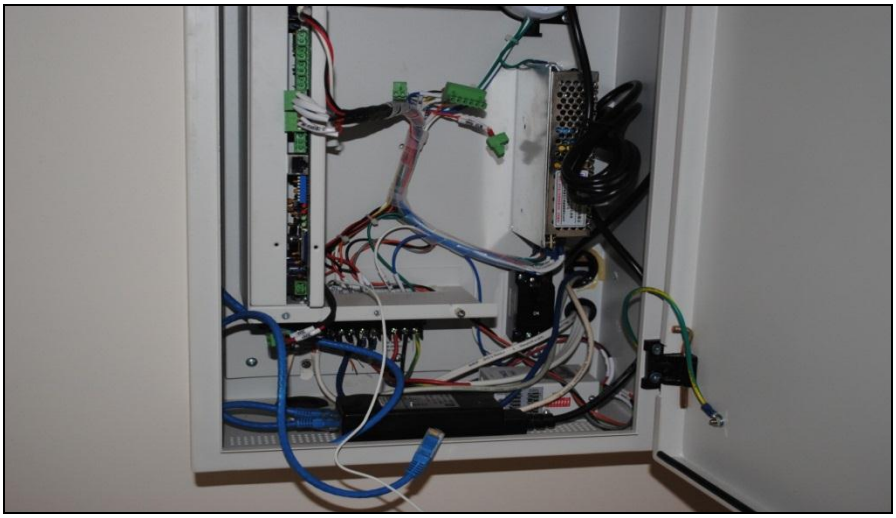

Figure 5. 7: Damaged Distributed Individual Villa Monitoring & Control System

Figure 5. 8: Damaged Battery

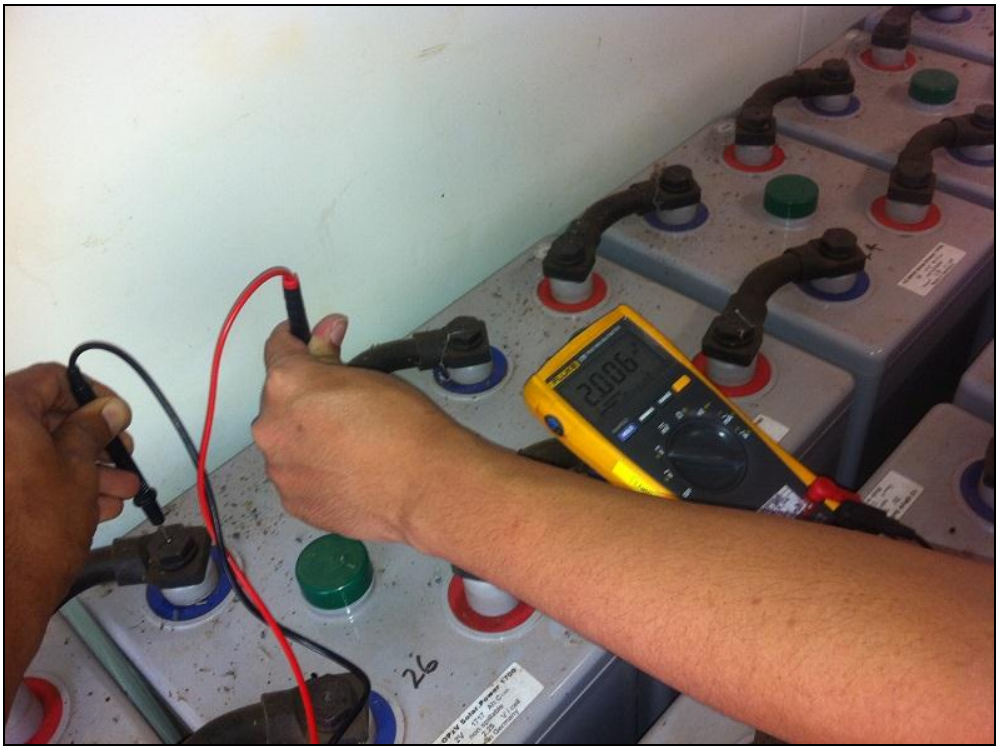

Figure 5. 9: **Damaged Battery**

Figure 5. 10: **Damaged Battery**

The batteries were over cooked because of the sudden surge in voltage from the lightning. Figures 5.7, 5.8 and 5.9 show the battery damage that occurred and the testing that was conducted. The entire bank of 180 batteries needed to be replaced. The solar panels and inverters in each villa were not affected by the storm. In contrast the remote control and wireless system were damaged, and as a result, the battery bank did not charge properly and started to give off a burning smell. Technical personnel visited the site on July 04 2011 for 5 days, tested the system, and confirmed that the battery bank and distribution inverter controllers were damaged. The system review also identified a malfunction in the monitoring system. For this reason, the Hybrid automation system (HAS), remote monitoring unit and control system were shut down so that the system could be further reviewed, and as a consequence, the diesel generators provided all power to the premises during this period.
While attending the maintenance work on site, the author proposed the system upgrade to the owner of the Eco Resort who agreed to the purchase of additional solar panels and a variable speed generator.

5.3 Software and Components used for Modelling

5.3.1 HOMER Modelling

With HOMER software, the constraints on a small power system can be varied, allowing the user to identify the best options for any subsequent modelling. The program first runs an hourly simulation of all possible system configurations. The load efficiency of diesel generators including lower efficiency when not fully operating can be determined. Analysis is repeated to optimize various user-defined factors, such as fuel price, load size, reliability requirement, and resource quality [14].

5.3.2 PSpice Modelling

The time domain response, small signal frequency response, total power dissipation, transient analysis and transfer functions were investigated using PSpice modelling. Three types of analysis were performed [15]:

- DC Analysis was used to calculate nodal voltages and branch current for circuits with time.
- Transient Analysis was used with variant sources to calculate all nodes voltage and

branch currents over a time interval.

- AC Analysis was used for signal analysis of all circuits with varying frequencies and to calculate all nodal voltage and branch currents over a range of frequencies.

5.3.3 MATLAB Modelling

Matlab modelling is an efficient and cost effective way to analyse and implement a project. Key aspects of a system, including the requirements, components, and communication strategies can be represented. Models can be referenced and divided into a hierarchy, which allows individual modelling of specific components [16].

5.3.4 Modelling System Components

- **Solar Modules**

Solar PV for the extension would be installed on the roofs of the villas. Capital and replacement costs were estimated at $8.50/W, including installation and dealer mark-ups. The panels were modelled as fixed and tilted north at an angle of 25 degrees.

The proposed panels for extension project will cost an estimate of $4/W, inclusive of installations and dealer mark ups since the global solar price has decreased. Roof mounted array frames can be used which need very little maintenance, as necessary for the panels. A de-rating factor of 90% was applied to the electric production from each panel to approximate the varying effects of temperature and dust. A range of sizes were used for the optimized simulations, up to 150kW, which would cover around 1200m^2.

- **Batteries**

Batteries were presented as a “two tank” system. The capacity of one tank would be immediately available while the second could only be discharged at a limited rate. Since the original system included a 2V, 1500Ahr generic gel battery this was chosen for the

simulation. Batteries were indicatively priced at $1,200 per 2V, 1500Ahr cell, including installation, all associated fusing, enclosures and required signage.

- **Inverters**

Island type inverters of 4 sizes- 15kW, 30kW, 45kW and 60kW, the minimum size required for provision of three phase power, were analysed for the project. The inverter and rectifier efficiencies were assumed to be 93% and 85%, respectively, for all sizes considered. Indicative pricing was $21,000 for each 15kW of inverter power, including installation and extra equipment.

The basic expansion project does not require any modification to the existing island inverter and grid inverters. However, the connection of an additional 70kW of solar panels would require the addition of 4 extra 17kW grid-connected inverters.

- **Generators**

A vast range of diesel generators is available. The various manufacturers and distributors provide different information that can be difficult to compare. The generators were not allowed to operate at less than 50% capacity. Operation and maintenance costs for the generators are listed per hour of operation. Two different types of control strategies were used in the modelling. Under the load-following strategy, the generator provides only the power necessary to meet the load at the time. With the cycle-charging strategy, once the generator is operating, it uses as much power as possible to charge the batteries in addition to meeting the load.

A variable speed diesel generator which described in chapter 4 and Deutz generators were used to model the fuel consumption. We decided to model variable speed diesel generator and dual generator system, with two 50kW generators provided as both a backup to the solar system, should it be required to shut down, and as a dual redundant system, so that the system should work well, even if one genset is undergoing an overhaul.

For the new variable speed diesel generator the price was estimated at $20,000, while the existing generators were priced at $21,000 each.

5.4 System Control

The connection topology for the proposed Eco Beach extension is shown in Figure 5.10 as a single line diagram. The main loads are located at the villa grid, and represents the main system feeders. The distributed 24 x 2kW PV arrays and field inverters are seen in the green box, with their remote wireless monitoring interface back to the central resort energy monitoring centre. At the power house, the central inverter is directly connected to the villa grid. The DGs form a separate grid, and the connection between the 2 grids is formed through the bus coupler controlled by the inverter. CT's and voltage sensors monitor both the DG bus and the net feeder load. Main system parameters such as the battery SOC, net load, DG load, inverter load and time of day are monitored by the HCUU, which predicts future energy requirements and selects the optimal mode of inverter operation.

The split bus topology of the switchboard control for Eco Beach allowed the inverter controller to call for DGs, synchronize them on a separate bus and then feed power to the loads. The interconnection between the load bus and DG bus was controlled using a large motorized circuit bus coupler breaker. In an emergency situation, conventional DG plant-type operation could be obtained by disengaging the inverter control, opening the main inverter CB, and manually closing the bus coupler. The additional panels will ensure that the load can be supplied during daylight hours by solar PV, with any excess power being used to charge the batteries. Once battery SOC is reached, the set point priority will go to the variable speed generator, followed by other standby generators, depending on the power requirements of the load.

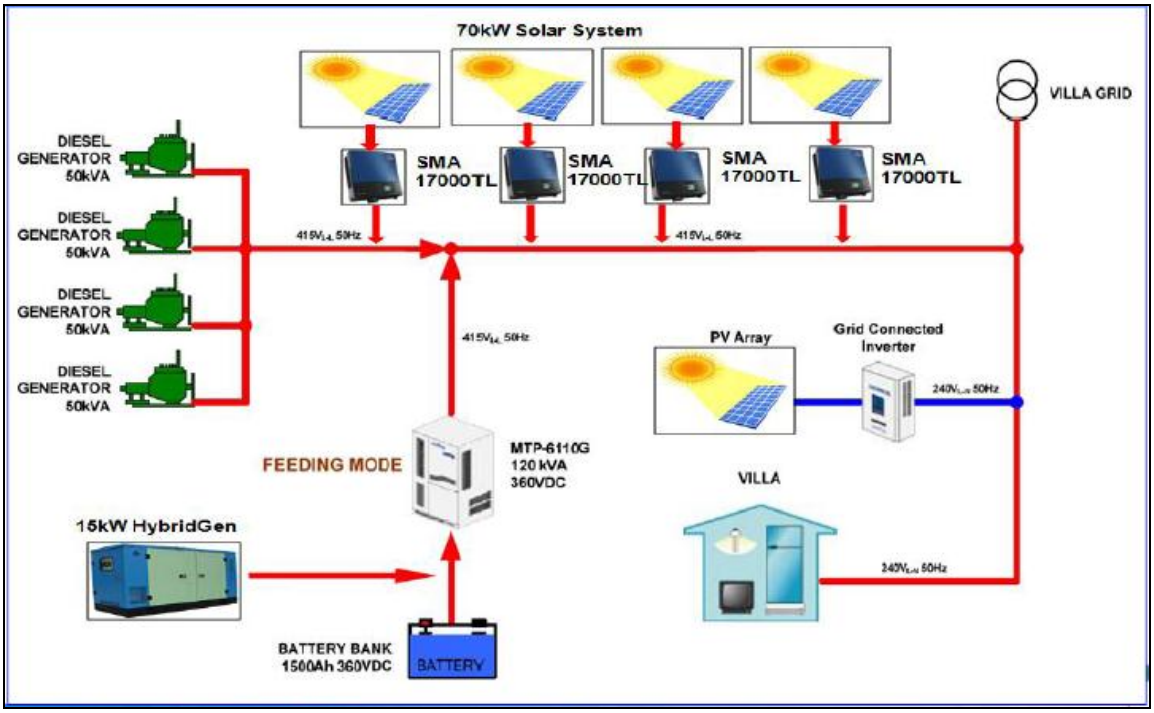

Figure 5. 11: Eco system diagram

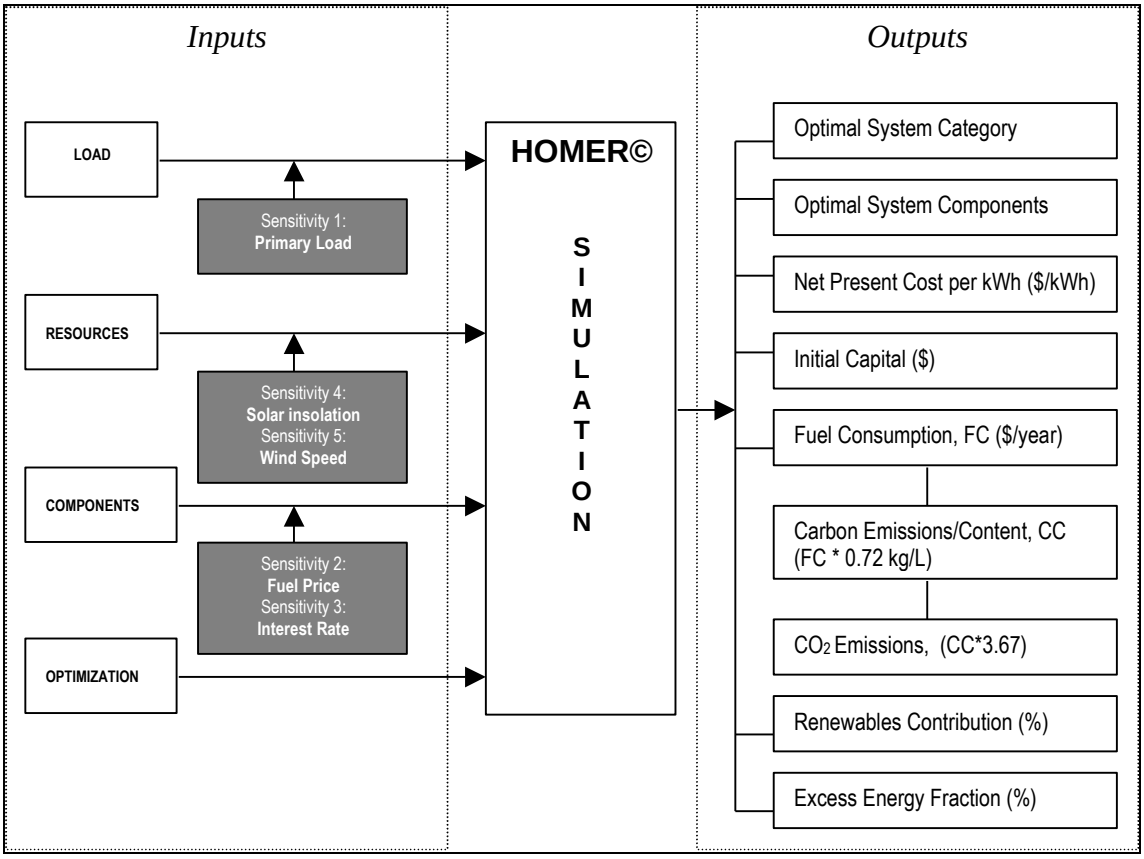

Figure 5. 12: **System control topology**

5.4.1 System Control Topology

The main objectives of the control of the system are to minimize the battery discharge cycle which will enlarge the battery life. By adding an additional renewable source (Solar PV) and DC variable speed generator, diesel consumption can drastically reduce. Variable speed generator's diesel consumption varies depending on the charging current, when the battery discharges heavily, that's the only time when full power is needed from the variable speed generator. Thus, diesel consumption is at a maximum only in such rare instances.

At other times variable speed generator runs at optimum speed to charge the batteries as required. Conventional diesel generators come into action only when the system hits a peak demand. The control system will take care of the conditions of the diesel generators to maximize operational efficiency of diesel generators.

The expansion system proposal models a high renewable energy fraction to maximize the renewable energy usage during all seasons at the resort.

The system is already designed and running on a minimized battery bank topology and the new expansion proposal maintains the same minimized battery topology even at increased load demand by adding variable speed control system, variable speed generator and solar panels.

The mini-grid system will operate in the following modes:

- Mode A: Operation with Low Sunshine and Peak Load
- Mode B: Operation with Full Sun Shine
- Mode C: Operation with No Sun Shine and Peak Load
- Mode D: Operation with Low Sun Shine and Low Load

The operation with low sun shine and peak load mode are Voltage Controlled Modes are implemented where the generators are all offline and the mini-grid is providing the source grid voltage which the distributed PV GCI's synchronize with.

The Current Controlled Modes are used where the generators are online and the mini-grid supplements, the power from the generators or can charge the batteries.

The mini-grid can add or draw power from the system to allow the generators to run at power levels close to their optimal efficiency points. The exact set points required for this operation can be evaluated at the next process. A possible implementation of this control topology is outlined in Table 5.1: Possible System Control Topology.

Table 5. 1: Possible System Control Topology

Eco Beach Control Topology						
Possible Implimentations						
Power Required from Gen/Inv System						
Load (kW)		Inverter/Charger	# Generator	Cont Type	Mode	
Range						
-30	-20	CHARGE	OFF	VC	B	
-20	-10	CHARGE	OFF	VC	B	
-10	0	CHARGE	OFF	VC	B	
0	10	INV	OFF	VC	A	
10	20	INV	OFF	VC	A	
20	30	INV	OFF	VC	A	
30	40	CHARGE	1	CC	D	
40	50	CHARGE	1	CC	D	
50	60	INV	1	CC	C	
60	70	INV	1	CC	C	
70	80	CHARGE	2	CC	D	
80	90	CHARGE	2	CC	D	
90	100	CHARGE	2	CC	D	
100	110	INV	2	CC	C	
110	120	INV	2	CC	C	
120	130	CHARGE	3	CC	D	
130	140	CHARGE	3	CC	D	
140	150	CHARGE	3	CC	D	
150	160	INV	3	CC	C	
160	170	INV	3	CC	C	
170	180	CHARGE	4	CC	D	
180	190	CHARGE	4	CC	D	
190	200	CHARGE	4	CC	D	
200	210	INV	4	CC	C	
210	220	INV	4	CC	C	
Make Battery Charge Prioirty Settings						
Mode	SOC	Action				
1	0<SOC<70	Feed all available power to recharge battery and inc generator to 95%				
2	70<SOC<98	Feed all PV generated power and run gen at max efficiency point				
3	98<SOC<100	Standby mode, use above power chart for energy use				
4	SOC = 100	Enable frequency change to drop off GCI in stages or DEB				

5.4.2 Overall System Monitoring

The hybrid system controller interfaces with a supplied computer which analyses all of the system information and presents this in a graphical user interface (GUI). The GUI is available on a screen display in the powerhouse as well as through the internet to access remotely. The system utilises the GSM through a modem or the GPRS through the internet to retrieve the data. This is outlined below in Figure 5.12: Remote Monitoring System and a sample screen shot from a previous system is shown in Figure 5.13: Sample Monitoring System Screenshot.

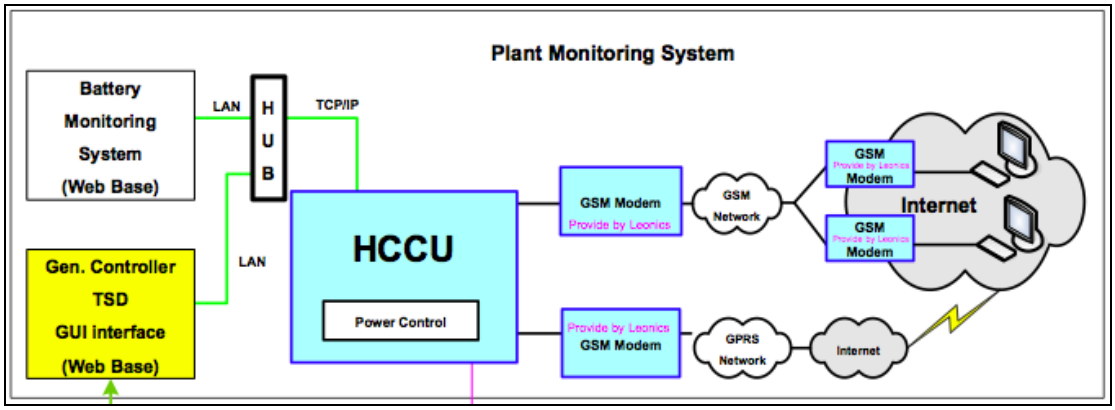

Figure 5. 13: Remote Monitoring System

5.4.3 System Protection

A surge arrestor has been installed between the mini-grid and the feed lines. This will prevent any voltage spike from propagating throughout the system in the event of a component failure or natural occurrence.

5.4.4 Economic Analysis

The economic analysis examines the cost effectiveness of the various hybrid systems that have been proposed and compares them to a diesel only system, which uses two equally sized diesel generators that can operate parallel, and a hybrid system without variable speed

generator. The analysis primarily chooses the reduction in diesel fuel consumption as the main indicator of performance, and the time it takes those savings to pay off the capital cost of the equipment.

5.5 System operation

The HCCU is designed to control automatically the operation of system in each mode (inverter mode, feeding mode, standby mode or charging mode) by sending command functions to BD-INV after that system operation is controlled by BD-INV. Moreover, this supervised controller used also handles the PV generated power by sending command to solar charger (SCM) (if any) through RS-485 communication interface to control current for charging battery from PV power.

The system operation can be explained as follows, as the system initially starts, all generators are started to be the prime power supply of the remote grid. HCCU starts monitoring load demand, battery SOC and then sends command to start the BD-INV or DG.

The operation will separate to 2 modes as follows:

In **Mode 1**- under normal healthy condition, Master Control have to inhibit auto function, HCCU is the master to control system operation and do the following procedure; now DG running and supply load if total load demand < 90% of bi-directional inverter capacity, then MTP take over all loads to work in inverter supply mode by transfer all load to inverter after that MTP sending command to open MC1 and wait to receive Aux. MC1 Signal (No. contact) to check MC1 already opens. After MC1 already confirm that it is open MTP will send MTP Demand signal to stop DG. If load start increasing > 95% of bi-directional inverter capacity, then HCCU will select the suitable operation mode that have 3 modes as following;

The central inverter can operate in four different basic modes; inverter, charging, feeding and standby. During inverter only mode, VC-VSI, Figure 5.14, the central inverter controls the voltage frequency on the grid. All DG are off and any excess energy generated by the distributed PV CC-VSI's can be used to charge the battery. This system can operate in VC-VSI mode with a negative charging current. If the battery is

full frequency variation is adopted to allow the central inverter to vary the power generated by the distributed field inverters. This technique was developed collaboratively with the manufacturer to prevent overcharging of the battery bank. A frequency band between 50.5Hz and 52Hz is used by the central inverter and monitored by the field inverters. A linear power shedding regime is used within this frequency band so that at 52Hz the power from the field inverters is down to 0%.

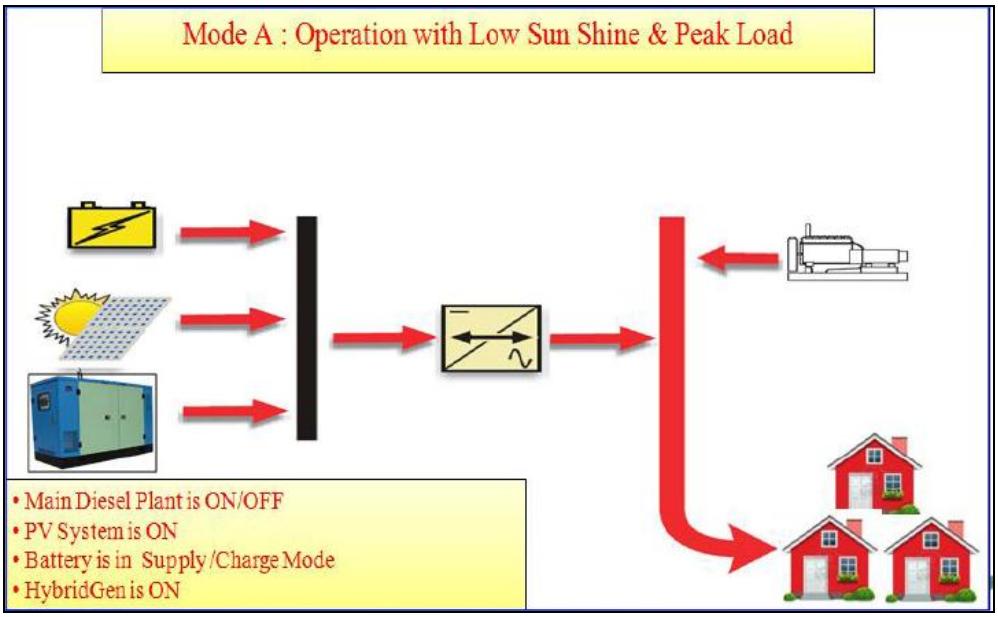

Figure 5. 14: Mode A Operation with Low Sunshine and Peak Load

The charging mode is used when the battery bank has a reduced SOC, and the DGs require to be optimised by drawing extra current, and the battery has some spare capacity or the battery SOC needs to be increased to allow night time operation. The power flows during this mode are seen in Figure 5.15.

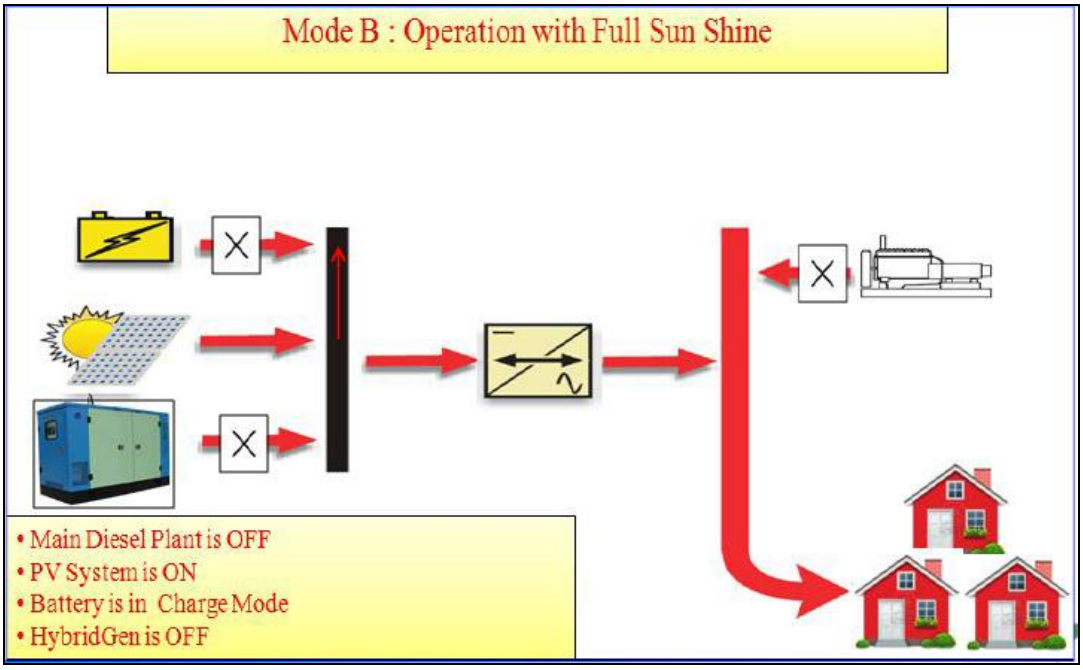

Figure 5. 15: Mode B Operation with Full Sun Shine

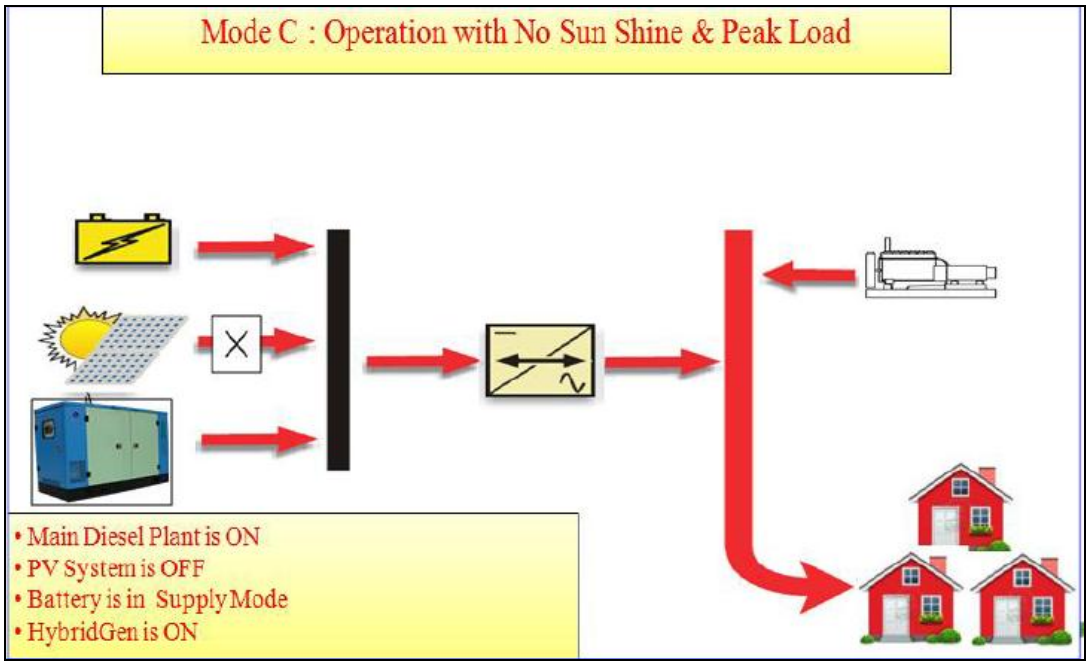

Figure 5. 16: **Mode C Operation with No Sun and Peak Load**

Feeding mode operation, Figure 5.16, is used when the battery is at a high SOC and the DGs are operating at a high level. The inverter will operate as a CC-VSI and feed power to optimize the loading of the DG or prevent another DG from starting from a transient load such as a fridge compressor or finally, allow an additional DG to shut down as the load is at an inefficient level between one and two generators.

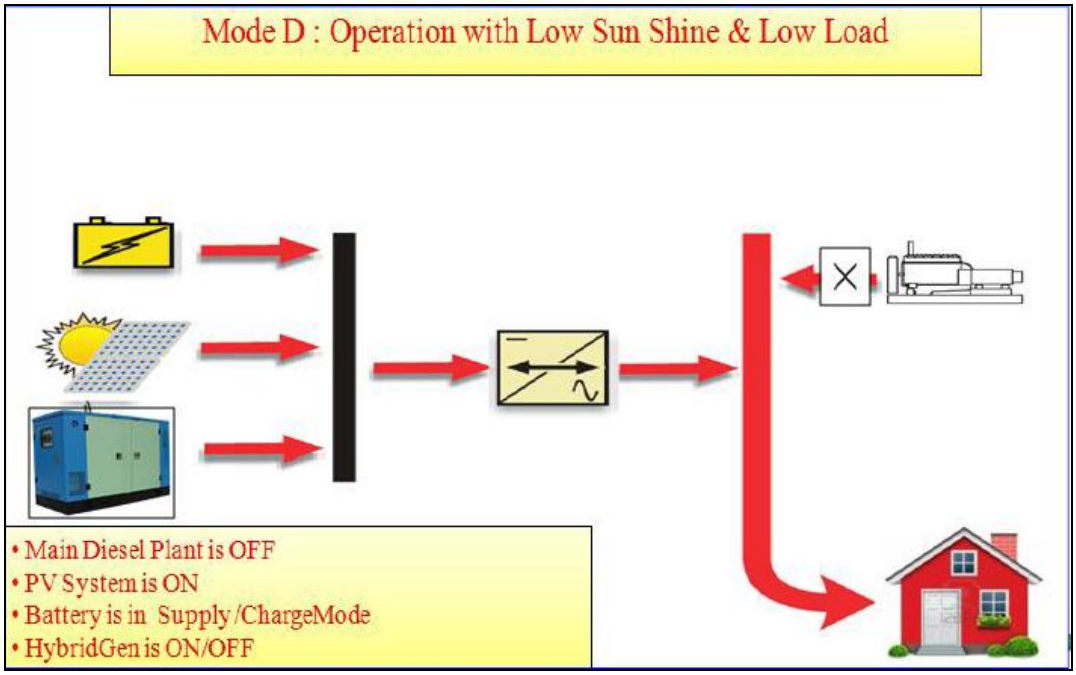

Figure 5. 17: Mode D Operation with Low Sun Shine and Low Load

Standby operation is selected when the battery is at a high enough SOC for the general time based variables and the DG are naturally operating at a power level which is quite efficient. This is a UPS type operation where if for some reason a DG fault occurred the inverter could quickly pick up the load and either prevent or only cause a momentary blackout. The difference between blackout and momentary blackout is determined by the instantaneous load, this transient power must be sourced quickly by the DC bus capacitor storage. If the load is too great the inverter's internal capacity cannot cover the energy and must start slowly to carry the load and prevent damaging current transients within the inverter.

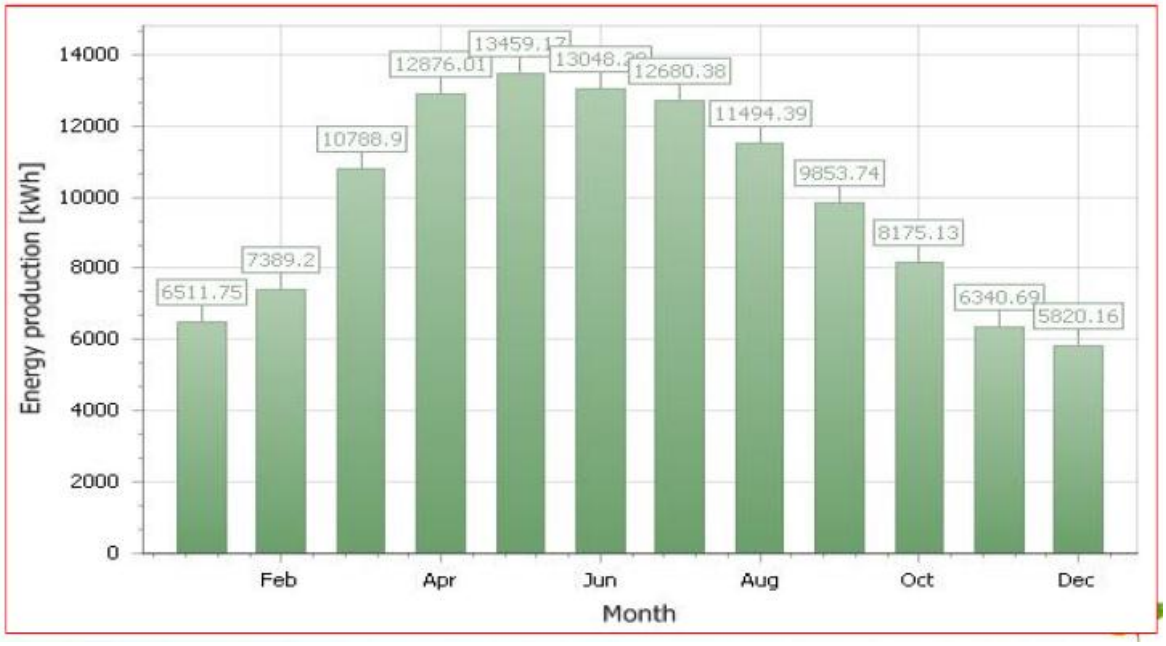

Figure 5. 18: **70kW PV average Monthly Energy Output**

In charging mode, The MTP will send command to start 3DG by sending MTP Demand signal. After generator already start and run up to normal operation speed, MTP will send command to close MC1 and receive Aux. MC1 Signal (No. contact) to check MC1 function before goes to charging mode. After that generator controller can control parallel of DG for suitable loads. All loads are transferred to use power from DG and MTP works in charging mode by getting power from DG to charge battery. In this mode, HCCU must know that which DG is running by checking Gen No.1 CB Signal, Gen No.2 CB Signal, Gen No.3 CB and Gen No.4 Signal to balancing energy.

In standby mode, The MTP will send command to start 3DG by sending MTP Demand signal. After generator already start and run up to normal operation speed, MTP will send command to close MC1 and wait to receive Aux. MC1 Signal to check MC1 function before goes to standby mode. After that generator controller can control parallel of DG for suitable loads. All loads are transferred to use power from DG and MTP works in standby mode. In this mode, HCCU must know that which DG is running by checking Gen No.1 CB Signal, Gen No.2 CB Signal, Gen No.3 CB and Gen No.4 Signal to balancing energy.

In feeding mode: If total load power consumption is higher than 80% of DG capacity to run only 3 DG, MTP feeds power under feeding mode to support loads together with DG. At this time, load is supplied by DG and MTP which controlled to feed power by hybrid system controller. The MTP will send command to start 3DG by sending MTP Demand signal. After generator already start and run up to normal operation speed, MTP will send command to close MC1 and wait to receive Aux. MC1 Signal to check MC1 function before goes to feeding mode. After that generator controller can control parallel of DG for suitable loads. Diesel generator supplies power to loads and MTP will feed power to support load power to maximize the uses of generator power and always energy balances. In this mode, HCCU must know that which DG is running by checking Gen No.1 CB Signal, Gen No.2 CB Signal, Gen No.3 CB and Gen No.4 Signal to balancing energy.

In **Mode 2**, Inverter fail mode or MTP fail contact open, If Master control receive the MTP Failure signal, Master control should control the whole system by sending command as following; Start all Generators then automatically close the MC1 to operate in bypass mode and send close MC1 in bypass mode signal to HCCU. In this mode generator controller should control to start necessary Generator if load is increased. After user repair the faults according to the causes as shown on LCD display and LED indicators the operators have to do the procedure to run MTP in normal mode.

5.5.1 MATLAB Simulation Results

Mode A: Operation with low sunshine and peak loads

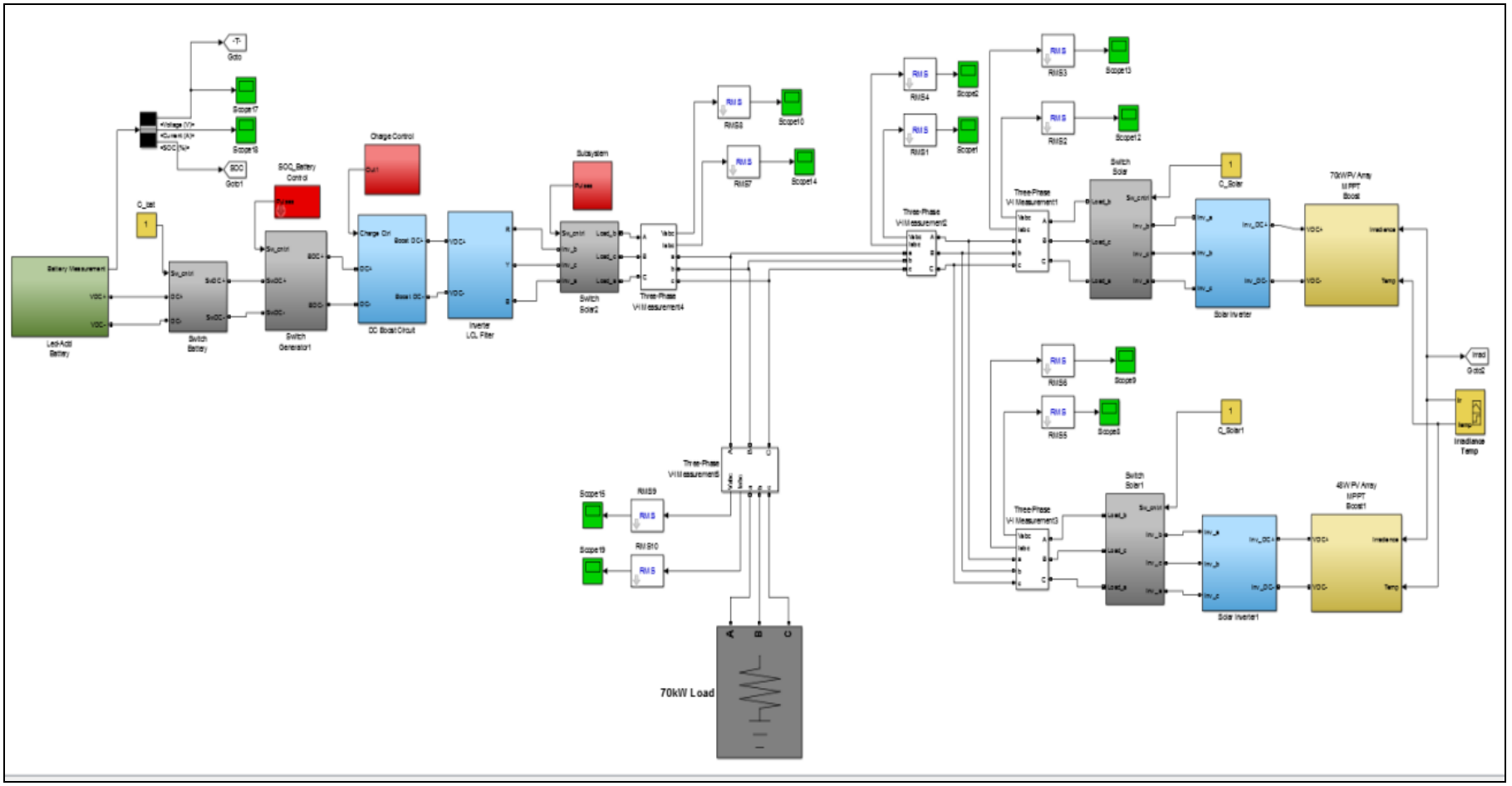

Figure 5. 19: MATLAB model of Mode A

The Simulink model of mode A operation is presented in Figure 5.19. Irradiance of 250W/m^2 was selected to represent low sunshine. Solar inverter loading was as per the MPPT control algorithm. Table 5.3 shows the simulated results of low sunshine and peak loads. The battery inverter would provide additional load once the maximum power had been drawn from both PV inverters. The main diesel generator and hybrid generator were not included in the simulations due to the degree of difficulty involved when a settling time of 4-5 seconds is required.

For Load power of 54.4kW (P_PVINV1+P_PVINV2+P_BATT)

- Power drawn from 70kW Solar Inverter is 14kW
- Power drawn from 48kW Solar Inverter is 10kW
- Power drawn from Battery Inverter is 30.5

Table 5. 2: Low sunshine peak load simulation results

Irradiance	70kW Solar Inverter			48kW solar inverter			Battery Inverter			Battery			Load		
	Voltage	Current	Power	Voltage	Current	Power	Voltage	Current	Power	Voltage	Current	Power	Voltage	Current	Power
250	353	23	14	353	16.5	10	353	50	30.5	435	76	33	353	89	54.4

Table 5. 3: Low sunshine peak load simulation results

Irradiance				250
	Voltage (UNIT)	Current (UNIT)	Power (UNIT)	
70kW solar inverter	353	23	14	
48 kW solar inverter	353	16.5	10	
Battery Inverter	353	50	30.5	
Battery	435	76	33	
Load	353	89	54.4	

Mode B: Operation with full sun shine and peak load.

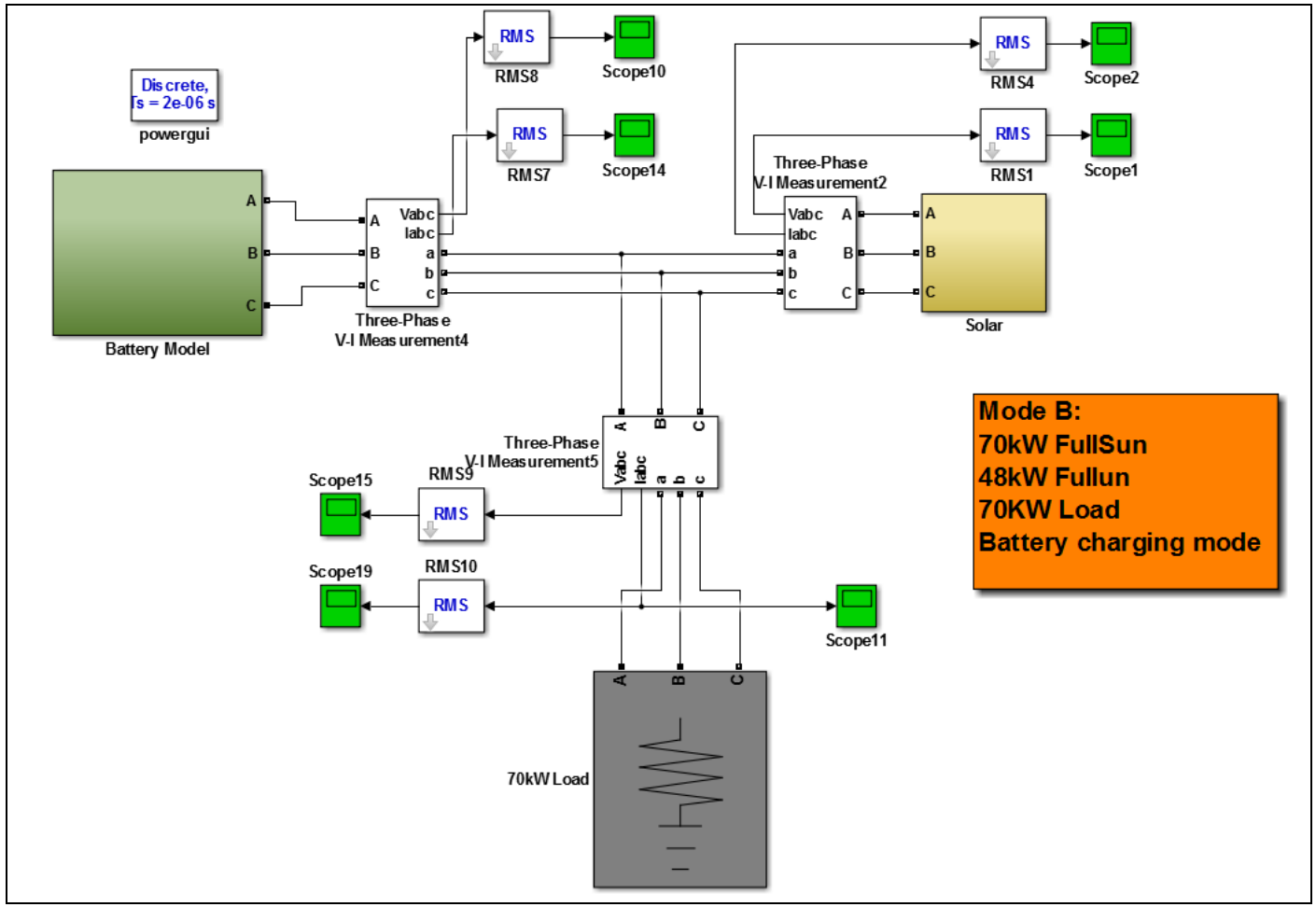

Figure 5. 20a: MATLAB model of Mode B

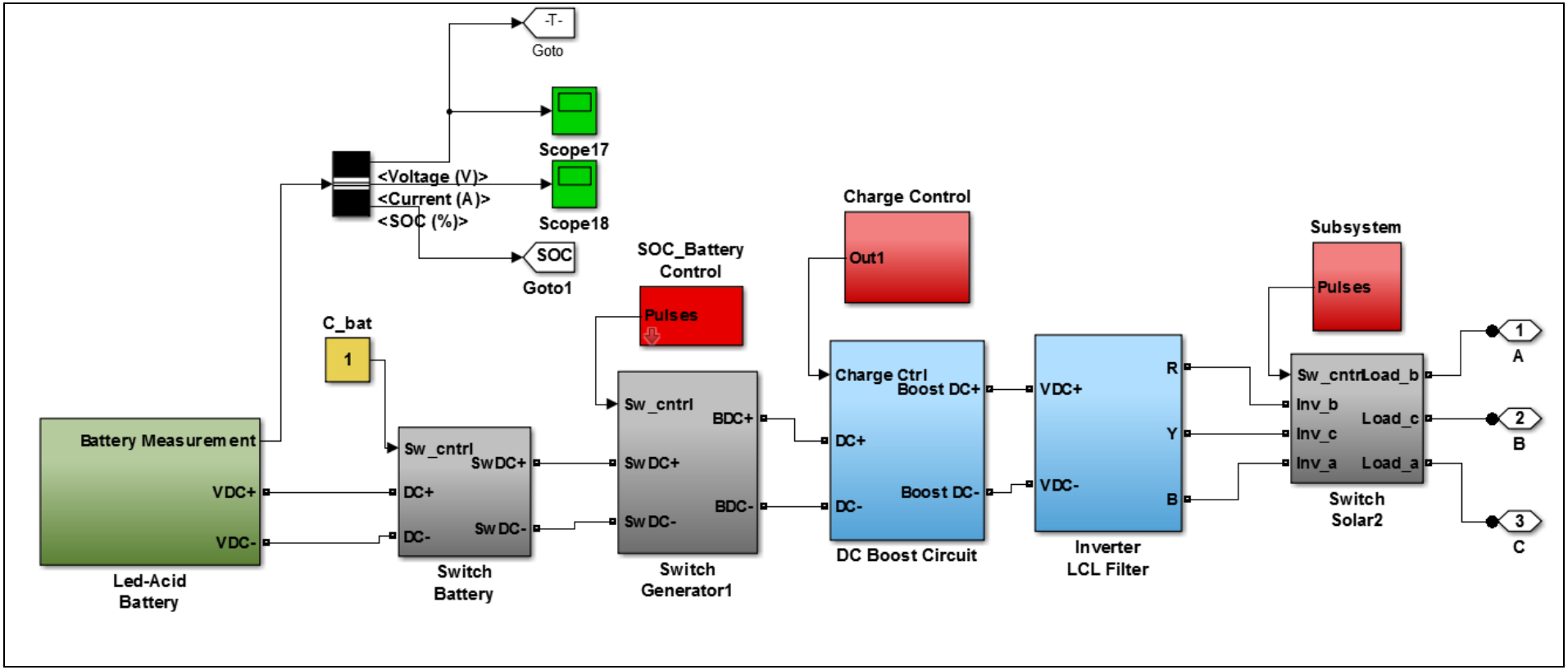

Figure 5. 21b: MATLAB model of Mode B (Battery model_Boost_Inverter)

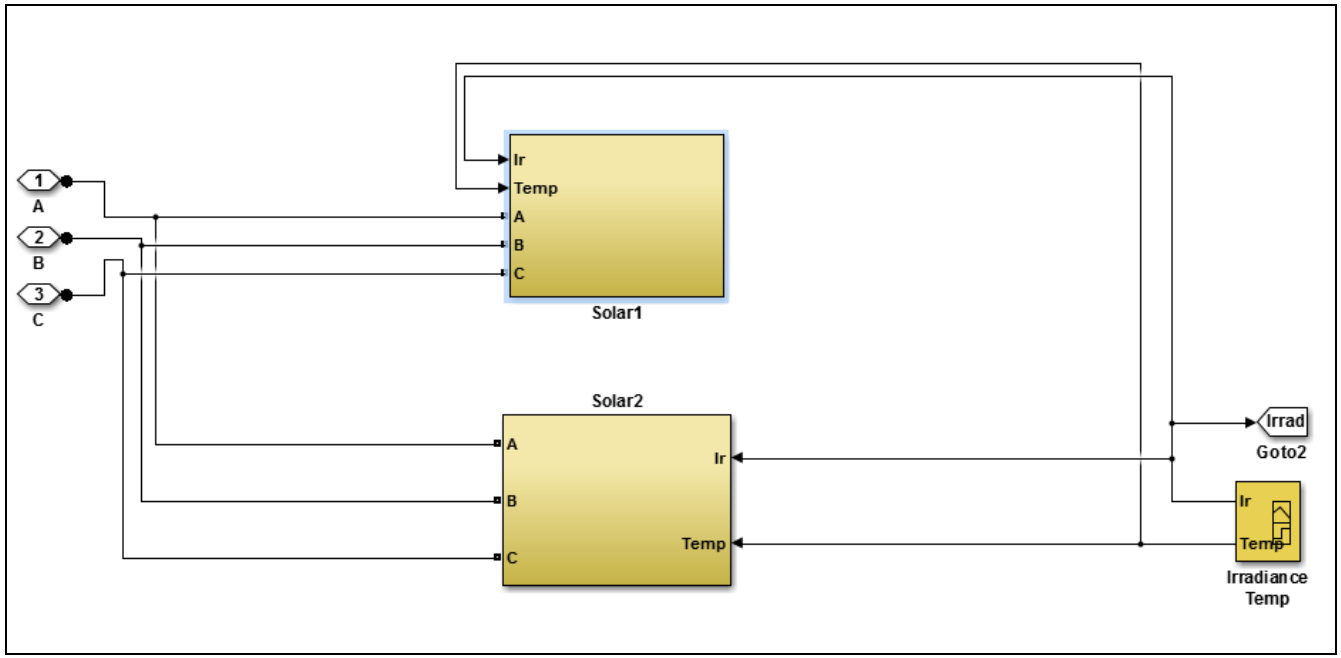

Figure 5. 22c: MATLAB model of Mode B (Solar Model)

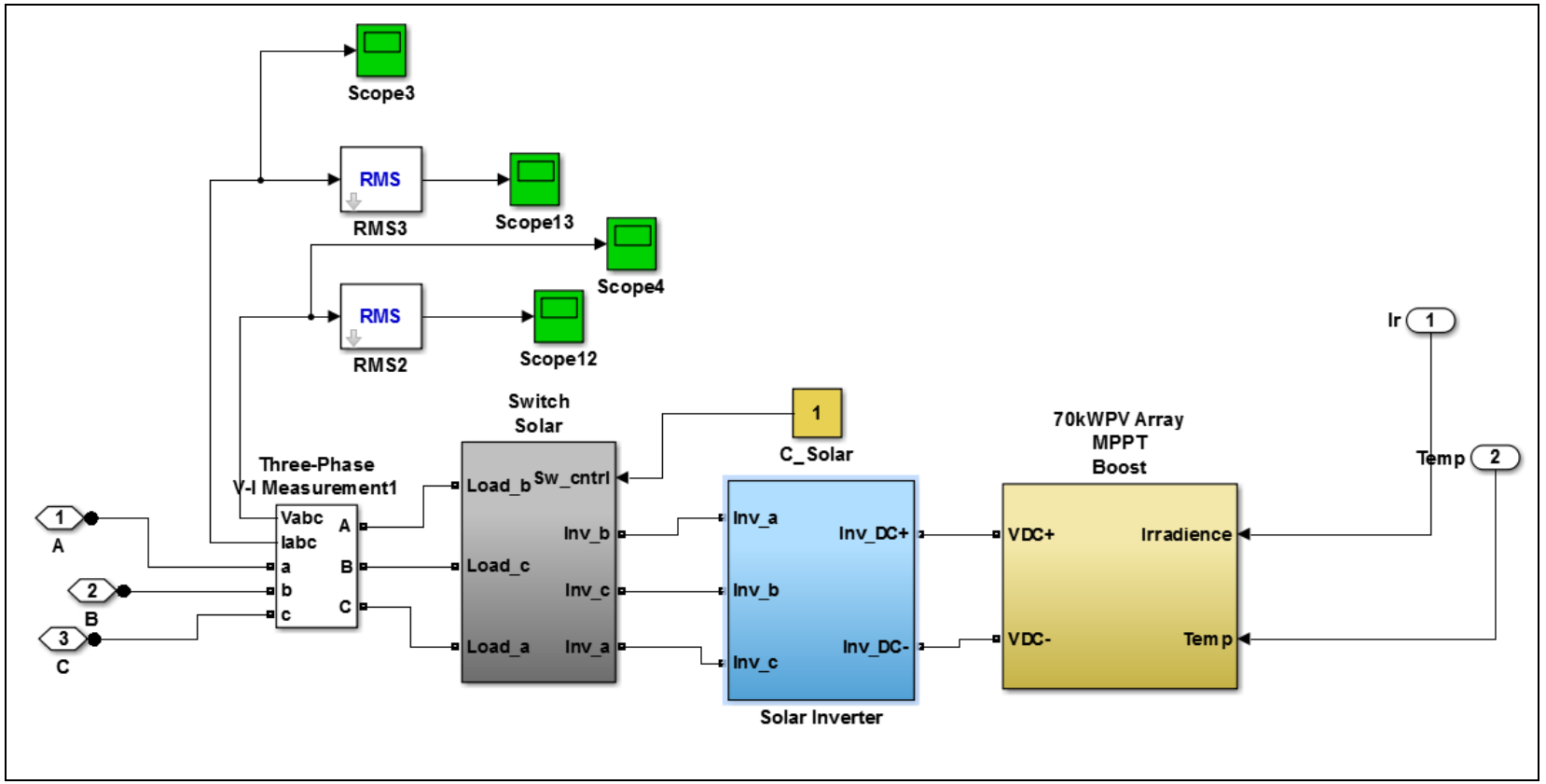

Figure 5. 23d: MATLAB model of Mode b (Solar1 & Solar 2 model_Boost_Inverter)

Figure 5.20 shows the Simulink model of Mode B operation. When the system is operating in full sun shine, total loading will be through the PV cell inverter. Load sharing between the PV panels will be as per the MPPT technique. The battery will be in charging mode, charging current will be as per the MPPT controller and buck converter current limit. Table 5.4 shows the simulation results of full sunshine mode.

Power flow is as shown below:

70kW Solar Inverter Power + 40kW Solar Inverter Power – Battery Charging Power = Villa load Power

Table 5. 4: Full sunshine simulation results

70kW Solar Inverter			48kW Solar Inverter			Battery			Villa Load			Comments
Vout	Iout	kW	Vout	Iout	kW	VDC	IDC	kW	Vload	Iload	kW	
400	62.4	43.2	400	52.2	36.2	404	-19.7	8	400	100	69.3	Battery in charging mode

Mode C: Operation with no sunshine and peak load:

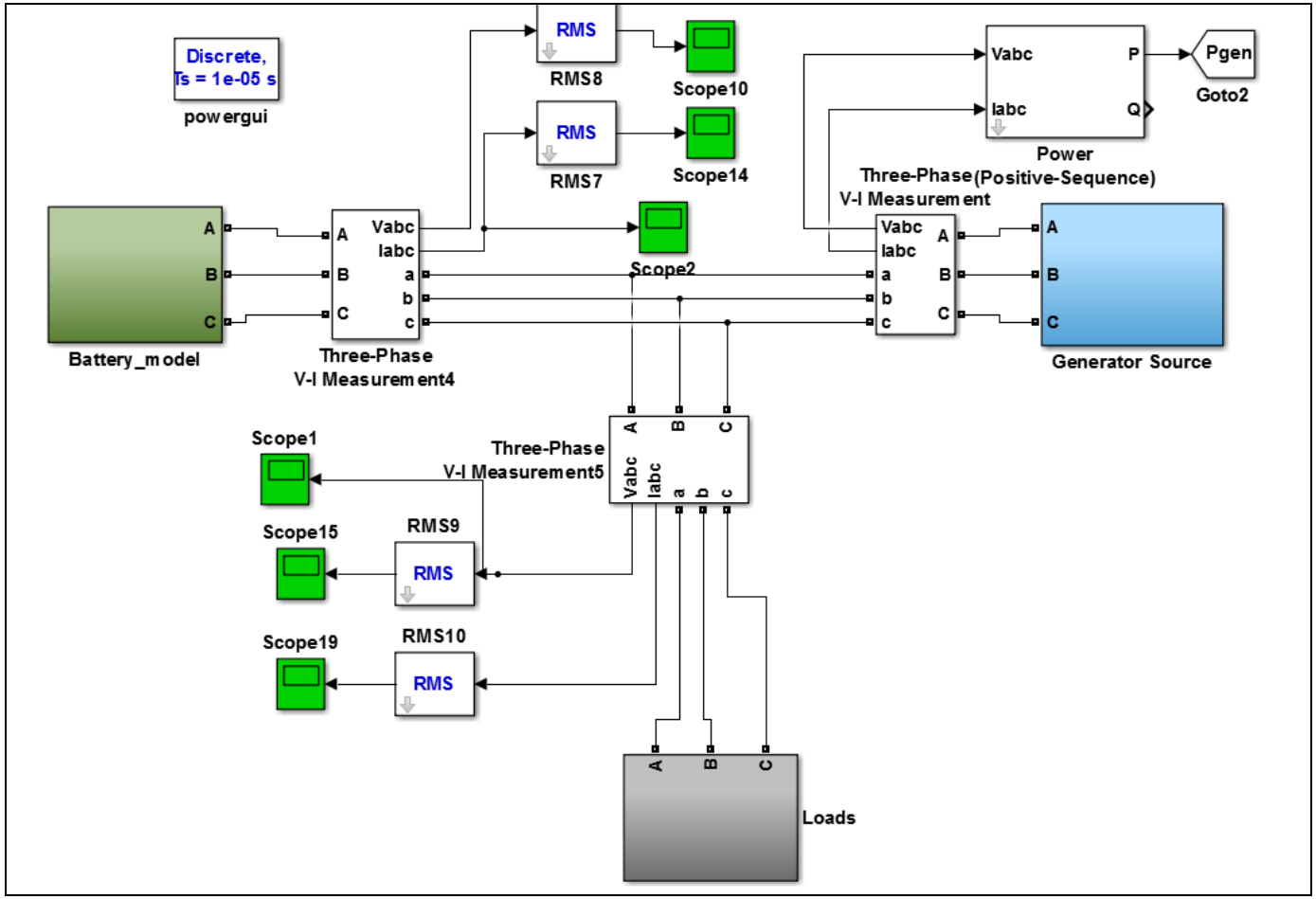

Figure 5. 24a: **MATLAB model of Mode C (Top Level)**

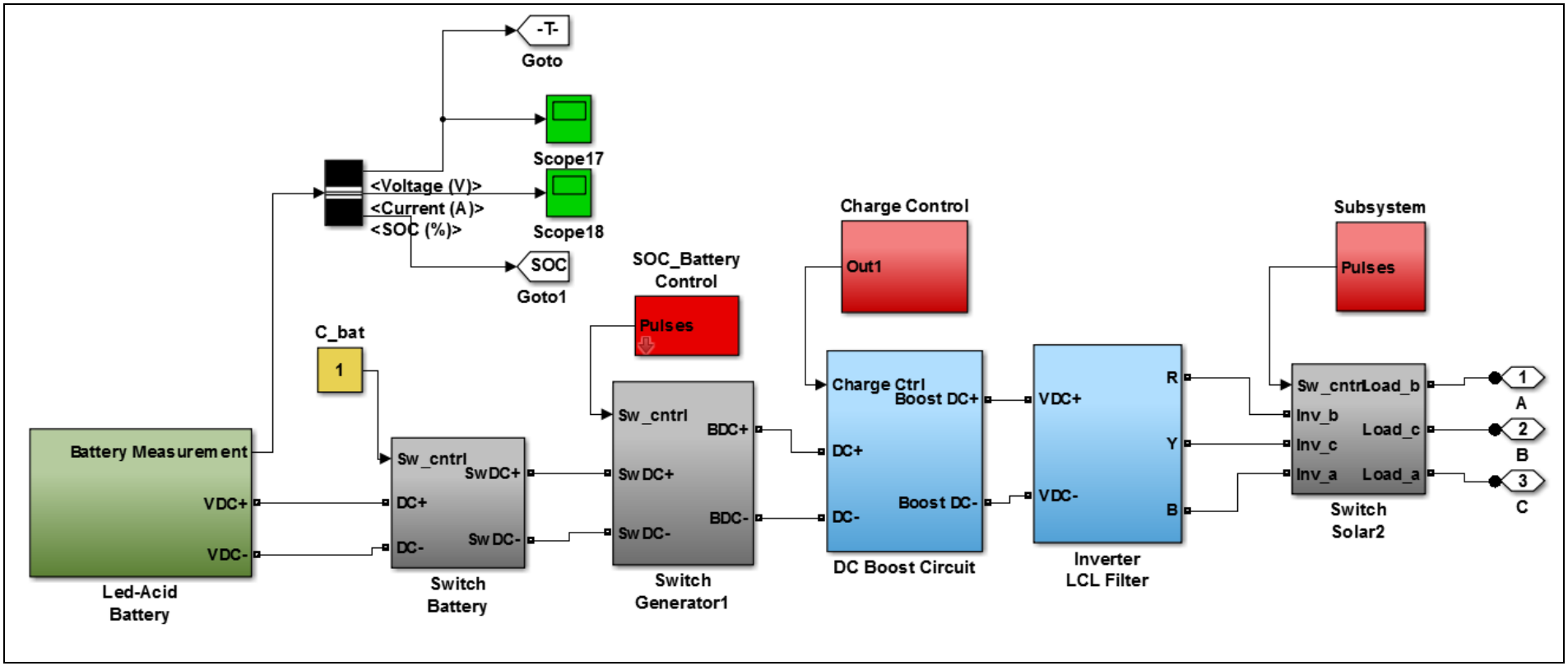

Figure 5. 25b: **MATLAB model of Mode C (Battery_Boost_Inverter)**

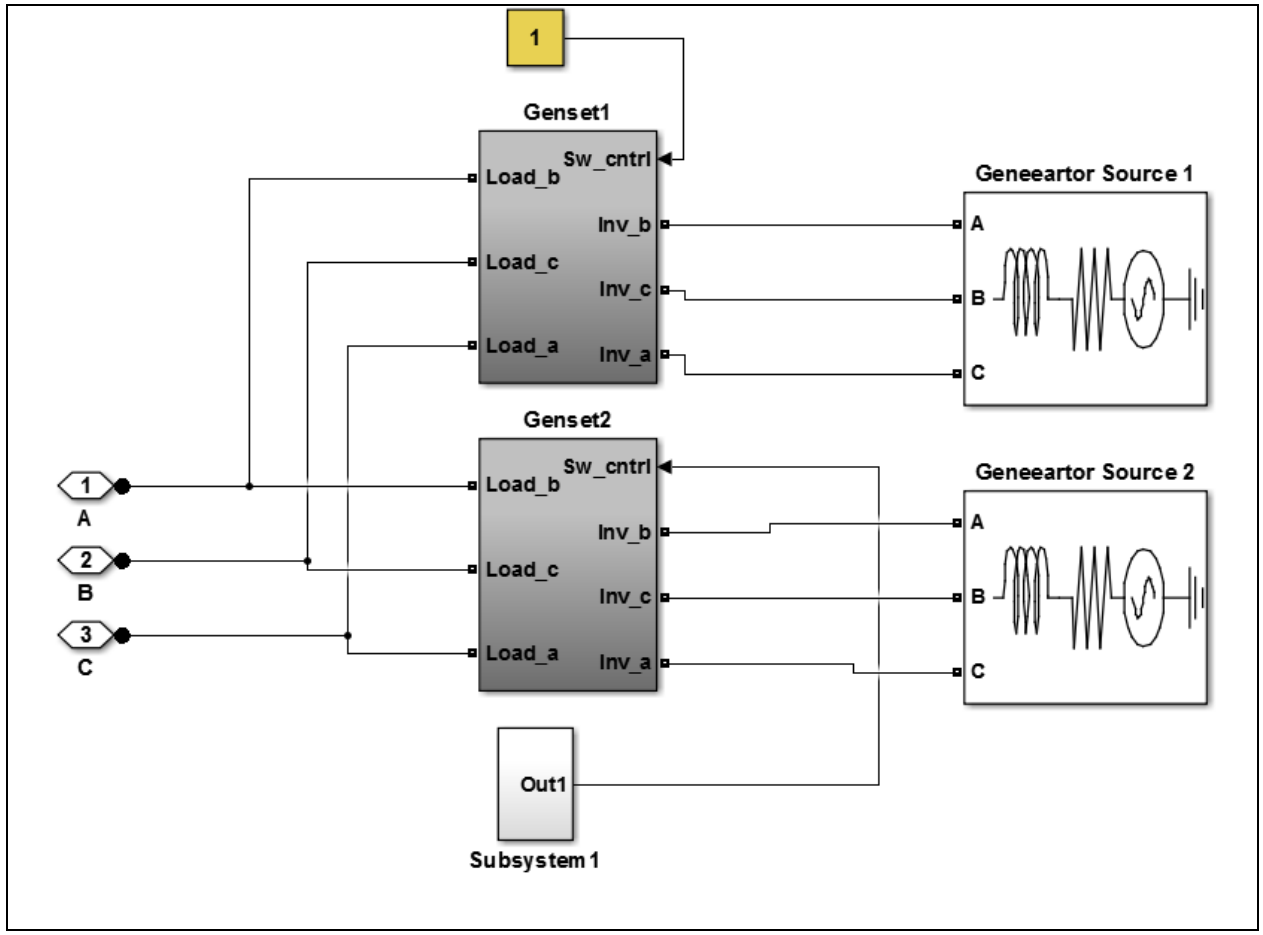

Figure 5. 26c: **MATLAB model of Mode C (Generator Source)**

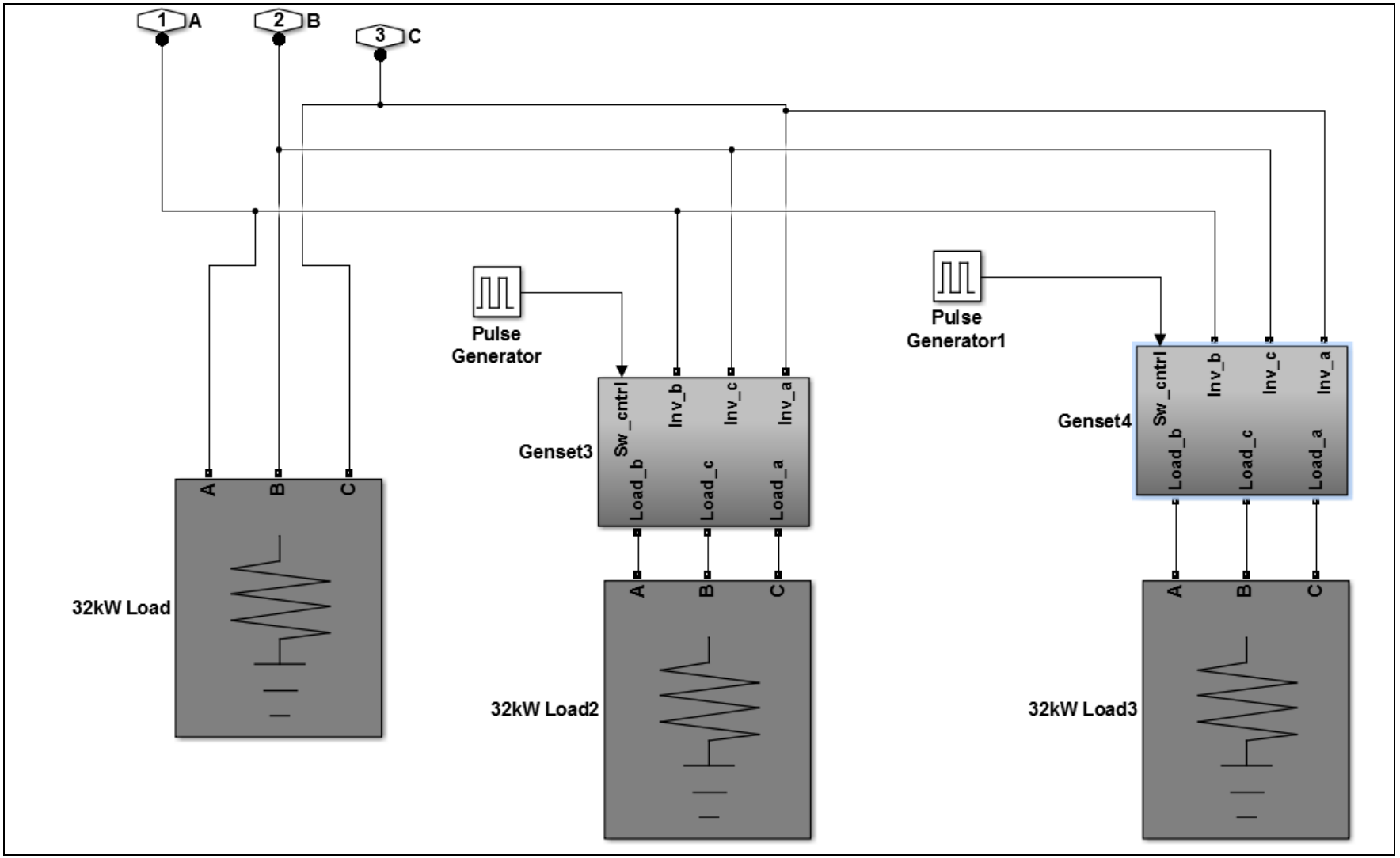

Figure 5. 27d: **MATLAB model of Mode C (Generator Source)**

Figure 5.21 shows the Simulink model of Mode C operation and Table 5.5 shows the simulated results.

The following assumptions were made to facilitate the analyses:

- A simple AC Power source was ~~is~~ used in place of the main diesel generator
- Only two main diesel generator units (AC Power sources) were used instead of four.

The following is the logic implemented in Simulink:

- Battery inverter is ON when load demand is in between 36kW to 50kW
- Main generator 2 is ON when load demand is >50kW and battery inverter is OFF

Table 5. 5: No Sunshine peak loads

Time	Main Generator 1			Main Generator 2			Battery Inverter			Load Power (kW)
seconds	Voltage	Current	Power (kW)	Voltage	Current	Power (kW)	Voltage	Current	Power (kW)	
0-0.5	370	56	36	0	0	0	0	0	0	36
0.5-1	370	56	36	0	0	0	363	23	14.4	51
1-1.5	370	56	36	370	56	36	0	0	0	71

Table 5. 6: No Sunshine peak loads

	0-0.5 seconds	0.5-1.0 seconds	1.0-1.5 seconds
Load Power (kW)	36	51	71
Main generator 1			
Voltage (UNIT)	370	370	370
Current (UNIT)	56	56	56
Power (kW)	36	36	36
Main generator 2			
Voltage	0	0	370
Current	0	0	56
Power	0	0	36
Battery Inverter			
Voltage	0	363	0
Current	0	23	0
Power	0	14.4	0

Mode D: Low sunshine and low loads:

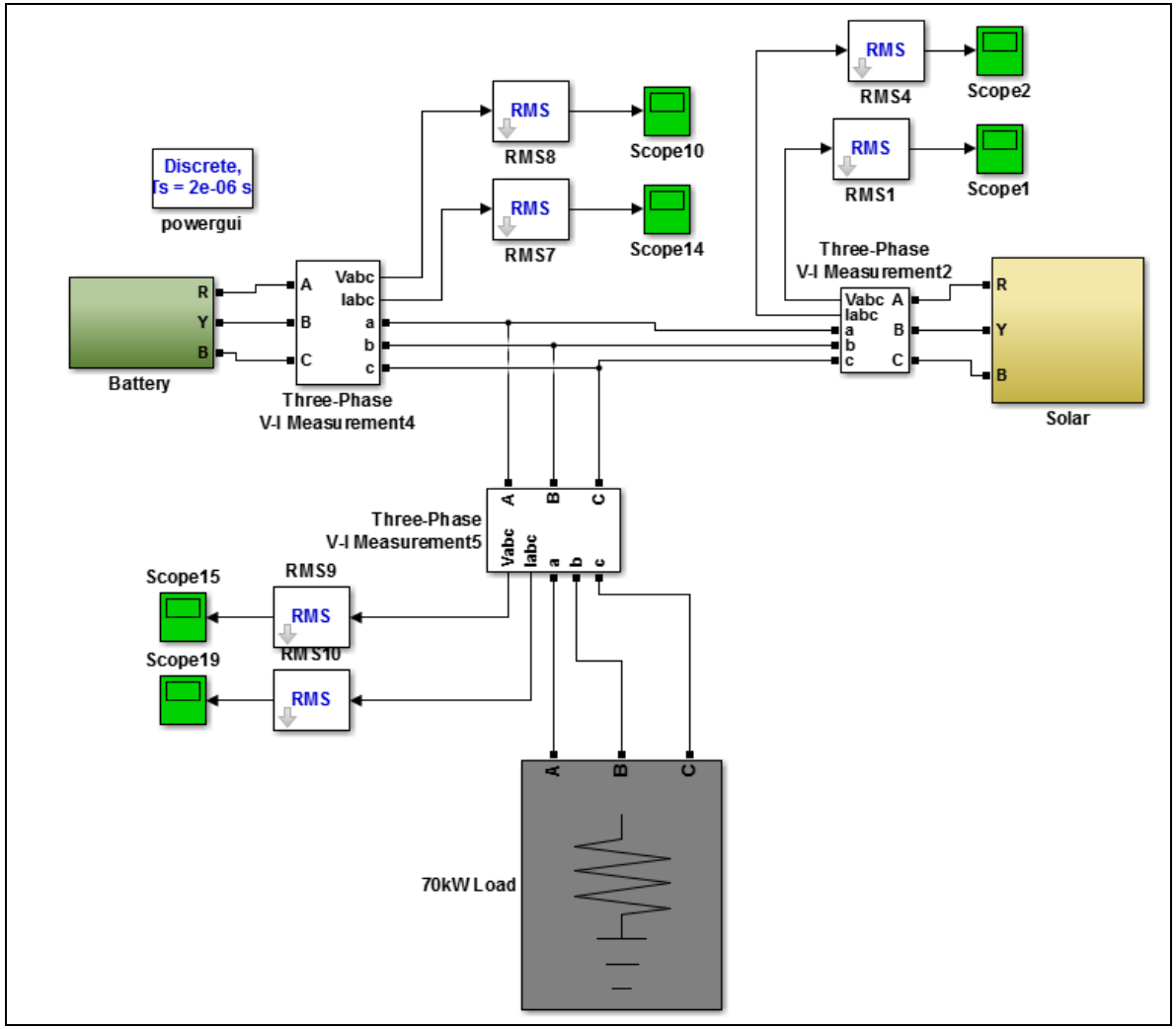

Figure 5. 28a: **MATLAB model of Mode D (Top Level)**

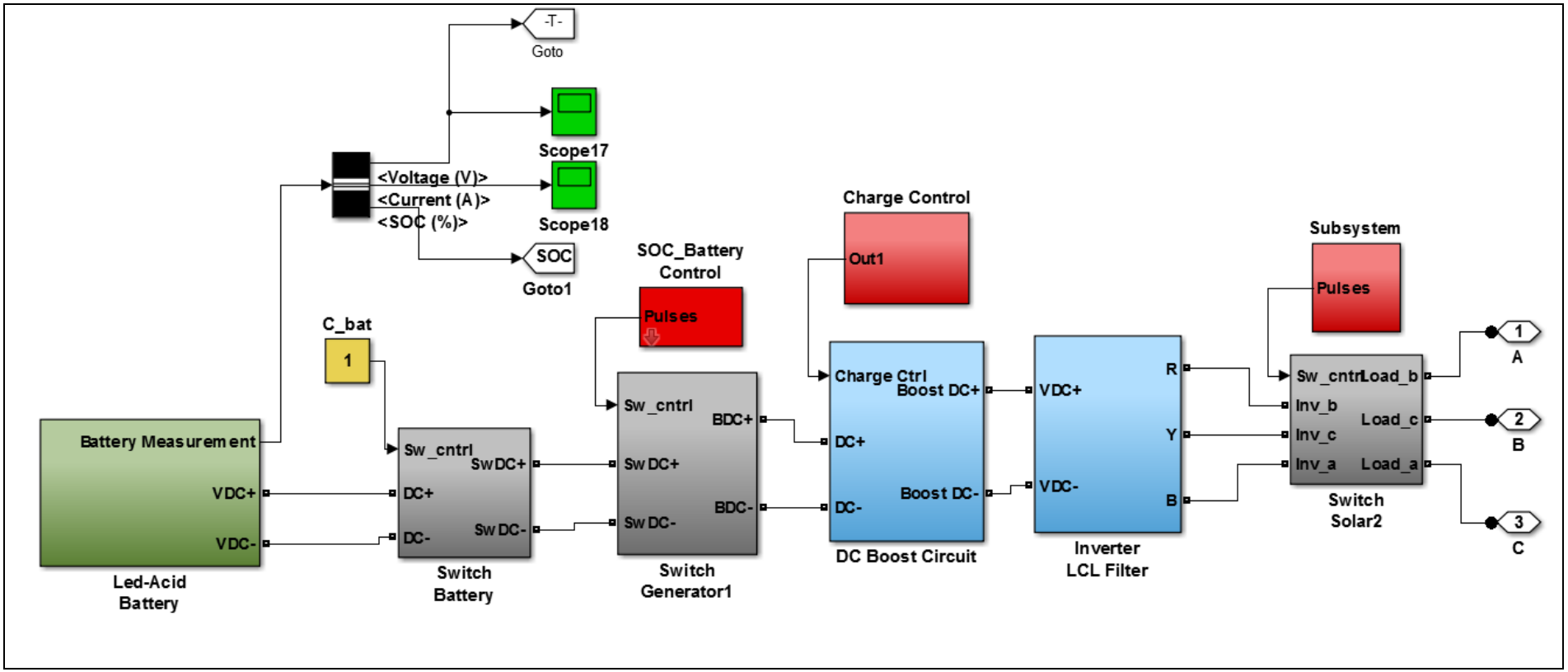

Figure 5.22b: MATLAB model of Mode B (Battery model_Boost_Inverter)

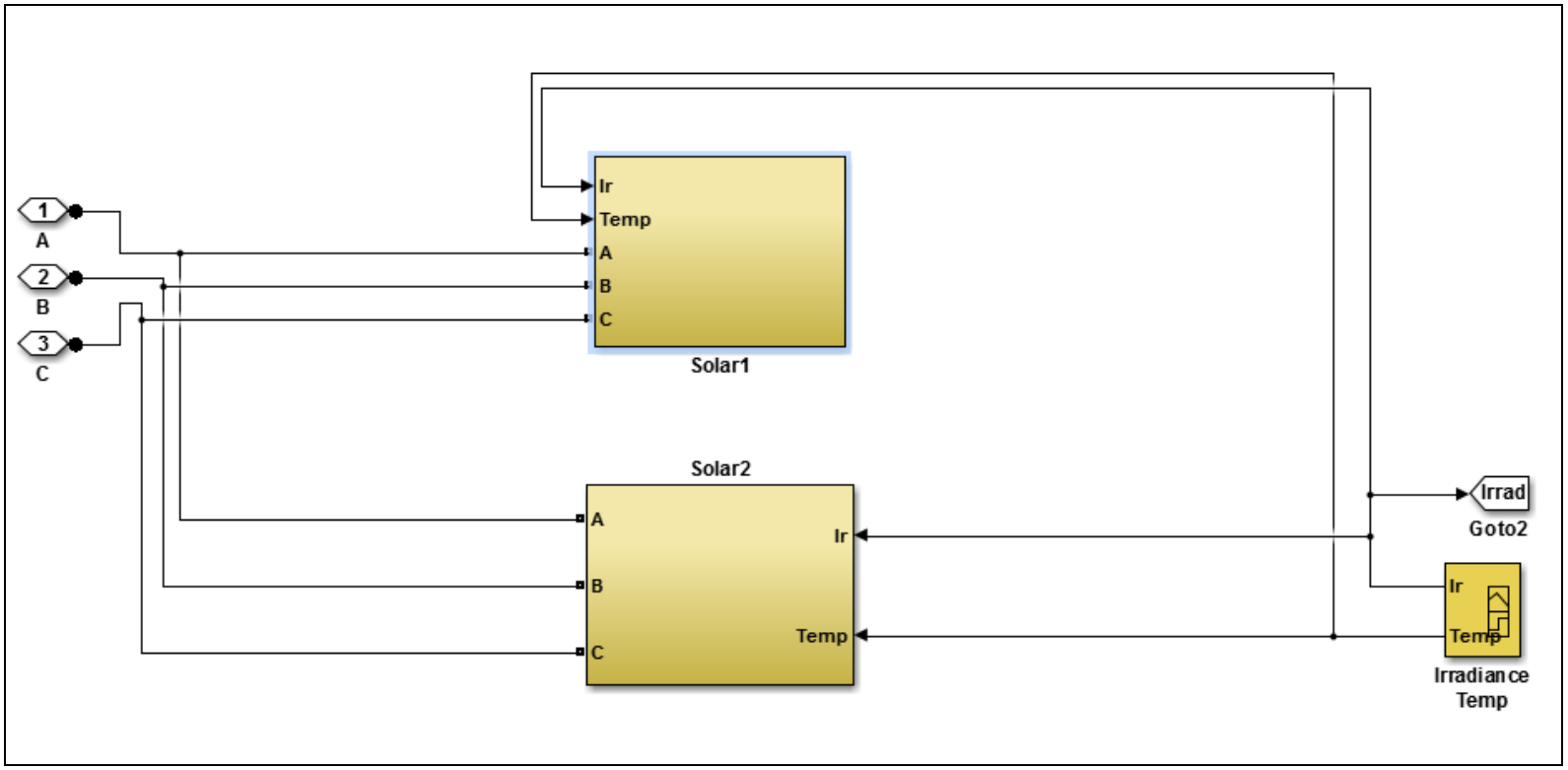

Figure 5.22c: MATLAB model of Mode B (Solar Model)

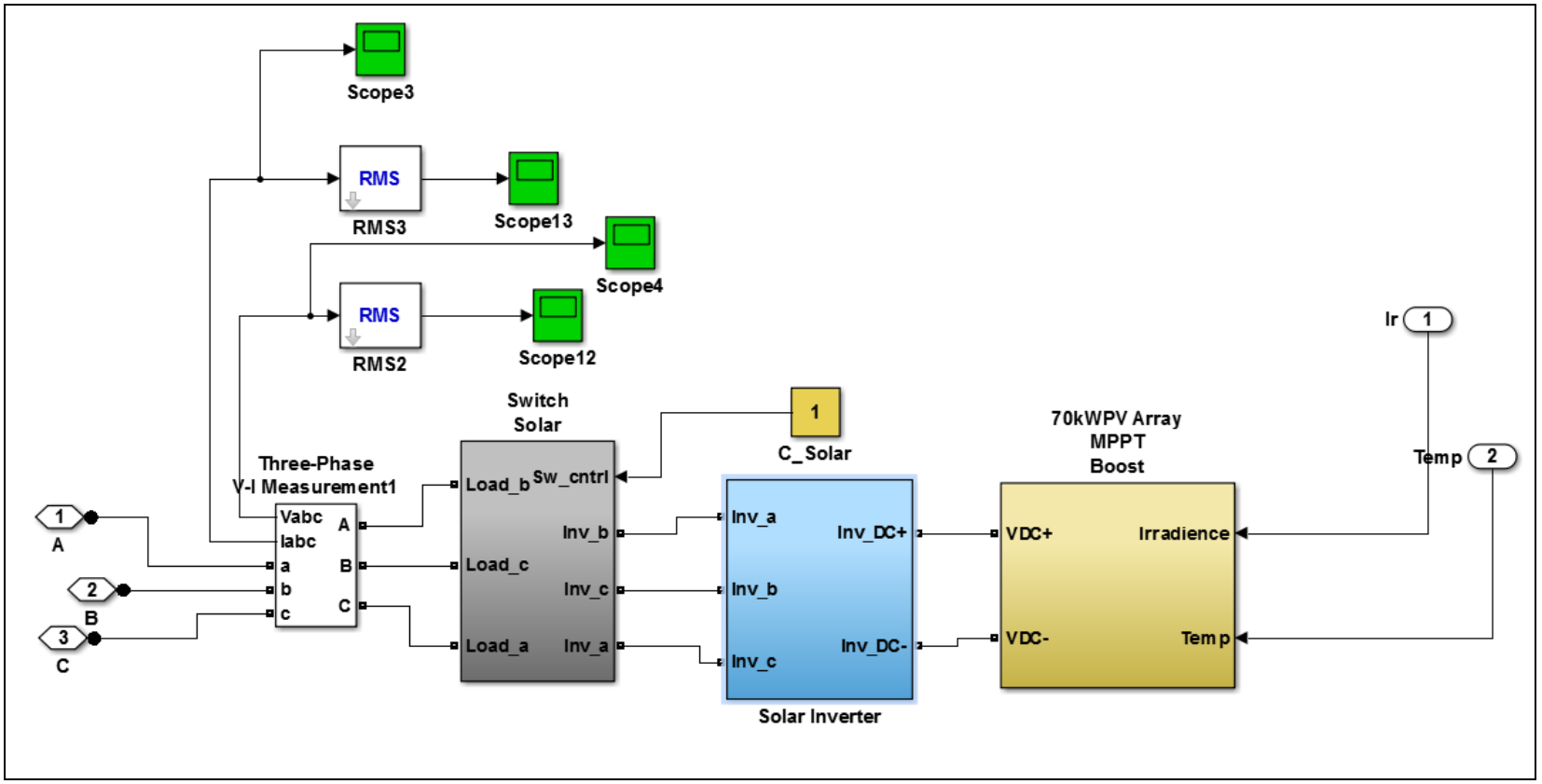

Figure 5.292d: MATLAB model of Mode b (Solar1 & Solar 2 model_Boost_Inverter)

Figure 5.22 shows the Simulink model of Case D operation and Table 5.6 shows the simulation results.

Note:

- Power drawn from the battery would be zero since the available irradiance is sufficient for providing the power to the load.

Table 5. 7: Low Sunshine low loads

Irradiance	70Kw solar Inverter			48kW solar inverter			Load		
	Voltage	Current	Power	Voltage	Current	Power	Voltage	Current	Power
500	410	30	21.3	410	23	16.3	410	52.5	37.3

Table 5. 8: Low Sunshine low loads

Irradiance				250
	Voltage (UNIT)	Current (UNIT)	Power (UNIT)	
70kWsolar inverter	410	30	21.3	
48kWsolar inverter	410	23	16.3	
Load	410	52.5	37.3	

5.5.2 Automatic mode after supervisory control PC (HCCU) fails

If BD-INV(MTP) detects low battery it will go to charging mode and after the battery is full it will remain in charging mode. If BD-INV(MTP) detects a high load for 1 second it will go to charging mode and return to inverter supply mode only when a command from HCCU is received. If BD-INV (MTP) detects low battery it will go to charging mode and start the generator, and revert to inverter supply mode when the battery is full. If BD-INV (MTP) detects high load for 1 second it will go to charging mode and start the generator.

5.5.3 System operation when battery voltage is high

When PV generated power is greater than the load demand power goes to charge the batteries connected to the MTP that is running in inverter mode. If the battery is fully charged and the battery voltage higher than 432 V DC then the MTP will shift frequency to 50+0.3 Hz. SMU is connected with G-303 through RS-485 and the AC frequency of G-303 monitored. If the AC frequency is greater than 50+0.3 Hz for 1 min, the SMU will send a command to limit O/P current by o/p current of G-303 equal to the load current. Once the battery voltage has been at the float voltage for a period of 5min, the MTP will reset the frequency to 50 Hz and the SMU will be required to inhibit current function.

System operation of each villa may also control the load when load current is greater than 10-15A (limit current). If the load current exceeds the limit current of each villa for a period of 1 min, then the SMU will send a dry contact signal to turn the air conditioner off. Once the load current has been reduced for 5 min, the SMU will send a dry contact signal to turn the air conditioner on.

The SMU is capable of gathering data from the system component, power meter and Grid-connected Inverter at intervals from 1 to 30 seconds. The information can be sent via an internet connection such as ADSL, Satcom, GPRS or 3G to a PC located at Jack's Bar. A year's worth of data can be logged on a system with an SD memory card, expandable to 104 weeks when data communication is lost. The PC at Jack's Bar is able to retrieve data from the SMU of any villas at intervals ranging from 5 seconds to 10 minutes, depending on the wireless signal. It can also retrieve data from the HCCU of the Hybrid system at similar intervals.

5.6 Eco Beach System Operations

The proposed upgrade has been delayed indefinitely because of financial constraints. Although the total load on the system has increased by an average of 20kW, peaking at 50kW during periods of high occupancy, the system continues to operate as expected. The generators run for approximately 5 hours per day during periods of low occupancy, and for up to 15 hours per day in times of high load. The fuel requirements for the system could be greatly reduced by the installation of a 25kW DC variable speed generator in the power house, and an additional 60kW AC coupled solar PV unit on the power house roof.

Overall, the power system for Eco Beach resort is operating as expected for the changing load requirements. However, it would greatly benefit with the addition of system proposed and designed in this paper.

5.7 Summary

This chapter presents the complete design, simulation and modelling of a large hybrid power system at Eco Beach Resort, and of a proposed extension to the site. The extension required the integration of an additional renewable energy source so that diesel consumption could be reduced, and the life of the existing diesel generators and storage battery could be increased. To this end, the quantity of power provided by the constant speed diesel generator sources was reduced by the inclusion of a variable speed generator and a hybrid control system in the proposal. The availability of operational data from the years 2009 meant that the design and implementation of the original project could be assessed. As with many renewable projects, financial constraints restricted the design of the system that was actually installed. The extension of the power system was delayed indefinitely for similar reasons. However, a recent drop in solar PV cost, and the addition of a variable speed generator to the design, may make the extension a financially viable option.

5.8 References

[1] C. V. Nayar, "High Renewable Energy Penetration Diesel Generator Systems, Paths to Sustainable Energy," 2010.

[2] K. E. M. Plunkett, "Eco Beach Broome Repot " 2012.

[3] F. Chun-Che, W. Rattanongphisat, and C. Nayar, "A simulation study on the economic aspects of hybrid energy systems for remote islands in Thailand," in *TENCON '02. Proceedings. 2002 IEEE Region 10 Conference on Computers, Communications, Control and Power Engineering*, 2002, pp. 1966-1969 vol.3.

[4] Y. Makarov, D. Pengwei, M. C. W. Kintner-Meyer, J. Chunlian, and H. Illian, "Optimal size of energy storage to accommodate high penetration of renewable resources in WECC system," in *Innovative Smart Grid Technologies (ISGT), 2010*, 2010, pp. 1-5.

[5] S. V. Mathews, S. Rajakaruna, and C. V. Nayar, "Design and implementation of an offgrid hybrid power supply with reduced battery energy storage," in *Power Engineering Conference (AUPEC), 2013 Australasian Universities*, 2013, pp. 1-6.

[6] C. Nayar, M. Tang, and W. Suponthana, "A case study of a PV/wind/diesel hybrid energy system for remote islands in the republic of Maldives," in *Power Engineering Conference, 2007. AUPEC 2007. Australasian Universities*, 2007, pp. 1-7.

[7] Broome Direct. (2014, 17/04/2014). *Weather and Tide in Broome, Average Monthly Temperature and Rainfall*. Available: http://www.broomedirect.com.au/weather_average.html

[8] P. Y. Lim and C. V. Nayar, "Photovoltaic-variable speed diesel generator hybrid energy system for remote area applications," in *Universities Power Engineering Conference (AUPEC), 2010 20th Australasian*, 2010, pp. 1-5.

[9] P. Y. Lim and C. V. Nayar, "Control of Photovoltaic-Variable Speed Diesel Generator battery-less hybrid energy system," in *Energy Conference and Exhibition (EnergyCon), 2010 IEEE International*, 2010, pp. 223-227.

[10] C. Nayar, M. Tang, and W. Suponthana, "Wind/PV/diesel micro grid system implemented in remote islands in the Republic of Maldives," in *Sustainable Energy Technologies, 2008. ICSET 2008. IEEE International Conference on*, 2008, pp. 1076-1080.

[11] C. V. Nayar, "Control and interfacing of bi-directional inverters for off-grid and weak grid photovoltaic power systems," in *Power Engineering Society Summer Meeting, 2000. IEEE*, 2000, pp. 1280-1282 vol. 2.

[12] Australian Government Bureau of Meteorology. (2014). *Broome Weather*. Available: http://www.bom.gov.au/wa/broome/

[13] Z. Bo, Z. Xuesong, C. Jian, W. Caisheng, and G. Li, "Operation Optimization of Standalone Microgrids Considering Lifetime Characteristics of Battery Energy Storage System," *Sustainable Energy, IEEE Transactions on*, pp. 934-943, 2013.

[14] NREL. (2014). *Homer Energy*. Available: http://www.homer.com/HOMER.html

[15] J. Yuncong, J. A. Qahouq, and M. Orabi, "Matlab/Pspice hybrid simulation modeling of solar PV cell/module," in *Applied Power Electronics Conference and Exposition (APEC), 2011 Twenty-Sixth Annual IEEE*, 2011, pp. 1244-1250.

[16] K. A. Cook, F. Albano, P. E. Nevius, and A. M. Sastry, "POWER (power optimization for wireless energy requirements): A MATLAB based algorithm for design of hybrid energy systems," *Journal of Power Sources*, vol. 159, pp. 758-780, 9/13/ 2006.

Chapter 6

6. High Solar PV Penetration into a township utility network: A Case Study

6.1 Introduction

In this chapter the effect of extensive solar PV penetration into a distribution network is investigated. The case study of Carnarvon, Western Australia, that was conducted by the Australian Photovoltaic Association (APVA) and Centre for Energy and Environmental Markets (CEEM) in 2012 is presented [1]. A proposal for resolving the issues faced by the township and the Horizon Power utility is provided, and computer modelling using the programs Matlab, PSpice and HOMER is described.

The case study in this chapter is based on the extensive penetration of PV into Carnarvon, Western Australia. Carnarvon is a coastal town situated approximately 900 kilometres north of Perth, Western Australia. It lies at the mouth of the Gascoyne River on the Indian Ocean. The popular Shark Bay World Heritage area lies to the south of the town and the Ningaloo Reef lies to the north. At the 2011 census, Carnarvon had a population of 4,559.

Carnarvon has a warm semi-arid climate with occasional tropical cyclones during the summer months that bring heavy rain and strong winds. Apart from this erratic source of rainfall, summers are normally dry. Temperatures range from an average maximum of 33 °C (91 °F) in February to 22 °C (72 °F) in July (Figure 6.2). Average minima are 23 °C (73 °F) and 11 °C (52 °F), respectively [2]. Such temperatures make Carnarvon an ideal place for Solar PV installations. However, as can be seen in Figure 6.1, Carnarvon receives lower mean levels of solar irradiation during the winter months, limiting the generation of power by PV at this time.

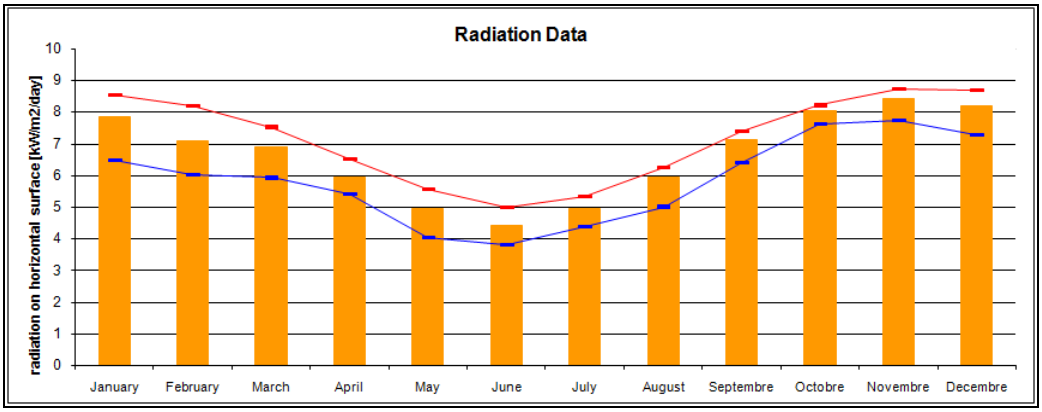

Figure 6. 1: Carnarvon mean daily solar exposure.

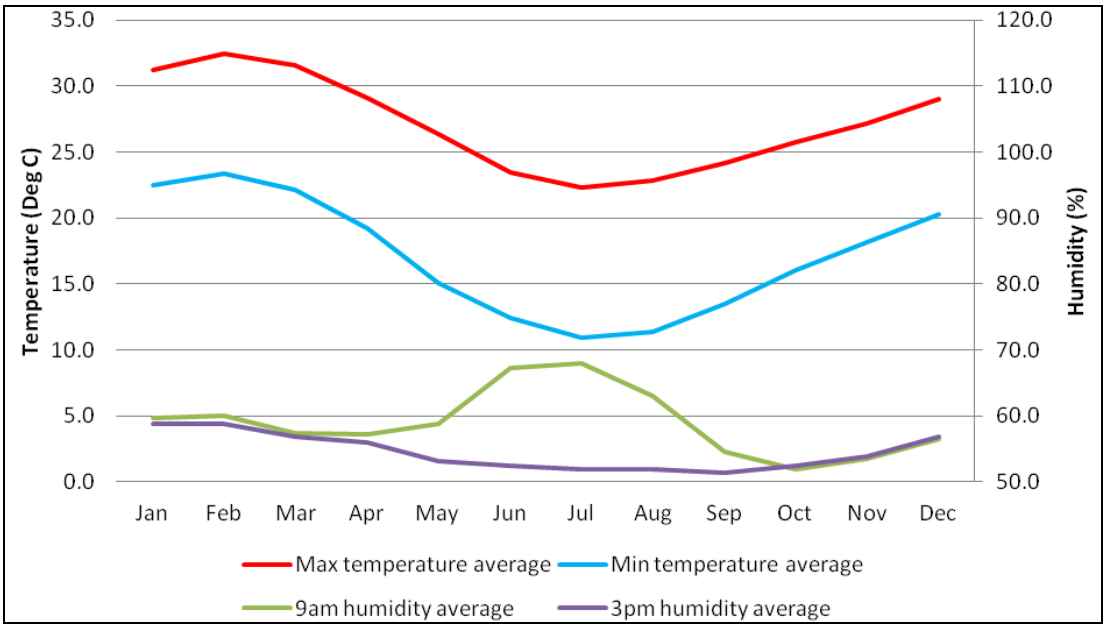

Figure 6. 2: Average temperature and humidity readings for Carnarvon [1]

At present, the Carnarvon distribution network consists of an isolated gas/diesel generation grid with more than 13 percent of embedded PV systems. This PV penetration is coupled with a strong solar resource (an average daily solar insolation of 6.2kWh/m^2). Such a high PV penetration could be expected to have an impact on the distribution network. This is indeed the case for Carnarvon, and in 2011 Horizon Power (the utility that owns and operates the Carnarvon distribution network) applied a limit of 1.15MWp of distributed PV system capacity on the distribution network.

The Carnarvon distribution network is primarily radial in nature with some long rural feeders, and comprises in total 200km of overhead lines servicing approximately 5300 people. The peak system load until 2012 was 11600kW, the average system midday loads were approximately 6800kW in summer and 5000kW in winter, 60% of the peak demand was from commercial/industrial loads and 40% from residential loads. The power station in Carnarvon is owned and operated by Horizon Power and comprises 13 generator sets which are predominantly dual fuelled by gas and diesel and have a nominal rating of 22100kW which is de-rated to 15900kW in summer[1]. The generating strategy in Carnarvon is to operate with enough spinning reserve to cover the loss of the largest online generator. This also sets the limit for the amount of distributed PV in the town, given the concern that some power system events might result in the disconnection of all PV at a time when maximum output is being generated.

Currently there is 1090kWp of nominal PV capacity connected to the distribution network. The majority (57%) of the systems were installed in 2010, in part due to the initially high state feed-in tariff. PV systems connected to the Carnarvon network have an average size of 8.30kWp, a value that is significantly higher than the average system size seen on the main grid within Australia. The PV distribution in Carnarvon is also quite clustered, with one medium voltage feeder loaded to 39% of its average midday load and distribution transformers loaded up to 70% of the rated capacity of the transformer.

6.2 Load Profile

The average and peak load profiles for Carnarvon in summer and winter are presented in Figures 6.3 and 6.4, respectively. This load profile is entirely different to most of utility scale load profile. From figure 6.3 we can see that in summer from 9am to 9pm the network feeding continues peak power unlike any other typical load profile. In winter also peak goes to high at morning and evening and maintaining near peak power consumption almost all day. So the selected location is ideally suited for one hundred percentage of renewable penetration. One hundred percentage of solar energy can integrate to the existing utility by adding variable speed genset, battery bank and bi-directional inverter.

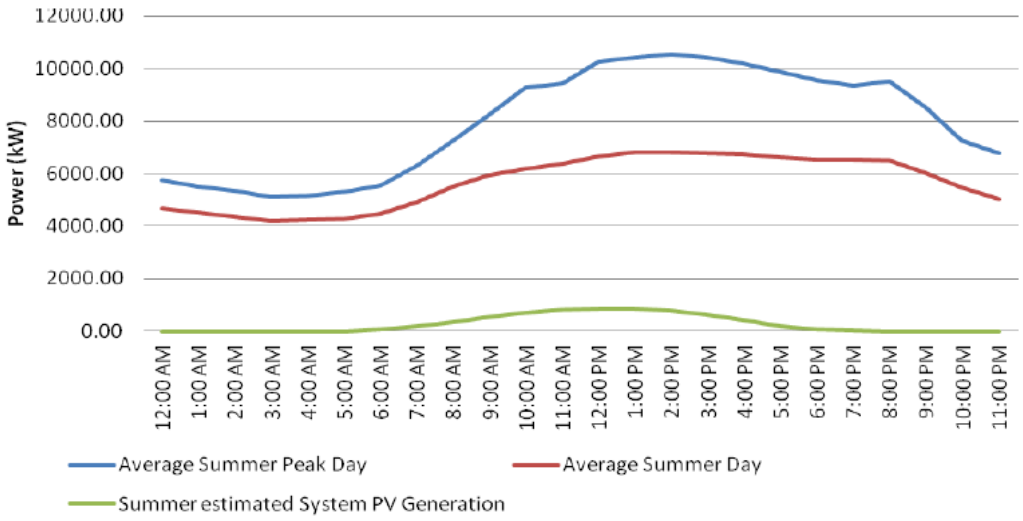

Figure 6. 3: **Carnarvon average and peak load profile in summer [1]**

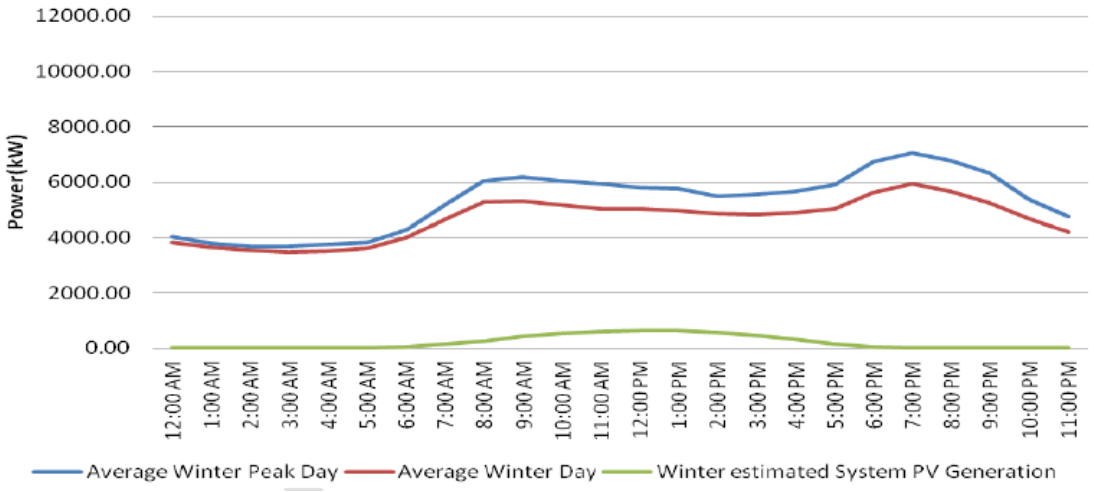

Figure 6. 4: **Carnarvon average and peak load profile in winter [1]**

6.3 The PV Issue in Carnarvon

Carnarvon has a small isolated grid with a relatively high density of PV as a function of system load (13% approx. of summer and winter midday loads). This relatively high level of PV penetration presents technical integration challenges that will likely emerge in the future for other isolated grids in Australia and internationally as the fuel and emissions savings of PV become increasingly valuable. Growing concerns about the potential impacts of high PV penetrations and the limitation of PV systems on the Carnarvon network include the lack of

resources available for the connection of the systems and the regulatory/commercial obligations of Horizon Power.

6.4 Electricity Supply System

The Carnarvon electricity supply system is quite diverse. The distribution system is radial in nature and comprises a mixture of rural and urban feeders, including some long rural feeders (Figure 6.5). The system is entirely overhead and contains 205km of supply lines. The supply system voltage levels include 6.6kV for the centralised generator, 22kV for the medium voltage network and a typical Australian 415V LV system which is supplied by 47 distribution transformers.

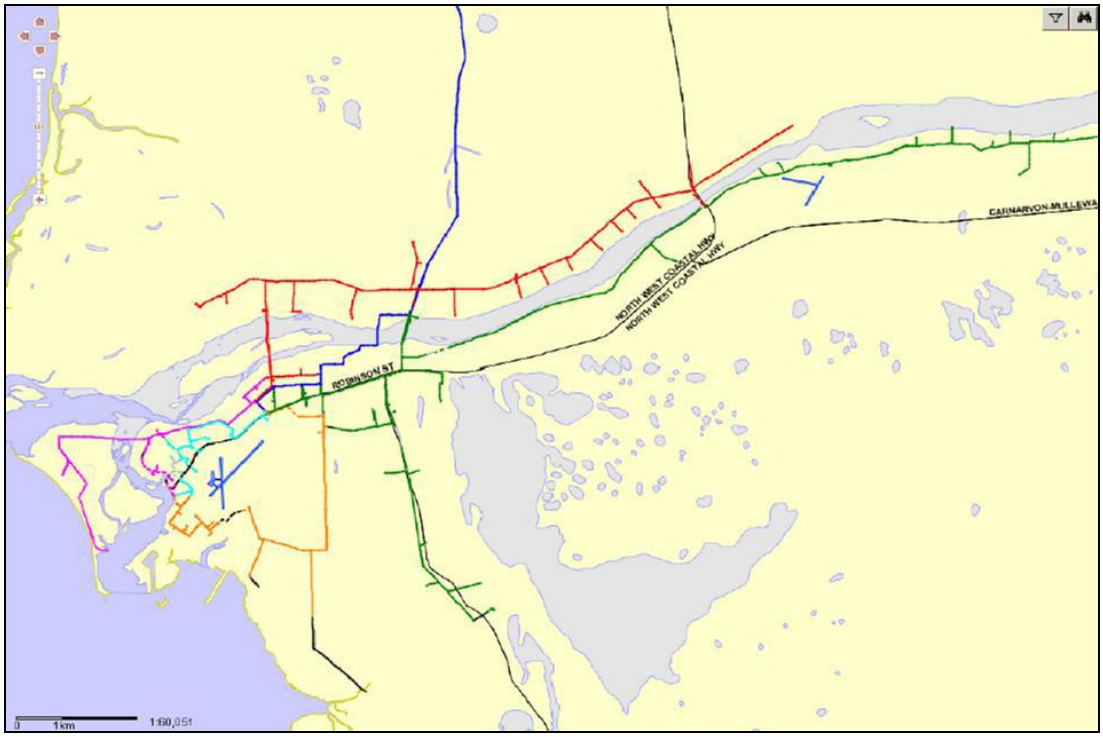

Figure 6. 5: The Carnarvon medium voltage (22kV) network [1].

The day time spinning reserve is the current limit for distributed PV systems in Carnarvon, which is currently 1.15MWp. This also allows for the loss of the largest online generator without a requirement for pro-active load shedding. Customers with large loads (in particular a nearby salt mine) provide warning on the timing of the start-up of these loads so that the spinning reserve can be appropriately adjusted and economic operation of the centralised generators maintained. The generator sets used in the Carnarvon power station are listed in Table 6.1. Mobile units are generally used to base load power.

Table 6. 1: Description of the generator sets utilised in the existing Carnarvon [1] power station.

Generator Set Description	**Quantity**	**Generator Speed (rpm)**	**Fuel Type**	**Nominal rating (KWp)**	**Summer rating level (KWp)**
Mobile Sets Cummins QSK45	5	1500	Diesel	1120	800
Mobile Set Detroit	1	1500	Diesel	1200	800
Wartsila 12V25SG	3	1000	Gas/Diesel hybrid	2340	1500
Allen GBC-8S37E	1	600	Gas/Diesel Hybrid	1200	1200
Mirrlees KP8-major	1	500	Gas/Diesel Hybrid	2240	1800
Mirrlees KP8-major	1	500	Gas/Diesel Hybrid	2500	1800
Mirrlees KP8-major	1	500	Gas/Diesel Hybrid	2305	1800
Totals	13	N/A	N/A	22065	15900

6.5 PV System Arrangement

The majority of the PV systems in Carnarvon are located within a 24km^2 area that represents the urban part of the township. The distribution transformers in Carnarvon show a more unequal PV system distribution than the 22kV feeders. The most highly loaded distribution transformers (the top 15 out of 47) are shown in Table 6.2, with the remaining transformers having a penetration of less than 10%.

Table 6. 2: Top 15 highly penetrated distribution transformers in Carnarvon [1].

Distribution Transformer	Transformer Rating	PV System nominal capacity (kWp)	PV Capacity as a % of Transformer Capacity
GIBSON	315	221	70%
NR122/6	63	40	63%
NR67/17/106	50	26	53%
NR129	63	30	48%
NR67/17/18	100	40	40%
BILCICH	63	20	32%
CARNARVON PONY CLUB	200	60	30%
NR90A/4	100	29	29%
FINNERTY	100	29	29%
CARNARVON CHRISTIAN SCHOOL	100	21	21%
RICHARDSON	200	35	17%
NELSON	200	30	15%
ANGELO NORTH	200	30	15%
SILVER CITY	100	12	12%
MUNGULLAH	200	20	10%

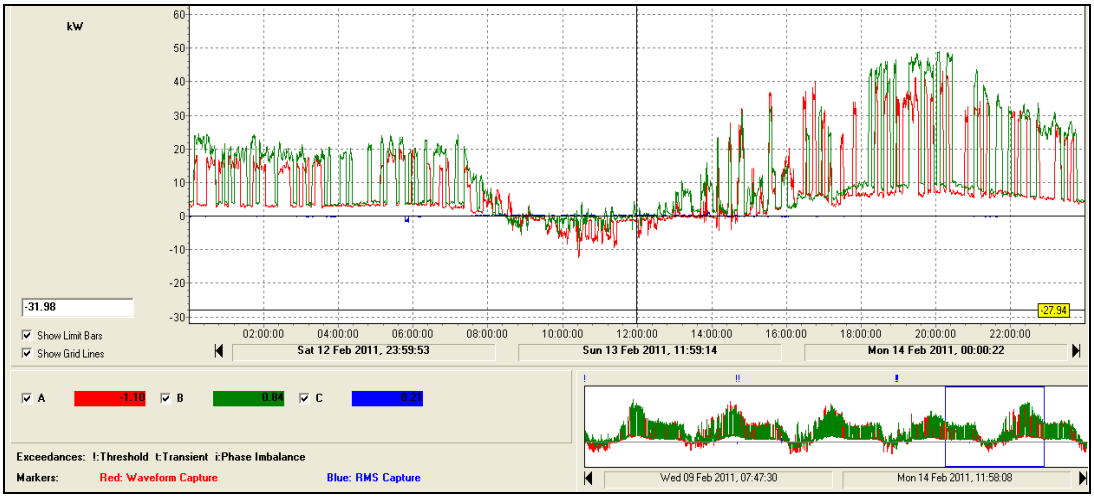

Figure 6. 6: Snap shot of real power on the Gibson transformer for one day in February [1].

Some customers with distribution transformers have already experienced problems with power quality and security issues. Inverters have disconnected from the network due to frequency and voltage fluctuations. Figure 6.6 shows the two types of technical challenges encountered with PV system integration: the first is the impact at the whole system network level solar PV penetration impact and the second is distribution networks level solar PV penetration impacts

6.6 Increasing PV Penetration Levels

It is essential that Horizon Power resolves the power and security issues that have arisen as a result of ongoing PV penetration of the Carnarvon Power Supply. As a first step, a 1.15MW limit on the connection of PV to the network has been implemented by Horizon Power.

Network stability may also be affected by the frequency anti-islanding protection. The simultaneous disconnection of all inverters on the network at times of high sunshine and hence high PV generation would be equivalent to a 700kW load switching on to the power station. Frequency deviation may happen as a result of a system disturbance, since the generators are likely to be stressed if they continue to operate during this time. When the frequency deviation is upwards (representing an excess of generation) PV disconnection

might assist in system management, although the step change involved would invariably raise control issues. For downwards frequency deviations representing a generation deficit the problem would be exacerbated by the addition of an effective 700kW of load [3].

6.7 PV System Impacts on System Stability from Cloud Fluctuations

Changes in solar irradiation affect PV system output. When the systems are highly clustered together (such as in the Carnarvon network), large clouds can effectively reduce a substantial proportion of the PV generated in a short period of time and, depending on generator ramp rates and spinning reserve, the system stability may be affected.

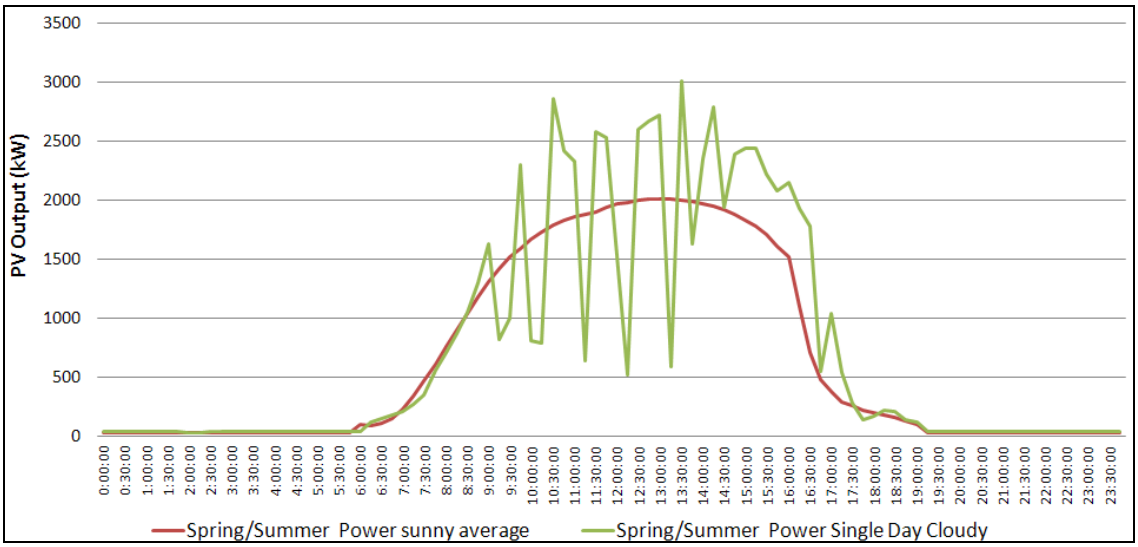

Figure 6. 7: Single day and average output of a 2.5kW PV system with a 5kW rated inverter, data taken at 15 minute intervals [1]

Horizon Power is currently mitigating this issue by ensuring that the generators have sufficient spinning reserve capabilities to accept this change in the load levels whilst keeping the network stable. Figure 6.7 shows the average power output from a 2.5KW PV system during spring/summer.

6.8 PV System Impact on Power System Planning Strategies

The high and somewhat uncertain variability in PV system output also has implications for power system planning in Carnarvon. This variability introduces difficulties in forecasting peak system loads and designing the network accordingly.

6.9 Distribution Level PV System Impacts

6.9.1 Voltage Rise in LV Networks

The rural nature of some of the feeders where PV systems are installed in Carnarvon and the clustered nature of the urban installations are both situations that are conducive to voltage rise problems on the various LV networks in the area. This is a problem because over voltage on the network can affect utility regulatory compliance, cause problems with some equipment (both for the network and the customer), increase equipment power consumption and cause the PV inverters to disconnect from the network.

The problems with over voltage can be exacerbated by a high underlying grid voltage independent of any PV impacts. Australian utilities have traditionally set the voltages on the network relatively high within the specified voltage range in order to accommodate voltage drops to the load. This is evident in the Gibson transformer case (Figure 6.6) with 95% of the recorded voltages at the transformer being greater than the nominal 240V. It is also expected that load variations would make the voltage at the load more variable. The presence of PV systems in a network having an already high grid voltage can cause more frequent over voltages for the consumer. Additionally, the AS4777 anti islanding voltage set points are established assuming a 230V nominal voltage as per the new AS61000.3.100 standard, so high voltages are more likely to lead to inverter disconnections [4].

The current options available to Horizon Power to rectify voltage problems on the network include:

- Change the phase of connection
- Lower the distribution tap setting
- Augment the network
- Load Shifting
- Implement voltage regulation technology

6.10 Network Power Flow

If the penetration levels of PV systems in a network are high enough, they can cause power to flow from the loads back through the MV network. The main problems in this scenario are the stability issues, reduced efficiency of distribution transformers and central generators, reactive power flow and network fault protection.

6.10.1 System Harmonics from PV Inverters

AS4777 limits the current harmonic output to 5% THD for individual inverters. Due to the comparatively small outputs of the PV systems compared to the loads, this 5% limit is usually sufficient to stop any significant harmonics being seen on LV networks.

6.11 Power System Benefits From PV Integration

6.11.1 Generator Fuel Savings and Carbon Dioxide Offset

A conventional diesel/gas power station incurs costs from the purchase of fuel to run the power station and for system maintenance, and emits high levels of greenhouse gases, predominantly CO2. PV systems may offer the utility the advantage of cost savings through the reduction in generator fuel use as well as the offsetting of greenhouse gas production. In

the system that was modelled for this study, the generator operating strategy was kept constant, and a set number of generating units was utilised. The operating strategy can change given different load situations (and variable PV system generation) and this will have an impact on fuel consumption and generator efficiency. Savings should be maximised by the implementation of a dynamic spinning reserve strategy. For the purposes of these calculations we were not able to dynamically estimate the generator fuel consumption with the data provided.

The diesel generators were assumed to operate at 0.26l/kWh (1MW generation per unit) and produce 1.22kg/kWh of carbon dioxide emissions. The gas generators were predicted to consume 0.24m 3 /kWh and produce 0.46kg/kWh of carbon dioxide emissions. If the operating strategy is kept constant, then these figures should also remain constant

6.12 Peak Load Shaving

Network size and generation for the expected peak system loads must be carefully designed by utilities, so that power is reliably and securely delivered to customers. In the Carnarvon network, the peak loads occur on average at 2pm in summer and 7pm in winter. The peak load for summer has always been greater than for winter. The network was designed to meet a peak load of 10.7MW. Furthermore, thermal limits on wires and network equipment are more problematic in the higher ambient temperatures of summer. Summer PV generation on a sunny day at 2pm is approximately 580kW.

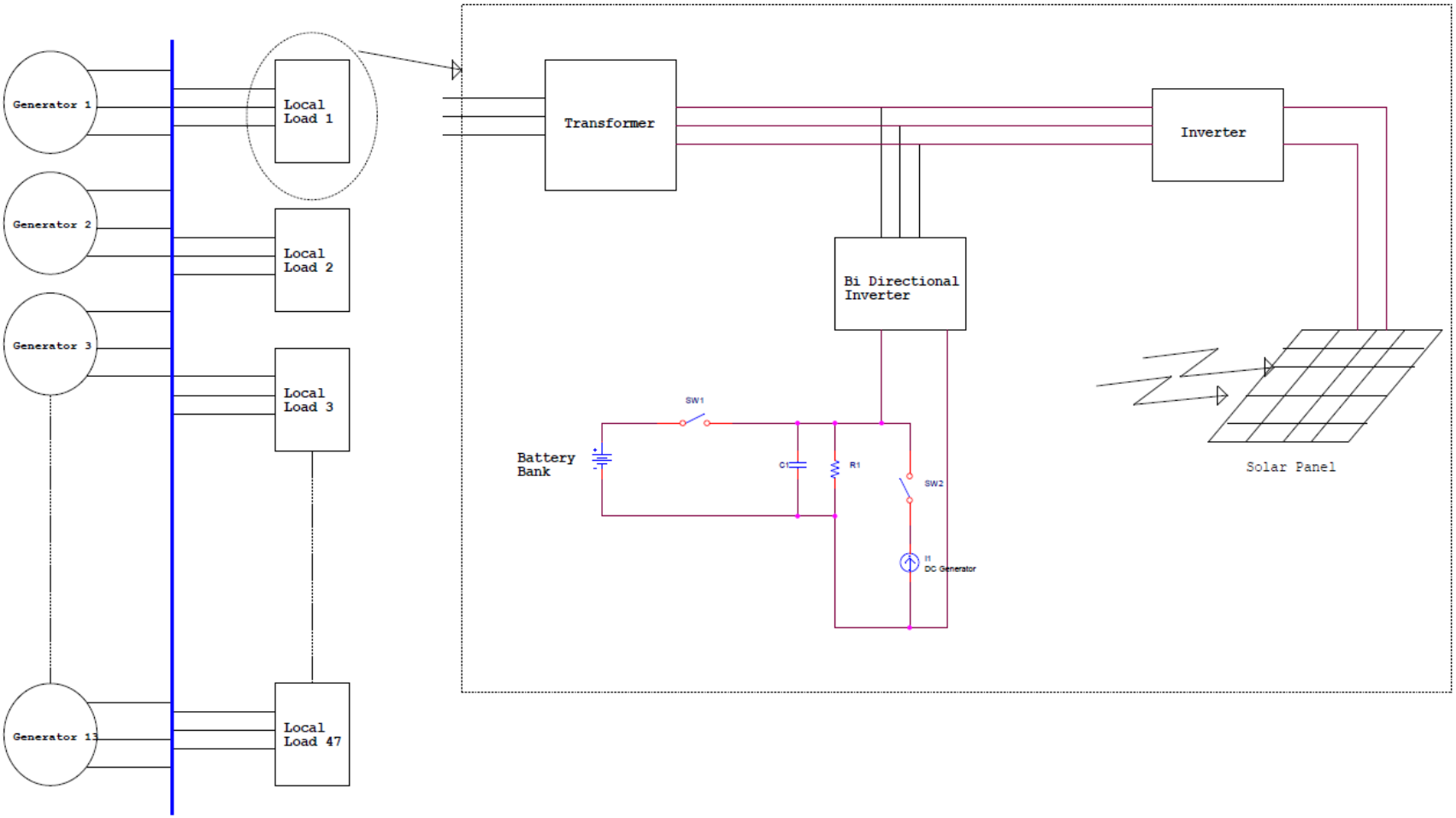

Figure 6. 8: Schematic diagram of the proposed system

6.13 Proposed System Modelling and optimisation

In this section, a Photovoltaic (PV) diesel hybrid-power system is modelled so that the operating cost can be minimized and the load on the aging generators can be significantly reduced. The proposal includes the installation of two 25kW DC variable speed diesel generators and a suitably sized advanced battery bank at each suburban transformer to ensure one hundred percent penetration of solar power by residential customers in the local area. Figure 6.8 shows the schematic diagram of the proposed system.

Figure 6.9 shows the comparative graph of the Ultrabattery VRLA against AGM VRLA battery. It clearly shows that Ultrabattery has the highest Partial State of Charge (HRPSoC) cycle numbers.

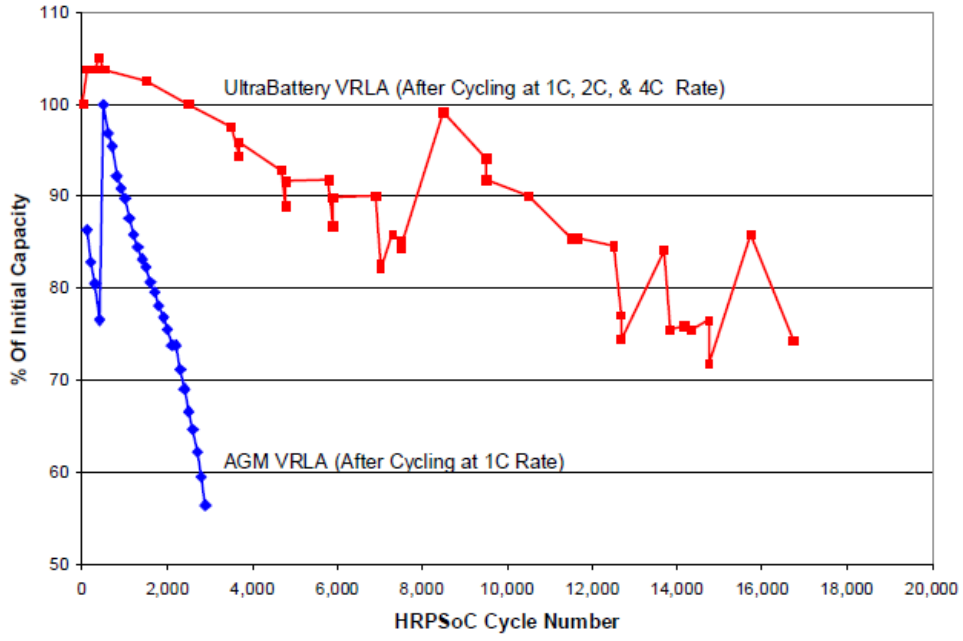

Figure 6. 9: Ultrabattery HRPSoC Utility Cycle Aging Effect Between 2,500 and 16,740 Cycles, At 1C 1 Rate for 6 min [5].

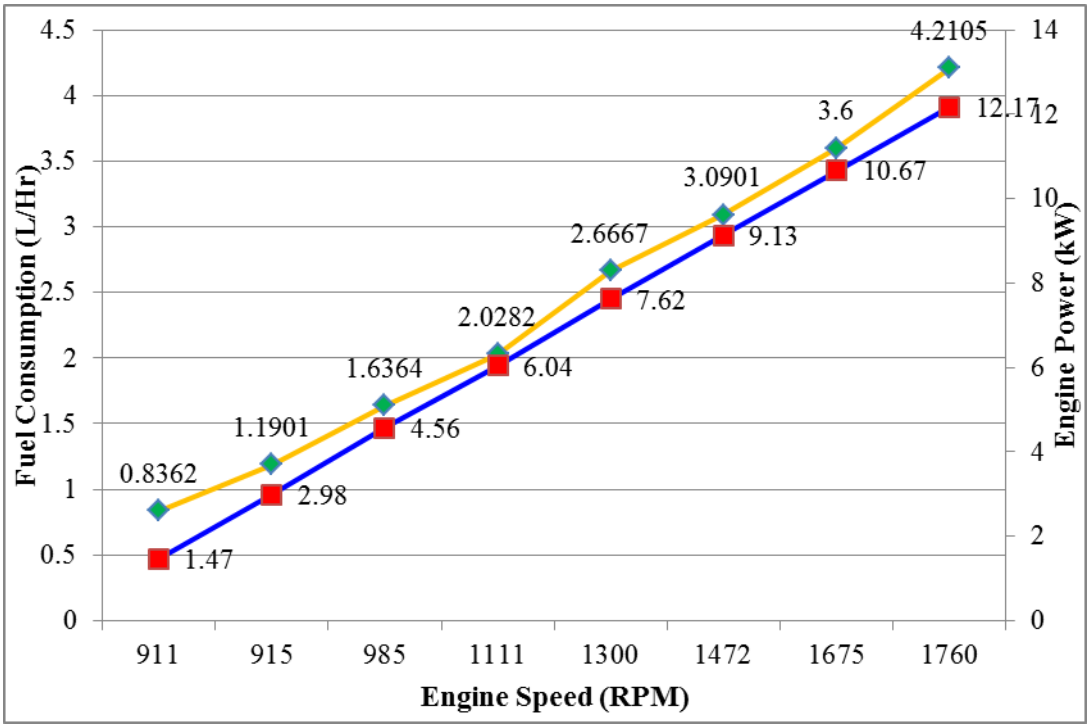

Figure 6. 10: Fuel consumption (orange) and output power (blue) curve of a diesel engine in variable speed

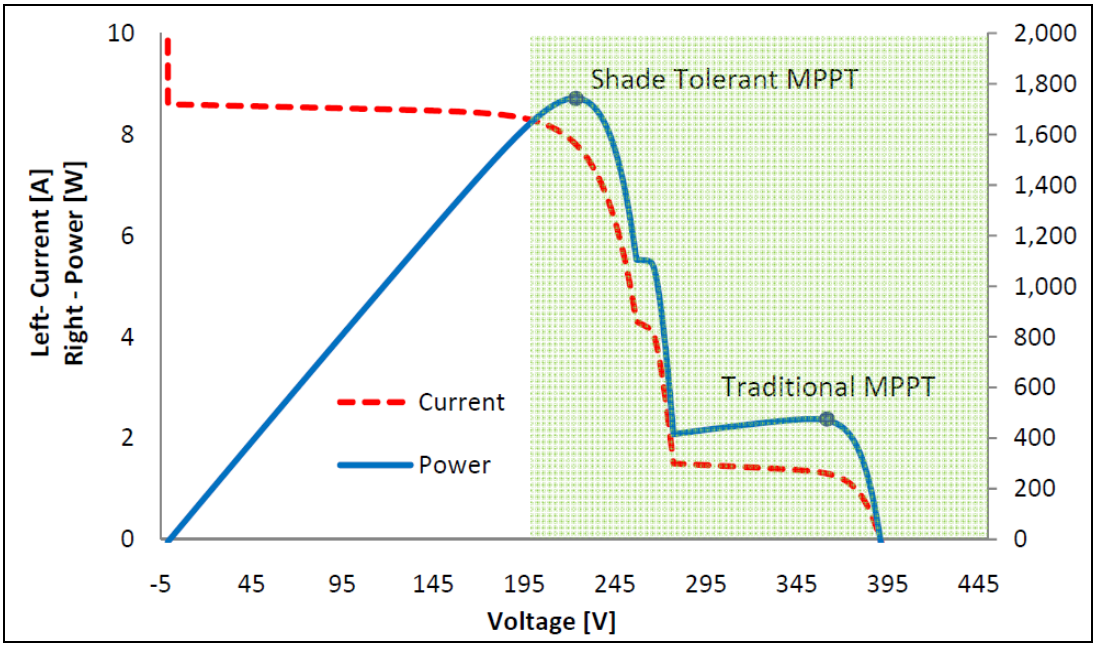

Figure 6. 11: Shaded Array String I-V curve [6]

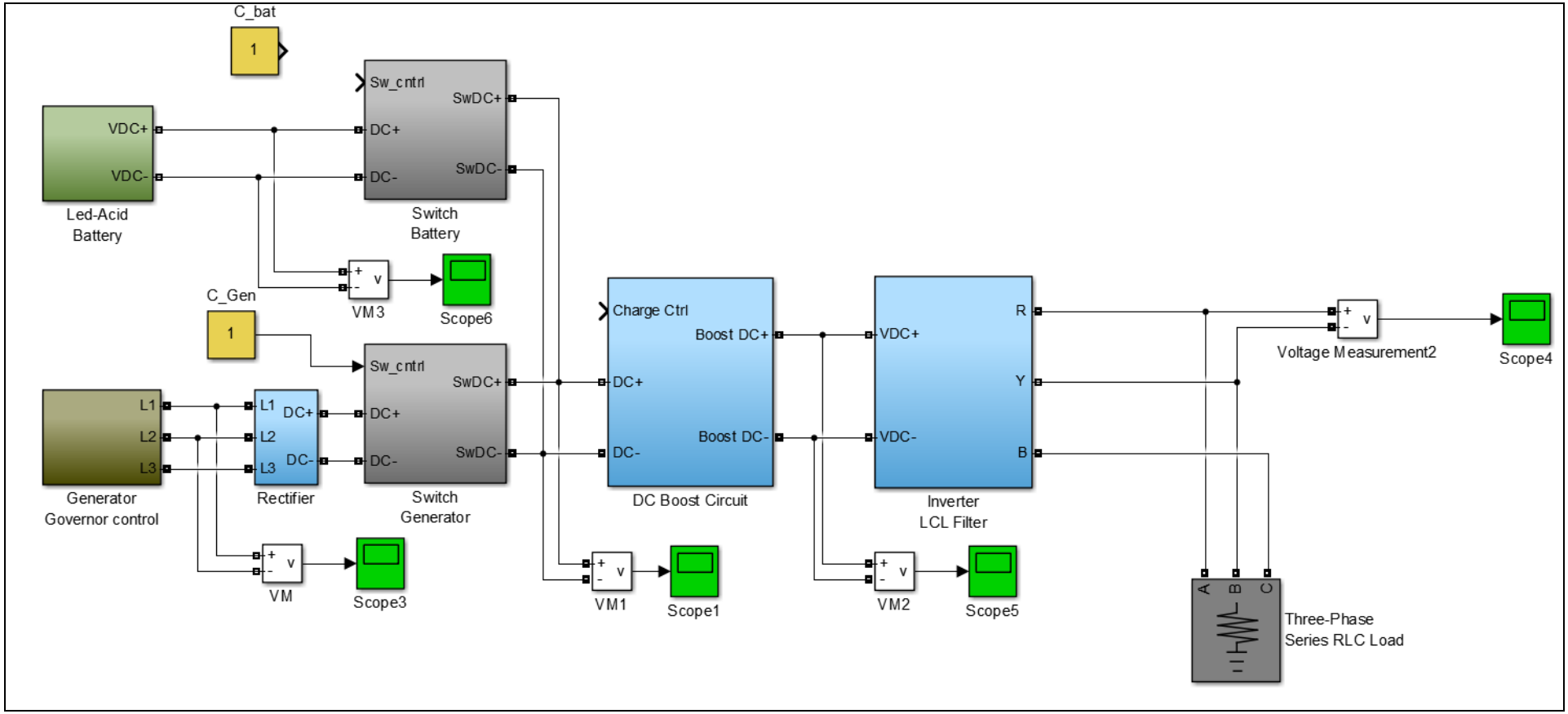

Figure 6. 12: Matlab model of proposed system

The fuel efficiency and output power curve for a diesel engine in variable speed is presented in Figure 6.10. When operating at a variable speed, the engine requires only approximately 4L per hour to produce around 12.5 kW of power, actually the minimum fuel level. Figure 6.11 shows a shaded array string I-V curve of a newly developed shade tolerant maximum power point tracker (MPPT) inverter. So by integrating an advanced battery bank, newly developed MPPT inverter, variable speed generator and newly developed control system we can reduce the high dependency of fossil fuel and utilise one hundred percentage of renewable energy penetration. In this session is investigating the integration of all this components and its size to get best optimised system.

Remote area power systems can benefit from harnessing renewable energy sources. Renewable energy sources, by nature, tend to be uncontrollable and intermittent. Therefore, they need to be operated in parallel with a diesel generator or battery bank. However, this parallel operation may, in many cases, result in the conventional diesel generators operating at low efficiency due to either low load or high renewable energy source penetration. It is possible that the use of a VSDG and an optimized battery bank may alleviate this problem.

The following software was used to model the proposed system and allow the selection of the most appropriate, cost-effective components.

a) HOMER Modelling

HOMER software was used to identify the best possible options for the system by varying the constraints of small power systems to give the best options by doing economic analysis for modelling and investigations. The program first runs an hourly simulation of all possible system type configurations. Analysis is repeated to optimize various user-defined factors, such as fuel price, load size, reliability requirement, and resource quality.

b) PSpice Modelling

PSpice modelling was used to analyse the time domain response, small signal frequency response, total power dissipation, transient analysis and transfer functions as mentioned in previous chapter.

c) Matlab Modelling

Matlab/Simulink provides a user-friendly, modular and visual simulation environment for the transient analysis of power electronics. This environment facilitates design and

simulation of the power systems and it is very convenient to perform transient analyses for the academic and industrial proposes. Although there are wind turbine models in SimPower Systems library of Simulink, a general purpose PV module component working in conjunction with power electronic circuit is still needed. The PV modules used for transient simulations of large-scale renewable source integration should not only be reconfigurable for wide-range of panel models but also present low-computational complexity in grid simulations due to the memory and calculation time limitation of computers. Recent PV models have low computational complexity or electrical characteristics well suiting for PV modules.

6.14 Modelling System Components

The transition to renewable energy-based consumption with economical, safe, and environmentally sound energy storage solutions and backup systems can be affected by high renewable energy penetration. In these situations, it may be possible to use the breakthrough capabilities of variable speed diesel generator and high quality energy storage to deliver solutions that make immediate and effective economic sense. The following components were selected for the studies of the integration of renewable energy into the grid:

a) Solar Modules

Solar Modules, or Photovoltaic panels (PV), can be installed on the roofs of residential and commercial buildings and/or near each suburban transformer as required and can be integrated into the system by AC coupling.

b) Batteries

The newly developed UltraBattery technology performance enhancing features that exploit the performance benefits of the Partial State of Charge (PSoC) band, while mitigating the deteriorating effects of conventional lead-acid technology. This technology avoids the upper and lower bands of charge in its normal operation, therefore improving efficiency and battery life.

c) Inverters

There are two types of inverters; the island type that controls the batteries and provides the start and stop signals for the generators and maintain grid voltage and frequency also reactive power, and the grid type inverters that will converter distributed solar PV DC power into AC and directly feed to load and remaining going to battery through bidirectional inverter.

d) Variable Speed Generators

Conventional fossil fuel based generators are designed to produce electricity at a fixed frequency which is rotating at a constant speed regardless of the power demand. Research in [7] and [8] shows that fuel consumption of a VSG is actually lower than the CSG during light load operation. This is an important characteristic of a fossil fuel based generator if fuel savings and the CO2 emissions reduction are the main concerns in the operation of a HPS. The fossil fuel based generators are modelled using the fuel consumption versus loading power characteristics. It is worth noting that, in HOMER the fuel load characteristic of a fuel-powered generator is assumed to be linear. This approximation may not be suitable table for the variable speed generator as its characteristic can be approximated as a polynomial curve that signifies lower fuel consumption for the operation below rated power.

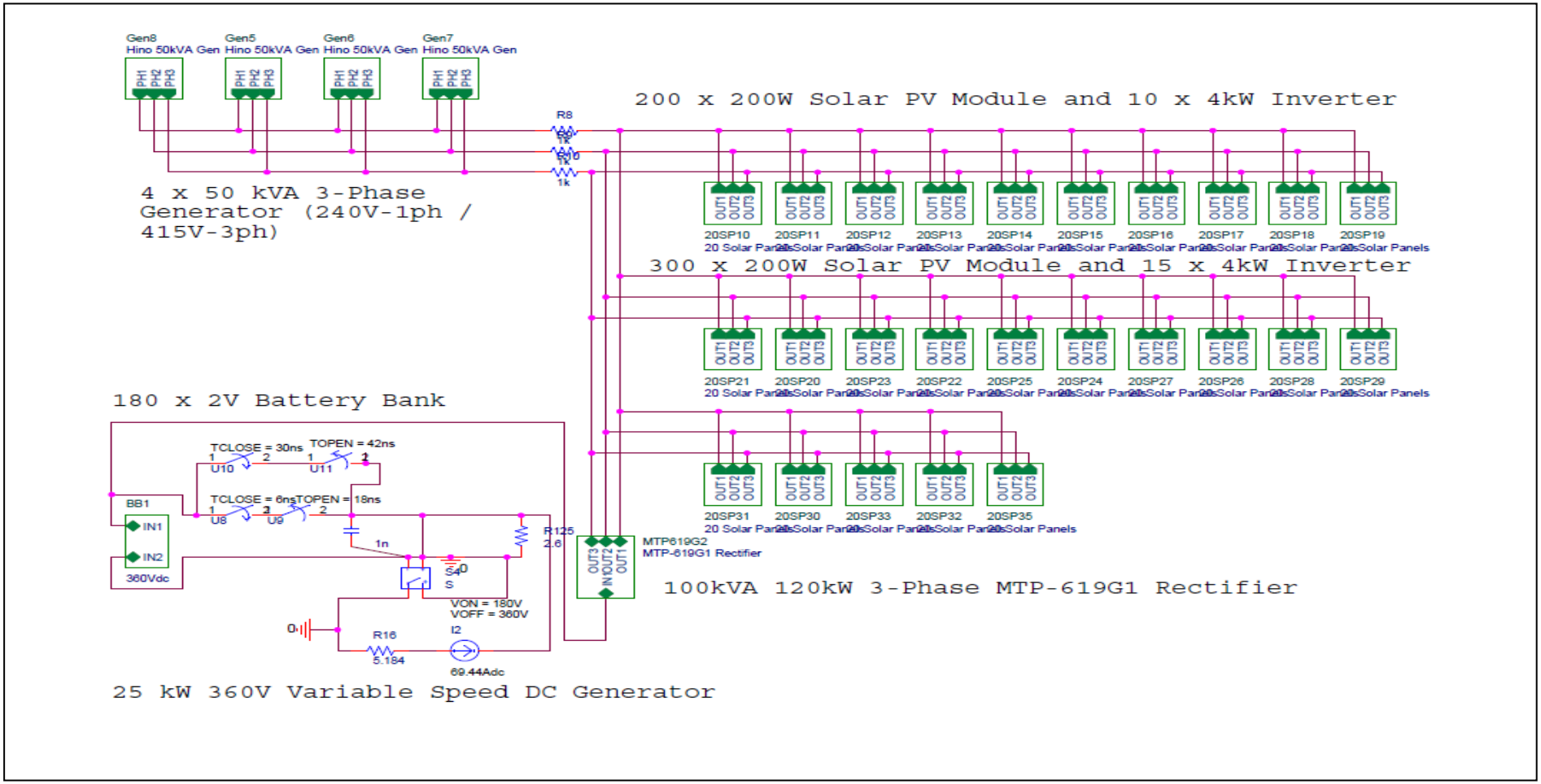

Figure 6. 13: System configuration

There are two operating conditions of a fossil fuel based generator. During a deficit of renewable sources, the generator and battery bank power supply have to match the load demand. Alternatively, the generator power can charge the battery and supply the load demand simultaneously during light load demand.

Figure 6.12 shows the Matlab simulation of a system with a lead acid battery and a variable speed diesel generator integrated with the network through a bidirectional inverter. In this system, AC coupled distributed solar PV can be integrated as required for each suburban transformer. Figure 6.13 shows the PSpice simulation for the same combination and all the components existing generators, network and proposed components modelled to compare the performance. Simulation results provided in appendix.

The fuel consumption characteristics of CSDG and VSDG that were used for the simulation are presented in Figures 6.14 and 6.15. When operating without a load, the fuel consumption of the VSDG would be only 0.67L/hour, 30% less than the 0.96L/hour value of the CSDG. Therefore, a system that contains a VSDG should have better fuel consumption than one with a CSDG.

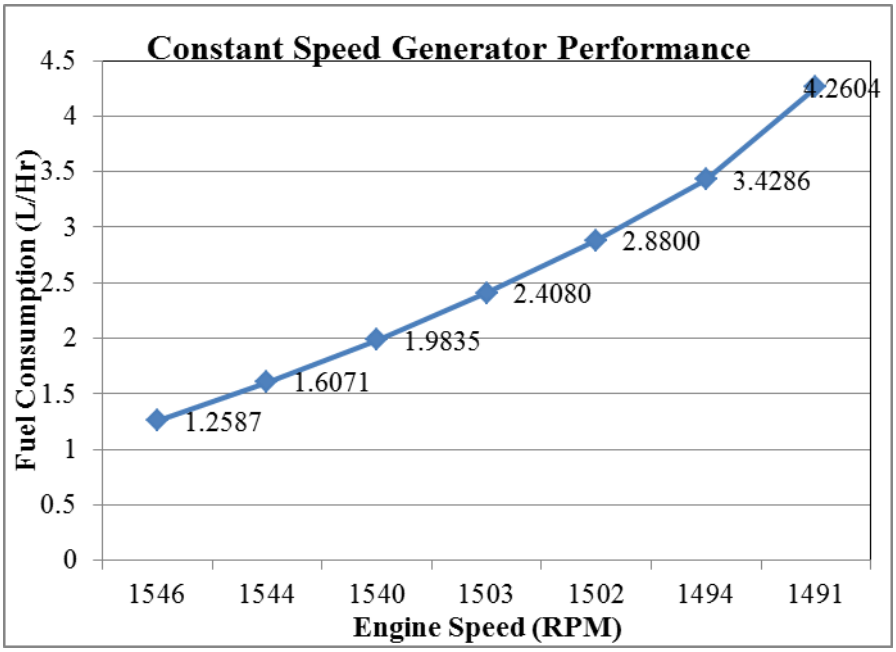

Figure 6. 14: Fuel consumption versus power production of a CSDG [9]

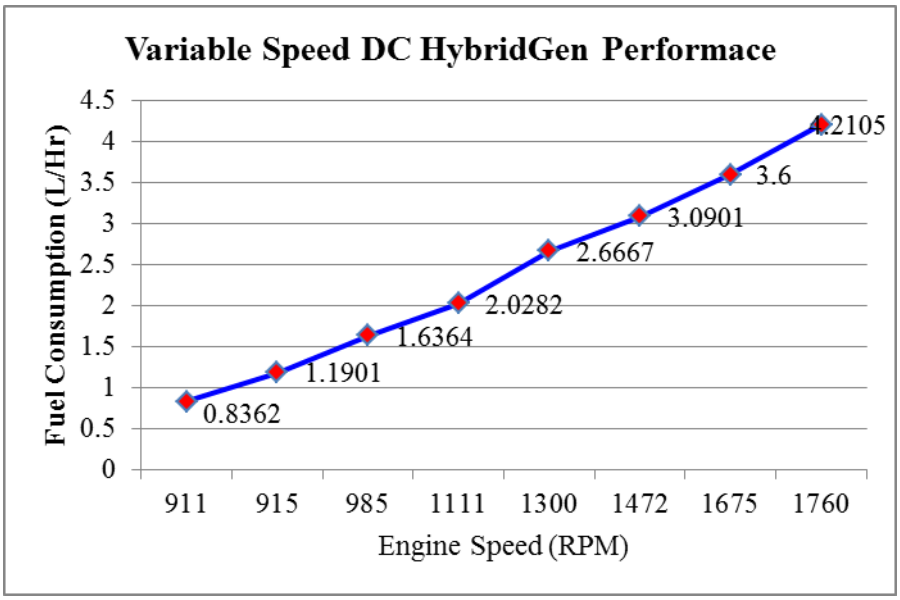

Figure 6. 15: Fuel consumption versus power production of a VSDG [9]

Analysis of the performance of hybrid power systems containing either a CSDG or a VSDG was completed. Dynamic and fast response operation was not included in the modelling. The system simulations were based on the following assumptions:

- System operations remained in a steady state
- Power supply and demand were balanced at any time step simulated
- System operation was continuous (breakdowns and maintenance were disregarded)
- Renewable energy source and load demand remained constant for each simulated time step

Selection of the appropriate simulation tools was a critical factor in the hybrid power system performance analyses. Although HOMER is the most commonly used software for hybrid power systems simulation for the purpose of general logistic performance analyses, the versatile simulation environment provided by PSpice MATLAB/Simulink [10-14] was better suited to this research study. All system components were modelled using this simulation tool and the results validated through comparison with those obtained using the benchmark simulation tool.

The validated Simulink models were then used for analysing the long-term performance of systems with either CSDG or VSDG in terms of fuel consumption and carbon dioxide emissions. In HOMER, diesel generators are represented by a linear fuel consumption model,

an assumption that is only valid for a hybrid system containing a CSDG. With Simulink, the VSDG fuel curve could be represented more accurately as a polynomial function [15].

6.15 Analytical Performance Models in Simulink

Simulation models are based on two types of parameter. The first group, modelling inputs, represents the physical characteristics of the components. These are usually entered only once through the Graphical User Interface (GUI) of each system component model. The second group, simulation inputs, are obtained either from the simulation source file or are based on the calculation obtained during each simulation time step. Simulation models of system components including the PV source, diesel generators, batteries and the supervisory controller are presented in the following sections.

6.16 Photovoltaic Model Representation

Modelling of a PV module requires an understanding of the current-voltage characteristics of PV cells under varying levels of solar radiation and cell temperature [16, 17]. A one-diode PV cell model was used in this study. A basic equivalent circuit of this model is presented in Figure 6.16.

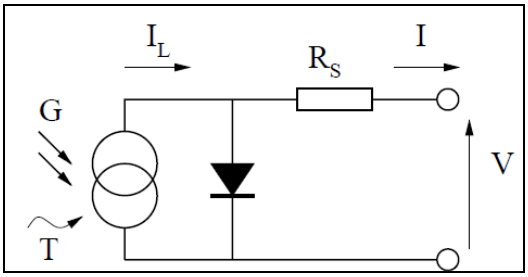

Figure 6. 16: Basic equivalent circuit of PV array

This basic PV cell model was developed in *Simulink* using solar irradiance and ambient temperature as the input variables Figure 6.17 shows the top level Simulink model implementation and the diode and R_p model is presented in Figure 6.18.

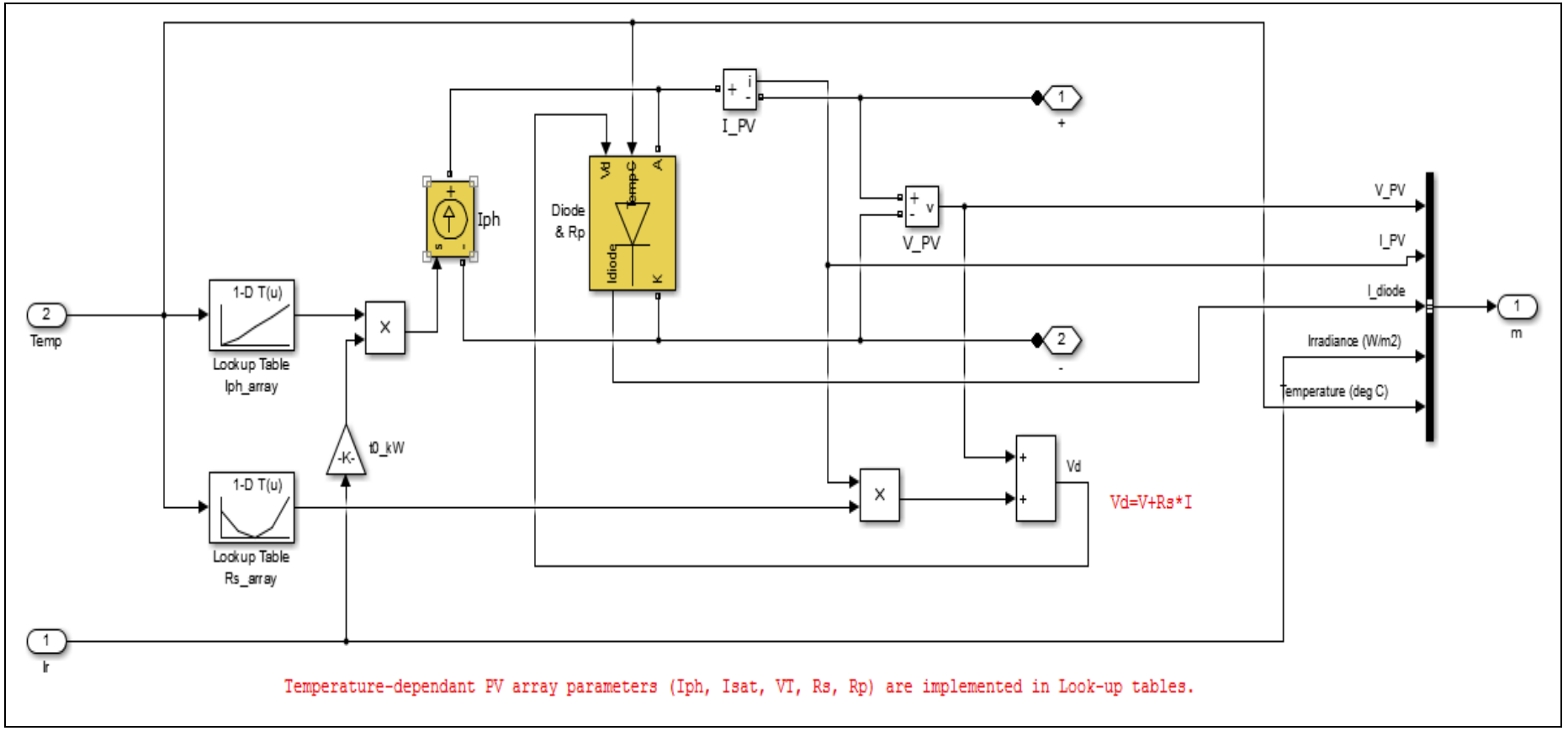

Figure 6. 17: Top level PV cell model.

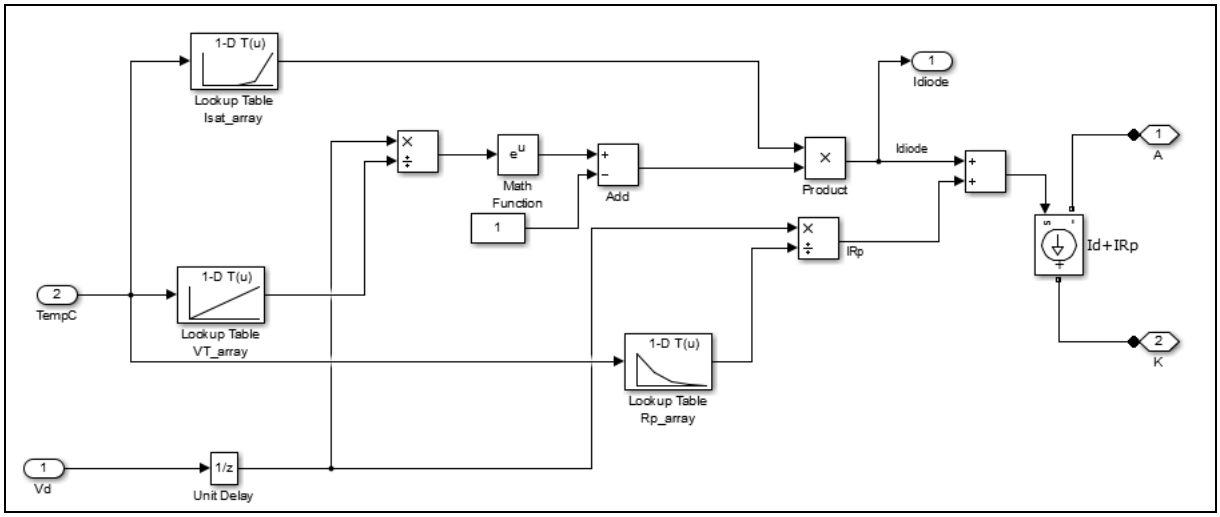

Figure 6. 18: Diode and Rs model**.**

Temperature dependent PV array parameters (I_{ph}, I_{sat}, V_T, R_s and R_p) were implemented in Look-up table. The diode characteristics and associated parameters used in the Simulink model are explained below.

Diode characteristic:

$I_d = I_{sat} \times [\exp (V_d/V_T) -1]$

Where:

I_d = diode current (A)

V_d = diode voltage (V)

I_{sat} = diode saturation current (A)

V_T = temperature voltage = $k \times T/q \times Qd \times Ncell \times Nser$

T = cell temperature (K)

k = Boltzmann constant = 1.3806e-23 $J.K^{-1}$

q = electron charge = $1.6022e^{-19}$ C

Qd = diode quality factor

Ncell = number of series-connected cells per module

Nser = number of series-connected modules per string

The PV module voltage and current were be obtained using Equation (6.1) and Equation (6.2). The PV output power will be the effect of incident solar irradiance striking on the panel. Given the meteorological data, the PV module power can be solved by computing the product

of the PV module's voltage and current as given in Equation (6.3). In order to obtain the PV power at the inverter input terminal, the total solar energy productions from the PV array can be calculated using Equation (6.4), which includes the PV cell temperature, module quantity and averaged de-rating factor of the PV modules. In particular, the higher the cell temperature, the lower the PV cell conversion efficiency.

$$I_{mod} = C_p \times I \quad (6.1)$$

$$V_{mod} = C_S \times V \quad (6.2)$$

$$PV_{mod} = V_{mod} \times I_{mod} \quad (6.3)$$

$$P_{PV} = M \times P_{PV,mod} \times DF \times [1 + \alpha(T_{cell} - T_{cell,STC})] \quad (6.4)$$

Where, M is the module quantity

In this way, the Simulink PV model could be used to investigate the effect of varying weather conditions, represented by solar irradiance and ambient temperature, on the power produced by a hybrid system.

Modelling inputs define the basic PV panel electrical characteristics, and these parameters are usually provided in the data sheets supplied by the manufacturers. The data given is normally referred to the standard test conditions (STC) that includes the incident radiation of 1kW/m^2 (1-sun) and a cell temperature of 25°C. These parameters are the control parameters and can be changed in the Simulink model.

There are a number of parameters defining the electrical characteristics of a PV panel:

- Short-circuit current, I_{SC}
- Open-circuit voltage, V_{OC}
- Power temperature coefficient
- Open-circuit voltage temperature coefficient

Several adjustable parameters were also included in the *Simulink* model to allow the users to vary the simulation conditions. These include:

- Quantity of PV module, M
- PV cell temperature at STC, $T_{cell,STC}$
- Solar irradiance at STC, G_{STC}
- Nominal operating cell temperature, $NOCT$

- Solar irradiance at normal operating conditions, G
- PV cell temperature at normal operating conditions, T_{cell}

The Sun Power SPR-305-WHT PV module was used for the simulation. Figure 6.19 shows the SPR-305-WHT parameters that were obtained from the datasheet for use in the Simulink model.

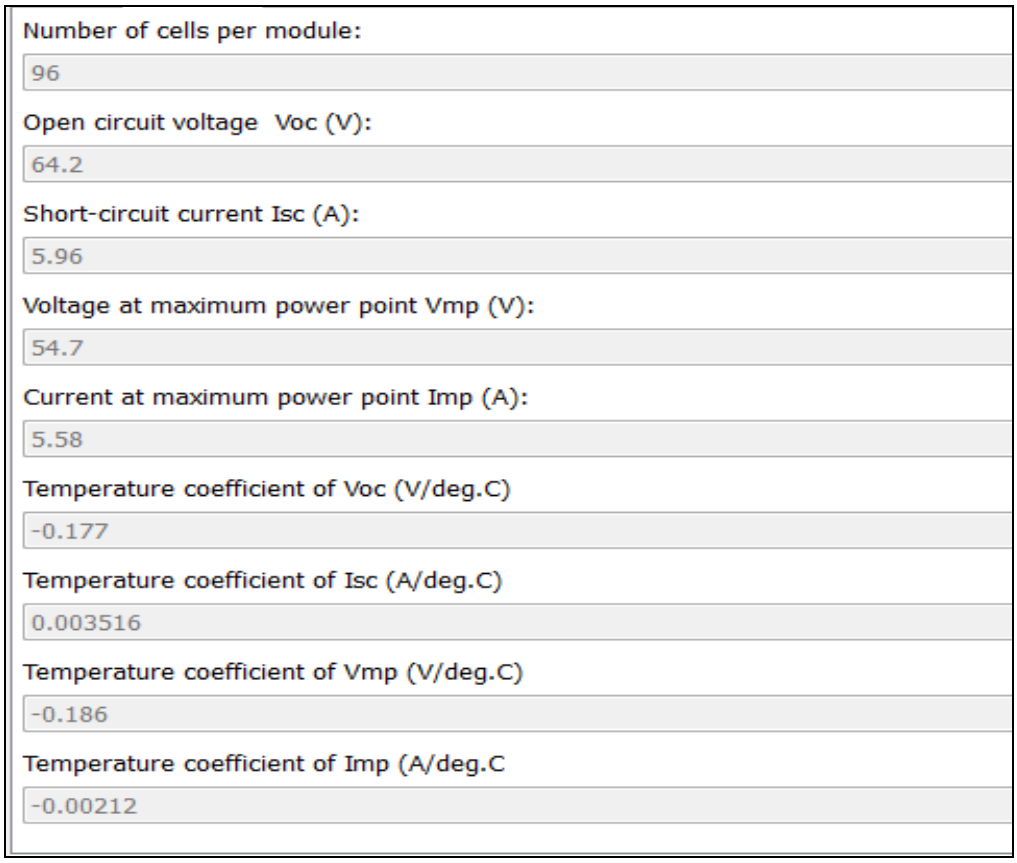

Figure 6. 19: SPR-305-WHT parameters.

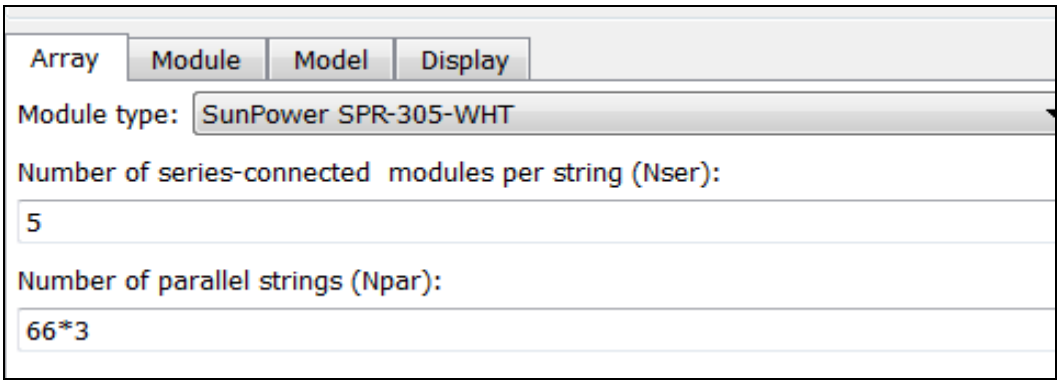

Figure 6. 20: Series and Parallel control of PV Modules

The Simulink program provides the option of modelling the modules in series (Nser) or parallel (Npar). Figure 6.20 shows the Simulink front view when we double clink on PV Model.

Note: Total power @ STC (Standard test condition) of PV module is: 305×5×193 = 301.95kW

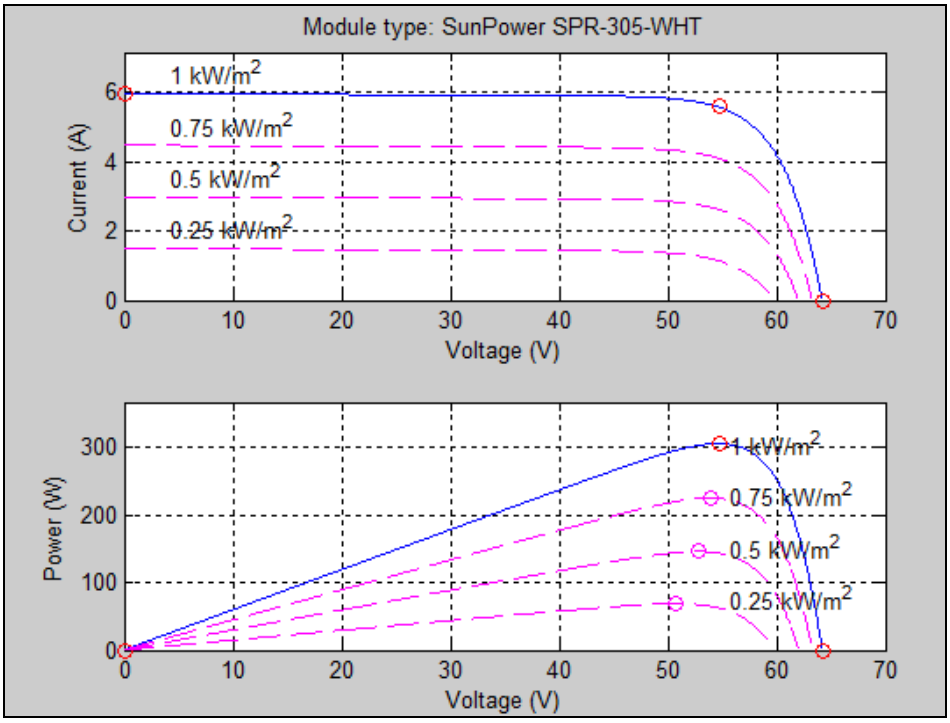

Figure 6. 21: I-V and P-V characteristics of SPR-305-WHT single module.

The I-V and P-V characteristics of single module and series-parallel modules are shown in Figures 6.21 and Figure 6.22, respectively.

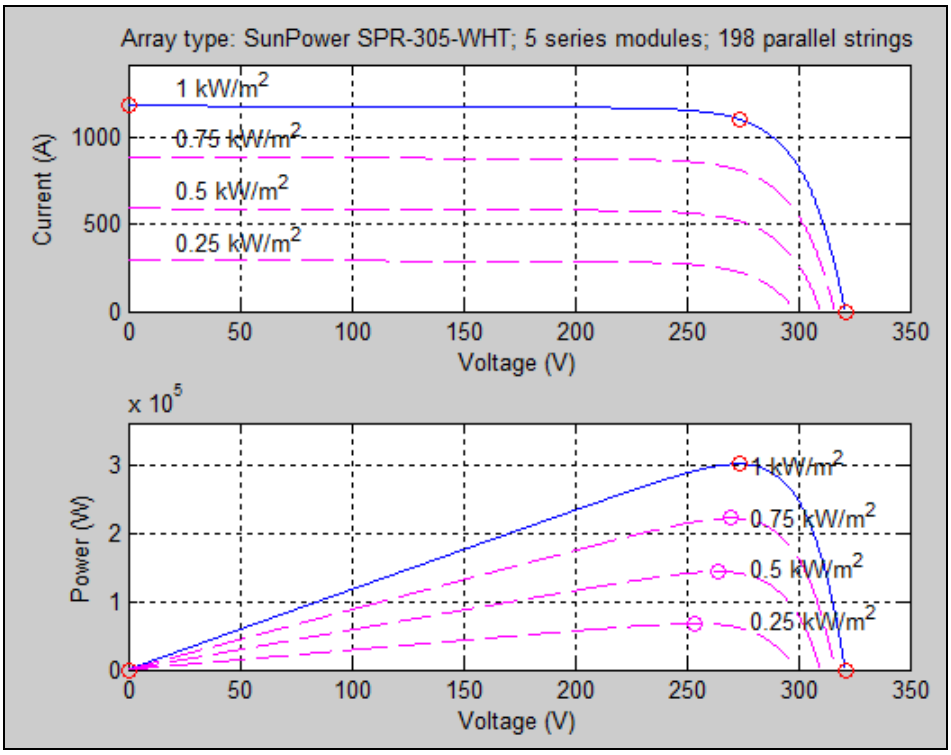

Figure 6. 22: I-V and P-V characteristics of SPR-305-WHT 5 series and 198 parallel modules.

6.16.1 MPPT Controller [15]

The efficiency of energy conversion from current PV technology remains low. In addition, the initial costs for implementation remain high. To achieve maximum efficiency in operation the use of techniques to extract the maximum power from these panels is essential. The point of maximum power (MPP) for each system varies according to climatic conditions. The photovoltaic power does not vary in a nonlinear manner, making the extraction of maximum power a complex task. For this study, the incremental control method was used for implementing Maximum Power Point Tracking (MPPT). A flow chart presenting the incremental control MPPT principle is presented in Figure 6.23.

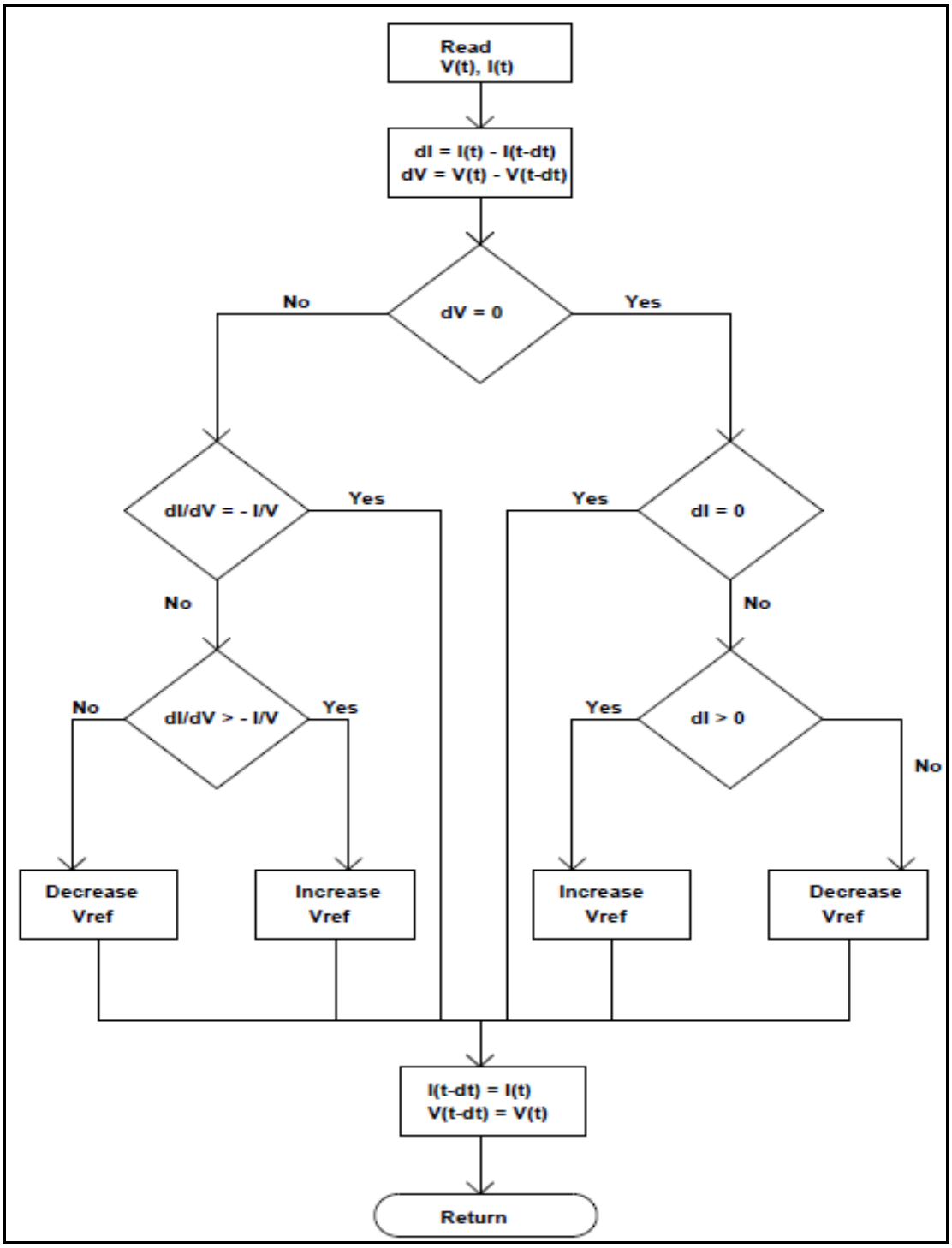

Figure 6. 23: Flow chart of IC Algorithm

The IC method is based on the fact that the power slope of the PV is null at MPP (dP/dV = 0), positive in the left and negative in the right. Therefore, the MPP can be found in terms of the increment in the array conductance. Using equation (6.5) it is possible to find the IC conditions presented by equation (6.6).

$$\frac{dp}{dv} = \frac{d(v.i)}{dv} = i + v.\frac{di}{dv} = 0 \qquad (7.5)$$

$$\frac{\Delta i}{\Delta v} = -\frac{i}{v}\,(a), \frac{\Delta i}{\Delta v} > \frac{i}{v}\,(b), \frac{\Delta i}{\Delta v} < \frac{i}{v}\,(c) \qquad (7.6)$$

Simulink models of a top level and internal MPPT controller are show in Figure 6.24.

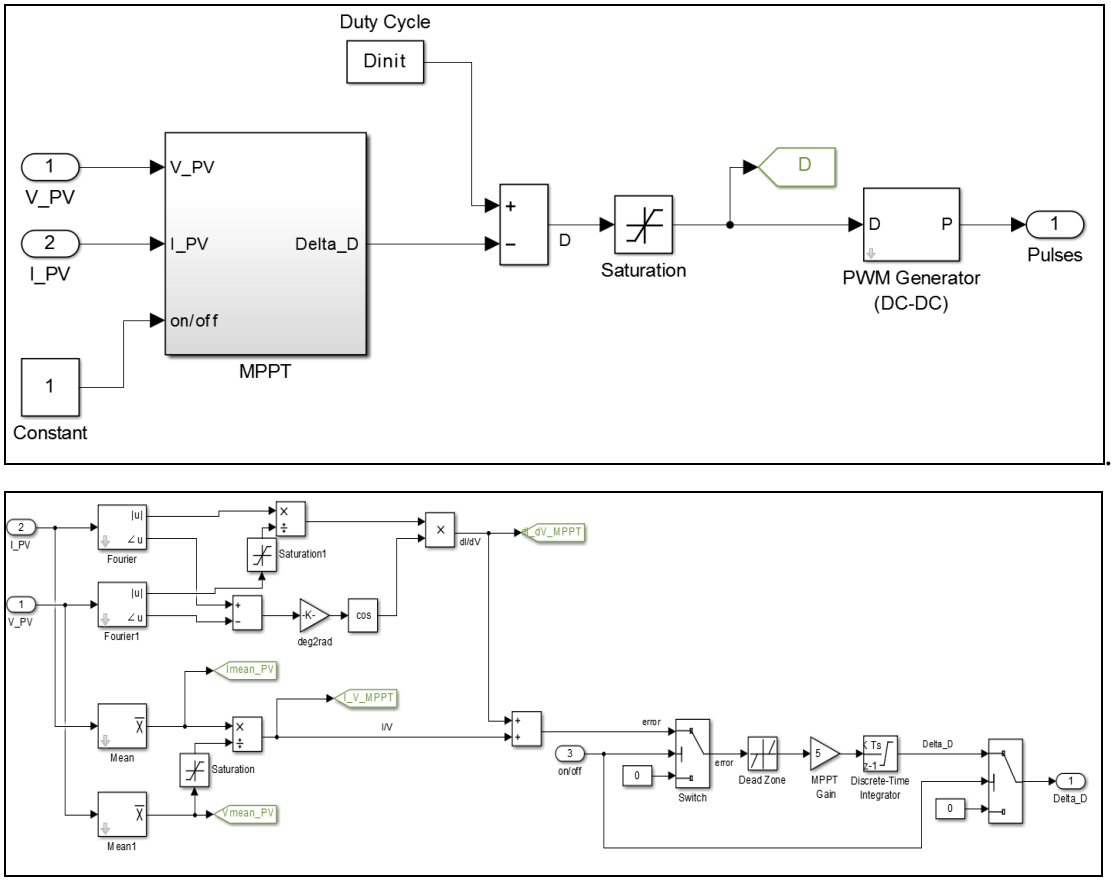

Figure 6. 24: Top level controller and detailed MPPT controller

Maximum power point is obtained when dP/dV=0 where P= V×I

d (V×I)/dV = I + V×d_I/d_V = 0

d_I/d_V = -I/V

dI, dV = fundamental components of I and V ripples measured with a sliding time window T_MPPT

I, V = mean values of V and I measured with a sliding time window T_MPPT

The integral regulator minimizes the error (dI/dV + I/V)

Regulator output = Duty cycle correction

6.17 Integrated PV array with Boost converter with MPPT control:

To implement a MPPT controller the power electronic equipment must be integrated with the PV array. Figure 6.25 shows the PV array integrated with a Boost converter and with an embedded MPPT controller.

- **Boost converter principle**:

A boost converter (step-up converter) is a DC-to-DC power converter with an output voltage that is greater than its input voltage. It is a class of switched-mode power supply (SMPS) containing at least two semiconductors (a diode and a transistor) and at least one energy storage element- either a capacitor or an inductor, or the two in combination. Filters made of capacitors (sometimes in combination with inductors) are normally added to the output of the converter to reduce output voltage ripple.

The Boost converter output voltage equation is:

$Vo = Vi \times [1/ (1-D)]$, where D is the duty cycle.

When used in a PV system, the MPPT controller duty cycle of is decided by the Maximum power point control algorithm

To implement a MPPT controller the power electronic equipment must be integrated with the PV array. Figure 6.25 shows the PV array integrated with a Boost converter and with an embedded MPPT controller.

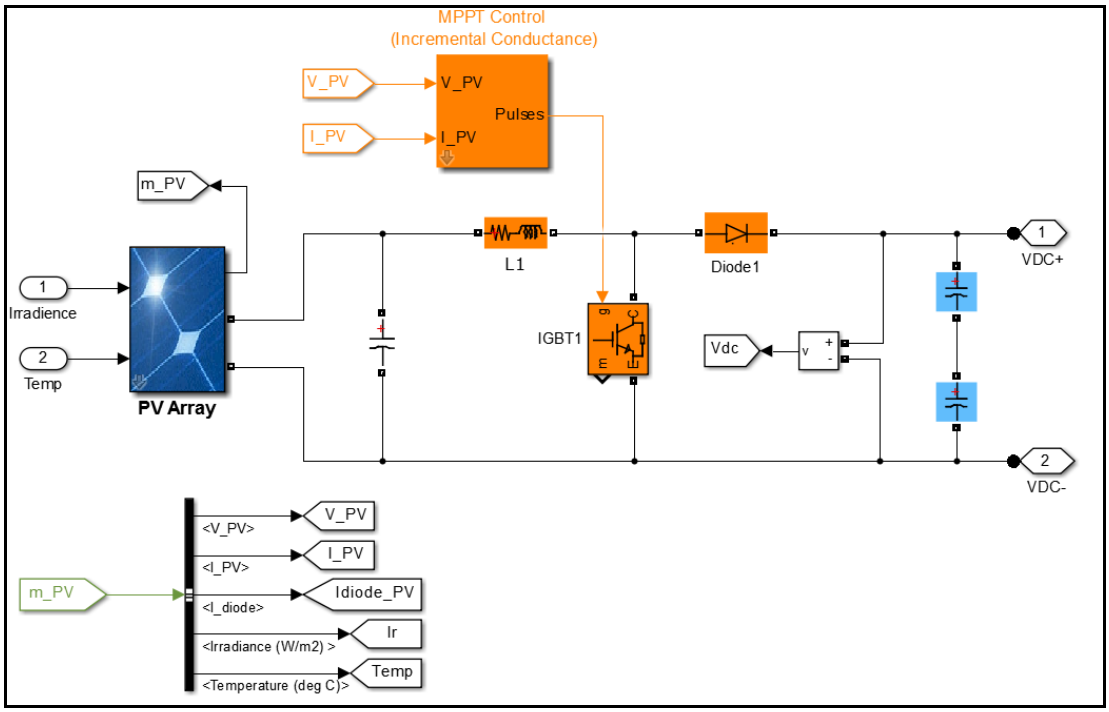

Figure 6. 25: PV array with Boost converter and MPPT controller.

The PV array monitors the irradiance and temperature and produces the appropriate output voltage. The Boost converter monitors the PV array output voltage and PV array current and can switch to deliver the maximum power at any point of time.

6.17.1 Solar (PV) Inverter

A solar inverter converts the variable direct current (DC) output of a photovoltaic (PV) solar panel into a utility frequency alternating current (AC) that can be fed into a commercial electrical grid or used by a local, off-grid electrical network. Solar inverters have special functions adapted for use with photovoltaic arrays, including MPPT.

PV Inverter output will have a sine wave filter to convert the PWM output voltage to sine wave. A basic PV inverter block is shown in Figure 6.26.

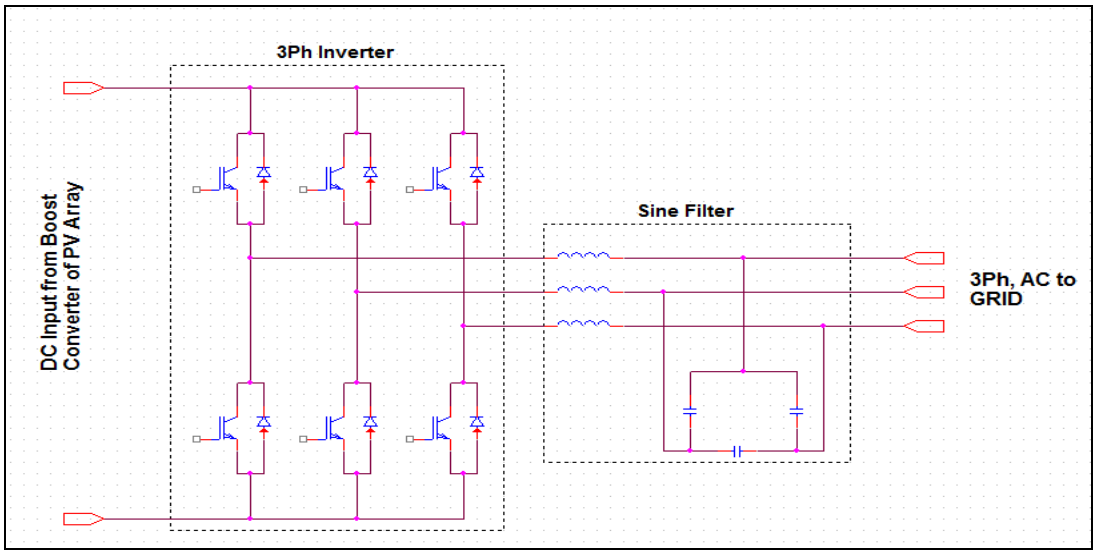

Figure 6. 26: PV Inverter and Sine filter block

6.17.2 PV array, Boost and Inverter simulation results

MATLAB simulations were carried out to determine the functionality of the PV array, MPPT, Boost converter and Inverter. A constant grid side load of 220kW was applied. Load variation was modelled by varying the irradiance from 1000W/m^2 to 500W/m^2. Figure 6.27 shows the irradiance and temperature plot with respect to time that was used for simulation. The high level block that was used for simulation is presented in Figure 6.28. The simulation results are presented in Table 6.4. When irradiance was set at 1000 W/m^2, output power was 192kW. When irradiance was 500 W/m^2, the output power was limited to 141kW at Maximum power output of PV cells.

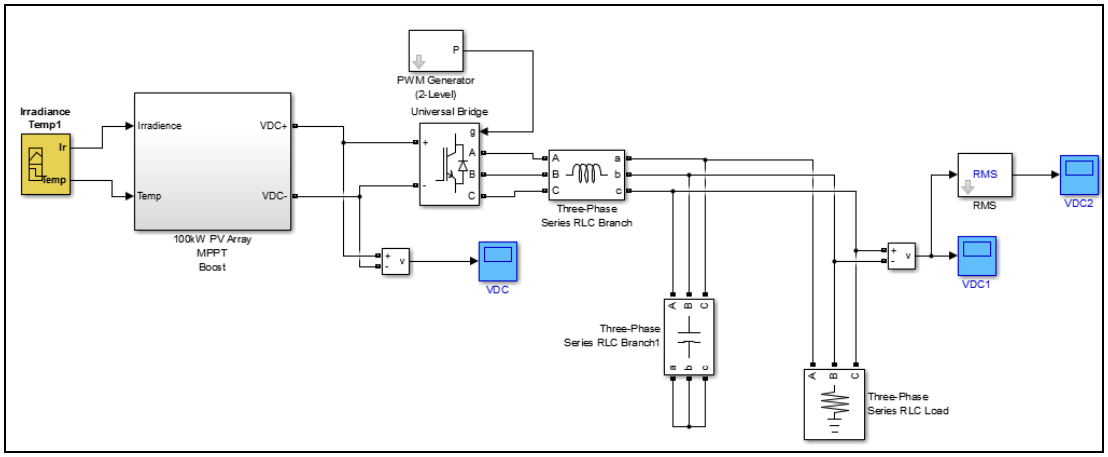

Figure 6. 27: Solar system connected to external load

Table 6. 3: Simulation results of PV cell, MPPT and PV Inverter

Irradiance (W/m^2)	Load Power (kW)	Boost DC voltage (V)	Inverter Output Voltage [L-L] (Vrms)
1000	192	615	373
500	141	526	320

6.17.3 Diesel Generator Model Representation

An analytical performance model of the diesel generator was developed based on the power versus fuel consumption characteristics or measurements in datasheets provided by the manufacturer. Figure 6.28 shows the Simulink model containing the diesel generator and controller. A 400V, 325kVA, 1500RPM diesel generator with governor control was used in the model. Figure 6.29 shows the generator parameters in PU.

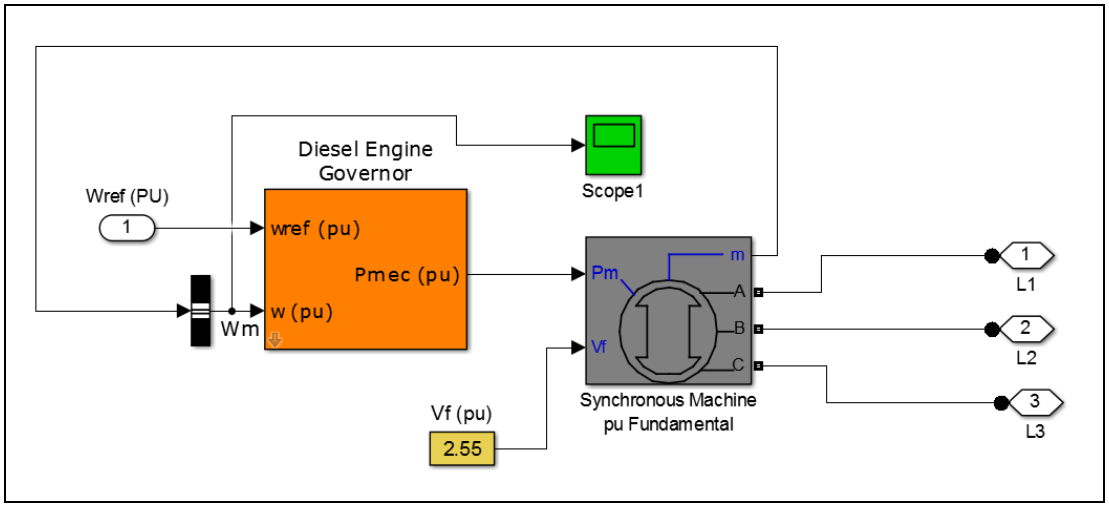

Figure 6. 28: Simulink model of diesel generator and Speed controller

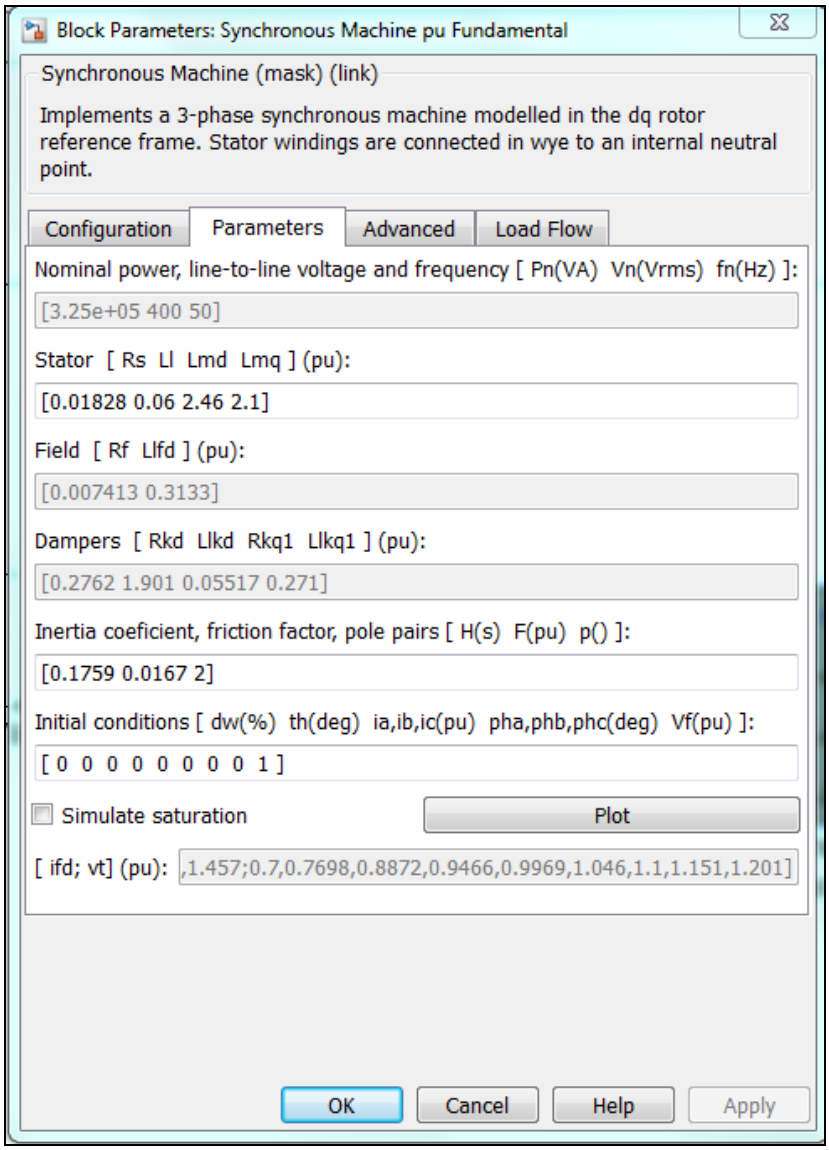

Figure 6. 29: Generator parameters in Simulink

In figure 6.30, Wref (pu) is per unit of the input speed setting value, w (pu) is per unit of generator set actual speed which is tested through generator detection unit, P_{mec} (pu) is per unit of diesel engine output power, used to drive generator. The main controller and scale-up unit constitute the proportion, differential and second-order inertial link control unit which by adjusting the diesel engine accelerator actuators to speed adjustment effect. Output speed of diesel engine is through integral unit conversion for torque because diesel engine is a large time delay system, the torque first through delay unit then multiplied the speed signal of multiplier to reach machinery power signal.

The function of excitation control system mainly in the following aspects:

- Maintain generator terminal voltage constant

  Usually when load changes, generator terminal voltages will change, according to the change of terminal voltages adjusting generator excitation current, to make the terminal voltage maintain in certain level.

- Control reactive power allocation of parallel operation generator

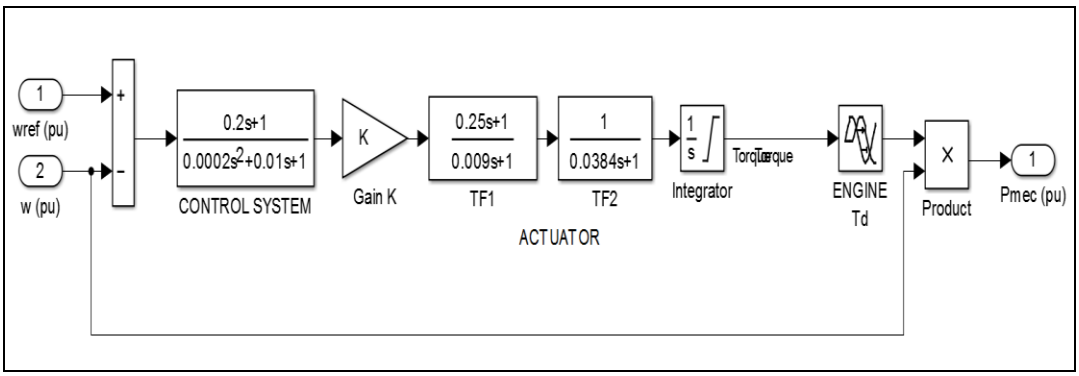

Figure 6. 30: Diesel engine governor control block.

6.17.4 Rectifier

A variable speed generator requires a rectifier to convert AC voltage to DC voltage. Figure 6.32 shows the rectifier block with LC filter to filter the DC ripple. The LC filter was tuned to a resonant frequency around 98Hz – 105Hz. Filter performance was evaluated in Simulink.

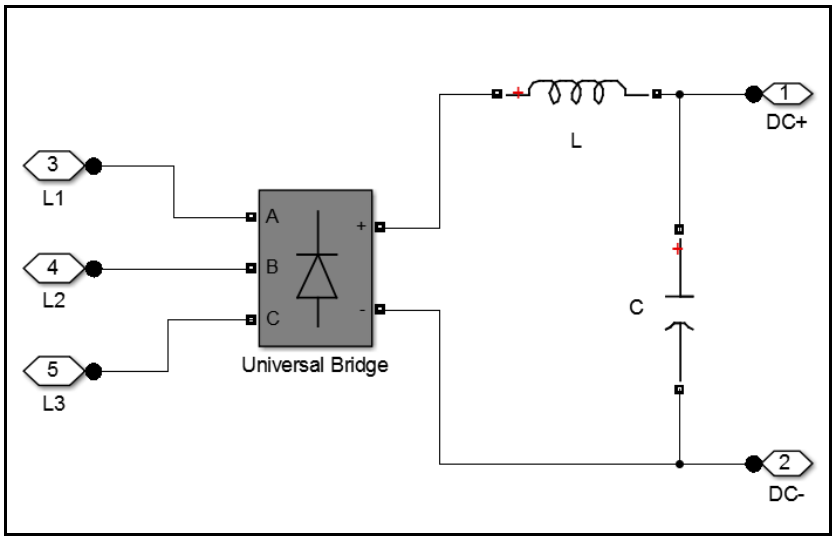

Figure 6. 31: Rectifier with DC filter.

6.17.5 Simulation results for Generator and Rectifier with variable loads

Figure 6.33 shows the blocks implemented for understanding the Variable Speed generator performance with respect to variable loads and generator speed. Load and speed were varied as shown in below Table 6.5 for getting constant DC output voltage at rectifier output.

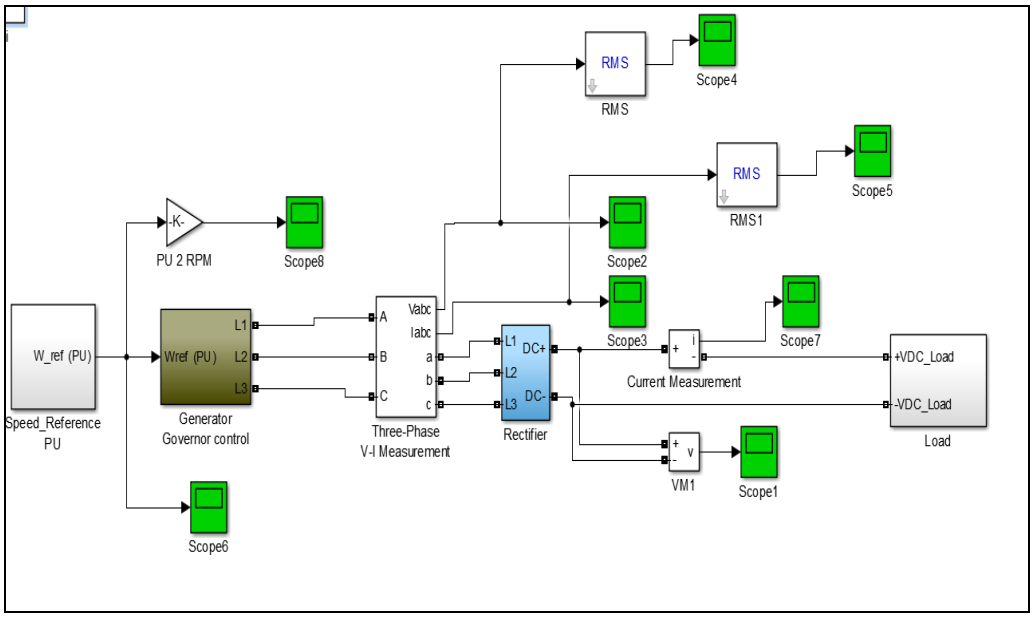

Figure 6. 32: Generator & rectifier Simulink model

Table 6. 4: Simulation results

Load	VSDG		Load (Rectifier Output)		VSDG
	Voltage (AC)	Current (AC)	DC Voltage	DC Current	Speed
KW	V_g	I_g	V_{load}	I_{load}	rpm
70kW	310	145	410	170	502.5
140kW	320	280	410	340	652.5
210kW	328	398	410	511	1200
140kW	320	280	410	340	652.5
70kW	310	145	410	170	502.5

Power vs. Speed for constant DC output voltage:

Figure 6.34 shows the power versus speed (PU) for the generator selected for the simulation.

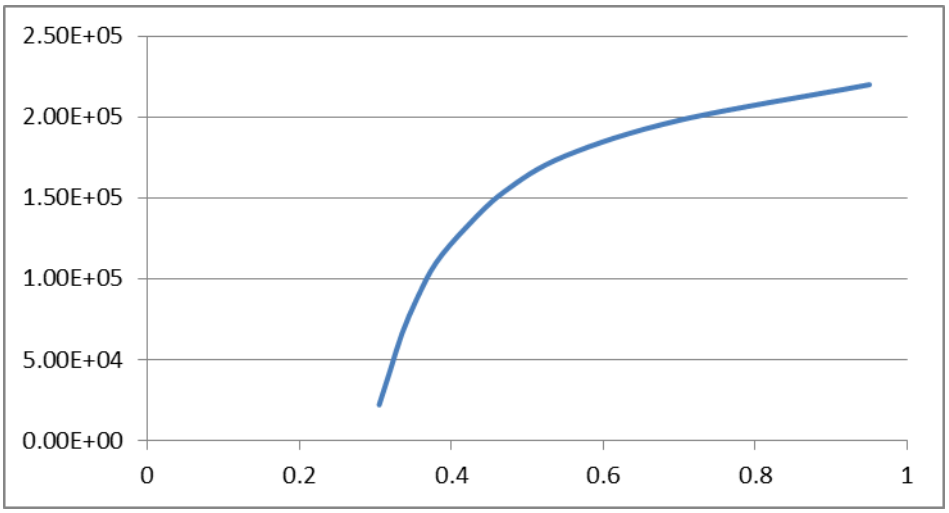

Figure 6. 33: Speed (PU) vs. Power output

When power reduces on the generator, to maintain constant output voltage, speed of the generator is controlled which saves diesel requirement. Generator output voltages and rectifier output voltage at various load levels are shown below in Figures 6.35 to 6.46.

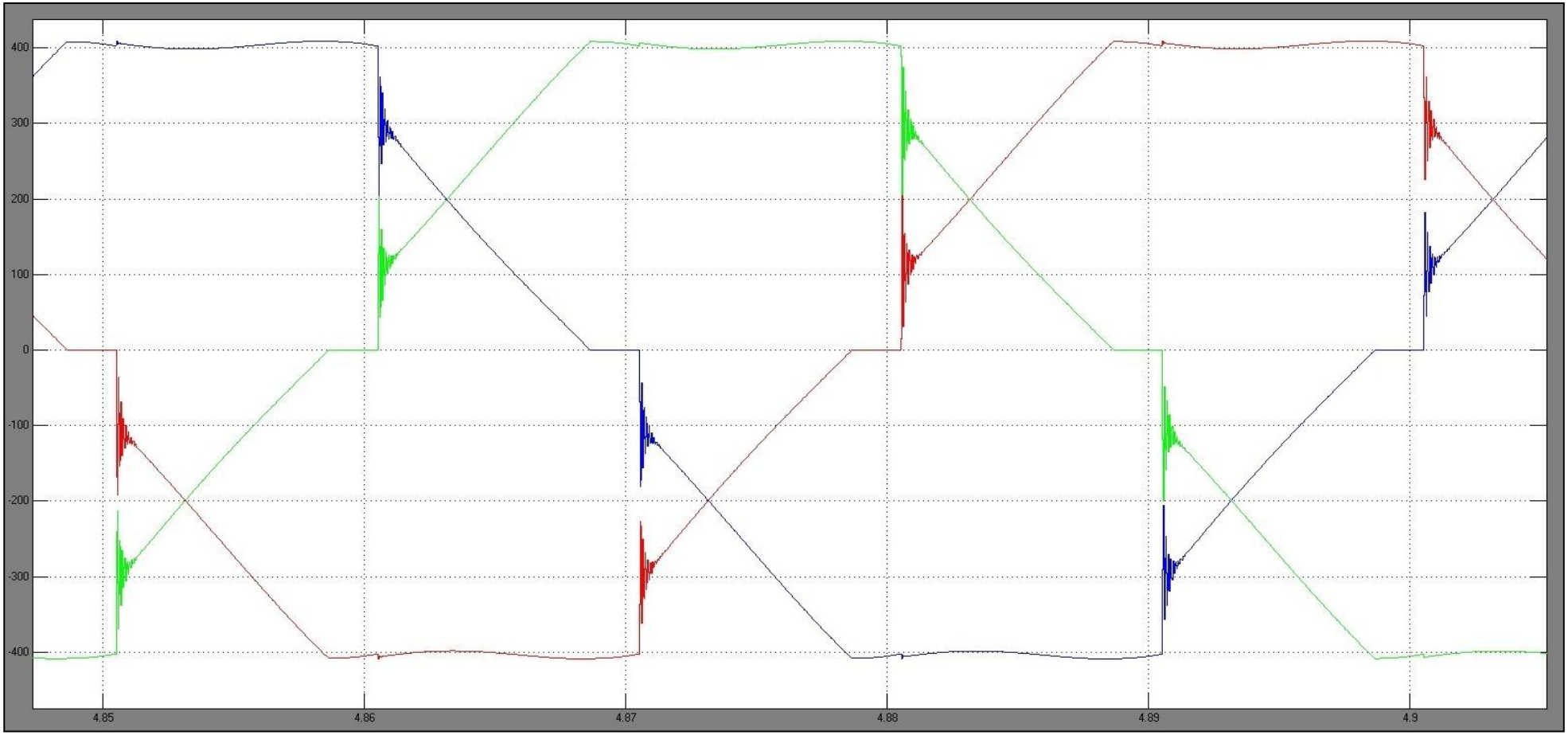

Figure 6. 34: Generator Voltage at 70KW

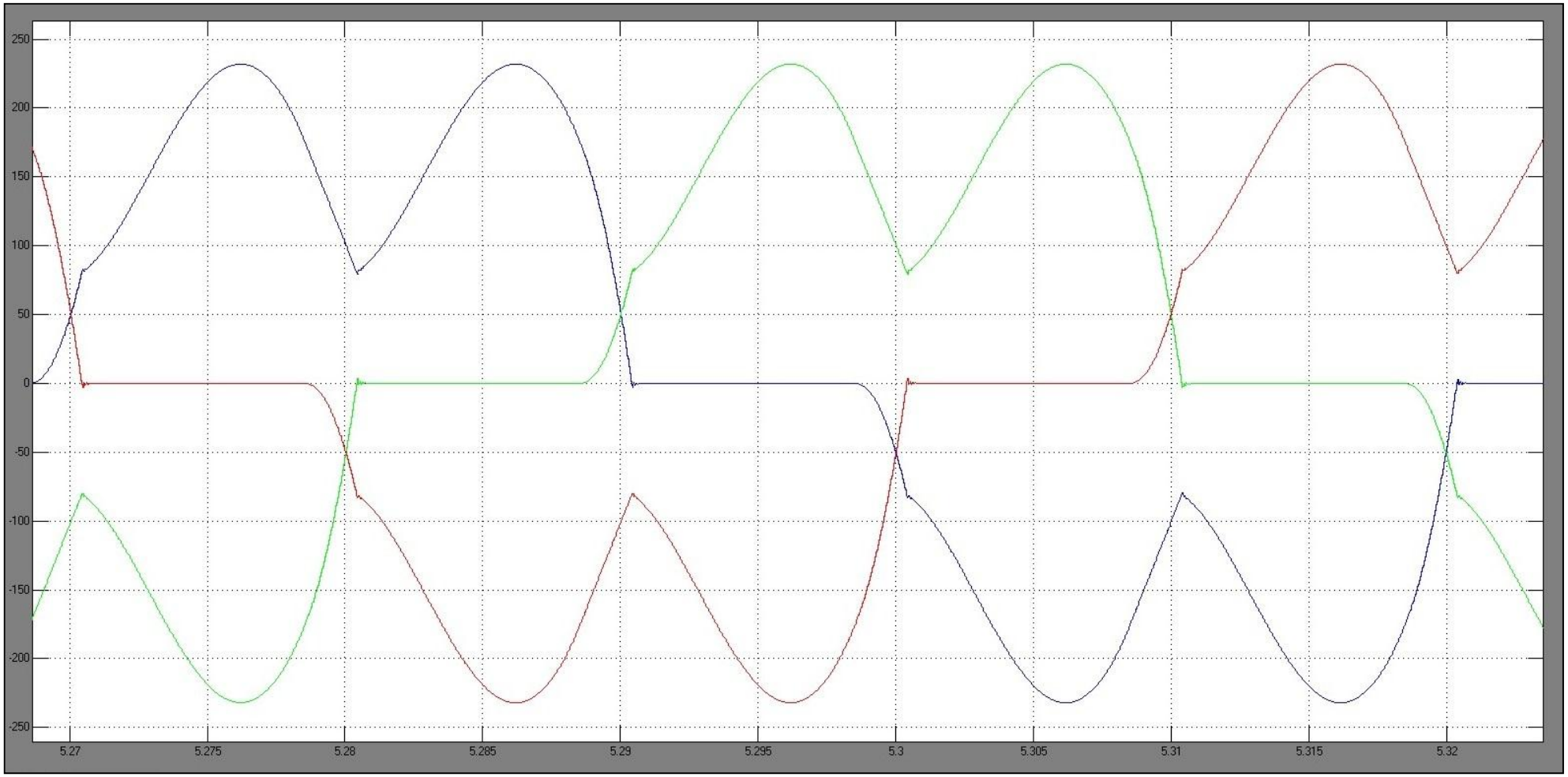

Figure 6. 35: Generator current at 70KW

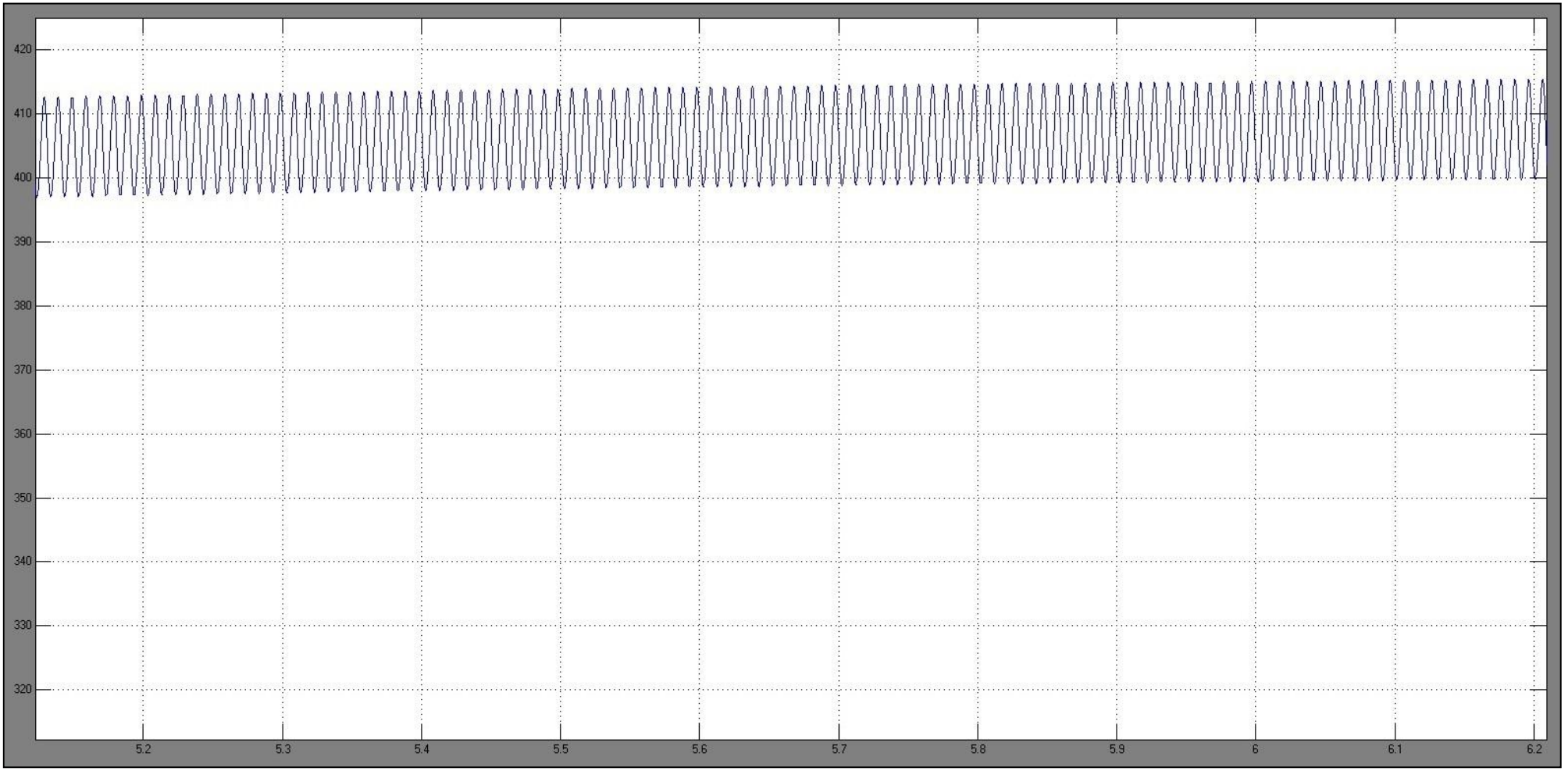

Figure 6. 36: DC Voltage at 70KW

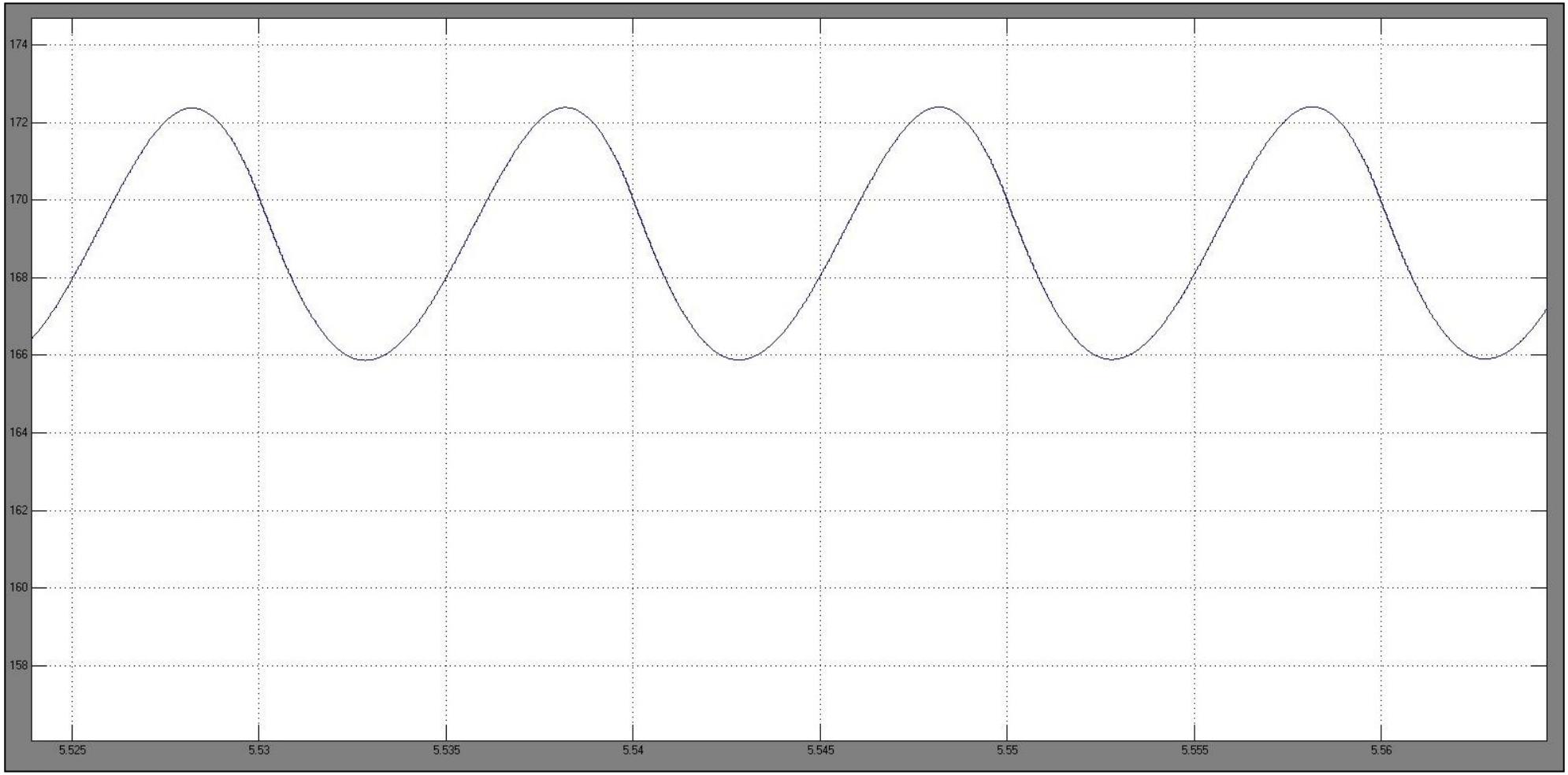

Figure 6. 37: DC current at 70KW

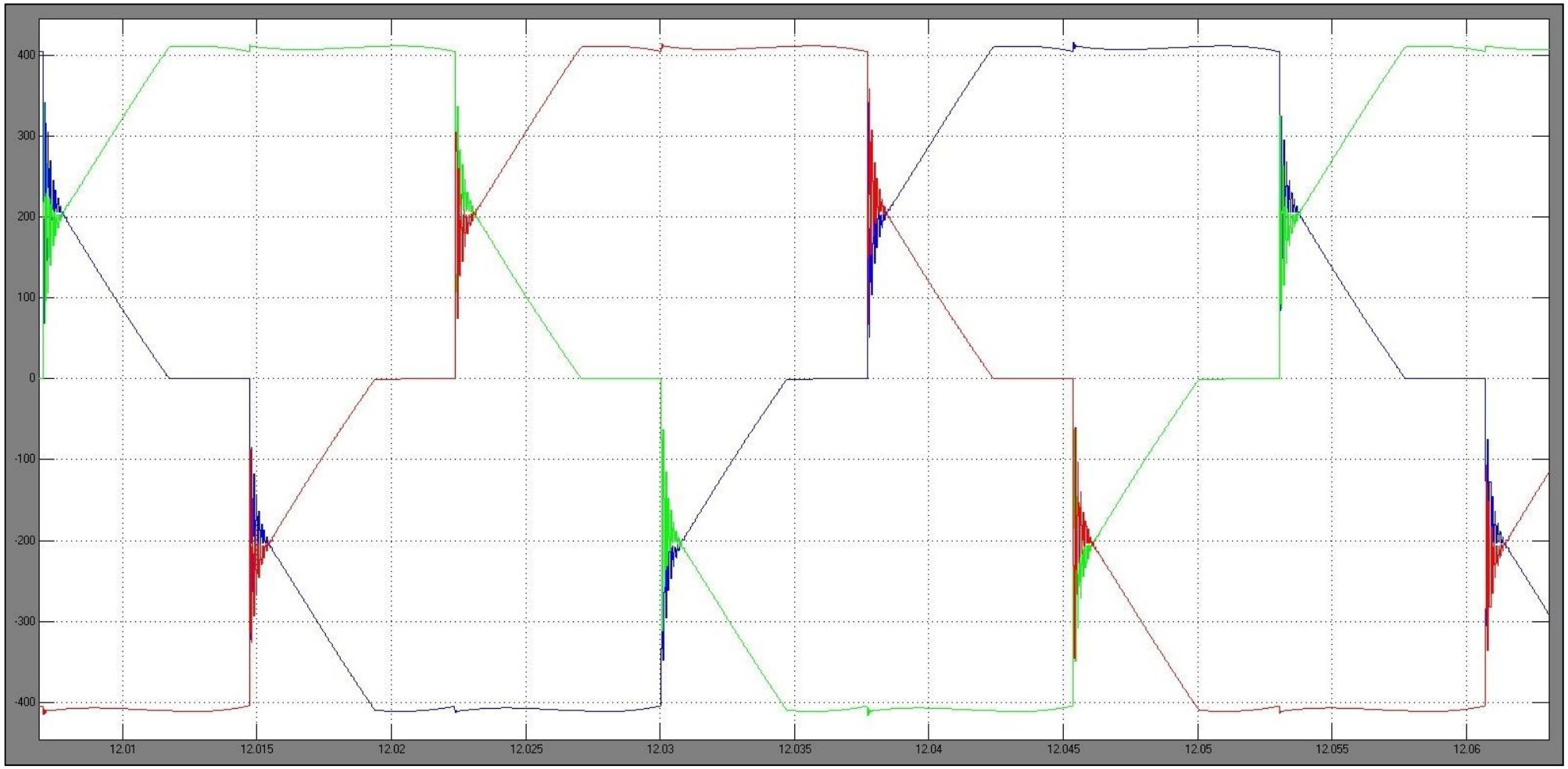

Figure 6. 38: Generator voltage at 140KW

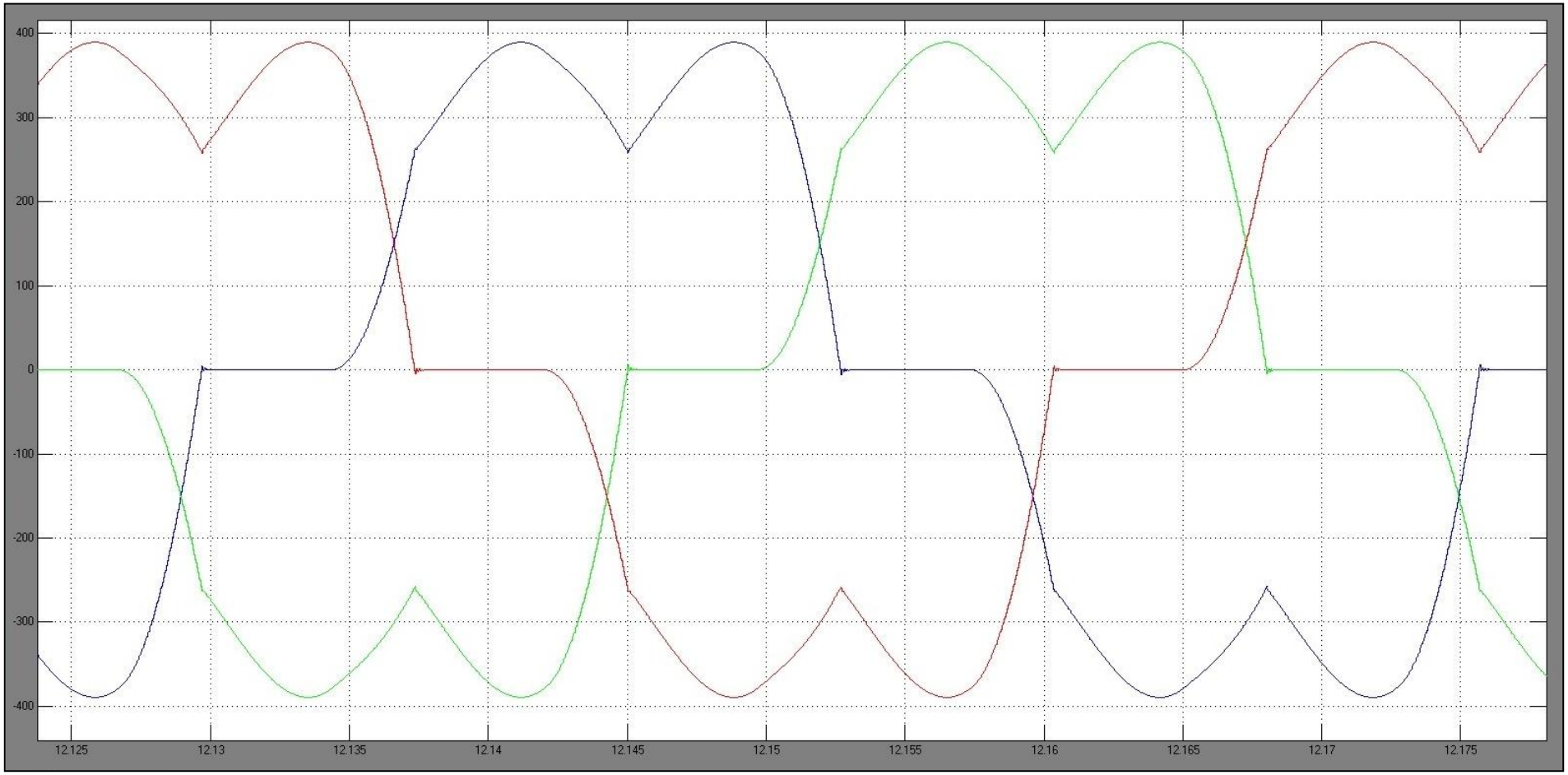

Figure 6. 39: Generator current at 140KW

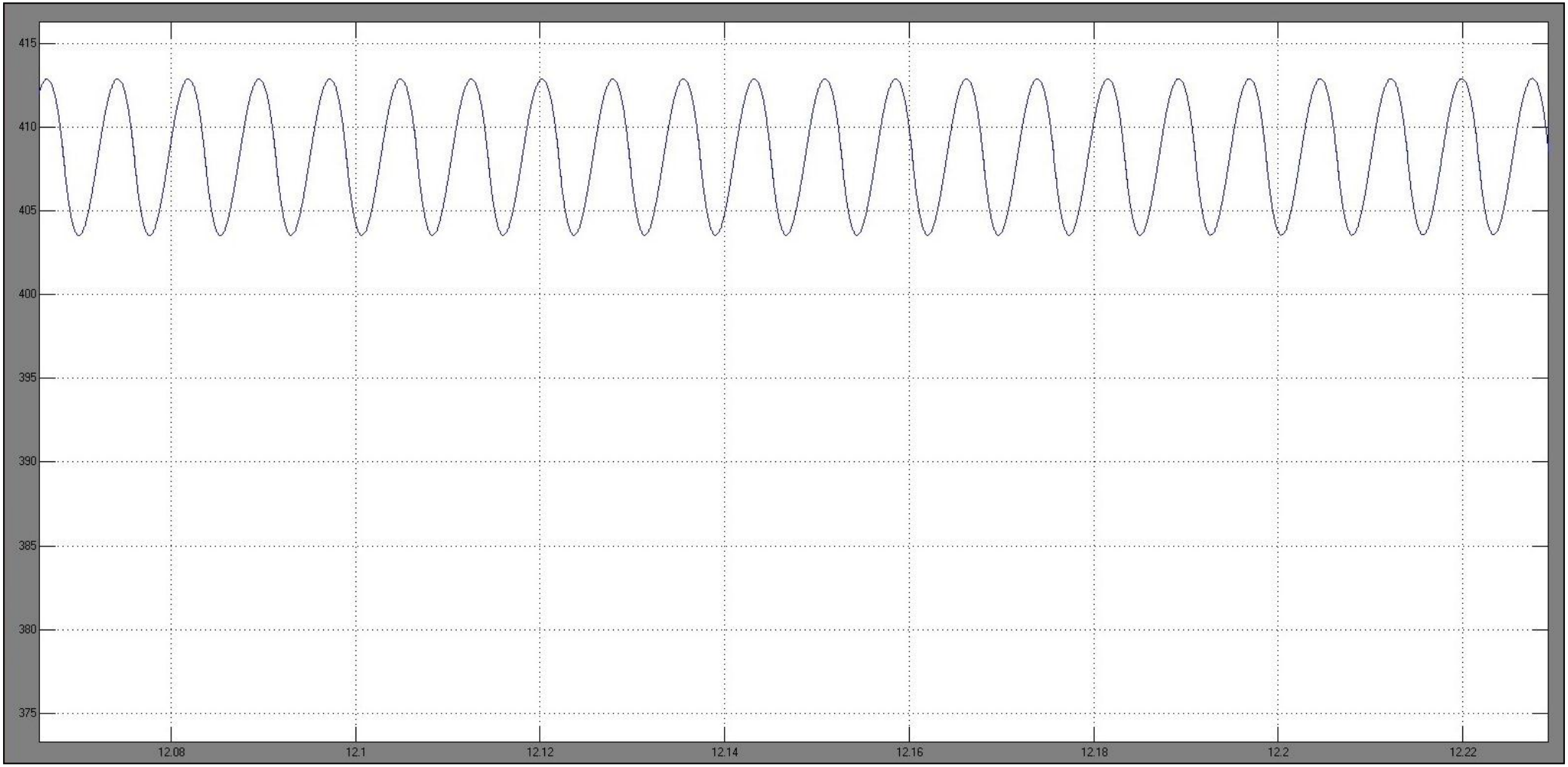

Figure 6. 40: DC Voltage at 140KW

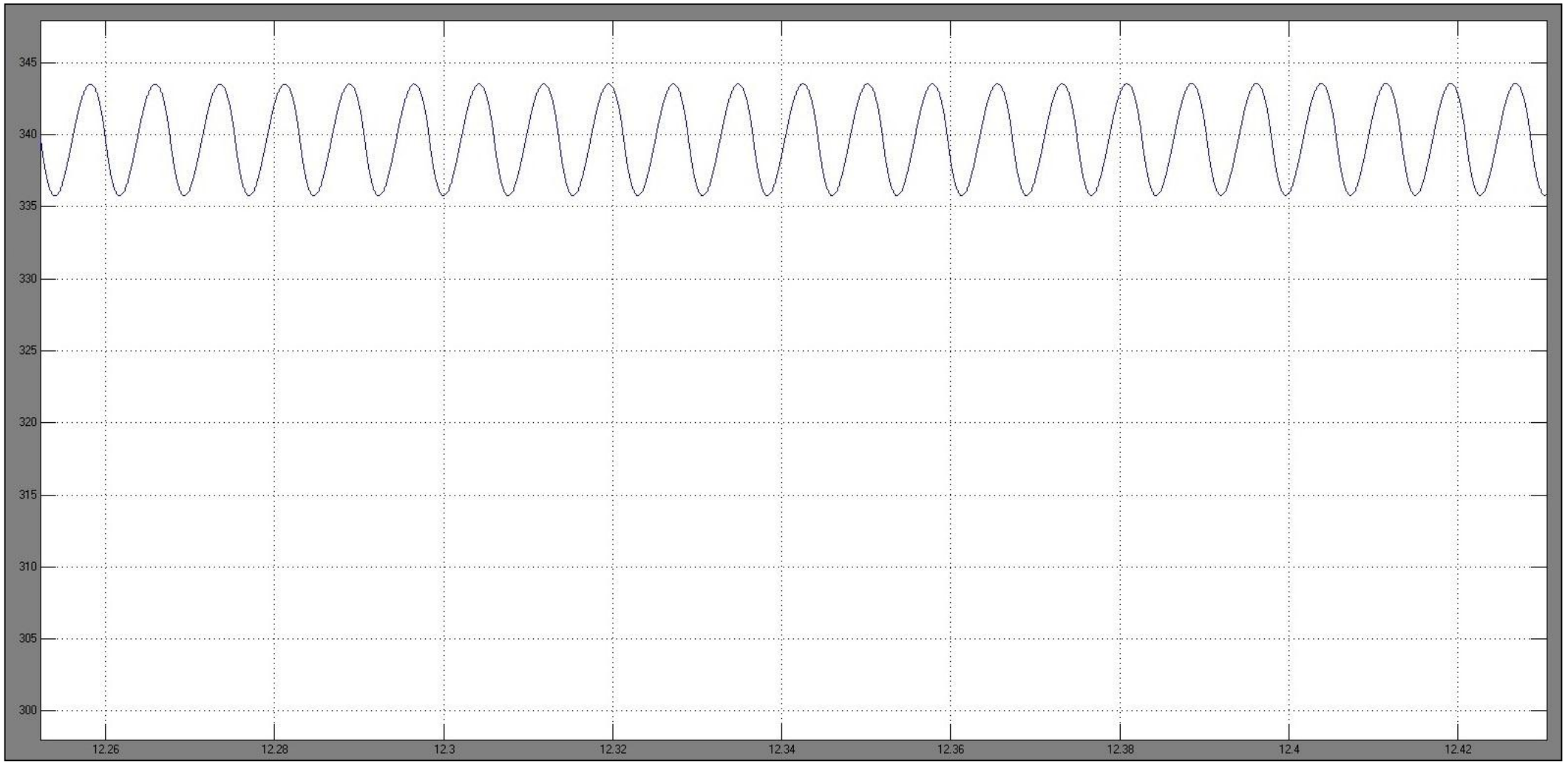

Figure 6. 41: DC Current at 140KW

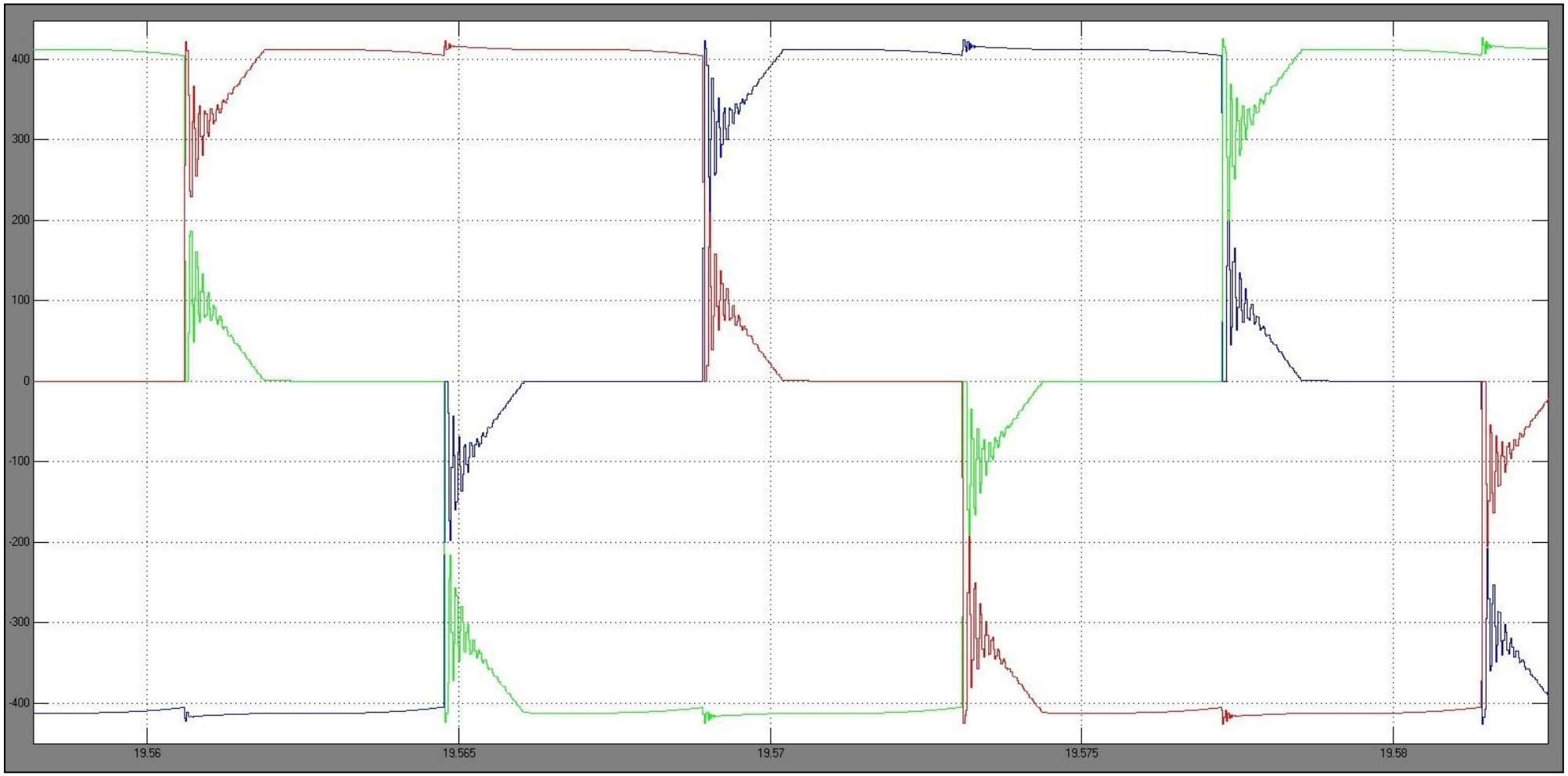

Figure 6. 42: Generator Voltage at 210KW

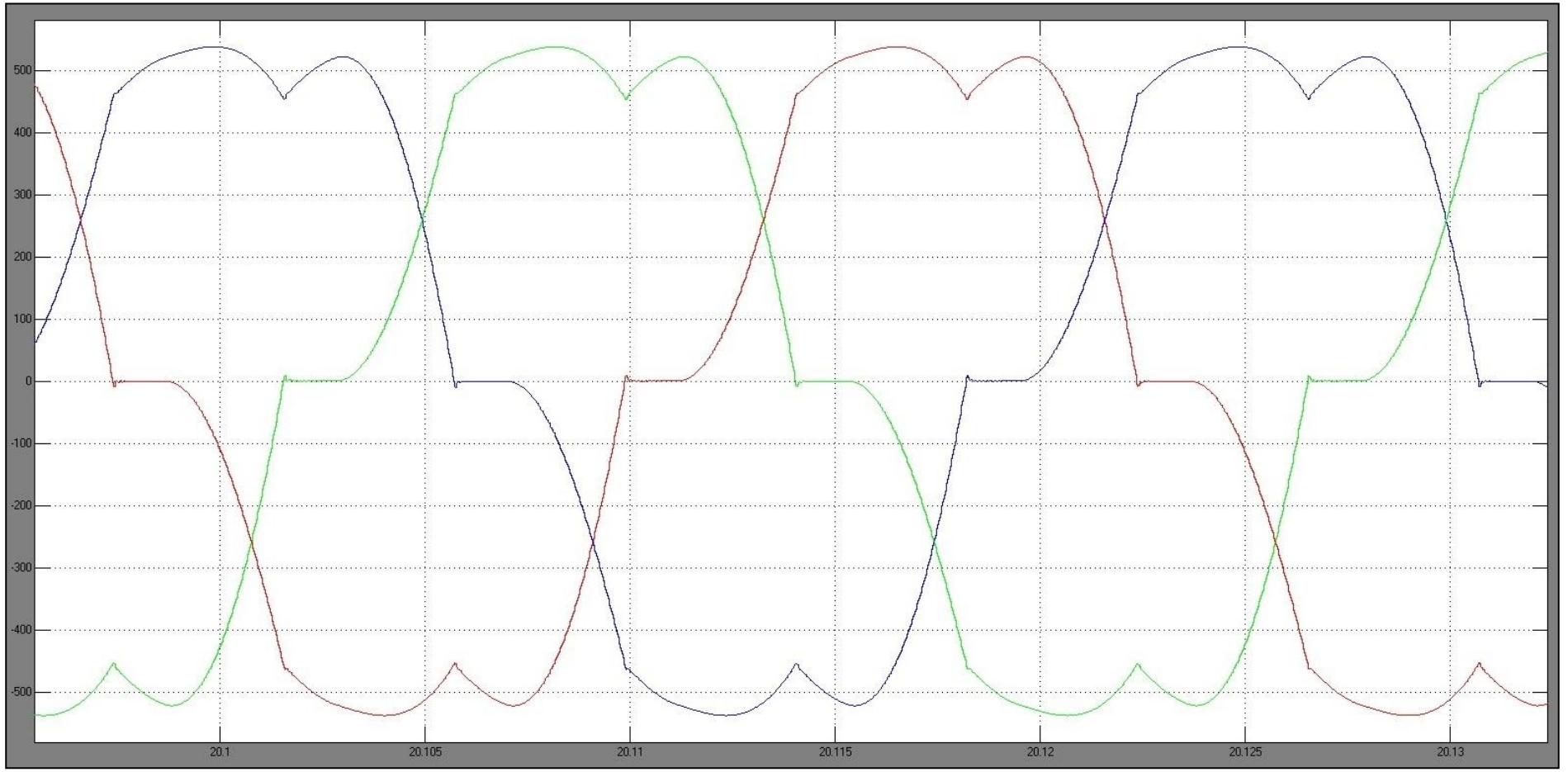

Figure 6. 43: Generator Current at 210KW

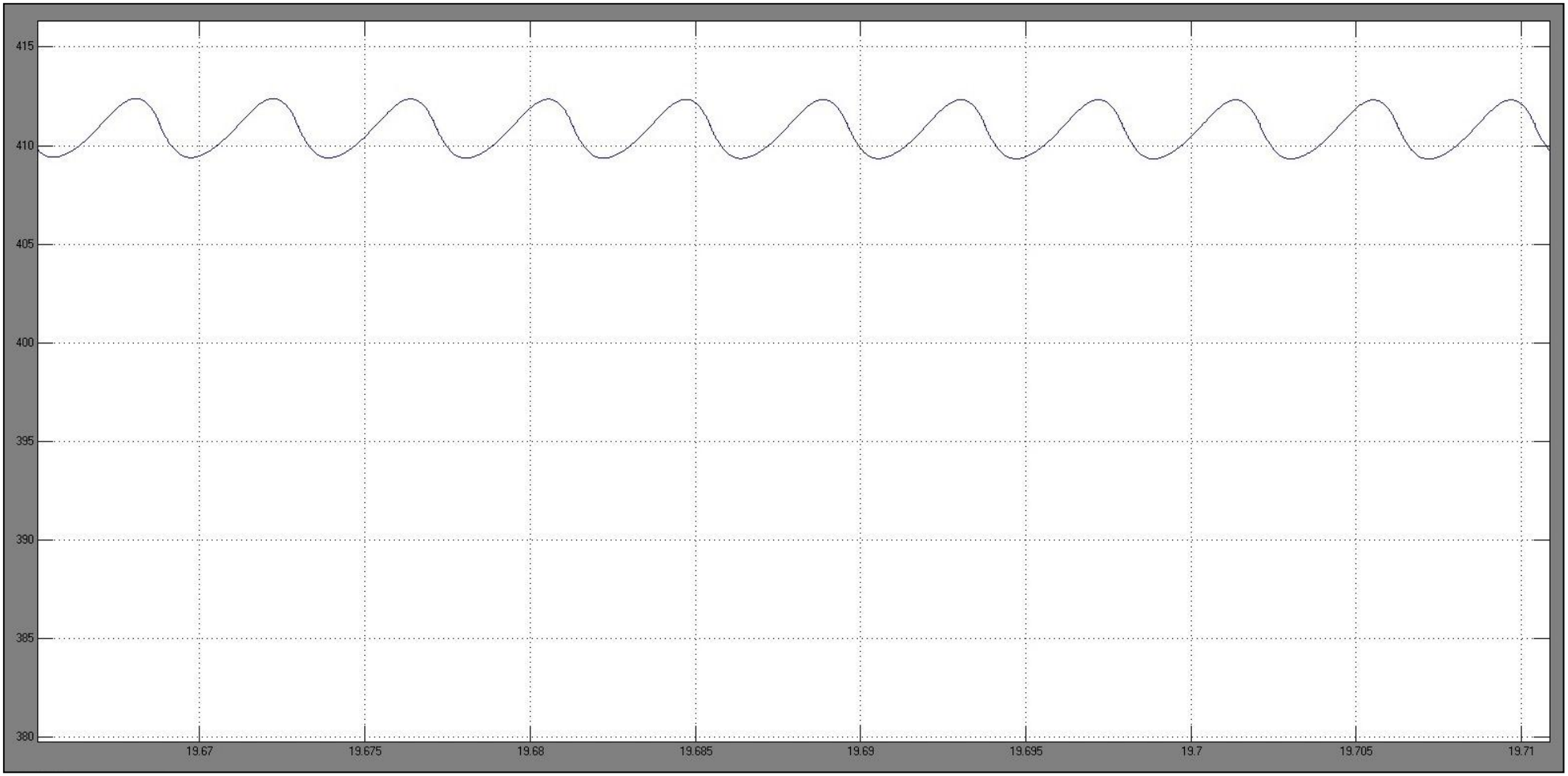

Figure 6. 44: DC Voltage at 210KW

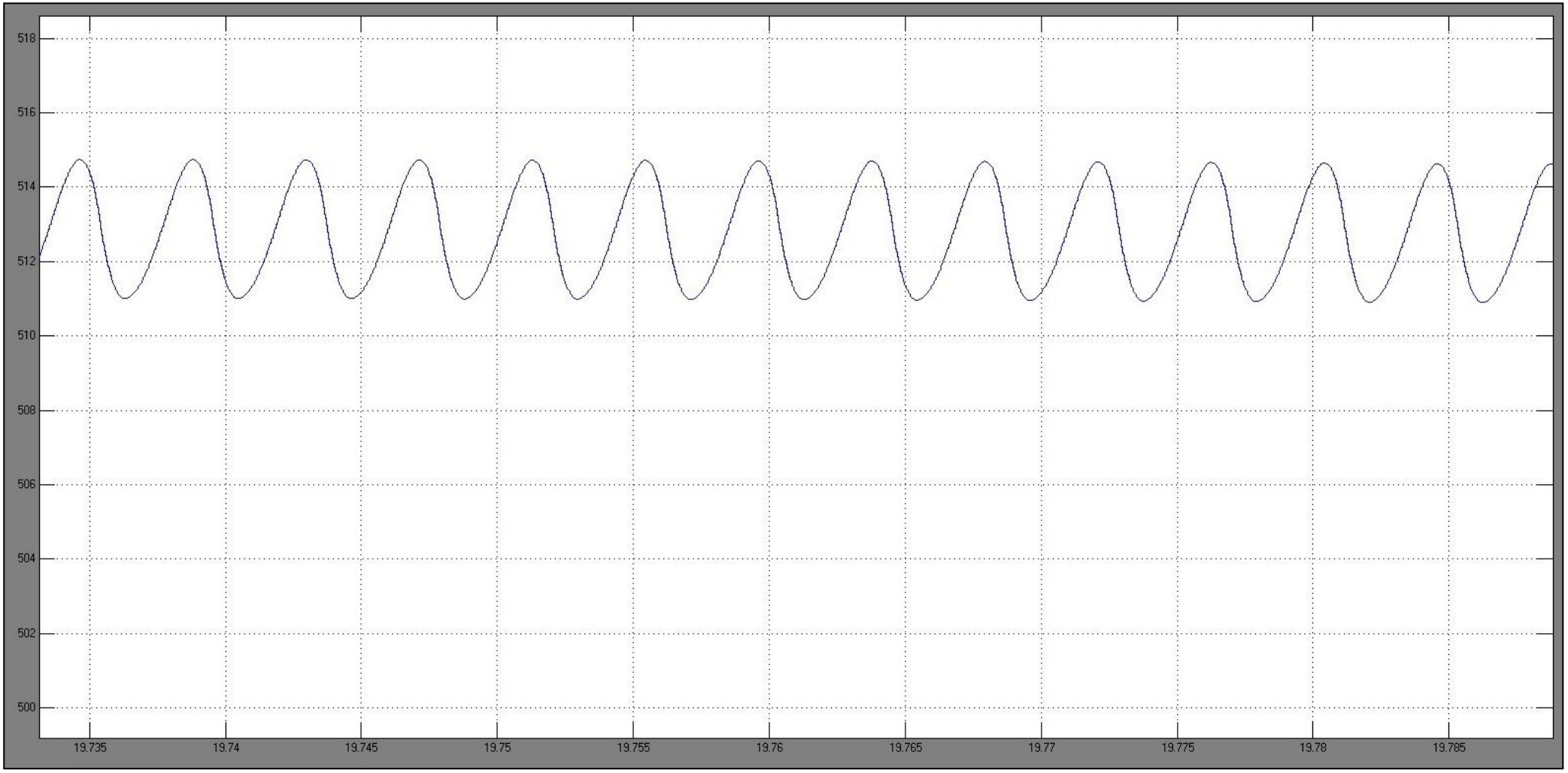

Figure 6. 45: DC Current at 210KW

6.18 Battery and Boost Circuit model

A Lead Acid battery (could not use Ultrabattery topology as it is not available in Simulink library) was used for simulating the battery model in Simulink. Boost circuit was used to boost the voltage to the required level from battery voltage. Rectifier output of Diesel generator was also connected to the boost circuit. Same boost circuit IGBT can be disabled when Battery has to be charged from solar power. Charge control IGBT should be activated for this operation.

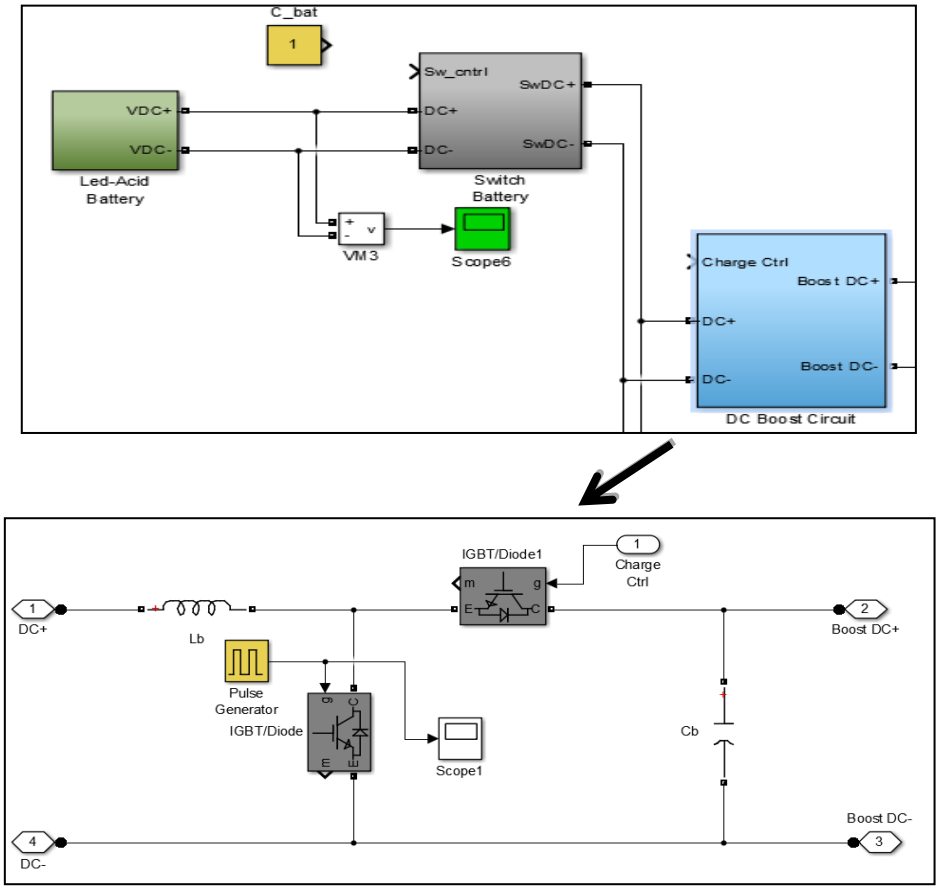

Figure 6. 46: Battery and Boost circuit blocks in Simulink

6.18.1 Bidirectional Inverter

DC boost converter converters (steps up) the DC input voltage of battery or generator DC voltage into the required DC voltage. This DC voltage is converted to AC which is filtered and provides power to grid. Conversion of DC to AC is done by Three-Phase inverter. Inverter should operate in bidirectional mode since if we have excess energy from solar power battery can be charged through inverter. In the case of battery charging inverter should operate in rectification mode so that battery can be charged. Since the three-phase inverter is operated in inverter mode and rectifier mode it is called bi-directional inverter. Figure 6.48 shows the inverter and LC filter block used in simulation.

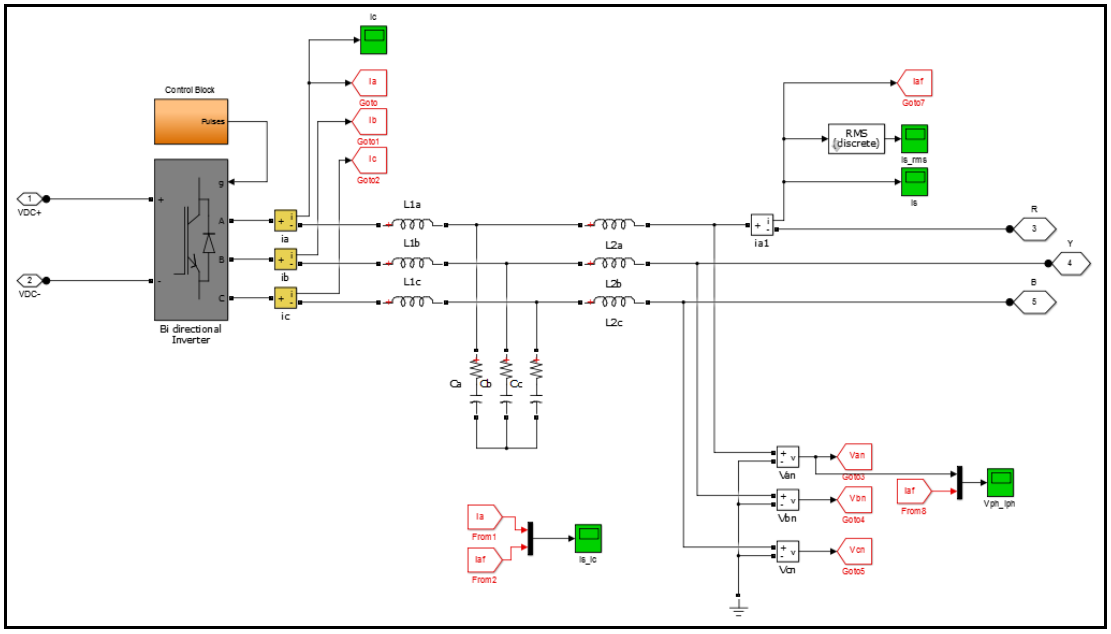

Figure 6. 47: Simulink model of Inverter and LC filter

Since inverter operation requires a rectifier mode it requires a complex control system to operate in both modes. Figure 6.49 is the control block used simulating the system in Simulink. This control block is used for operating Bi-directional inverter in rectifier mode. For inverter mode standard PWM block from Simulink library is used for simulating.

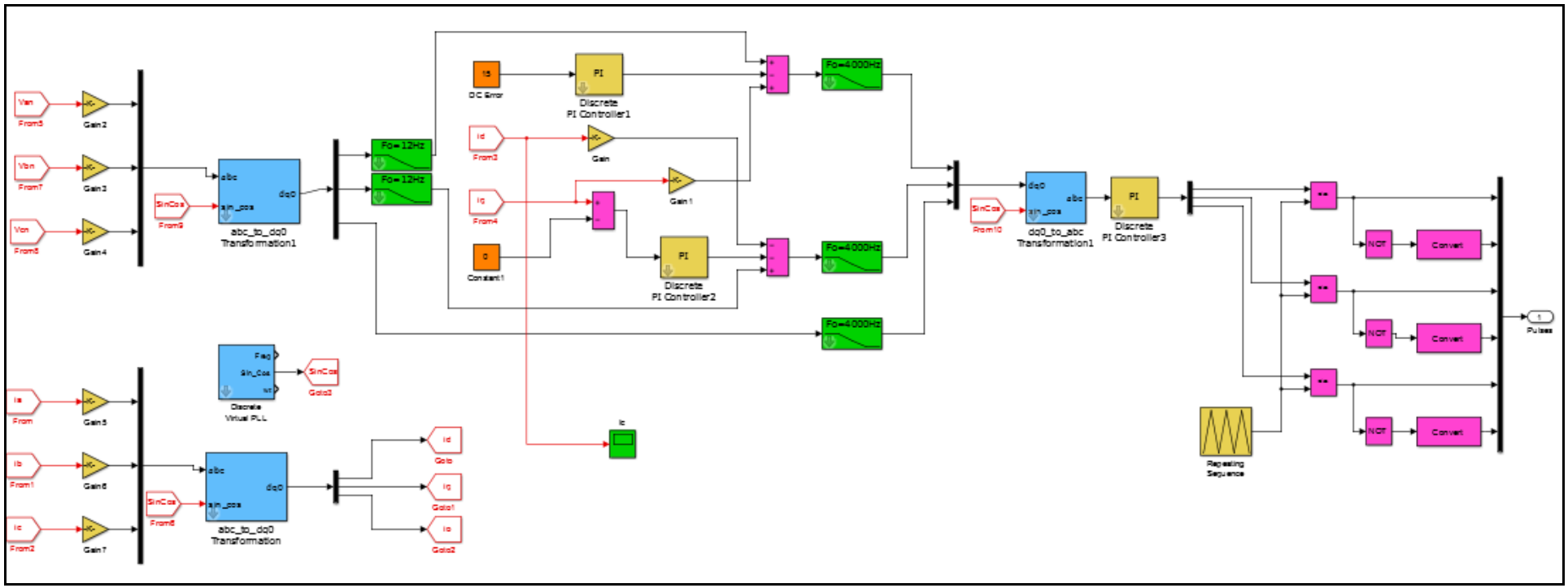

Figure 6. 48: Simulink model of PWM rectifier control block

6.19 Integrated System

The Simulink models developed were integrated and simulated in the Parallel hybrid power system configuration as show in Figure 6.50. Figure 6.51 shows the integrated system in Simulink model.

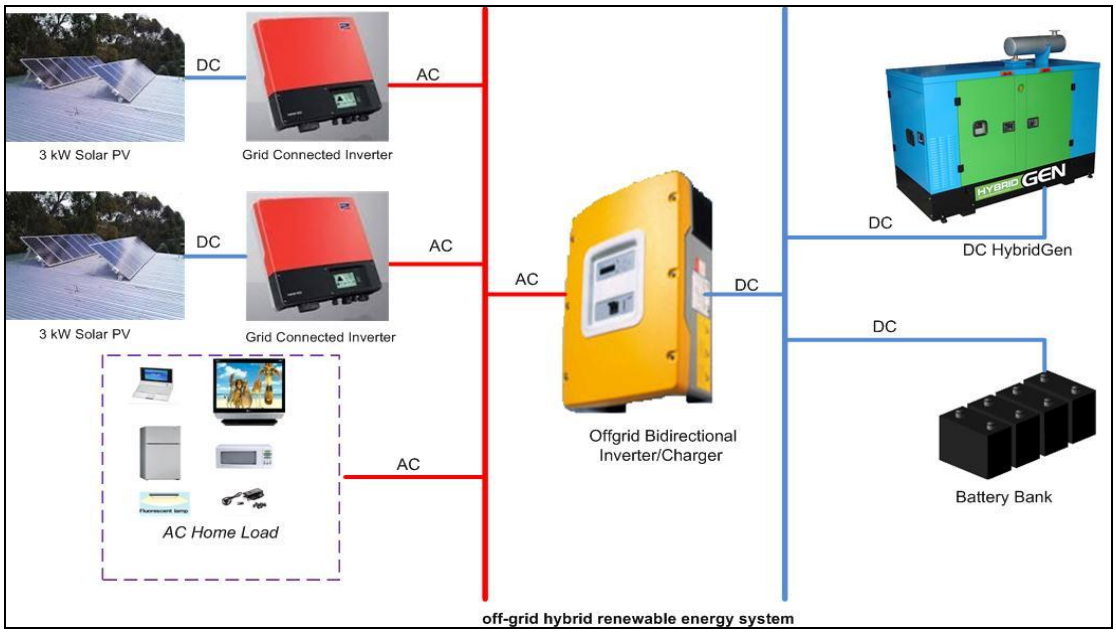

Figure 6. 49: Parallel hybrid power system configuration

Basic system operation:

- If we have an adequate solar energy, home loads are powered with solar power
- If solar energy is not sufficient then battery will power the additional loads
- If load power requirement is less than the available solar power then the battery bank will be charged through the bi-directional inverter
- Diesel generator will be used whenever peak demand is high
- Diesel generator will be used for charging the battery bank when necessary
- Bi-directional inverter will be disabled when the battery reaches SOC
- Diesel generator will charge the battery (when battery SOC is less than the specified value) and supply power to load when there is no solar or grid power

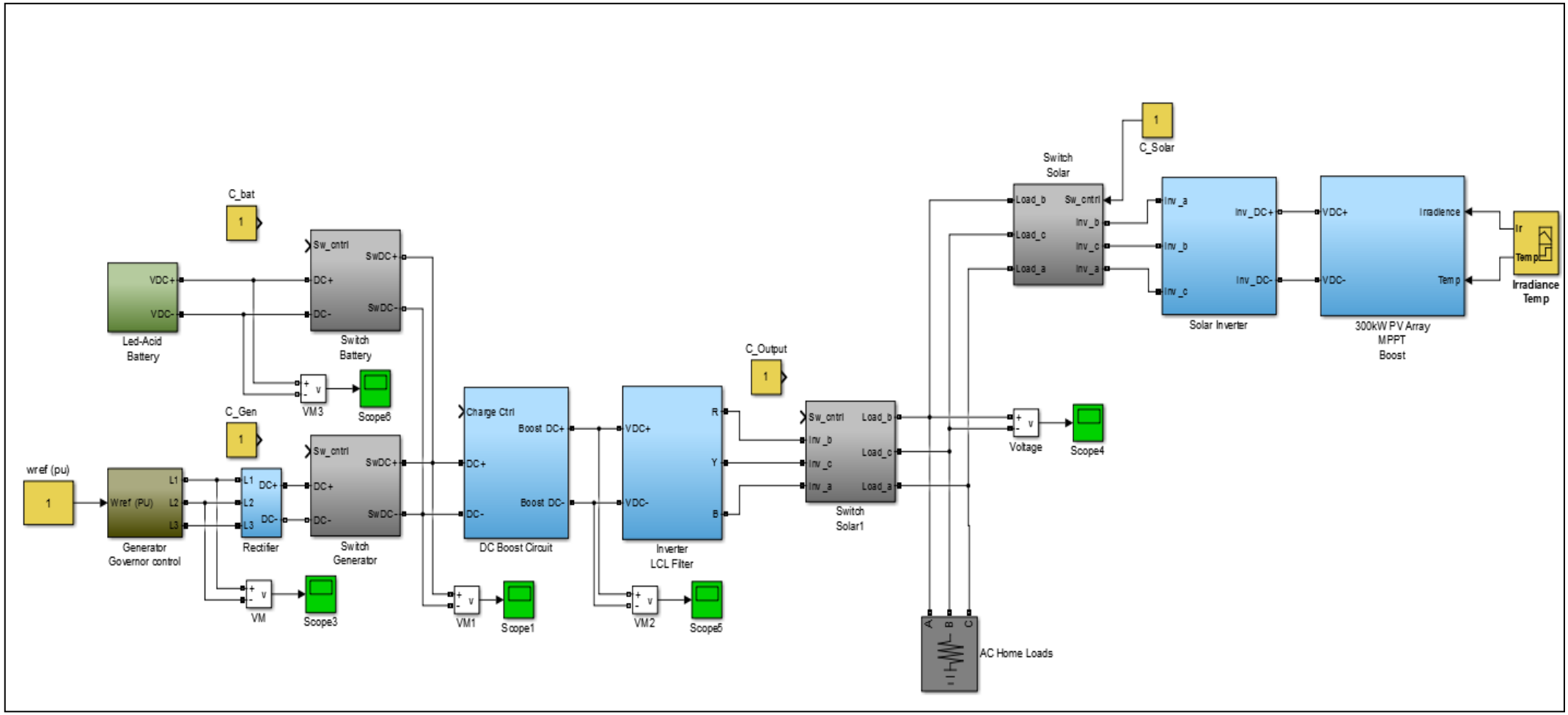

Figure 6. 50: Simulink model in parallel hybrid configuration

6.19.1 Simulation Results of Integrated System

Generator simulation was performed independent of the integrated system due to the dynamics of a diesel generator in Simulink model. An extended period of time would be required for simulation of a diesel generator because the machine takes approximately 4 seconds to stabilise, which is in contrast to the 1µsecond of discrete time required by a PV cell, solar inverter, battery, or bi-directional inverter. Section 7.10.8 can be referred for generator simulations.

These systems were integrated in the simulations:

- PV array
- Solar inverter
- Lead-acid battery
- DC boost circuit
- Bi-directional inverter

6.19.2 Control blocks

a) SOC battery control

Figure 6.52 shows the battery switch control. When the battery SOC reaches the target value, the switch connected to the boost converter and the bi-directional inverter will be disabled, which will disconnect the battery connection to load. In this case the diesel generator will be charging the battery.

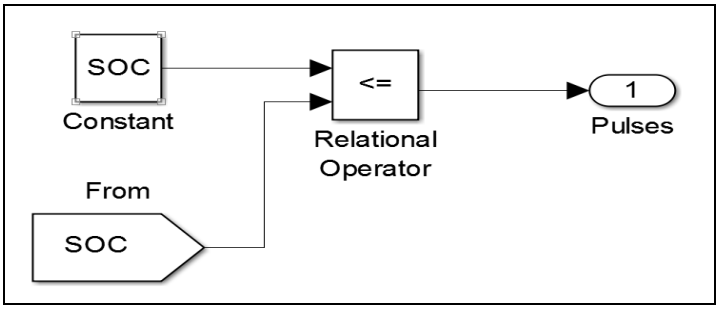

Figure 6. 51: Battery SOC controller

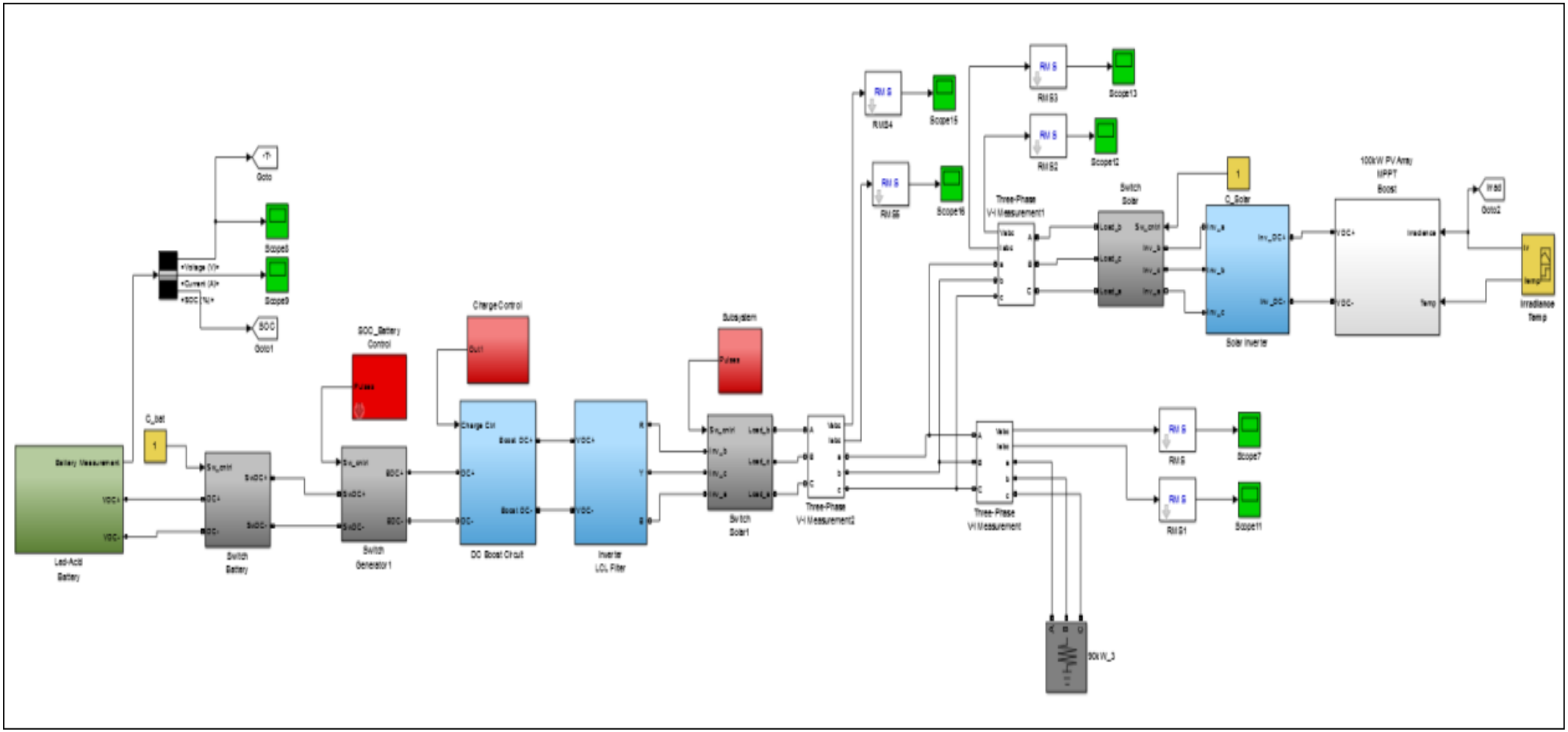

Figure 6. 52: Integrated System in Simulink

b) **Battery charge control**

Figure 6.53 shows the charge control when the battery SOC is less than the specified level. The charge control will be activated and enable the IGBT connected across the boost converter diode. Pulses to boost IGBT are disabled in this situation. In this mode the DC-DC converter will be operating in Buck mode.

When there is excess solar power the battery is charged through the charge control. The charge control output is in turn connected to the current controller. Figure 6.54 shows the current controller of a buck converter. The battery will be charged at a constant 30Amps.

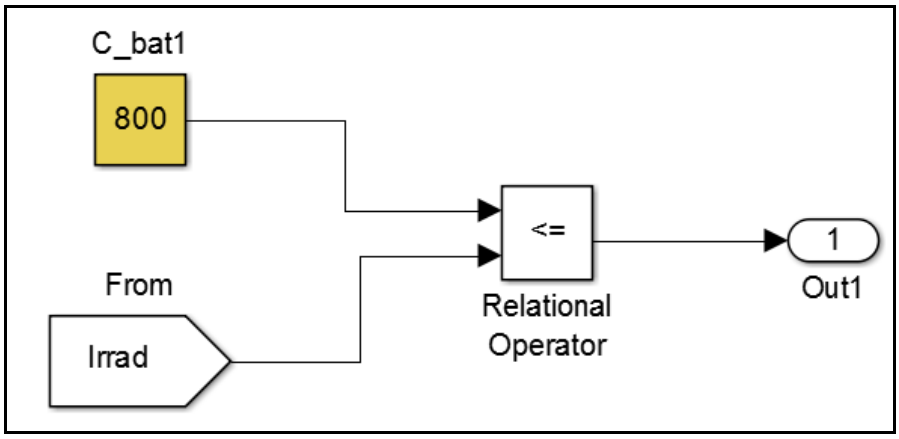

Figure 6. 53: Charge control block.

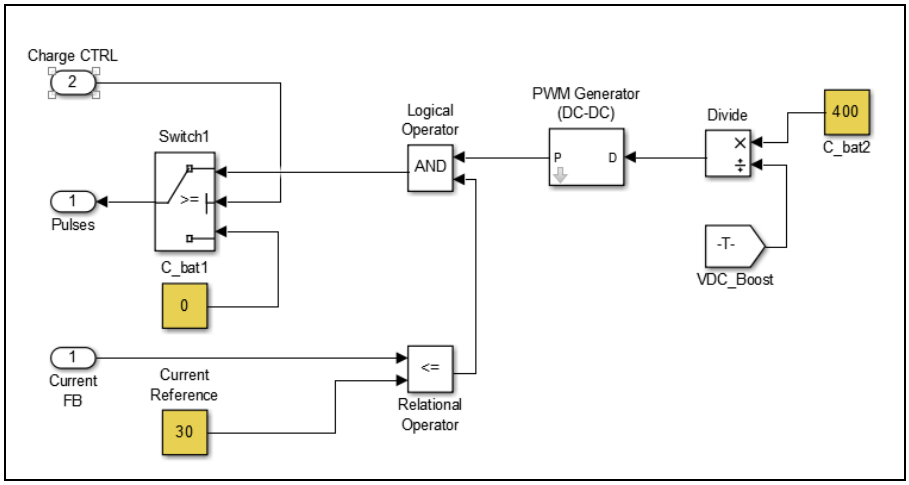

Figure 6. 54: Buck current controller

c) **Simulation waveforms to verify current controller**:

Figure 6.55 shows the Simulink model to verify the current controller. A DC voltage of 350V connected at the buck chopper output was used in the simulation. Since the output voltage is less than the specified limit (400VDC), the buck chopper should produce a constant output current (in this case 30Amps).

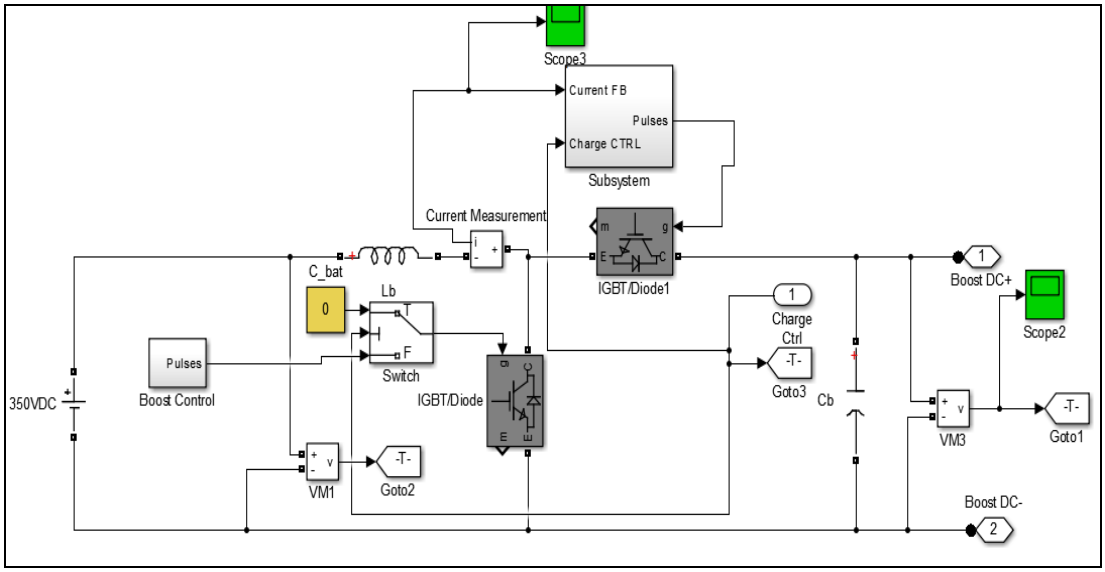

Figure 6. 55: Simulink model for verifying current controller

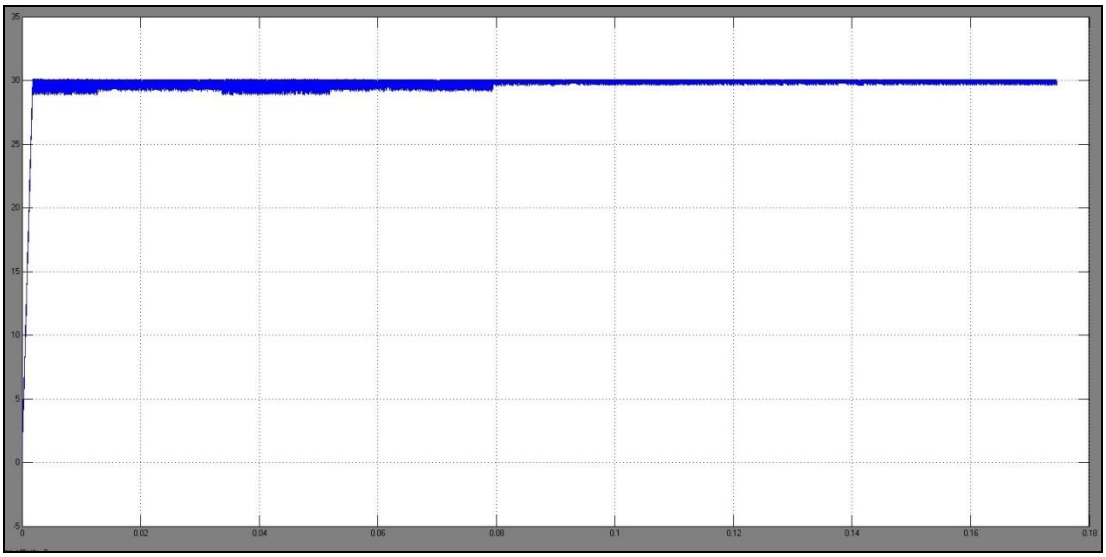

Figure 6. 56: Buck converter output current

d) Bi-directional inverter control:

Figure 6.58 shows the bi-directional inverter control. 2Level PWM generator pulses will be activated when the bi-directional inverter is delivering power to a load. When the battery charge control is activated the rectifier control will also be activated and deliver power to the battery for charging. Refer to Figure 6.49 for the PWM rectifier control block.

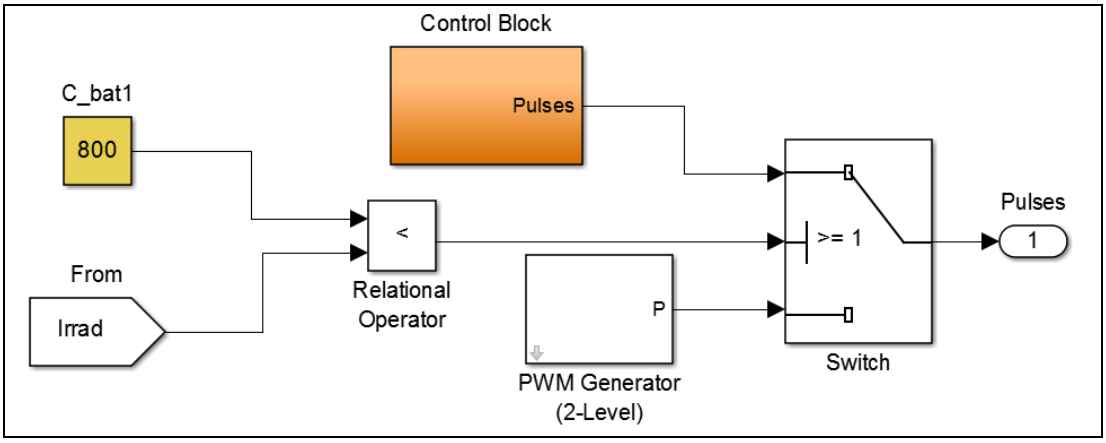

Figure 6. 57: Bi-directional inverter control.

6.19.3 Simulation results (Integrated system):

Table 6.5 shows the simulation results of different operating conditions.

Condition 1: Irradiance: 1000 W/m^2.

Full load power and battery charging current is provided by solar energy. Battery is charged through the bi-directional inverter with the charge control IGBT in ON state.

In the simulated results battery is charged fully, therefore current drawn by battery is zero. Figure 6.56 and Figure 6.57 shows that the current control of battery is working and the battery will be charged with constant current source of 30Amps when SOC is less than the specified limit (in simulation battery charges when SOC is < 80%)

Condition 2: Irradiance: 200 W/m^2.

Major part of the power to load is provided by battery with partial load from solar power.

Condition 3: Irradiance: 500 W/m2

Major part of the power to load is provided by battery with partial load from solar power.

The waveforms of voltage at current at irradiance levels of 200, 500 and 1000 are presented in Figures 6.51- 6.61.

Table 6. 5: Integration system simulation results

Irradiance	**Load**	**Solar Inverter**			**Battery**			**Bi-directional Inverter (Battery Power)**			**Load**		**Comments**
		Voltage	**Current**	**Power**	**Voltage**	**Current**	**Power**	**Voltage**	**Current**	**Power**	**Voltage**	**Current**	
	KW	V_{inv}	I_{inv}	KW	V_{bat}	I_{bat}	KW	V_{inv}	I_{inv}	KW	V_{load}	I_{load}	
1000	178	360	286	178	435	0		360	0	0	360	286	Battery is fully charged, therefore battery is not charging in this case
200	146	325	90	50.6	393	307		325	168	94.6	325	260	
500	162	344	130	77.4	399	260		344	141	84	344	272	
200	146	325	90	50.6	393	307		325	168	94.6	325	260	
1000	178	360	286	178	435	0		360	0	0	360	286	Battery is fully charged, therefore battery is not charging in this case

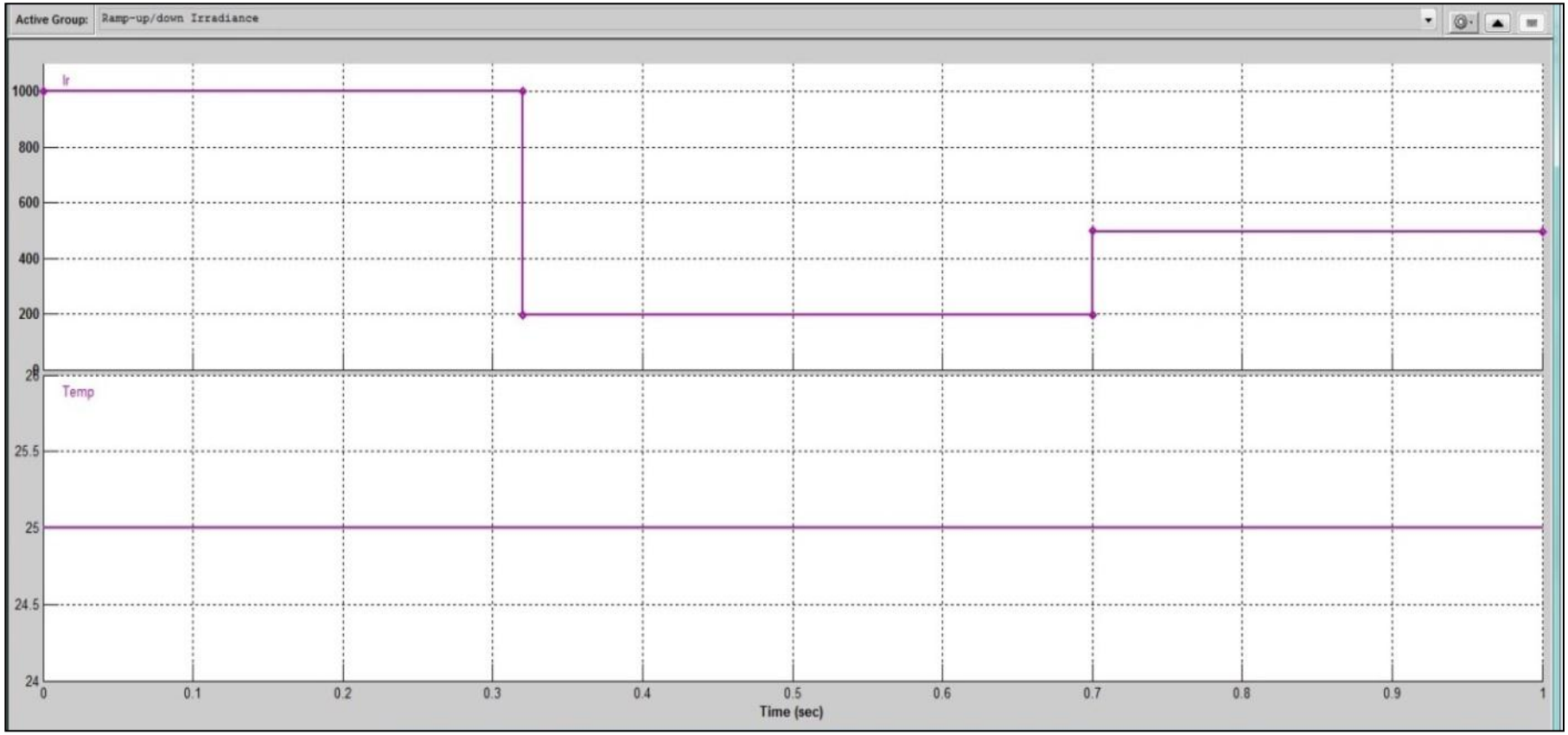

Figure 6. 58: Irradiance and Ambient temperature.

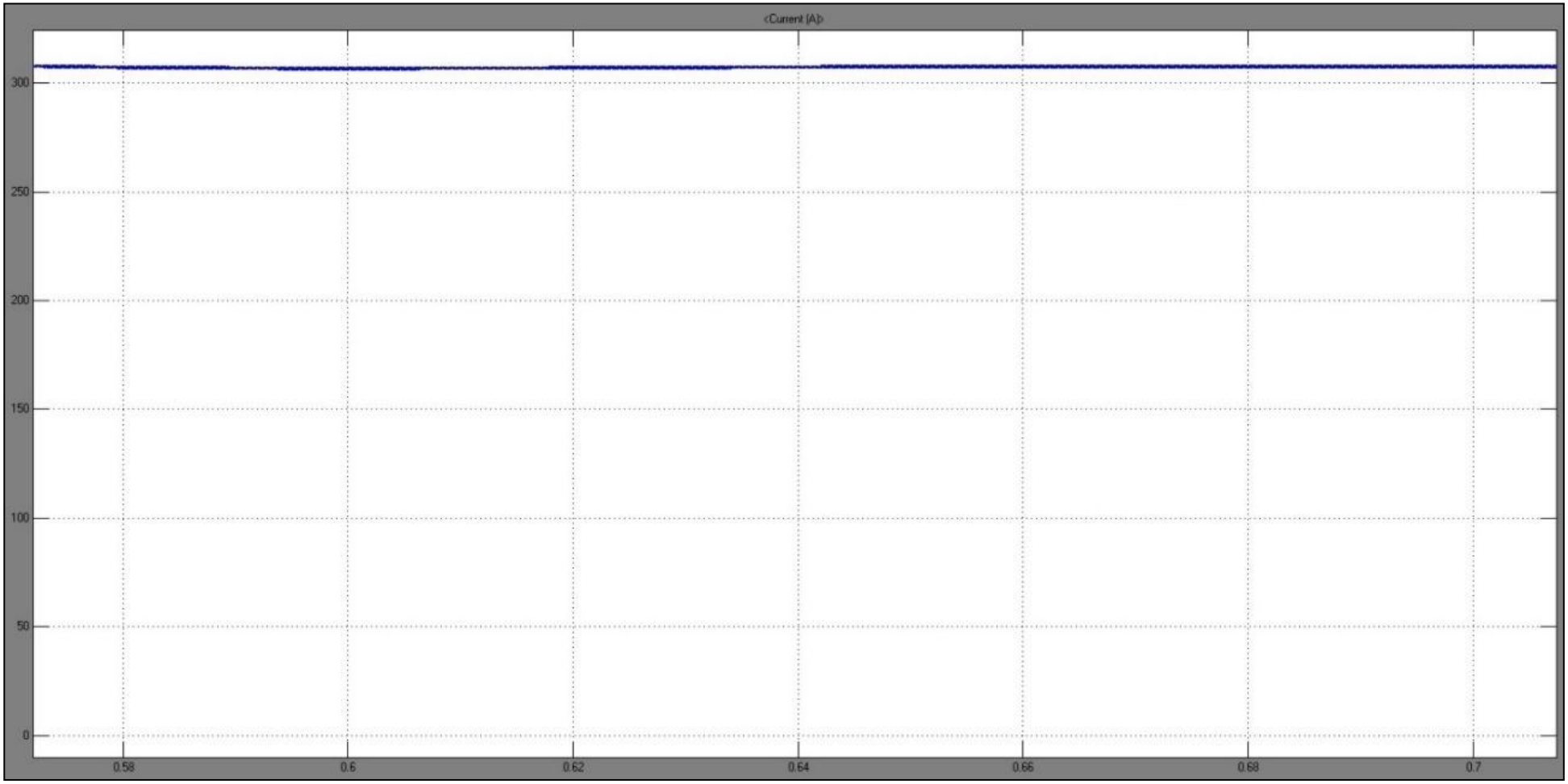

Figure 6. 59: Battery Current at 200 Irradiance.

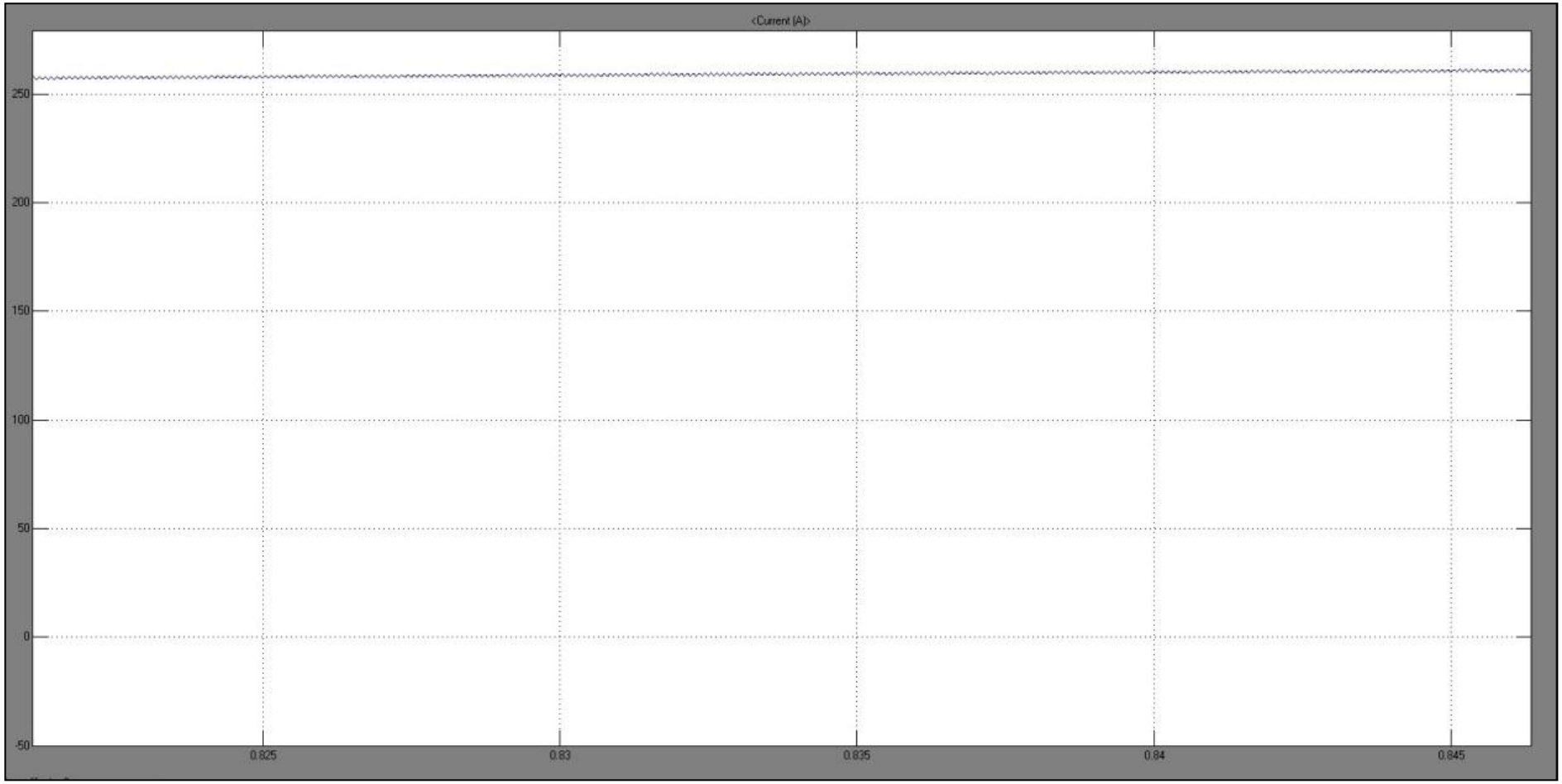

Figure 6. 60: Battery Current at 500 Irradiance**.**

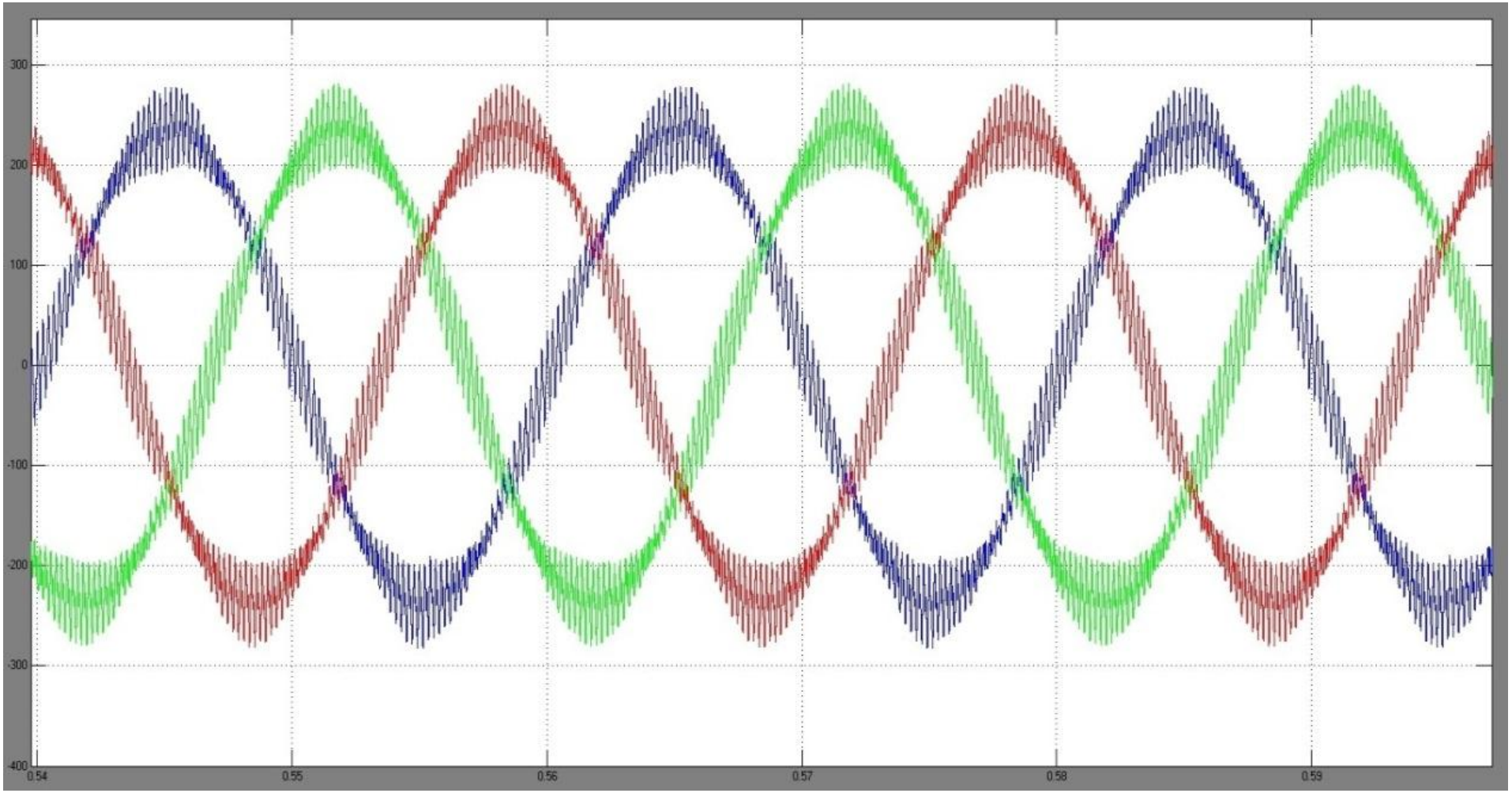

Figure 6. 61: Bi-directional current at 200 Irradiance.

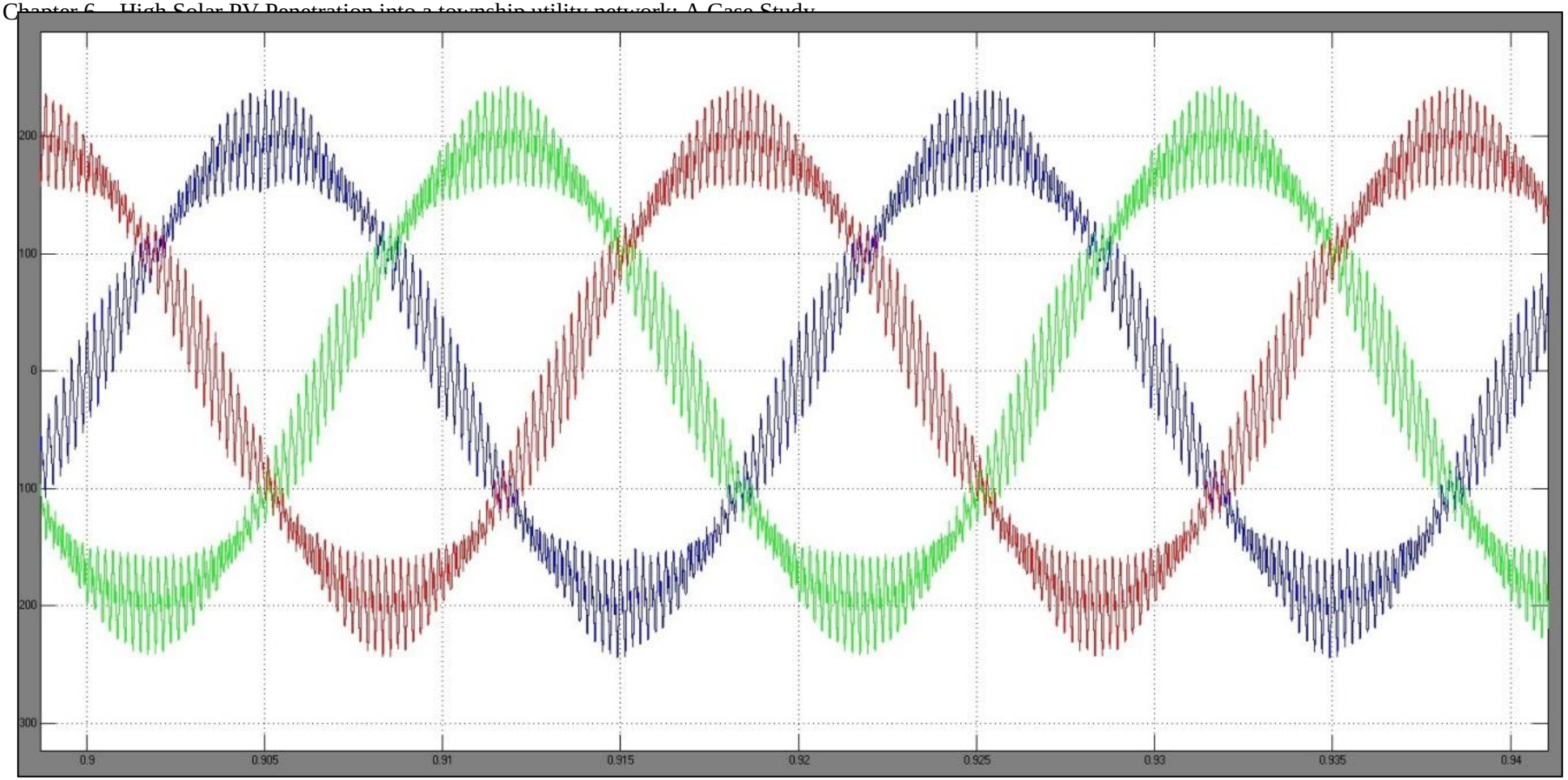

Figure 6. 62: Bi-directional Inverter current at 500 Irradiance.

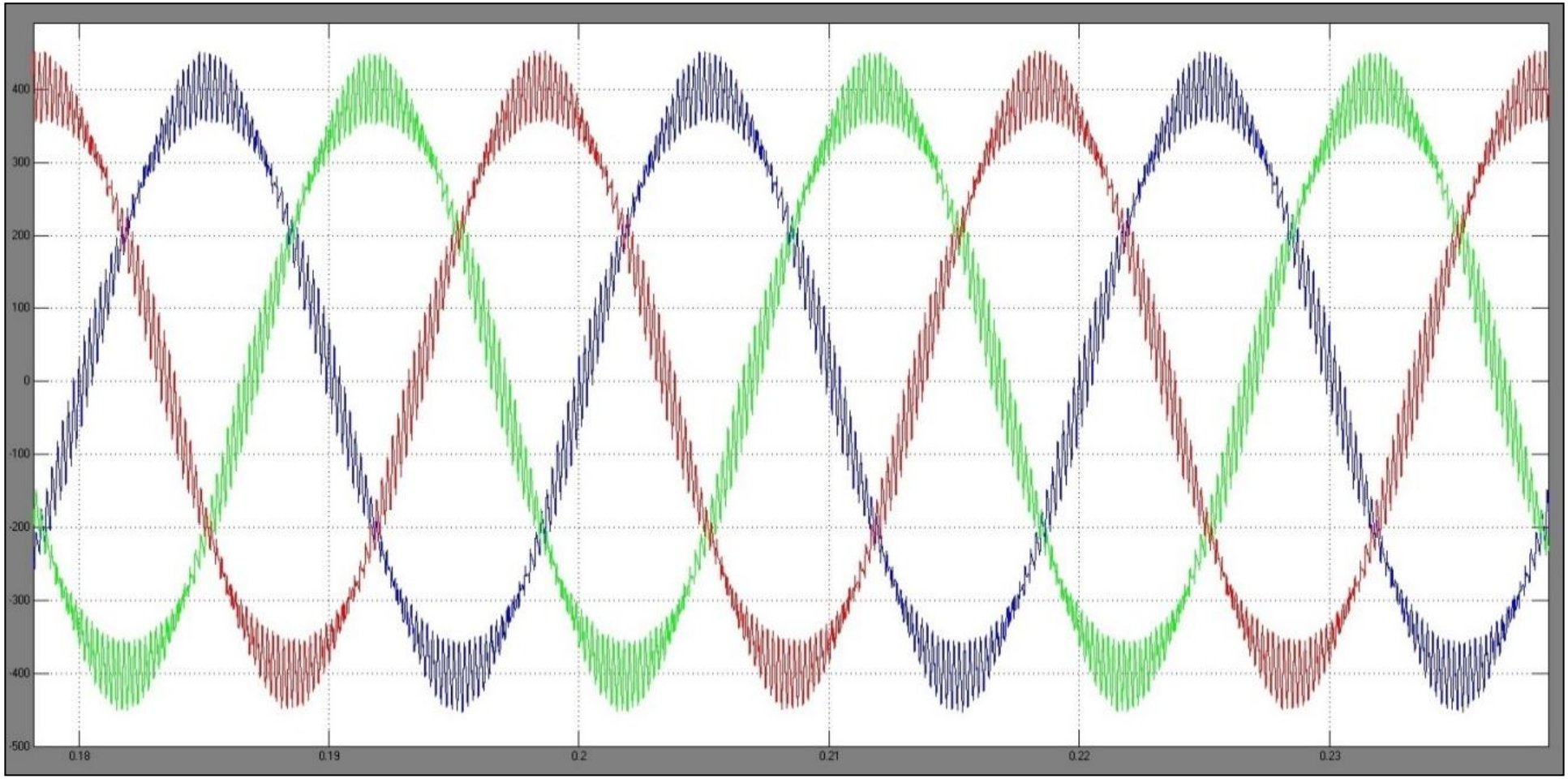

Figure 6. 63: Solar Inverter current at 1000 Irradiance**.**

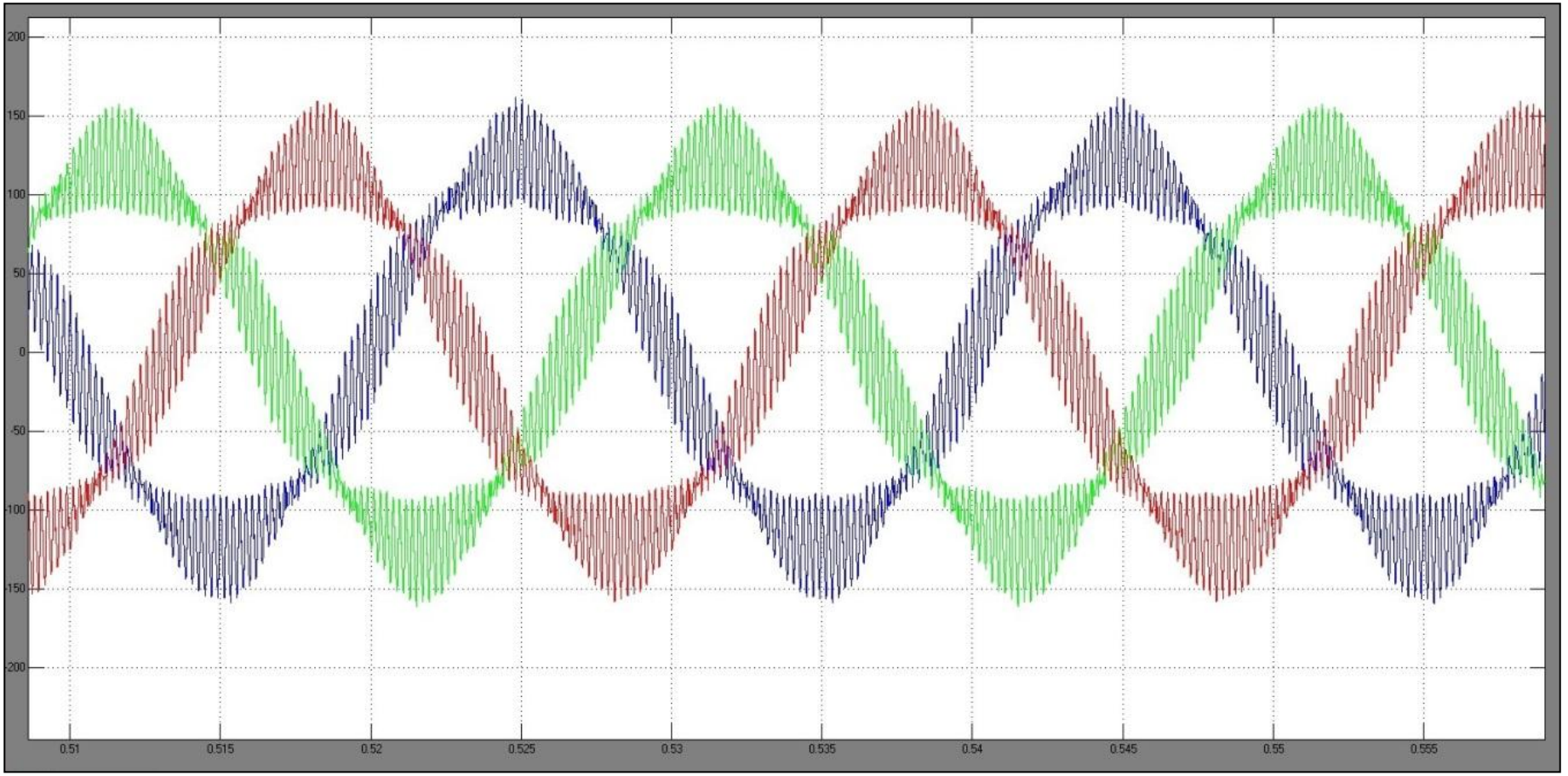

Figure 6. 64: Solar Inverter current at 200 Irradiance

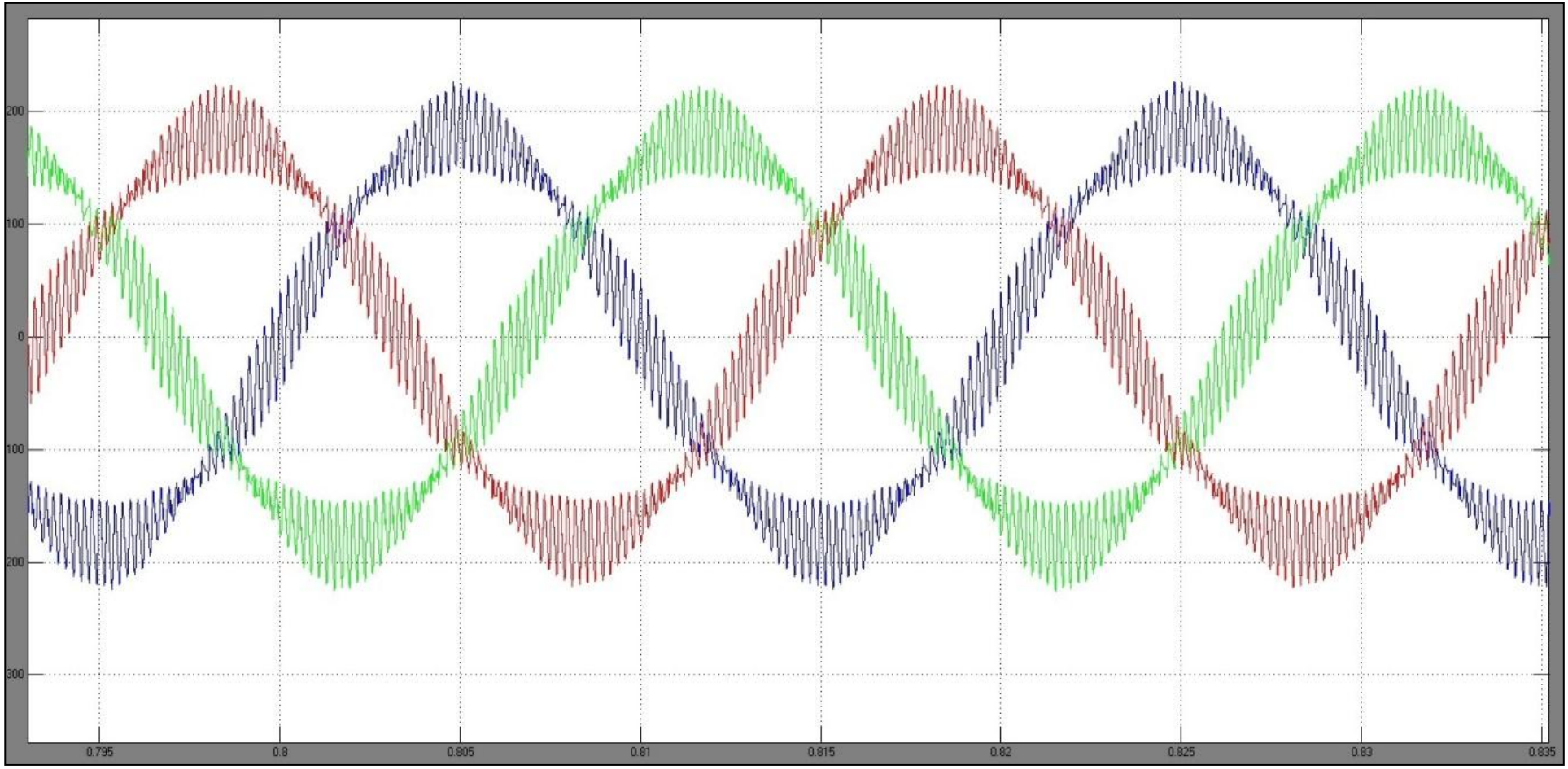

Figure 6. 65: Solar Inverter current at 500 Irradiance

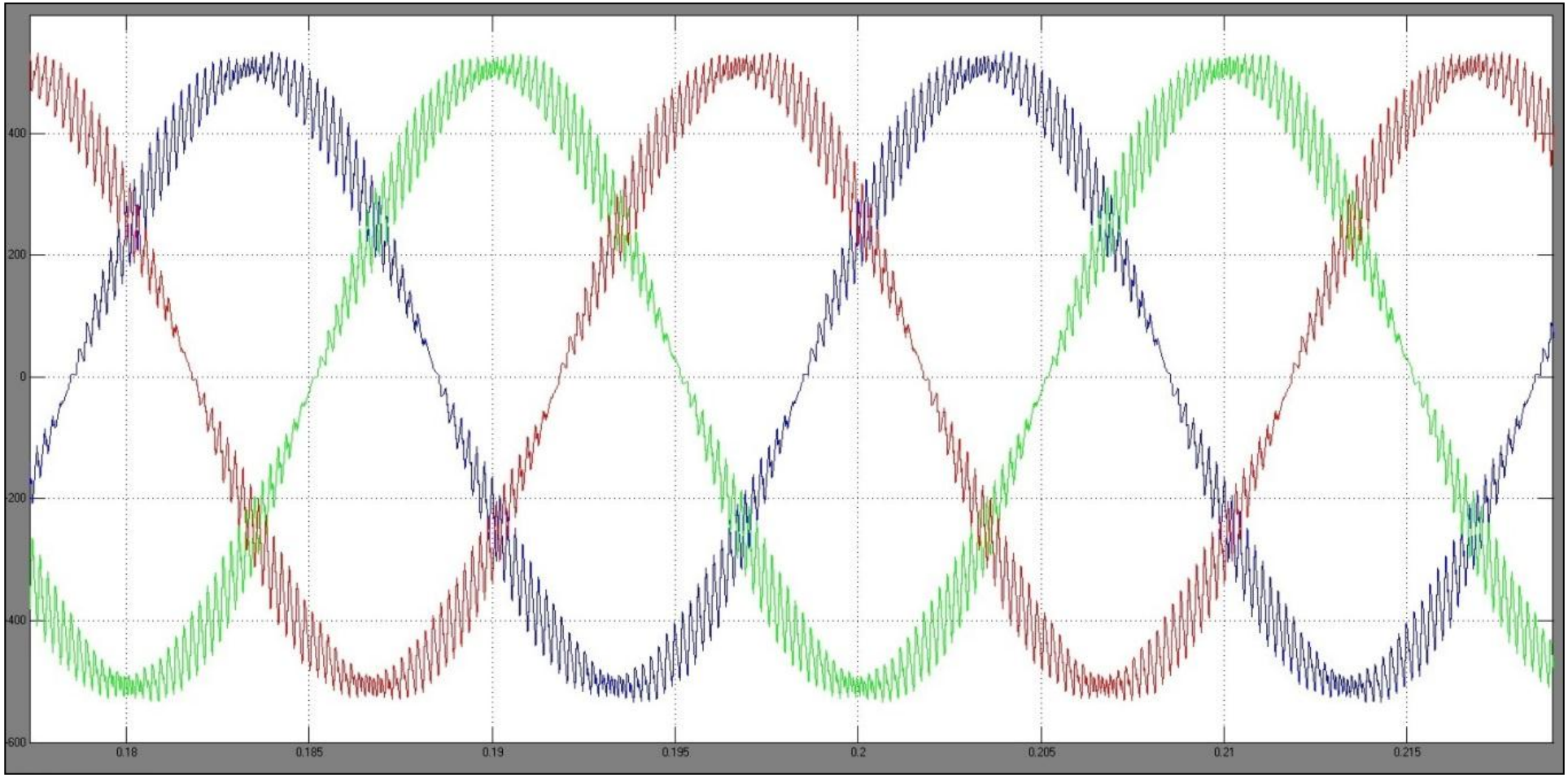

Figure 6. 66: load voltage at 1000 Irradiance

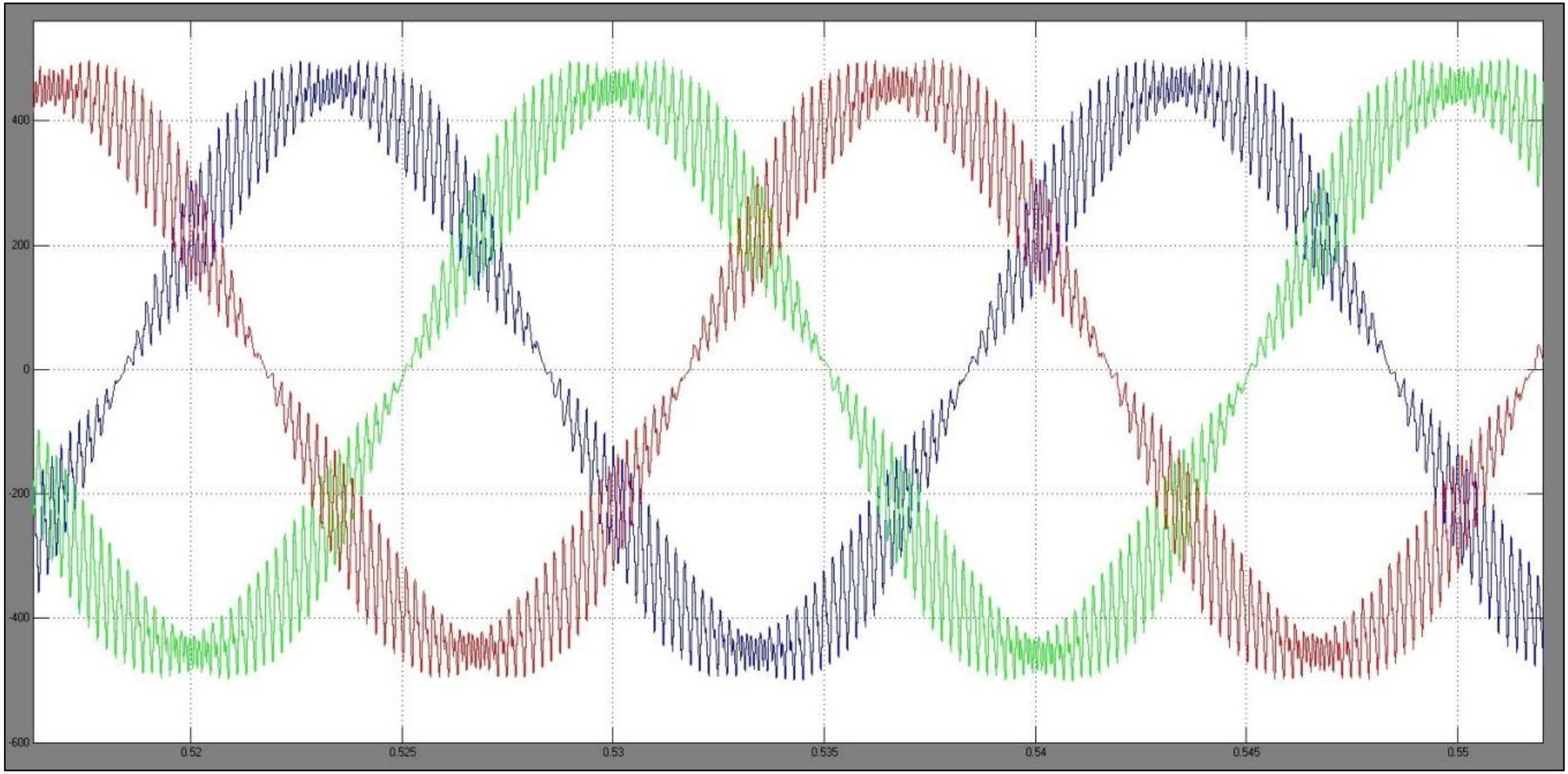

Figure 6. 67: load voltage at 200 Irradiance

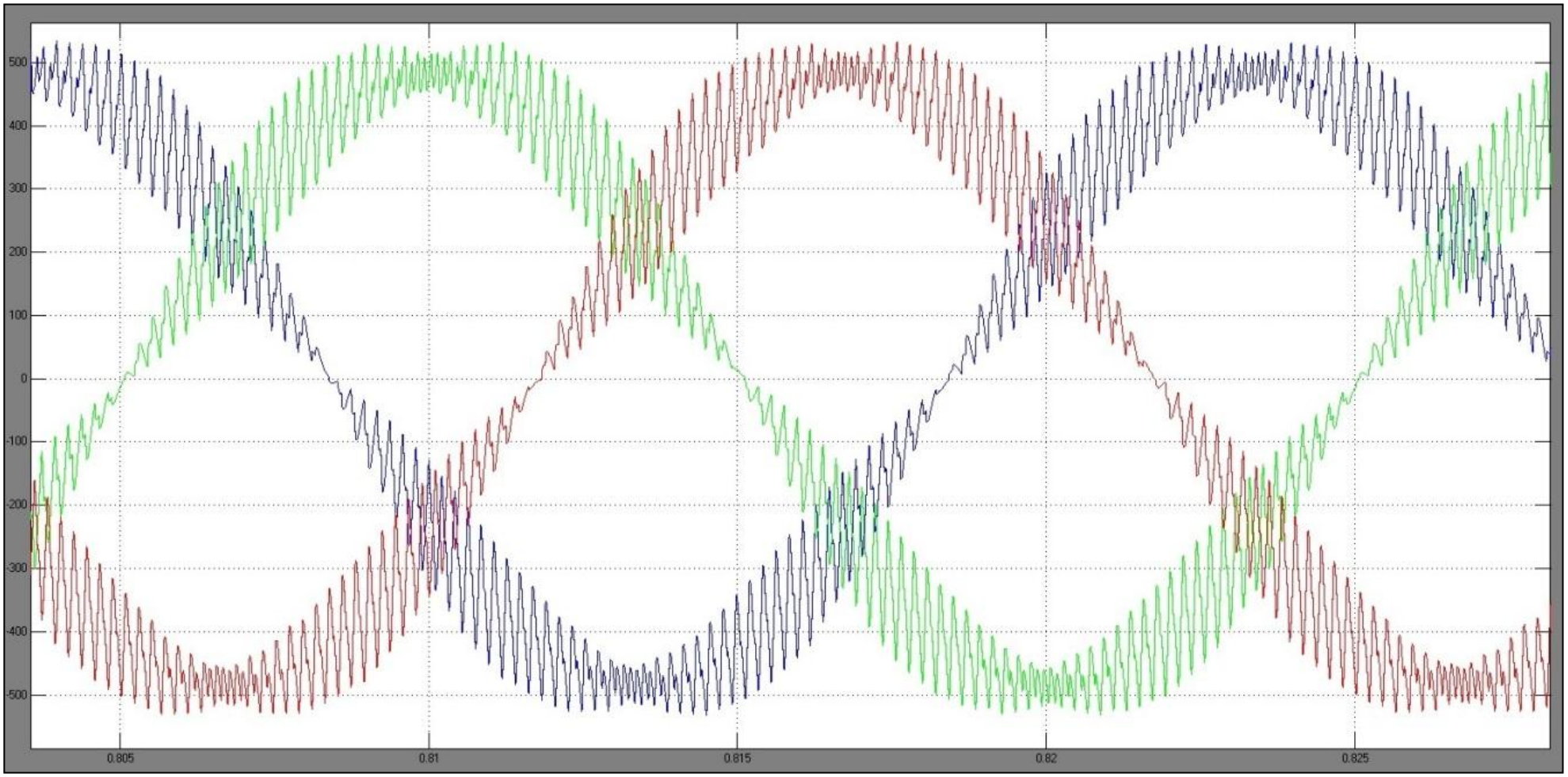

Figure 6. 68: Load Voltage at 500 Irradiance

6.20. Conclusions

This chapter presents design and modelling methodology to define hosting capacity of Horizon Power's isolated networks to accommodate hundred percentage integration of distributed PV installations. These include stability and reliability, network capacity, power quality and minimum loading of generating unit criteria. There is no doubt that rooftop solar and battery storage present the biggest threat to the grid operator's business in more than a century of poles and wires – and managing this will not only be the key to the business models of these operators, but also to the costs of the customers they serve. A mathematical model that gives a visual representation of the interaction between the various system parameters has been developed and implemented. The model can be used as an analysis tool to define the hosting capacity and to assess system impacts due to integration of PV generation, as demonstrated in the case studies and performance monitoring of the selected network (Carnarvon, Western Australia) that are presented.

6.21. References

[1] S. Lewis, CEEM, and U. o. NSW, "APVA/CEEM(2012) Carnarvon: A Case Study of Increasing Level of PV Penetration inan Isloated Electricity Supply System, a report by the UNSW Centre for Energy and Environmental Markets for the Australian PV Association," p. 49, 2012.

[2] A. G. B. o. Meteorology, "Carnarvon, Western Australia Daily Weather Observations," 2014.

[3] R. Passey, L. Chin, and M. Watt, "Impacts of photovoltaic systems and feed-in tariffs on Australian residential electricity consumers," The Australian PV AssociationMay 2011.

[4] *Western Australian Distribution Connections Manual 2013*, E. N. C. t. a. W. P. a. R. P. C. t. a. H. Power., 2013.

[5] J. Wood, "UltraBattery, Cloud Energy Storage for the Grid: Positioning Data Center and Telecommunication Backup Resources as Smart Grid Assets That Support," in *Telecommunications Energy Conference 'Smart Power and Efficiency' (INTELEC), Proceedings of 2013 35th International*, 2013, pp. 1-5.

[6] A. Swinger. (December 2010, 08/12/2013). Photovoltaic String Inverters and Shade-Tolerant Maximum Power Point Tracking: Toward Optimal Harvest Efficiency and Maximum ROI.

[7] L. Joon-Hwan, L. Seung-Hwan, and S. Seung-Ki, "Variable Speed Engine Generator with Super-Capacitor; Isolated Power Generation System and Fuel Efficiency," in *Industry Applications Society Annual Meeting, 2008. IAS '08. IEEE*, 2008, pp. 1-5.

[8] P. A. Stott and M. A. Mueller, "Modelling Fully Variable Speed Hybrid Wind Diesel Systems," in *Universities Power Engineering Conference, 2006. UPEC '06. Proceedings of the 41st International*, 2006, pp. 212-216.

[9] Regen Power Pty. Ltd. (Jan.). *Hybrid renewable energy penetration micro-grid power system using a variable speed constant frequency generator*. Available: http://www.dailylife.com.sg/HybridGen%20Writeup%20ver3.pdf

[10] *MATLAB 7 Getting Started Guide*. Natick, MA: The Math Works, Inc., 2008.

[11] *MATLAB 7 Programming Fundamentals*. Natick MA: The Math Works, Inc., 2008.

[12] *MATLAB 7 Programming Tips*. Natick MA: The Math Works, Inc., 2008.

[13] D. Gupta, S. C. Solanki, and J. S. Saini, "Heat and fluid flow in rectangular solar air heater ducts having transverse rib roughness on absorber plates," *Solar Energy*, vol. 51, pp. 31-37, 7// 1993.

[14] *Simulink 7 User's Guide*. Natick, MA: The Mathworks, Inc., 2008.

[15] P. Y. Lim, C. V. Nayar, and S. Rajakaruna, "Simulation and components sizing of a stand-alone hybrid power system with variable speed generator," in *9th International Conference on Environment and Electrical Engineering (EEEIC)*, 2010, pp. 465-468.

[16] J. A. Gow and C. D. Manning, "Development of a photovoltaic array model for use in power-electronics simulation studies," *Electric Power Applications, IEE Proceedings -*, vol. 146, pp. 193-200, 1999.

[17] G. M. Masters, "Renewable and efficient electric power systems," 2004.

Chapter 7

7. Conclusions and Further Recommendations

7.1 Summary of Work

The authors' work is summarised below and the terms invention, creation, development and application are used to describe the originality of each section of work. The term invention describes a new concept that has come out of the research conducted for this thesis and is directly correlated to the author's work. The term creation defines a new piece of work that has stemmed from the research and has been used to prove a concept. The term development is used where the author has transcribed or converted a previous concept into a new model or simulation. The term application has been used where the author has applied a known method to a new situation.

The original contributions of the author include the invention of integration of variable speed diesel DC generator with solar energy and advanced battery bank with invention of new power electronics technology and development of Matlab simulation codes and Simulink models, development of prediction algorithms and codes, and implementation of the proposed prediction model within the predictive power management strategy, as well as the simulation and analyses of systems performance.

The thesis has been divided into chapters to further analyse, discuss and study both the ongoing projects as well to give proposals that enhance energy usage for the network authorities at sites where maximum output can be handled safely.

Chapter two reviews and investigates the current status of all sources of energy and describes the recent developments in the renewable energy sector. The developments in major countries and understanding of how government policies have influenced the development of renewable energy over the recent years are also discussed.

Chapter three identifies the new invention, the Ultra battery, new shade tolerant MPPT control and the topologies of inverters, DC- DC conversion and MPPT. The Ultra battery achieves a typical DC-DC efficiency of 93–95% in contrast to the typical 70% efficiency of VRLA batteries. Due to the reduced energy loss during PSoC operation, more energy is available to supply the load especially when performing variability management

applications, such as grid regulation services or renewable ramp rate smoothing at 1C peak power in a Partial State of Charge (PSoC) regime.

Chapter four covers the theoretical analysis, modelling and simulation of the variable speed diesel generator using various new generation technologies. Matlab/Simulink software was used to simulate and the results validated using VSDG to realize variable speed operation for diesel engine. The use of different vector control algorithms for different operation modes showed that such a system could provide acceptable power quality. The experimental results also showed that the variable speed system produced high quality DC voltages independent of diesel engine speed. Chapter four also highlights the advantages of off-grid hybrid power systems with VSDG and minimal battery storage, through a comprehensive comparison of economic aspects. In addition, drawbacks of the system with integrated energy storage were also explained. The system operation and performance characteristics of practical cases have been discussed. Starting from Chapter four the thesis takes on the major contributions by the author including a discussion of the current developments in remote hybrid power systems, and the investigation and development of a novel DC variable speed generator which is suitable for renewable energy integration on a small scale.

Chapter five presents the small scale hybrid system with a reduced battery bank. One of the projects investigated was a place, where it was hard to fix the load profile which meant a volatile load profile design. This was then integrated into a system with a renewable energy generator and a small battery bank with backup DC. The variable diesel generator would help provide uninterrupted power with less capital investment and reduced running cost. A control logic was developed, and a system implemented that now operates to the satisfaction of both the clients and occupants. Mathematical simulations were presented for each of the systems. Modelling of the system components was done using PSpice. These models were verified through comparisons of simulation results with those obtained from HOMER.

In Chapter six, the implementation of the proposed prediction model within the expert system of the supervisory controller was elaborated. Flow charts of the predictive power management strategy were presented. The previously developed hybrid solar system was combined with more solar energy and a DC Genset to charge the battery, without upgrading existing battery bank, so that the increased load caused by a high guest turnout could be met.

Throughout this research there has been a need for a methodology to compare various sizes of the solar system to find the most suited for a particular location. This

work required careful analysis of the yearly insolation, guest occupancy rate and ambient temperature among many other varying factors. The requirements of diesel generators were now included from a control and interconnection point of view. The inverter control requirements for these differing modes of operation were described and simulated. Though the expansion of the project hasn't taken place yet due to the costs involved, there has been an effort from the management to re-think its decision due to the increasing demand and the introduction of newer inventions from industry experts like the author.

Chapter seven presented the design and simulations of a large hybrid power system which integrated their configurations with different types of diesel generator. Simulation results of these systems were taken and various power management strategies were presented and the long-term performances of these systems were discussed throughout. The complete design, simulation and implementation of a large hybrid power system into a real operating system was considered. A method of limiting the power from remote renewable energy sources using frequency shift was simulated and implemented. Methods to control the use of the renewable energy were investigated, with a controller using the predictable nature of the Sun to determine the battery charging states.

- Development of frequency shift control in decentralised distributed renewable systems.
- Creation of method in PSIM to simulate a combination VC-VSI and CC-VSI inverter controlled system.
- Development of a controller for the largest decentralised multi-function renewable power system in Western Australia.

Chapters six and seven describe the parallel hybrid system operating in different modes of operations. From the Matlab simulations it is evident that the hybrid power system utilizes most of the renewable energy to its maximum extent. Whenever there is excess renewable energy (example as full irradiance solar) the excess power can be used for charging the battery bank. Latest technologies are described that enable tracking of the maximum power from the solar. The hybrid generator can also be used as a source for loads. A speed-controlled generator saves energy when there is a low demand for power and it can also be a short term power distributor in emergencies.

7.2 Conclusions

It is undeniable that a simple, reliable and economically feasible system with a reduced energy storage element is more suitable for remote area applications. System economic and operation results presented in this thesis have suggested that the PV-VSDG system with predictive power management offers an alternative approach to remote applications. It has been demonstrated throughout the thesis that a PV-VSDG system could provide a comprehensive solution for remote applications without complex system control, and require only minimal technical expertise in handling the system operation. Economic and environmental analyses also showed that a PV-VSDG system is not only cost-competitive, if compared to the system with large battery bank storage, but also delivers environmental benefits when compared to those systems without a renewable energy generator. The main advantage of the PV-VSDG system configuration under study was direct utilisation of PV power along with variable speed operation of the diesel generator. Simulation results showed that fuel savings of a PV-VSDG system, compared to the PV-CSDG system, can contribute to very reasonable long-term economic and environmental benefits.

One of the challenges of this research has been to identify solar resource and load demand forecast models for the predictive power management strategy. Furthermore, it has been demonstrated that the integration of solar resource and load demand forecasting in an advanced predictive power management strategy provides optimal component dispatch for a PV-VSDG hybrid power system. This system topology and the proposed power management strategy offer an alternative to the off-grid hybrid power system design, with the aims of overcoming the complex technical issues associated with massive energy storage elements and of contributing to extension of the market for off-grid hybrid power systems.

This thesis is a culmination of four years of successful research under the guidance of Professor C.V. Nayar and Dr Sumedha Rajakaruna. The author was delighted to have the research lead to a practical conclusion in the form of the system designed, developed and implemented at Veterans retreat, Eco Beach Wilderness Resort in Broome, Western Australia among other projects.

The author believes the key aspects of this research were the development, modelling and demonstration of the complimentary hybrid system. This combination of solar and advanced battery bank and novel variable speed DC diesel generator allows a hybrid system to increase its energy output and inverter utilisation. Mathematical modelling was carried out to show exactly where this type of system is advantageous over conventional power electronic topologies. The system was developed for both the stand alone and grid connected configurations.

A key aspect of the research comes from the control and configuration of larger hybrid power systems. These systems use a compartmental approach to allow solar or wind systems to be AC coupled to the distribution network. A central inverter and controller are used as the brain for the system and this determines generator runtimes and energy storage requirements based upon likely future free energy availability.

Power generated in power stations pass through large & complex networks like transformers, overhead lines, cables & other equipment and reaches at the end users. It is a fact that the amount of electric energy generated by a Power Station does not match with the units distributed to the consumers. Some percentage of the units is lost in the Distribution network. EIA estimates that national electricity transmission and distribution losses average about 6% of the electricity that is transmitted and distributed in the United States each year.

A parallel hybrid power system is one way to overcome these losses since renewable energy sources are located near the loads. The transmission and distribution system will be available when a renewable energy source is not available.

When there is low sunshine and peak load demand then a battery bank with inverter provides the remaining demanded power for the loads. If necessary, the required energy can also be taken from the transmission line.

From the above operations it is evident that the parallel hybrid configuration will provide users with a better power system network and an uninterrupted power supply. It also makes excellent use of renewable energy and reduces the total energy lost by the system.

Finally, the author is grateful to have had this opportunity for pursuing study and completing research in the area of renewable energy engineering. This invaluable experience will definitely allow the author to make a contribution to the development of off-grid power supply in remote communities across Australia.

7.3. Further Areas of Research

The development of a simulation program with a graphical user interface that allows analytical performance simulation for hybrid power systems with a variable speed diesel generator would be a task beneficial to creating a user-friendly simulation environment that facilitates engineering designs.

Based on the work of this thesis in developing the use of solar power in remote and desert applications, these predictive models can be modified and extended for other renewable energy resources that have a high frequency of fluctuation, such as the wind.

The inclusion of other renewable resources in the simulation model could be useful to test the power management algorithms and to provide a clear perception of the advantages of employing VSDG and the proposed strategy with multi-renewable resources integrated into a hybrid power system.

New electrical and hybrid cars with good energy storage or capacity batteries will be on the market soon. These cars will be parked at a garage with a lot of energy, and with a proper control mechanism, without adding more centralised battery bank; more energy can be stored or discharged without affecting the entire network system or affecting the quality of the power. These car batteries will also need to be discharged in the evening, when the day shift workers are at home, and if the network can be supported by this procedure, the centralised battery system would not need to be increased.

Remote monitoring and regulation is an important area for research. These types of systems can be in isolated places with the support of GPS. Improved technology will markedly reduce the running cost.

The author hopes that this thesis represents advancement in the area of hybrid power systems and control for remote area applications. However, much work is still to be carried out on the optimal balance between renewable energy extraction, the storage of this energy and increasing the reliability of the overall system.

7.4. An Exciting and Invaluable Area to Research

Australia, like many locations across the globe, will have an ongoing requirement to bring electricity to remote and isolated locations. The research presented in this thesis draws on the energy source of solar with advanced novel battery storage system and conventional diesel systems to provide reliable electricity. The enabling technology with allows this to be possible is power electronics. This area of research is likely to be undergoing a revolution in the next few years as switching devices change from being Silicon based to Silicon Carbide. This new material will vastly decrease switching losses allowing higher power and faster switching devices, and providing a new level of efficiency for power electronics.

8. Appendices

8.1 Additional graphs and figures of chapter 6.

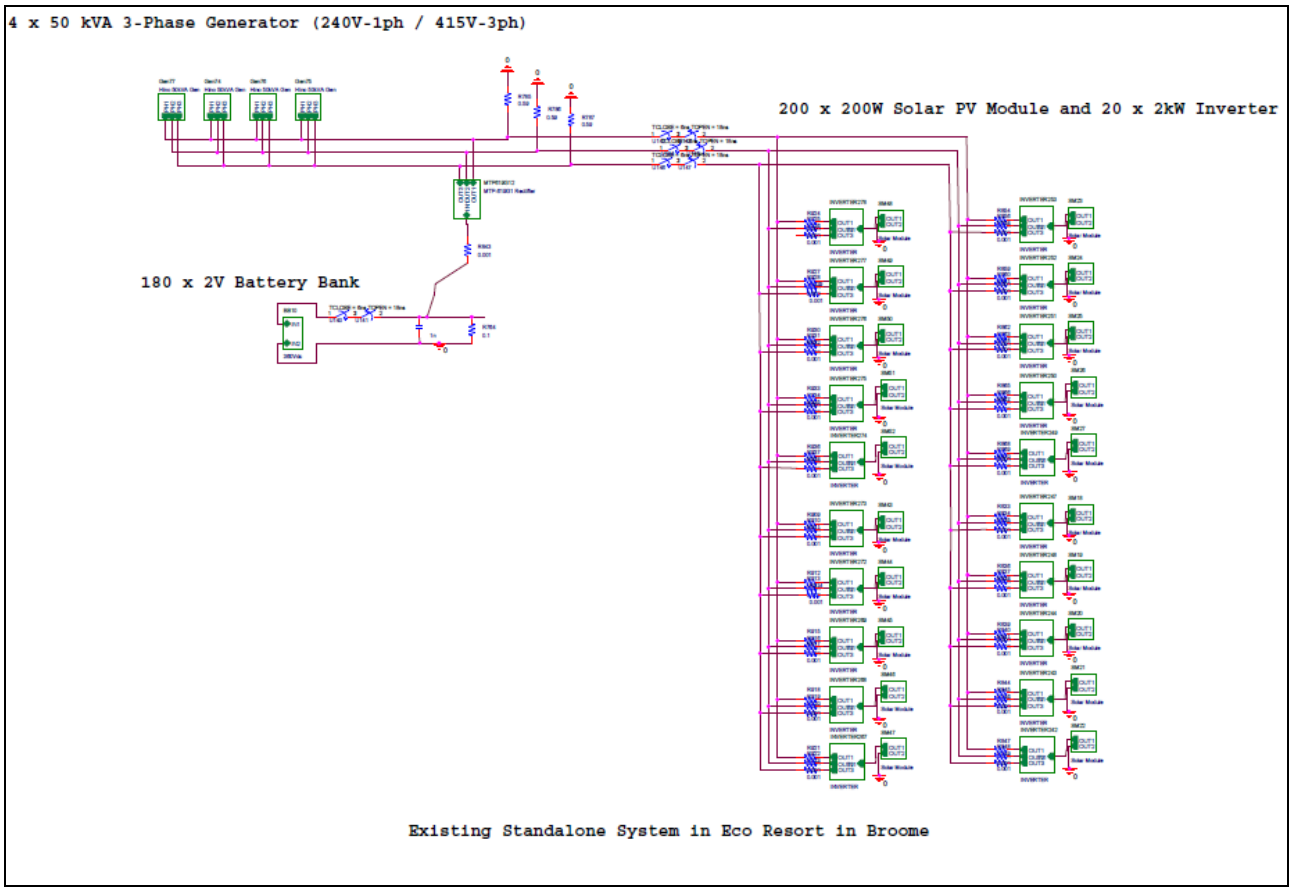

Figure 8. 1: Existing Standalone System in Eco Resort in Broome

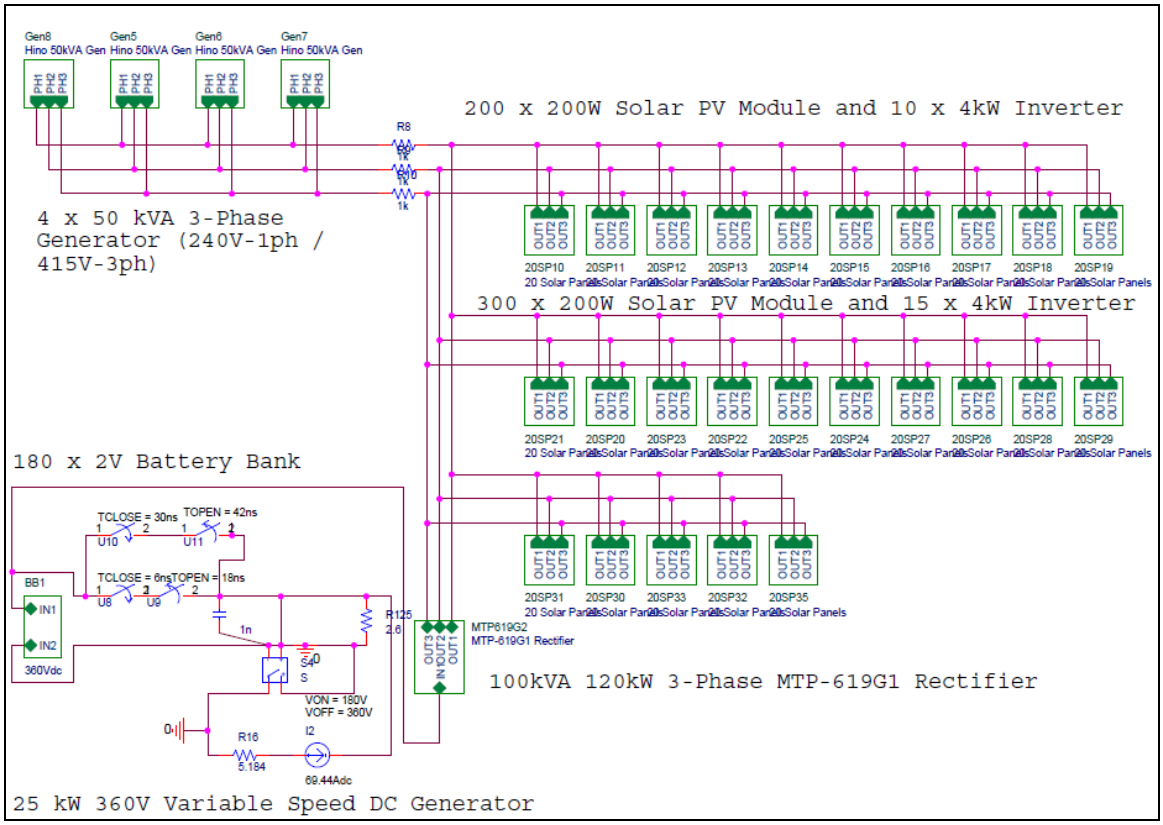

Figure 8. 2: New Standalone System in Eco Resort in Broome

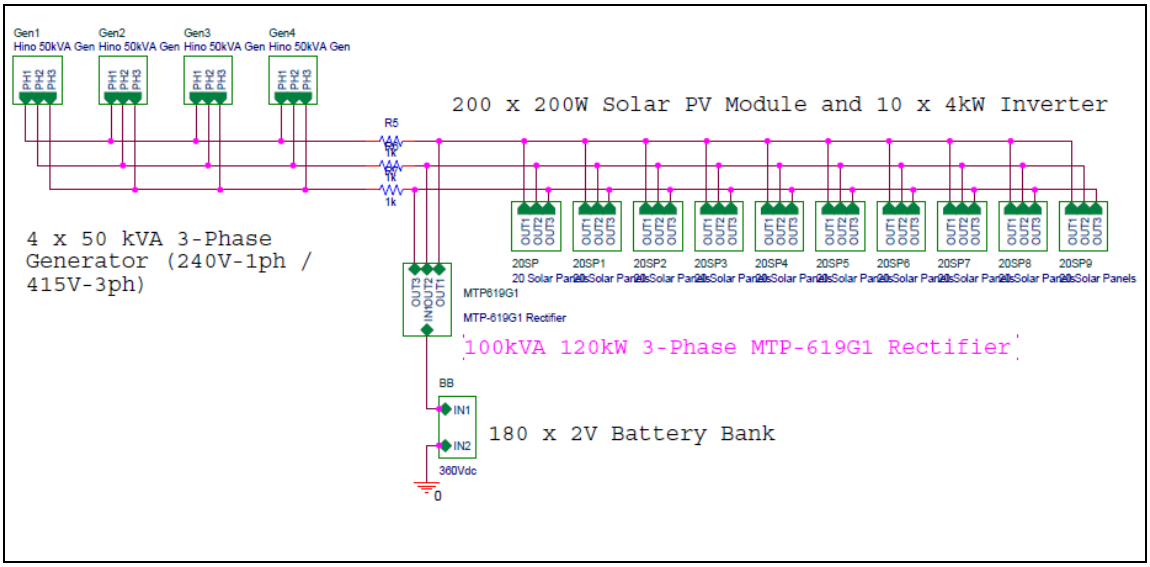

Figure 8. 3: Existing Standalone System Schematic

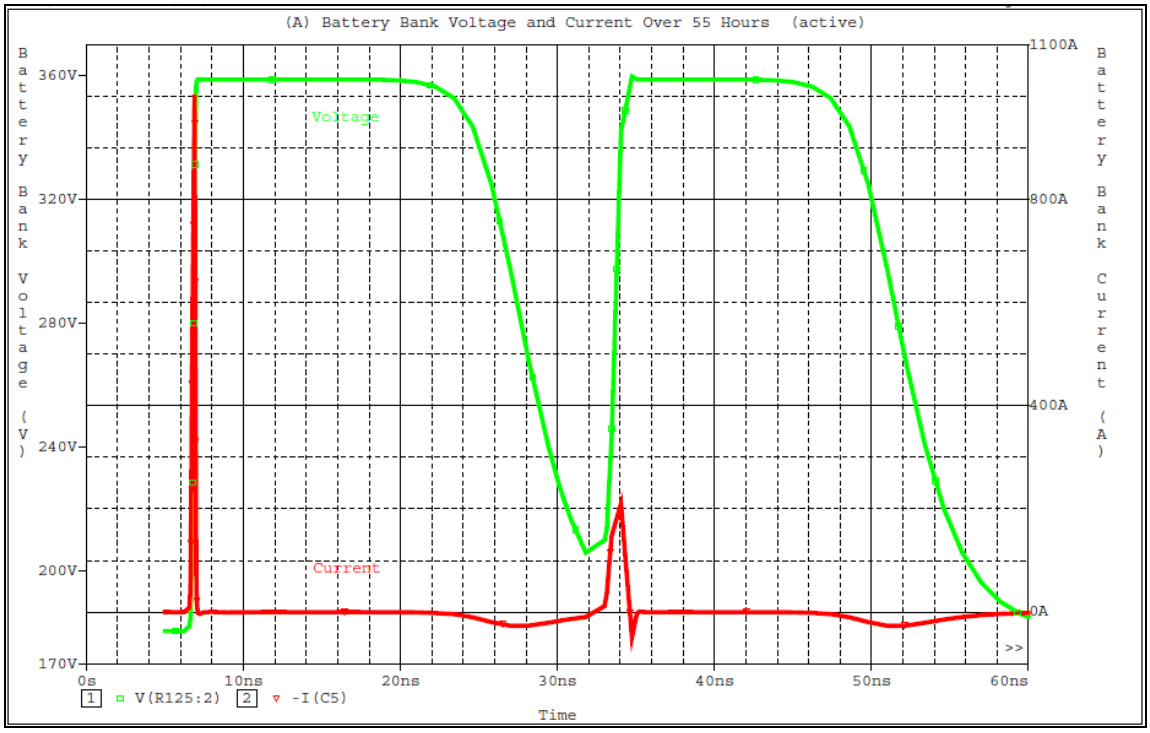

Figure 8. 4: Battery Bank Voltage and Current Over 55 Hours

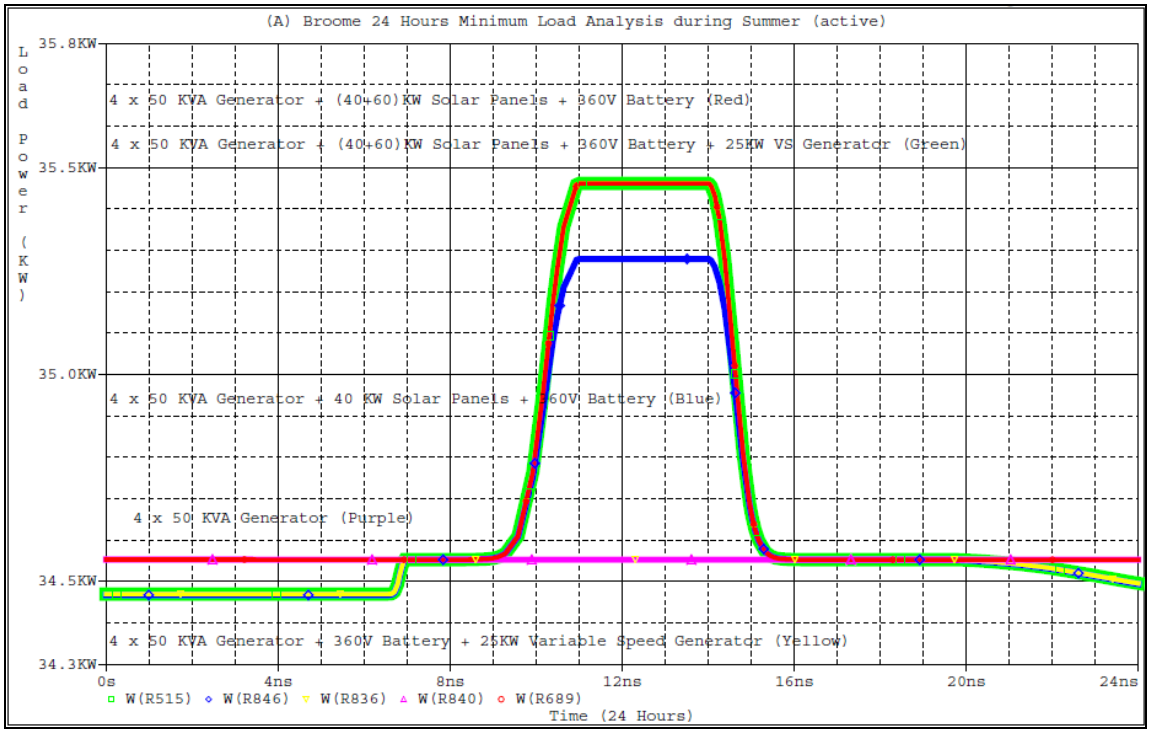

Figure 8. 5: Broome 24 Hours Minimum Load Analysis during Summer

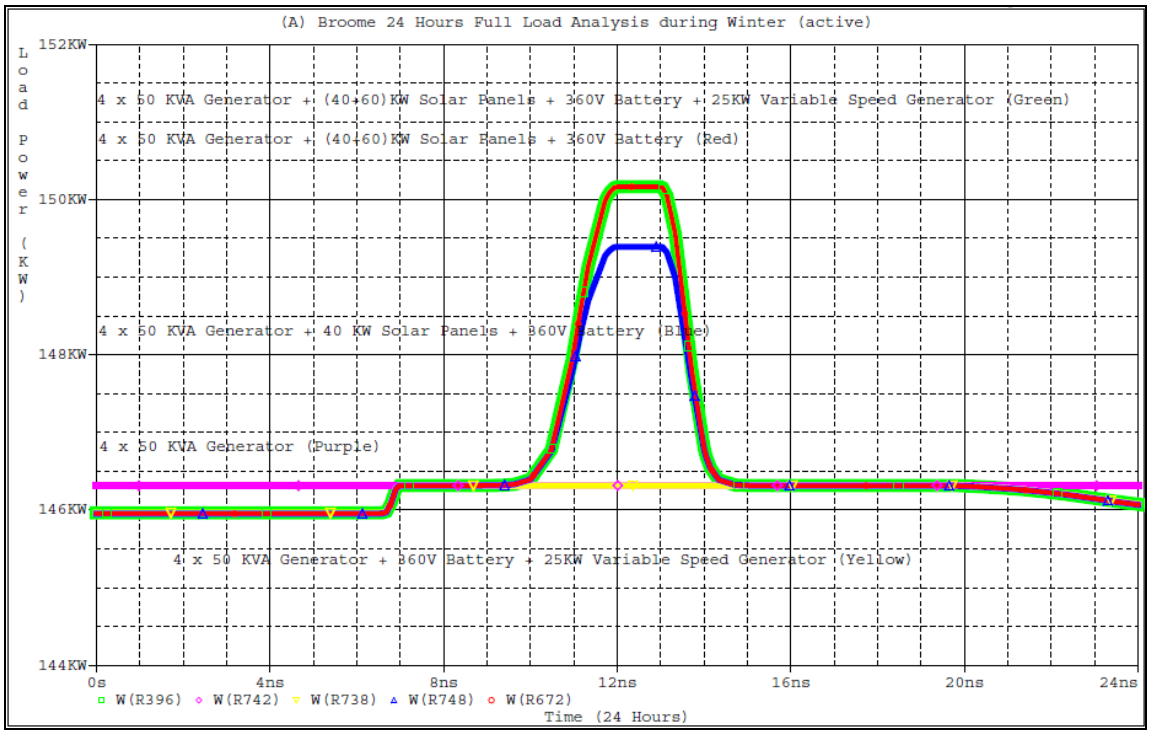

Figure 8. 6: Broome 24 Hours Full Load Analysis during winter

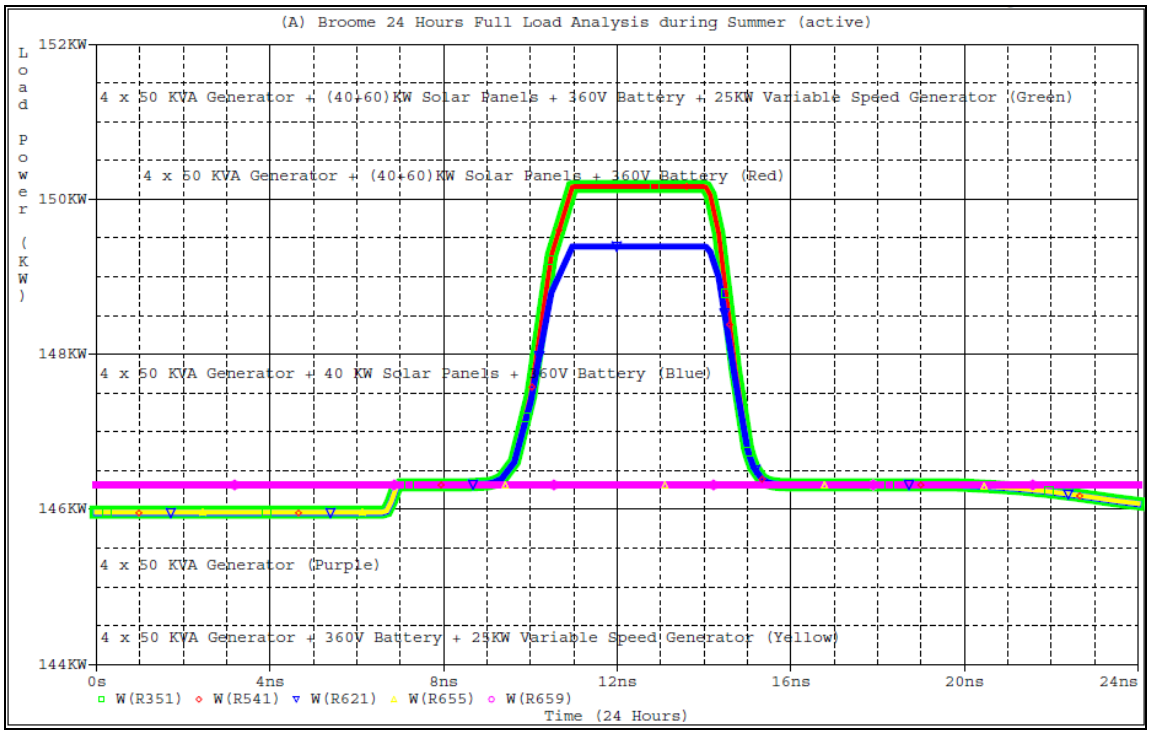

Figure 8. 7: Broome 24 Hours Full Load Analysis during summer

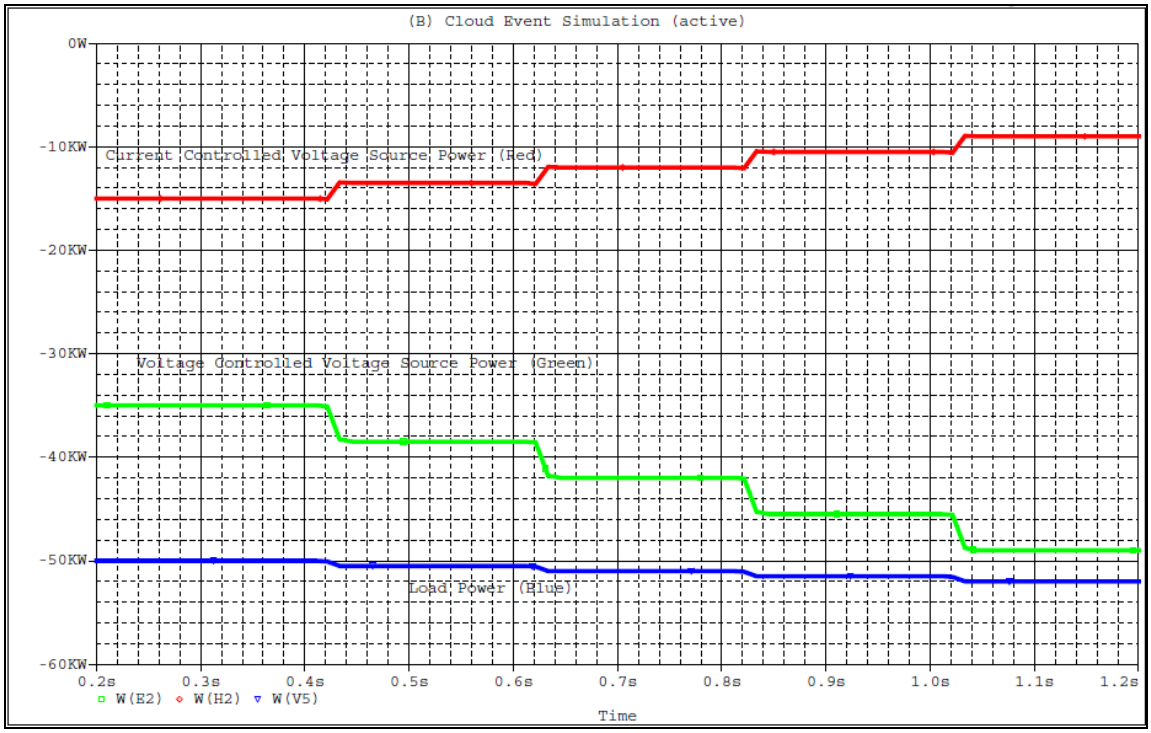

Figure 8. 8: Cloud Event Simulation

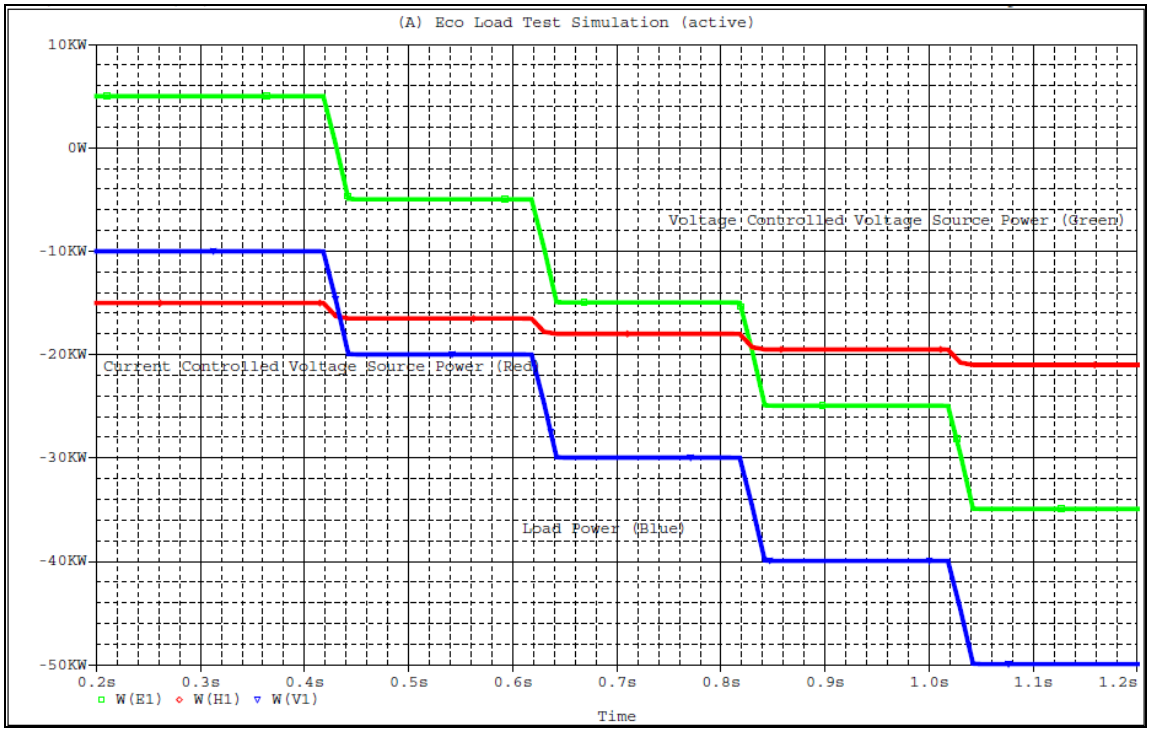

Figure 8. 9: Eco Load Test Simulations

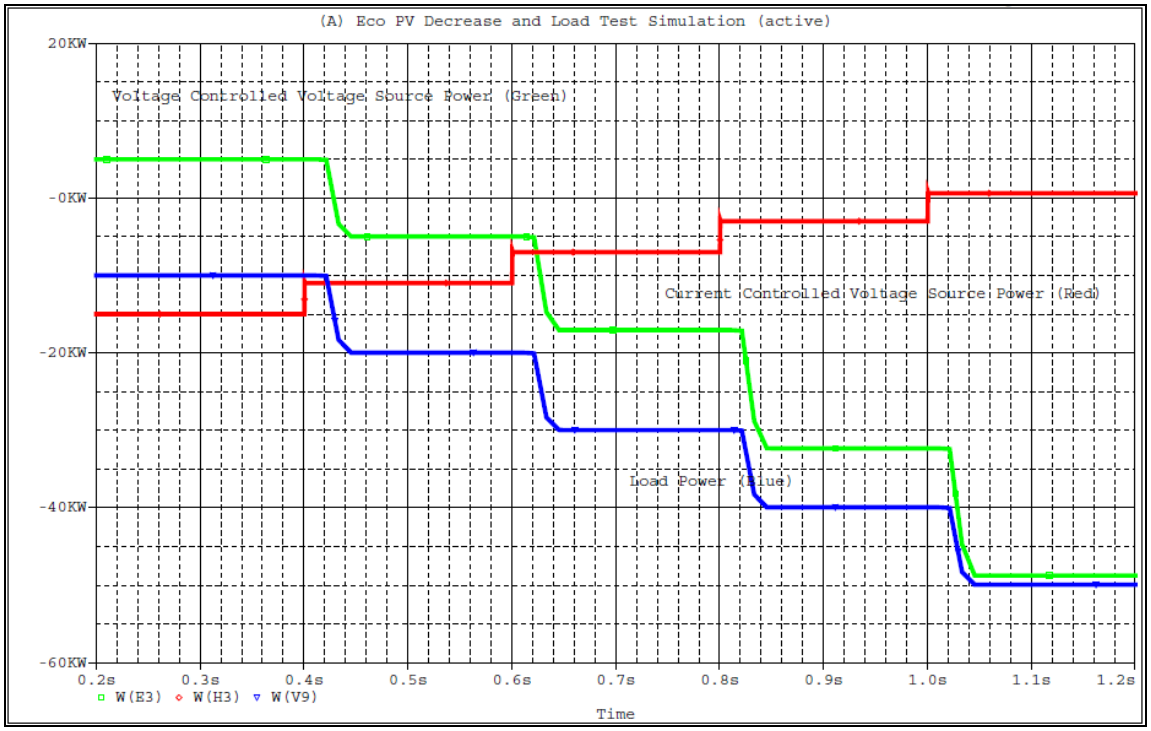

Figure 8. 10: Eco PV Decrease and Load Test Simulation

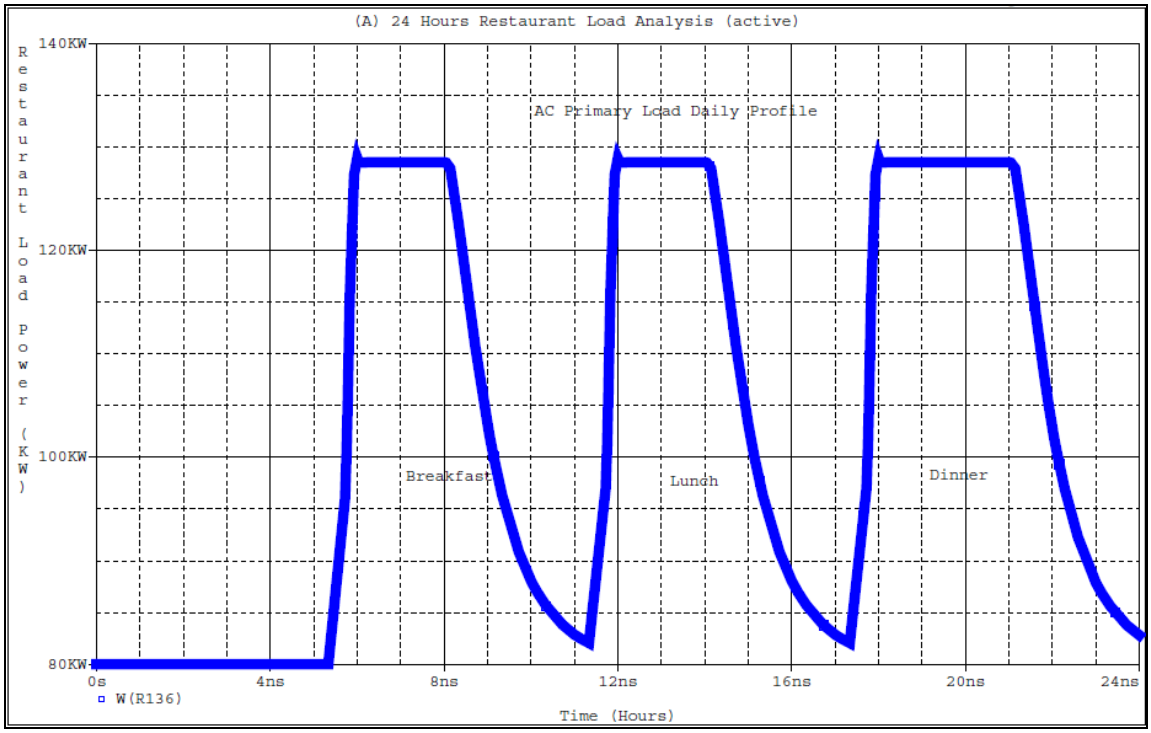

Figure 8. 11: 24 Hours Restaurant Load Analysis

A. System Report_EcoProject_new_proposalvers2

8.2. System architecture

PV Array	134 kW
Generator 2	50 kW
Generator 3	50 kW
Generator 5	50 kW
Generator 1	25 kW
Battery	180 Hoppecke 12 OPzS 1500
Inverter	1 kW
Rectifier	1 kW
Dispatch strategy	Cycle Charging

8.3. Cost summary

Total net present cost	$ 4,099,041
Levelized cost of energy	$ 0.777/kWh
Operating cost	$ 195,166/yr

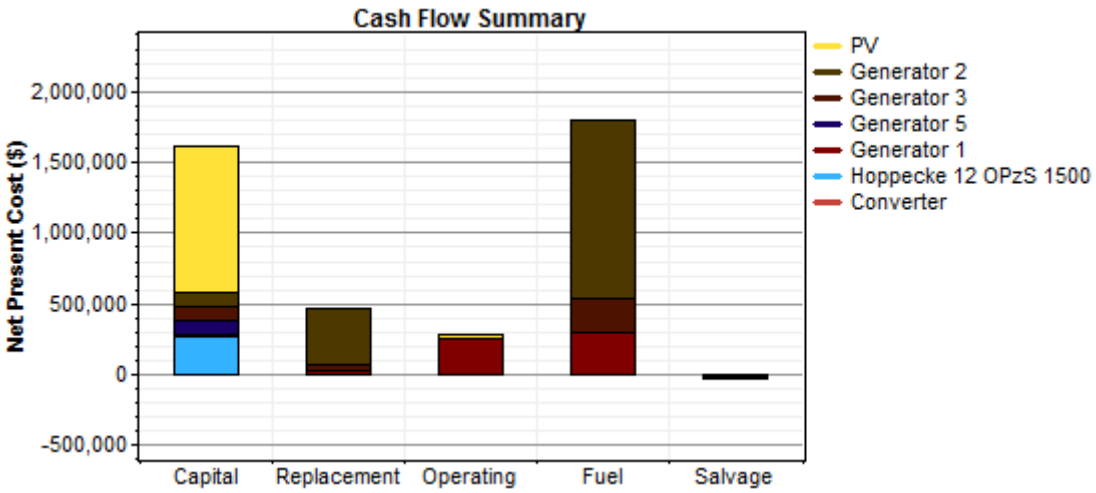

Net Present Costs

Component	Capital	Replacement	O&M	Fuel	Salvage	Total
	($)	($)	($)	($)	($)	($)
PV	1,032,946	0	15,861	0	0	1,048,807
Generator 2	100,000	401,608	0	1,266,484	-9,669	1,758,423
Generator 3	100,000	45,663	0	241,233	-3,301	383,595
Generator 5	100,000	0	0	197	-23,261	76,935
Generator 1	15,000	19,746	256,102	284,751	-536	575,063
Hoppecke 12 OPzS 1500	255,060	0	0	0	0	255,060
Converter	1,158	0	0	0	0	1,158
System	1,604,164	467,016	271,963	1,792,666	-36,767	4,099,042

Annualized Costs

Component	Capital	Replacement	O&M	Fuel	Salvage	Total
	($/yr)	($/yr)	($/yr)	($/yr)	($/yr)	($/yr)
PV	80,804	0	1,241	0	0	82,045
Generator 2	7,823	31,416	0	99,073	-756	137,556
Generator 3	7,823	3,572	0	18,871	-258	30,007
Generator 5	7,823	0	0	15	-1,820	6,018
Generator 1	1,173	1,545	20,034	22,275	-42	44,985
Hoppecke 12 OPzS 1500	19,953	0	0	0	0	19,953

Converter	91	0	0	0	0	91
System	125,489	36,533	21,275	140,234	-2,876	320,655

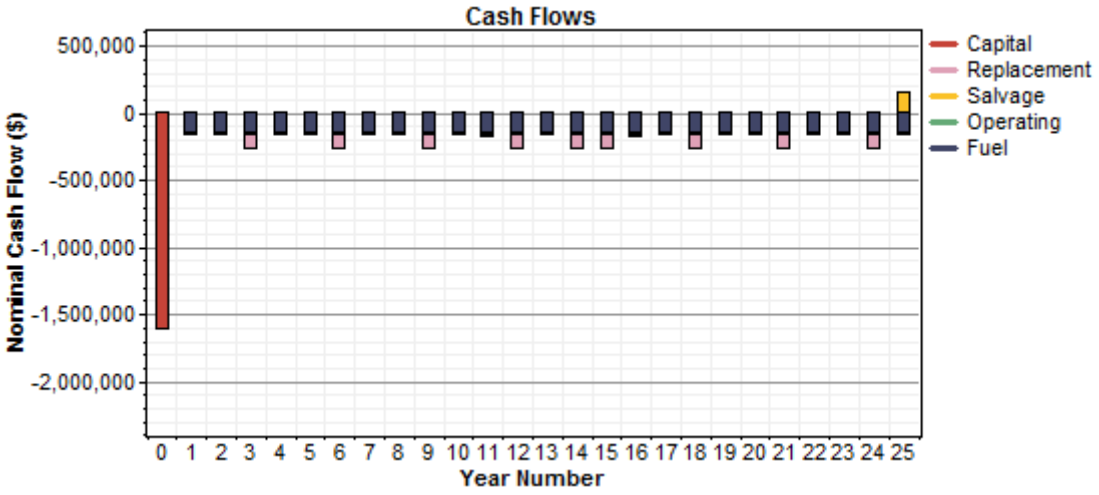

Electrical

Component	Production (kWh/yr)	Fraction
PV array	249,046	50%
Generator 2	181,779	36%
Generator 3	32,482	6%
Generator 5	25	0%
Generator 1	36,504	7%
Total	499,837	100%

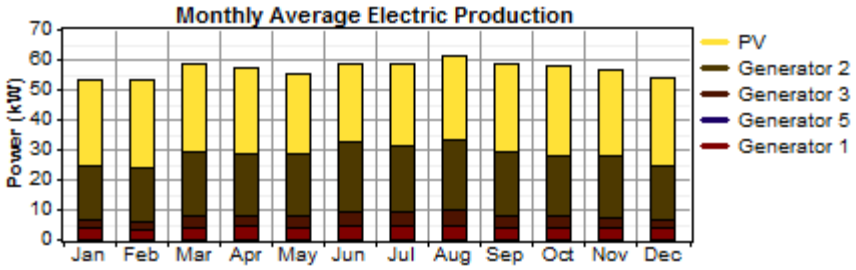

Load	Consumption (kWh/yr)	Fraction
AC primary load	412,815	100%
Total	412,815	100%

Quantity	Value	Units
Excess electricity	85,228	kWh/yr
Unmet load	0.000153	kWh/yr
Capacity shortage	0.00	kWh/yr
Renewable fraction	0.498	

PV

Quantity	Value	Units
Rated capacity	134	kW
Mean output	28.4	kW
Mean output	682	kWh/d
Capacity factor	21.2	%
Total production	249,046	kWh/yr

Quantity	Value	Units
Minimum output	0.00	kW
Maximum output	100	kW
PV penetration	60.3	%
Hours of operation	4,398	hr/yr
Levelized cost	0.329	$/kWh

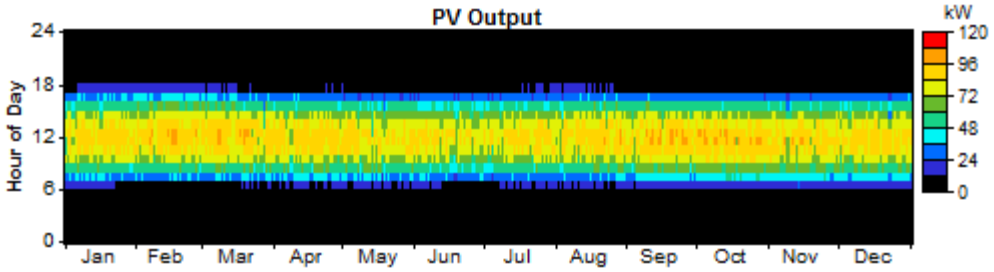

Generator 2

Quantity	Value	Units
Hours of operation	5,151	hr/yr
Number of starts	761	starts/yr
Operational life	2.91	yr

Capacity factor	41.5	%
Fixed generation cost	12.7	$/hr
Marginal generation cost	0.375	$/kWhyr

Quantity	Value	Units
Electrical production	181,779	kWh/yr
Mean electrical output	35.3	kW
Min. electrical output	25.0	kW
Max. electrical output	50.0	kW

Quantity	Value	Units
Fuel consumption	66,049	L/yr
Specific fuel consumption	0.363	L/kWh
Fuel energy input	649,918	kWh/yr
Mean electrical efficiency	28.0	%

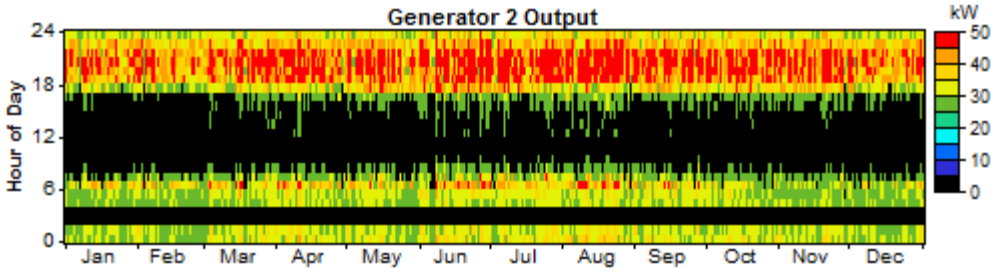

Generator 3

Quantity	Value	Units
Hours of operation	1,115	hr/yr
Number of starts	569	starts/yr
Operational life	13.5	yr
Capacity factor	7.42	%
Fixed generation cost	12.7	$/hr
Marginal generation cost	0.375	$/kWhyr

Quantity	Value	Units
Electrical production	32,482	kWh/yr

Mean electrical output	29.1	kW
Min. electrical output	25.0	kW
Max. electrical output	50.0	kW

Quantity	Value	Units
Fuel consumption	12,581	L/yr
Specific fuel consumption	0.387	L/kWh
Fuel energy input	123,793	kWh/yr
Mean electrical efficiency	26.2	%

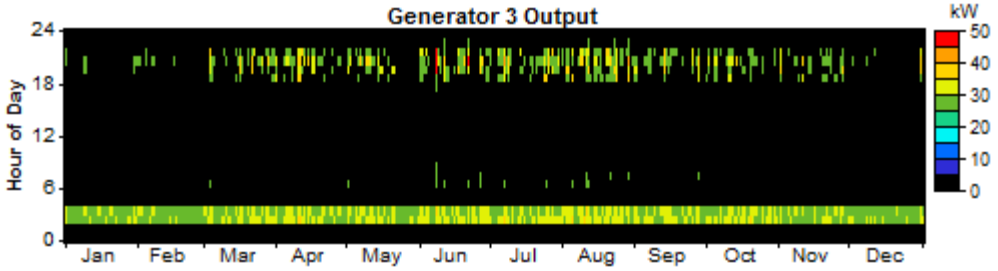

Generator 1

Quantity	Value	Units
Hours of operation	2,862	hr/yr
Number of starts	1,432	starts/yr
Operational life	5.24	yr
Capacity factor	16.7	%
Fixed generation cost	10.7	$/hr
Marginal generation cost	0.375	$/kWhyr

Quantity	Value	Units
Electrical production	36,504	kWh/yr
Mean electrical output	12.8	kW
Min. electrical output	12.5	kW
Max. electrical output	19.9	kW

Quantity	Value	Units

Fuel consumption	14,850	L/yr
Specific fuel consumption	0.407	L/kWh
Fuel energy input	146,125	kWh/yr
Mean electrical efficiency	25.0	%

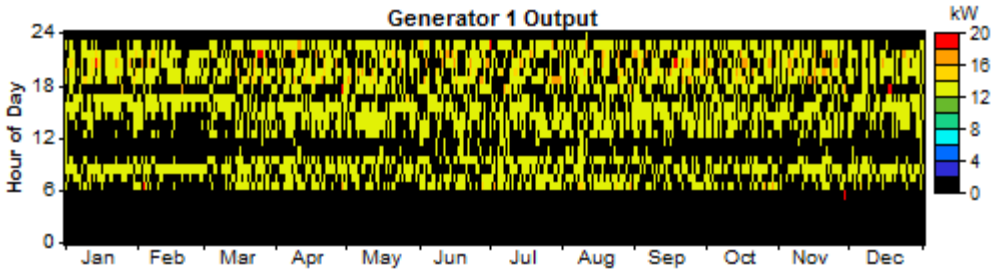

Battery

Quantity	Value
String size	180
Strings in parallel	1
Batteries	180
Bus voltage (V)	360

Quantity	Value	Units
Nominal capacity	540	kWh
Usable nominal capacity	378	kWh
Autonomy	8.02	hr
Lifetime throughput	924,480	kWh
Battery wear cost	0.000	$/kWh
Average energy cost	0.137	$/kWh

Quantity	Value	Units
Energy in	4,833	kWh/yr
Energy out	4,185	kWh/yr
Storage depletion	26.2	kWh/yr
Losses	621	kWh/yr
Annual throughput	4,513	kWh/yr

Expected life	20.0	yr

Emissions

Pollutant	Emissions (kg/yr)
Carbon dioxide	246,189
Carbon monoxide	608
Unburned hydrocarbons	67.3
Particulate matter	45.8
Sulphur dioxide	494
Nitrogen oxides	5,422

8.2 Additional Graphs and Figures of Chapter 7.

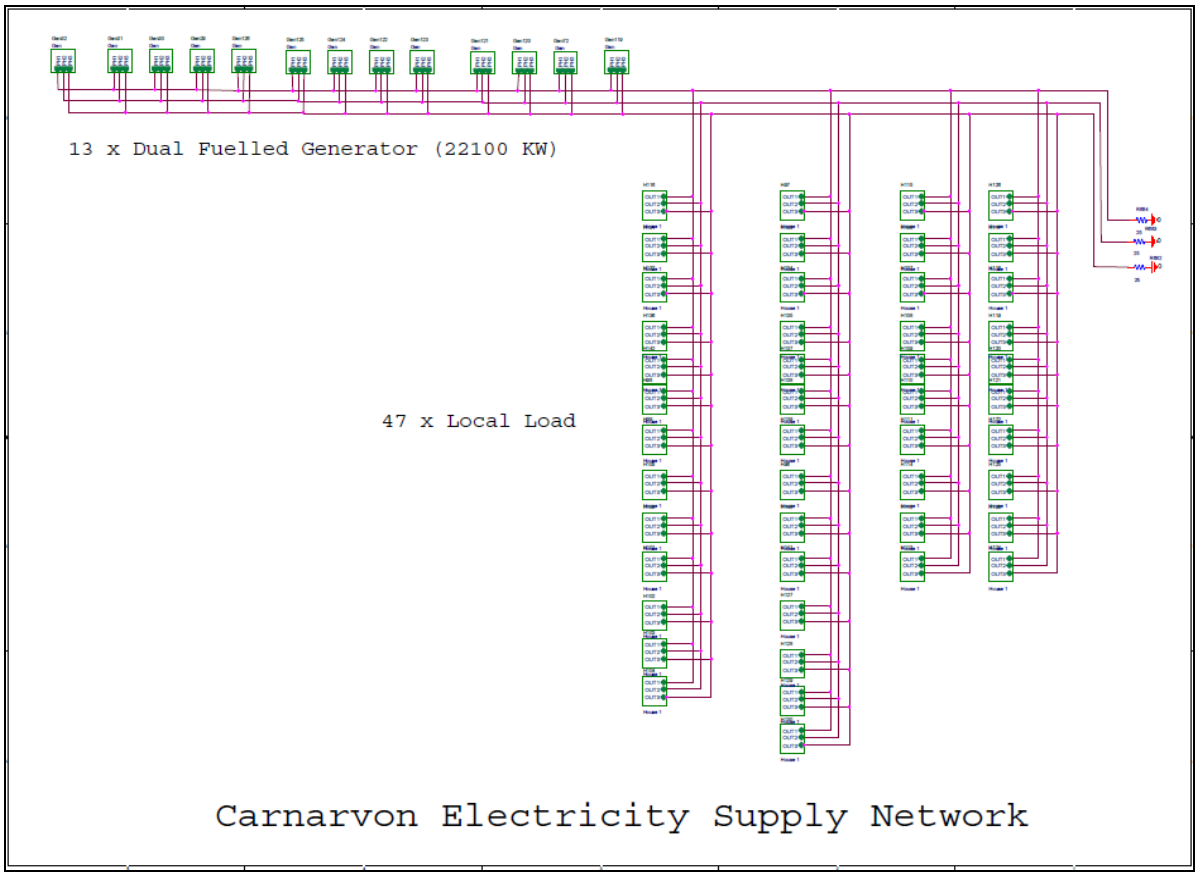

Figure 8. 12: Carnarvon Electricity Supply Network Schematic

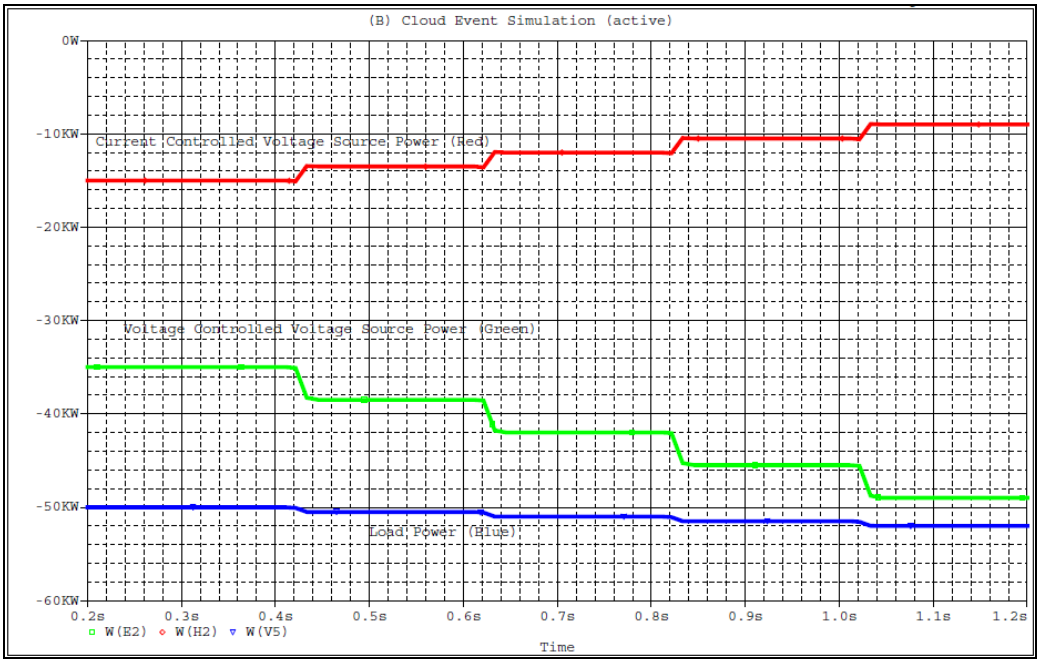

Figure 8. 13: Cloud Event Simulation

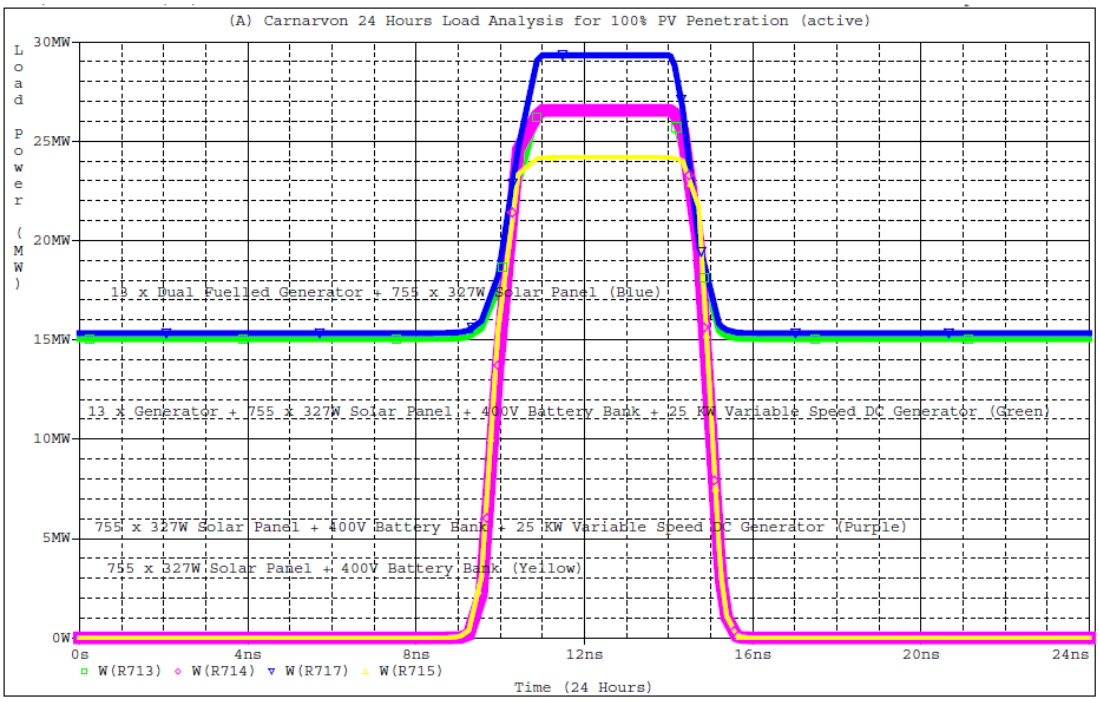

Figure 8. 14: Carnarvon 24 Hours Load Analysis for 100% PV Penetration

(Full Load - summer)

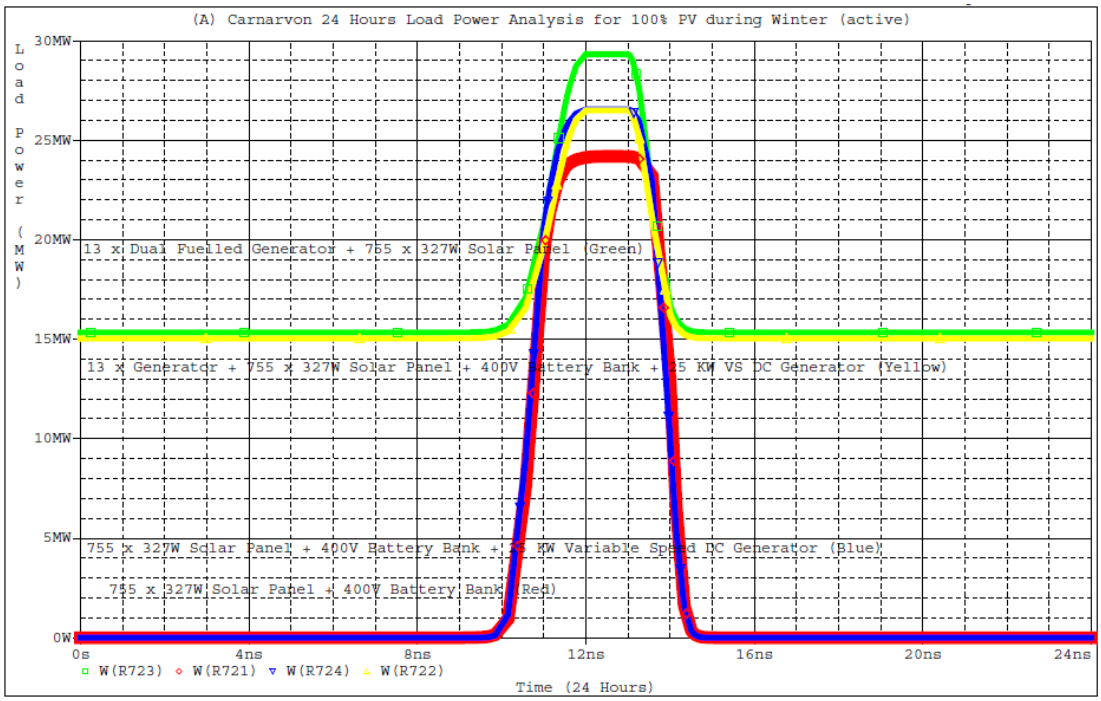

Figure 8. 15: Carnarvon 24 Hours Load Analysis for 100% PV Penetration

(Full Load - winter)

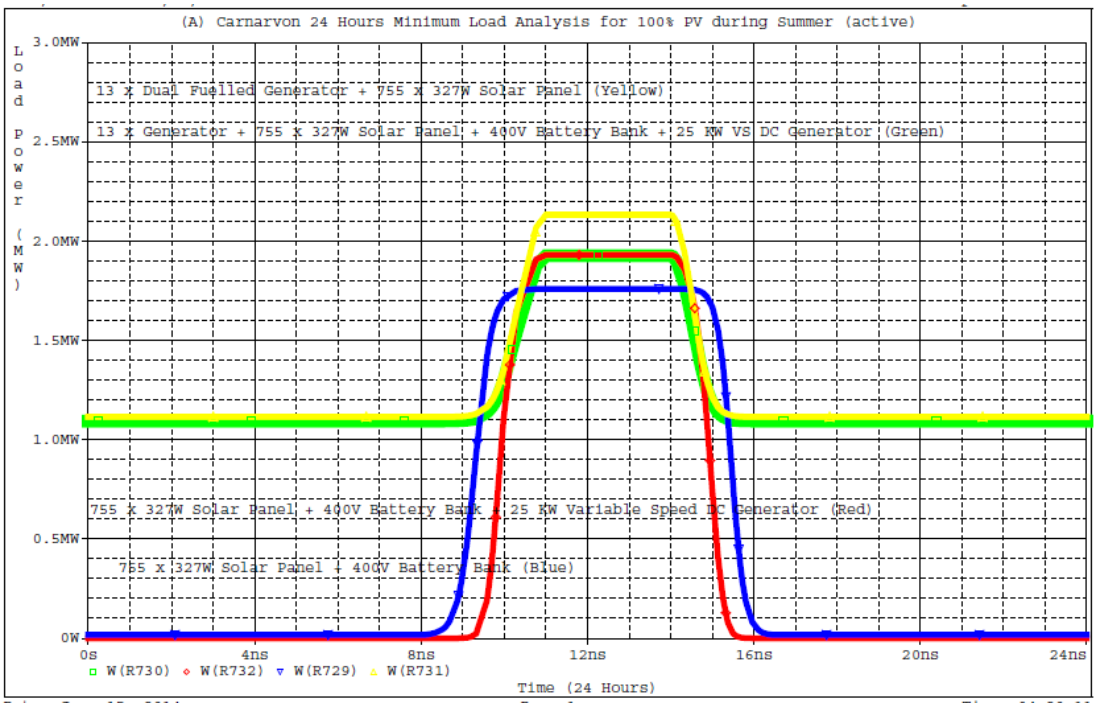

Figure 8. 16: Carnarvon 24 Hours Load Analysis for 100% PV Penetration
(Minimum Load - summer)

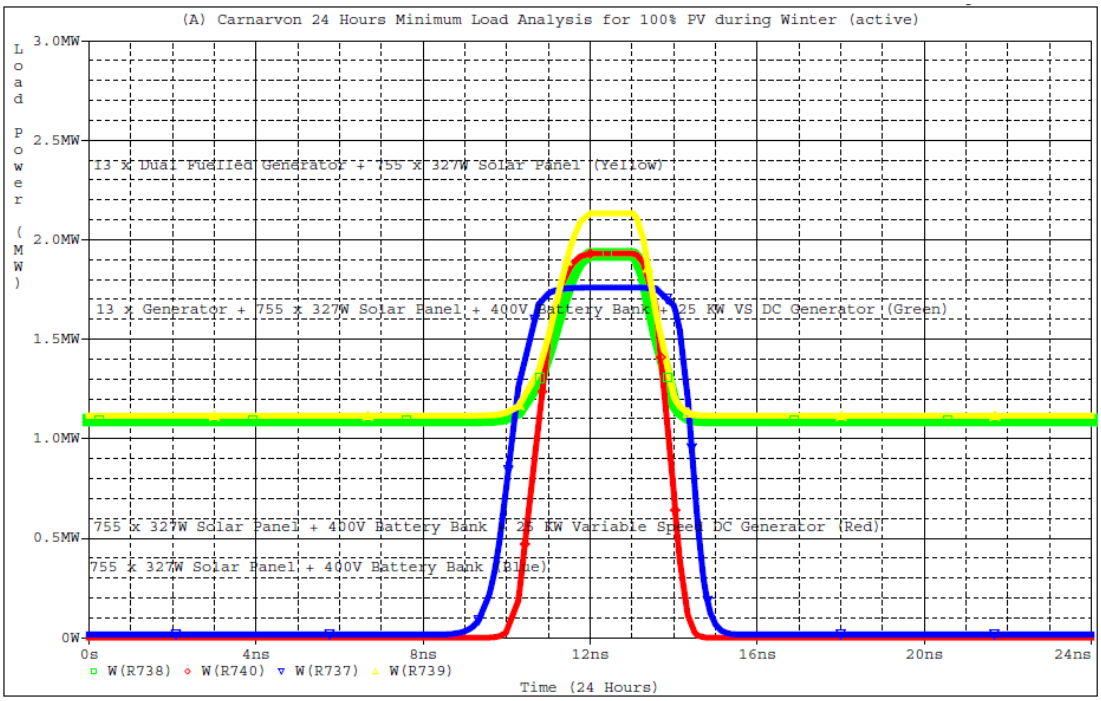

Figure 8. 17: Carnarvon 24 Hours Load Analysis for 100% PV Penetration (Minimum Load - winter)

8.3 DC Gen battery setup for Carnarvon grid

8.4 System architecture

PV Array	13,000 kW
DC HbG20kW	1,500 kW
Battery	360 Hoppecke 20 OPzS 2500
Inverter	15,000 kW
Rectifier	15,000 kW
Dispatch strategy	Cycle Charging

8.5 Cost summary

Total net present cost	$ 113,244,808
Levelized cost of energy	$ 1.318/kWh

Operating cost	$ 3,864,003/yr

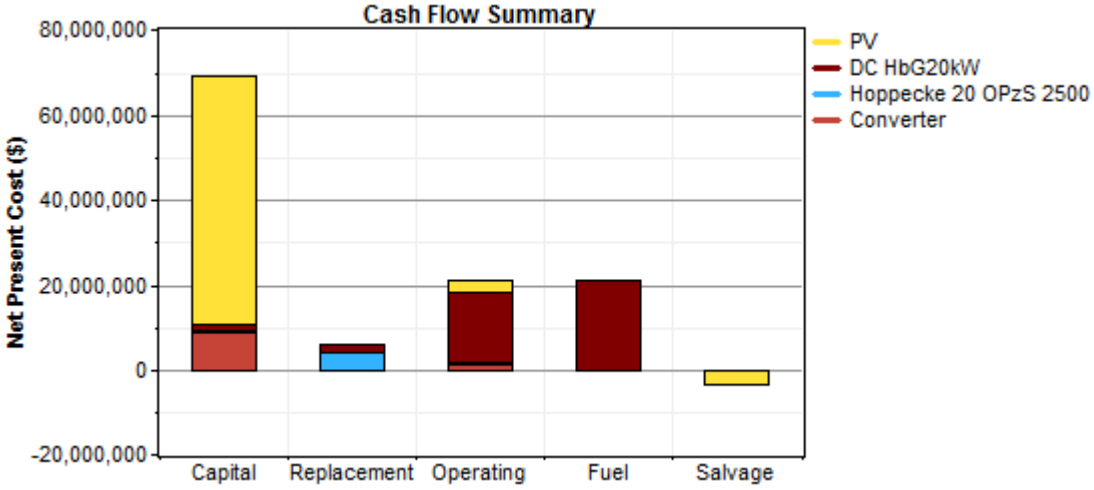

8.5.1 Net Present Costs

Component	Capital	Replacement	O&M	Fuel	Salvage	Total
	($)	($)	($)	($)	($)	($)
PV	58,500,000	0	2,982,181	0	-3,242,773	58,239,408
DC HbG20kW	1,200,000	1,978,437	16,470,587	20,945,504	-123,849	40,470,676
Hoppecke 20 OPzS 2500	225,000	3,980,732	412,917	0	-230,898	4,387,751
Converter	9,000,000	0	1,146,993	0	0	10,146,994
System	68,925,000	5,959,168	21,012,676	20,945,504	-3,597,520	113,244,816

8.5.2 Annualized Costs

Component	Capital	Replacement	O&M	Fuel	Salvage	Total
	($/yr)	($/yr)	($/yr)	($/yr)	($/yr)	($/yr)
PV	5,100,297	0	260,000	0	-282,720	5,077,577
DC HbG20kW	104,621	172,489	1,435,981	1,826,125	-10,798	3,528,418

Hoppecke 20 OPzS 2500	19,617	347,058	36,000	0	-20,131	382,544
Converter	784,661	0	100,000	0	0	884,661
System	6,009,196	519,547	1,831,981	1,826,125	-313,648	9,873,199

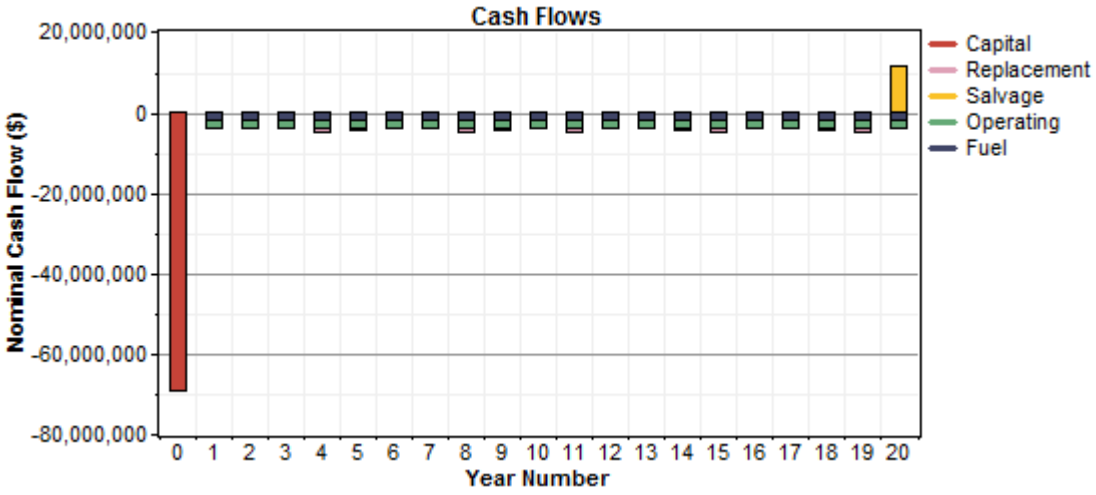

8.6 Electrical

Component	Production (kWh/yr)	Fraction
PV array	22,332,640	86%
DC HbG20kW	3,596,317	14%
Total	25,928,956	100%

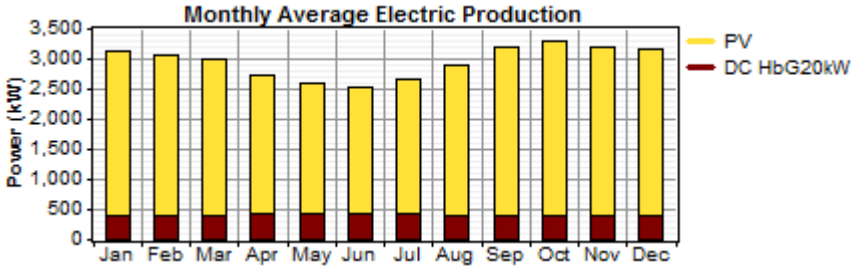

Load	Consumption (kWh/yr)	Fraction
AC primary load	7,492,356	100%
Total	7,492,356	100%

Quantity	Value	Units
Excess electricity	17,915,764	kWh/yr
Unmet load	0.00336	kWh/yr
Capacity shortage	0.00	kWh/yr
Renewable fraction	0.861	

8.7 PV

Quantity	Value	Units
Rated capacity	13,000	kW
Mean output	2,549	kW
Mean output	61,185	kWh/d
Capacity factor	19.6	%
Total production	22,332,640	kWh/yr

Quantity	Value	Units
Minimum output	0.00	kW
Maximum output	10,891	kW
PV penetration	298	%
Hours of operation	4,371	hr/yr
Levelized cost	0.227	$/kWh

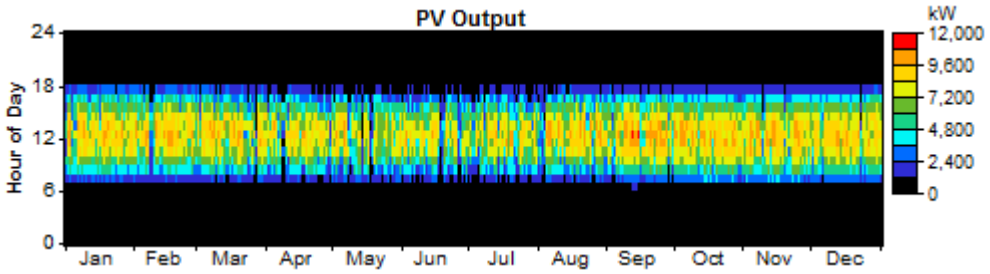

8.8 DC HbG20kW

Quantity	Value	Units
Hours of operation	3,419	hr/yr

Number of starts	1,462	starts/yr
Operational life	4.39	yr
Capacity factor	27.4	%
Fixed generation cost	503	$/hr
Marginal generation cost	0.486	$/kWhyr

Quantity	Value	Units
Electrical production	3,596,317	kWh/yr
Mean electrical output	1,052	kW
Min. electrical output	450	kW
Max. electrical output	1,500	kW

Quantity	Value	Units
Fuel consumption	1,217,416	L/yr
Specific fuel consumption	0.339	L/kWh
Fuel energy input	11,979,372	kWh/yr
Mean electrical efficiency	30.0	%

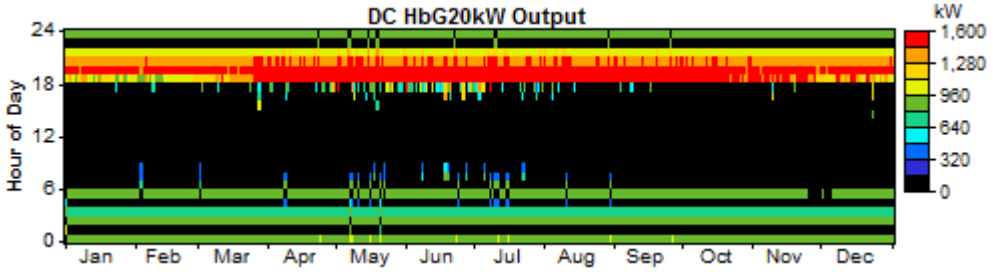

8.9 Battery

Quantity	Value
String size	24
Strings in parallel	15
Batteries	360
Bus voltage (V)	48

Quantity	Value	Units
Nominal capacity	1,800	kWh
Usable nominal capacity	1,260	kWh
Autonomy	1.47	hr
Lifetime throughput	3,068,280	kWh
Battery wear cost	0.506	$/kWh
Average energy cost	0.368	$/kWh

Quantity	Value	Units
Energy in	906,995	kWh/yr
Energy out	780,459	kWh/yr
Storage depletion	395	kWh/yr
Losses	126,141	kWh/yr
Annual throughput	841,591	kWh/yr
Expected life	3.65	yr

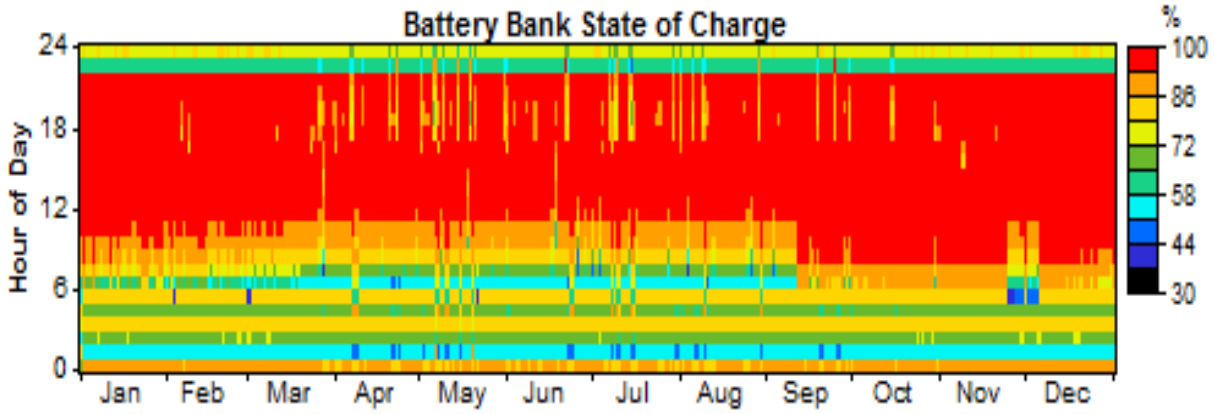

8.10 Emissions

Pollutant	Emissions (kg/yr)
Carbon dioxide	3,205,857
Carbon monoxide	7,913
Unburned hydrocarbons	877
Particulate matter	597
Sulphur dioxide	6,438
Nitrogen oxides	70,610